

Asymptotic Analysis and Numerical Analysis of the Benjamin-Ono Equation

by
Zhengjie Xu

A dissertation submitted in partial fulfillment
of the requirements for the degree of
Doctor of Philosophy
(Applied and Interdisciplinary Mathematics)
in The University of Michigan
2010

Doctoral Committee:

Professor John P. Boyd, Co-Chair
Professor Peter D. Miller, Co-Chair
Professor Sijue Wu
Associate Professor Jinho Baik

© Zhengjie Xu 2010
All Rights Reserved

To my parents and my wife

ACKNOWLEDGEMENTS

First of all, I would like to thank my thesis advisors, Professor Peter Miller and Professor John Boyd, for offering me such a great opportunity to work in this interesting area, and their guidance through my entire graduate life. I am very grateful to Professor Miller and Ms. Miller for their hospitality, tremendous help and warm regards. I am also indebted to Prof. Boyd for teaching me the skills in numerical analysis. This thesis would not be possible without their supports and advices.

I am grateful to Professor Sijue Wu and Professor Jinho Baik for being on my thesis committee and Professor Smadar Karni for being on my proposal committee. I would like to acknowledge funding support by the Department of Mathematics at University of Michigan. I would also like to thank many friends in Ann Arbor for their support and friendship.

I am greatly indebted to my parents Wenlai Xu and Lingdi Zhang for their love and encouragement throughout life. I also gratefully acknowledge my wife Xin Xu, who brings a lot of happiness to my life. Her love and support give me strength and courage. She makes my life in Ann Arbor more colorful and memorable.

TABLE OF CONTENTS

DEDICATION	ii
ACKNOWLEDGEMENTS	iii
LIST OF FIGURES	vii
LIST OF TABLES	xi
LIST OF APPENDICES	xii
CHAPTER	
I. Introduction	1
1.1 Zero Dispersion Limit of the BO Equation	3
1.2 Numerical Methods	6
1.3 Outline of Thesis	6
1.4 Notation	7
II. The Inverse-Scattering Transform for Integrable Evolution Equations	8
2.1 The Inverse-Scattering Transform for the KdV Equation	8
2.1.1 The Direct Scattering Problem	9
2.1.2 Time Dependence of the Scattering Data	11
2.1.3 The Inverse Scattering Problem	11
2.1.4 The Riemann-Hilbert Problem	11
2.2 The Inverse-Scattering Transform for the BO Equation	13
2.2.1 The Direct Scattering Problem	16
2.2.2 Time Dependence of the Scattering Data	23
2.2.3 The Inverse Scattering Problem	25
2.2.4 The Riemann-Hilbert Problem	26
2.2.5 The Soliton Solutions	27
2.2.6 The Multi-phase Solutions	29
2.2.7 The Conservation Laws	30
2.2.8 Matsuno's Method	32

2.3	An Example for the Scattering theory of the BO Equation . . .	35
III.	Zero dispersion limit of the BO equation for positive initial conditions	42
3.1	The Scattering Data in the Zero-Dispersion Limit	42
3.1.1	Admissible Initial Conditions	42
3.1.2	Formula for Phase Constants	45
3.1.3	Modification of the Cauchy Data	46
3.2	The Inverse-Scattering Problem in the Zero-Dispersion Limit	50
3.2.1	Main Theorem	50
3.2.2	Basic Strategy. Outline of the Proof of Main Theorem	54
3.2.3	Asymptotics of Traces of Powers of $\tilde{\mathbf{A}}_\epsilon$. Proof of Proposition III.7	58
3.2.4	Convergence of Measures and Locally Uniform Convergence of \tilde{U}_ϵ . Proof of Proposition III.8	71
3.2.5	Differentiation of \tilde{U}_ϵ . Burgers' Equation and Weak Convergence of \tilde{u}_ϵ	83
3.3	Strong Convergence Before Breaking	90
3.4	Numerical Verification	91
IV.	Generalizations of the Zero-Dispersion Limit of the BO Equation	97
4.1	Higher-Order BO Equations and Their Soliton Solutions . . .	97
4.2	Generalizations	98
4.3	Proof of Theorem IV.1	101
4.4	Proof of Proposition IV.2	102
V.	Numerical Methods	104
5.1	Fourier Pseudospectral Method	107
5.2	Rational Basis Function Method	108
5.3	Radial Basis Function Spectral Algorithm	114
5.3.1	Gaussian RBF Method	115
5.3.2	Uniform Grid: Toeplitz Matrices	116
5.3.3	Strengths of the RBF Method	118
5.3.4	Drawbacks of the RBF Method	118
5.4	Courant-Friedrichs-Lewy (CFL) Time Step Limit	119
5.5	Aliasing Instability and Dealiasing	121
5.5.1	Aliasing Instability	122
5.5.2	Dealiasing	125
5.6	Boundary Difficulties	126
5.6.1	Moving Coordinate System	126

5.6.2	Fourier Pseudospectral Method	128
5.6.3	Christov Method	128
5.6.4	RBF Method	129
5.7	Summary: Comparisons of Three Spectral Methods	130
5.7.1	Cost	130
5.7.2	Domain Truncation	131
5.7.3	Boundary Difficulty	131
5.7.4	Grid-Flexibility	132
5.8	Numerical Experiments on the Zero-Dispersion Limit of the BO Equation	132
5.9	Traveling Wave Solutions of the Cubic BO Equation	134
5.9.1	Derivation of the Cubic BO Traveling Wave Equa- tion and Its Scaling	136
5.9.2	A Numerical Method to Find A Traveling Wave So- lution of the Cubic BO Equation	137
5.9.3	Homotopy Perturbation Method	139
VI. Future Work		142
6.1	The Zero-Dispersion Limit of the BO Equation with Negative Initial Conditions	142
6.1.1	Introduction	142
6.1.2	Methodology and Preliminary Results Related to Conjecture VI.4	147
6.1.3	Methodology and Preliminary Results Related to Conjecture VI.5	151
6.2	Numerical Analysis for the Stability of the Traveling Wave Solution of the Cubic BO Equation and the Limited Area Model	156
6.2.1	Instability of the Traveling Wave Solutions of the Cubic BO Equation	157
6.2.2	Limited Area Model	157
APPENDICES		158
BIBLIOGRAPHY		171

LIST OF FIGURES

Figure

1.1	The evolution of a pulse under the BO equation. Top row: $\epsilon = 0.04$. Bottom row: $\epsilon = 0.02$. In both cases the initial condition is the same: $u_0(x) = 2(1 + x^2)^{-1}$	4
3.1	The graph of an admissible initial condition and the turning points $x_{\pm}(\lambda)$	44
3.2	Except along the caustic curves $x = x_{\xi}^{-}(t)$ and $x = x_{\xi}^{+}(t)$ the number of solutions of (3.34) is of the form $2P + 1$, and these solutions are simple roots. For this figure, $u_0(x) := 2(1 + x^2)^{-1}$	52
3.3	The multivalued solution (black) of (3.33) and the signed sum of branches (red) corresponding to $u_0(x) = 2(1 + x^2)^{-1}$. Left: $t = 0$. Middle: $t = 1$. Right: $t = 2$. Before the breaking time as well as afterwards but outside the oscillation interval there is only one solution branch and hence no difference between the red and black curves.	52
3.4	Histograms of eigenvalues of $\tilde{\mathbf{A}}_{\epsilon}$ corresponding to the initial condition $u_0(x) := 2(1 + x^2)^{-1}$, $x = 5$, and $t = 2$, normalized to have total area $M = 1$, compared with the density $G(\alpha; x, t)$ of the limiting absolutely continuous measure μ	55
3.5	The region of integration $-2\lambda(x + 2\lambda t - x_+(\lambda)) < \alpha < -2\lambda(x + 2\lambda t - x_-(\lambda))$ for $u_0(x) = 2(1 + x^2)^{-1}$ with $t = 0.7$. Left: $x = 2$ (to the left of the oscillatory region for $u_{\epsilon}(x, t)$). Center: $x = 2.5$ (within the oscillatory region for $u_{\epsilon}(x, t)$). Right: $x = 3$ (to the right of the oscillatory region for $u_{\epsilon}(x, t)$). The line $\alpha = 0$ of discontinuity of the integrand is superimposed, and the intersections of the boundary with this line are indicated with arrows.	58
3.6	The square $[-L, 0]^2$ in the (κ, λ) -plane is covered by the six regions $S_D, S_{OD}, B_D, B_{OD}, H_D$, and H_{OD}	78

3.7	The graphs of $a_-(\alpha) < a_+(\alpha)$ (black) and several graphs of $2 \arctan(\epsilon^{-1}\alpha)$ for $\epsilon \leq 1$ (gray).	82
3.8	Left: plots of $\tilde{U}_\epsilon(x, t)$ (black) and its locally uniform limit $U(x, t)$ (red) at $t = 4$ for various values of ϵ . For these plots, $u_0(x) := 2(1 + x^2)^{-1}$. Right: corresponding plots of the error $U(x, t) - \tilde{U}_\epsilon(x, t)$	94
3.9	Circles: $\log_{10}(\ \tilde{U}_\epsilon(\cdot, 4) - U(\cdot, 4)\ _\infty)$ for $\epsilon = 1/25, 1/30, 1/35, 1/40, 1/45, 1/50,$ and $1/100$, as a function of $\log_{10}(\epsilon)$. In red: The least-squares linear fit.	95
3.10	Left: plots of $\tilde{u}_\epsilon(x, t)$ (black) shown together with $u_\epsilon(x, t)$ (red) for the initial data $u_0(x) = 2(1 + x^2)^{-1}$ shown for several values of ϵ at $t = 4$. Right: The error $u_\epsilon(x, t) - \tilde{u}_\epsilon(x, t)$	96
5.1	The graphs of the Higgins functions $CH_4(x)$ (blue) and $SH_3(x)$ (red) with $L = 1$	109
5.2	The graphs of the Christov functions $CC_4(x)$ (blue) and $SC_5(x)$ (red) with $L = 1$	110
5.3	The graphs of the rational Chebyshev functions $TB_2(x)$ (blue) and $UB_2(x)$ (red) with $L = 1$	111
5.4	Comparison of the errors in $t \in [0, 5]$ using the Christov method to solve the BO equation with different choices of the parameter L and the number of the grid points N . Here the initial condition is $u(x, 0) = 2/(x^2 + 1)$ and the exact solution is $u(x, t) = 2/((x - t)^2 + 1)$	115
5.5	The CFL limit of the linear BO equation for the Fourier method, the RBF method and the Christov method.	121
5.6	The benchmark case used to demonstrate aliasing instability in the BO equation. With 256 grids points, a timestep of $\delta t = 0.004$ is stable. The initial condition evolves into three solitons on the periodic domain $x \in [-5\pi, 5\pi]$	123
5.7	Canonical run but with $n = 512$ grid points and a timestep of $1/1000$. The Fourier coefficients are plotted every one-fifth in t with the lowest curve showing the initial curve; the slope monotonically decreases with time.	124

5.8	Canonical run but with $n = 128$ grid points and a timestep of $1/250$. The Fourier coefficients are plotted every one-tenth in t with the lowest curve showing the initial curve; the slope monotonically decreases with time. At the final time, the error in physical space is 5000% (not illustrated on this graph).	125
5.9	Canonical run but with $n = 128$ grid points and a timestep of $1/250$. $u(x, t)$ are plotted every one-tenth in t ; the slope monotonically decreases with time. The flow blows up catastrophically with overflow between $t = 3.4$ and $t = 3.5$	126
5.10	Comparison of the exact benchmark solution at $t = 10$ with the solution as computed using Orszag-Phillips dealiasing with resolutions of $N = 32$, $N = 64$ and $N = 128$ grid points. In each frame, the true solution is shown as the dashed curve; the solid curve with the circles is the lower resolution dealiased approximation. The lower right shows the $N = 128$ grid point solution without dealiasing: there is no graph because the aliased computation is unstable and overflows to Not-a-Number (NaN) at every grid point. This difficulty cannot be fixed by shortening the timestep.	127
5.11	Waterfall plot using the Fourier pseudospectral method to solve the BO equation with $N = 512$ grid points and a timestep of $1/50000$. $u(x, t)$ plotted every one-tenth in t . The initial condition of $u(x, t)$ is $u(x, 0) = 2/(x^2 + 1)$ for $x \in [-\pi, \pi]$ and $u(x, 0) = u(x + 2\pi, 0)$ for all $x \in \mathbb{R}$	128
5.12	Waterfall plot using the Christov method to solve the BO equation with $N = 128$ grid points and a timestep of $1/1000$. $u(x, t)$ plotted every one-fourth in t . The initial condition of $u(x, t)$ is $u(x, 0) = 2/(x^2 + 1)$	129
5.13	Waterfall plot using the RBF method to solve the BO equation with $N = 256$ grid points and a timestep of $1/5000$. $u(x, t)$ plotted every two-tenth in t . The initial condition of $u(x, t)$ is $u(x, 0) = 2/(x^2 + 1)$	130
5.14	The red curve is the right hand side of the equation (5.66) and the blue curve is the left hand side of the equation (5.66) with $\epsilon = 0.05$. The initial condition used in the calculation is $u(x, 0) = 2/(x^2 + 1)$	134
5.15	The red curve is the right hand side of the equation (5.66) and the blue curve is the left hand side of the equation (5.66) with $\epsilon = 0.05$. The initial condition used in the calculation is $u(x, 0) = 2/(x^2 + 1)$	135

5.16	The red curve is the right hand side of the equation (5.66) and the blue curve is the left hand side of the equation (5.66) with $\epsilon = 0.05$. The initial condition used in the calculation is $u(x, 0) = 2/(x^2 + 1)$	135
5.17	Comparison of the errors of different methods for the cubic BO equation	141
6.1	Left: the curve Γ^s corresponding to x and t satisfying $x + 2Lt < x_0$ Right: the curve Γ^s corresponding to x and t satisfying $x + 2Lt > x_0$	148
6.2	The graph of the curve Γ^M	151
6.3	The graph of the curves Γ^m and $\bar{\Gamma}^m$	154
A.1	Two-layer Fluid	159

LIST OF TABLES

Table

5.1	Formulas for the CFL limit of the linear BO equation. The number W in the formulas is the width of the domain and L is a parameter in the Christov method.	122
5.2	Comparison of Numerical Methods	132
5.3	Error of small dispersion limit calculation. The initial condition of $u(x, t)$ is $u(x, 0) = (\cos x + 1)/2$	133
5.4	Maximum of δ such that $0 < \delta \leq 1$ and by using the solution we obtained as the first guess, Newton's method for the equation (5.85) will converge	140

LIST OF APPENDICES

Appendix

A.	Derivation of the BO Equation	159
B.	Proof of an Integral Identity	168

CHAPTER I

Introduction

Nonlinear evolution equations as mathematical models are widely used in almost all science disciplines. For most of nonlinear evolution equations, it is very difficult to find exact solutions and there is no general solution available in close form. However, there are some theoretical methods available to study some nonlinear evolution equations with special properties. For example, the inverse scattering transform can be used to investigate integrable evolution equations. Here, the integrable evolution equations are evolution equations that have a Lax pair developed by Lax [42]. The Lax pair of an integrable evolution equation is a pair of linear equations, whose compatibility condition is this integrable evolution equation. The inverse scattering transform based on the Lax pair is a very powerful tool to find exact solutions (soliton solutions) and analyze the Cauchy problem of integrable evolution equations. With the use of the Lax pair, instead of solving a nonlinear evolution equation, one deals with two linear equations and one of them is a single variable equation, which is easier to solve. Among integrable evolution equations, the Korteweg-de Vries (KdV) equation and the nonlinear Schrödinger (NLS) equation are most famous and well-studied. They can be derived from various physical phenomena. In this dissertation,

we study another integrable evolution equation, the Benjamin-Ono (BO) equation

$$(1.1) \quad u_t + 2uu_x + \epsilon \mathcal{H}(u_{xx}) = 0,$$

where ϵ is a constant and \mathcal{H} is the Hilbert transform defined by

$$(1.2) \quad (\mathcal{H}f)(x) := \frac{1}{\pi} \int_{-\infty}^{\infty} \frac{f(y)}{y-x} dy.$$

It arises in modeling internal gravity waves in deep water [5, 18, 59, 12] (see Appendix A for details). It also describes “morning glory cloud” in Northeastern Australia [64]. The Lax pair of the BO equation was discovered by Nakamura [57], Bock and Kruskal [6]. By using the Lax pair, Fokas, Ablowitz, Anderson [2, 25] introduced the inverse scattering transform of the BO equation. They investigated the solutions of the single variable equation in the Lax pair with four different boundary conditions and introduced the scattering data that characterize the relation among these solutions. The time evolution of the scattering data was derived from the other equation in the Lax pair. Fokas, Ablowitz, Anderson also studied the inverse scattering problem, which is to calculate solutions of the BO equation by using the known scattering data. Soliton solutions of the BO equation corresponding to reflectionless scattering data were obtained by solving the inverse scattering problem. Later, Kaup and Matsuno [39] analyzed the conservation laws of the BO equation and the asymptotic behavior of the scattering data. With the real initial condition assumption, they also proved two identities of the scattering data.

In this dissertation, theoretical methods (Chapter II-IV) and numerical methods (Chapter V) are used to investigate the BO equation. First, we review the inverse scattering transform of the BO equation and fill in many mathematical details and mathematical gaps to make it easy to understand. Next, we study the zero dispersion limit of the BO equation and its generalizations in Chapter III and IV

respectively. The contents of Chapter III and the proof of an identity in Appendix B were published in [56] and the contents of Chapter IV will be published in the future. In Chapter V, we use numerical methods to investigate the BO equation and the contents of this chapter will be published in the future. Moreover, we review the derivation of the BO equation and fill in some mathematical details in Appendix A and some new ideas to analyze the BO equation are provided in Chapter VI. To be more precise, first let us talk about the zero dispersion limit.

1.1 Zero Dispersion Limit of the BO Equation

The parameter $\epsilon > 0$ represents the relation between the nonlinear and dispersive effects in the BO equation (1.1). The dispersive effect is dominant in the system if the parameter ϵ is very large. In this case, a solution of the BO equation can be approximated by a solution of the linear BO equation with the same initial condition. On the other hand, if the parameter ϵ is very small, then the nonlinear effect becomes the dominant effect. One may expect a solution of the BO equation can be approximated by a solution of the inviscid Burgers equation (obtained by choosing $\epsilon = 0$ in (1.1)) with the same initial condition. This conjecture holds true only for $t < T$ (see Corollary III.6) because of the formation of a shock wave in the inviscid Burgers equation in finite time T . What happens to the solutions of the BO equation after that time is a very interesting question. For the KdV equation, the small dispersion term forces the shock wave to become approximately periodic traveling waves [43, 44, 45]. This phenomenon also appears in the solutions of the BO equation for small ϵ (see Figure 1.1). Here, Figure 1.1 is taken from [56]. This interesting phenomenon can be analyzed by studying the zero dispersion limit, where the zero dispersion limit is the limit of the solution of the Cauchy problem with ϵ -independent

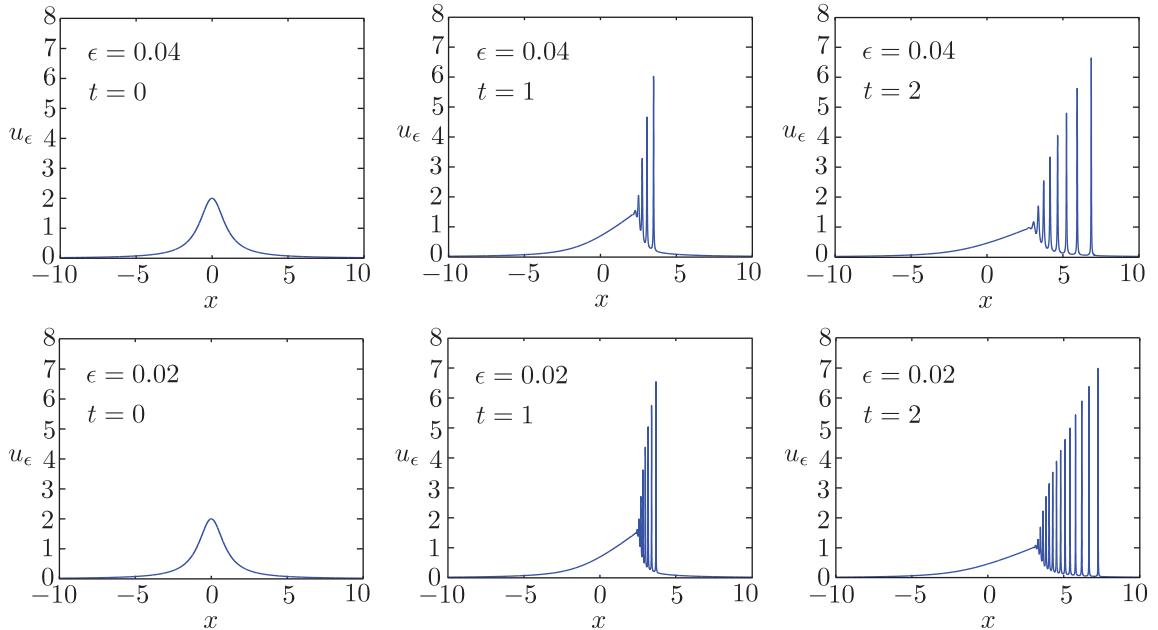


Figure 1.1: The evolution of a pulse under the BO equation. Top row: $\epsilon = 0.04$. Bottom row: $\epsilon = 0.02$. In both cases the initial condition is the same: $u_0(x) = 2(1 + x^2)^{-1}$.

initial condition $u_0(x)$ as $\epsilon \downarrow 0$. Before we talk about the history of the zero dispersion limit of the BO equation, let us first review that of the KdV equation. The KdV equation [41]

$$(1.3) \quad u_t + 2uu_x + \frac{1}{3}\epsilon^2 u_{xxx} = 0,$$

where ϵ is a constant, has very wide applications in various areas. The KdV equation describes shallow-water waves with weakly non-linear restoring forces, long internal waves in a density-stratified ocean, ion-acoustic waves in a plasma and acoustic waves on a crystal lattice, etc. The inverse scattering transform of the KdV equation introduced by Gardner, Greene, Kruskal and Miura [29, 30] is widely used to investigate the KdV equation. Especially, the inverse scattering transform provides a simple way to construct soliton solutions of the KdV equation. On the other hand, the formula for the N -soliton solutions of the KdV equation can be obtained via a bilinear

method introduced by Hirota [36]. This formula was used by Lax and Levermore [43, 44, 45] to analyze the zero-dispersion limit of the KdV equation with negative initial conditions. They approximated the solutions of the KdV equation with negative initial conditions by N -soliton solutions, which can be written in terms of the determinant of a huge matrix. Lax and Levermore analyzed the asymptotic behavior of the dominant part of the determinant and obtained a method to calculate the weak zero dispersion limit of the KdV equation.

The zero-dispersion limit of the BO equation was studied by Matsuno [52, 53], Jorge, Minzoni, and Smyth [38]. They assumed that the approximately periodic traveling waves can be modeled by the formula of periodic solutions of the BO equation where the parameters in the formula varies very slowly for small ϵ . Based on this conjecture, they estimate the zero dispersion limit of the BO equation via an analogue of the method developed by Gurevich and Pitaevskii [32] to study that of the KdV equation. In [52], Matsuno wrote:

From a rigorously mathematical point of view, however, the various results presented in this paper should be justified on the basis of an exact method of solution such as [the inverse-scattering transform], or an analog of the Lax-Levermore theory for the KdV equation.

In Chapter III, such a rigorous proof is provide. Similarly as the Lax-Levermore method, we approximate the solutions of the BO equation with admissible initial conditions by N -soliton solutions. The bilinear method applied to the KdV equation can also be used to the BO equation to construct N -soliton solutions, which was done by Matsuno [48]. These N -soliton solutions can also be written in terms of the determinant of a huge matrix. Instead of analyzing the determinant, we investigate the eigenvalues of this huge matrix to calculate the weak zero dispersion limit of the

BO equation. The most surprising result about the zero-dispersion limit of the BO equation is that the weak zero-dispersion limit can be simply written in terms of the multivalued solution of the inviscid Burgers equation with the same initial condition (see Theorem III.5 for details).

1.2 Numerical Methods

Compared to the other evolution equations, analyzing the Cauchy problem of the BO equation numerically is more challenging due to the presence of the Hilbert transform. The Hilbert transform in the BO equation is an integral operator, which is essentially nonlocal. To evaluate the Hilbert transform of a function at one point requires knowledge of the function at every other point. Thus if one discretizes the computational domain, one needs to use the values of the approximate solution at all of the grid points just to compute its Hilbert transform evaluated at only one grid point. To avoid this difficulty, spectral methods in which the Hilbert transforms of the basis functions are simple are used. This idea was used by Thomee, Vasudeva, Murthy [67], James and Weideman [37] to numerically study the BO equation. In this dissertation, we make a comparison of three different numerical methods and use one of these methods to illustrate and verify our results of the zero dispersion limit of the BO equation.

1.3 Outline of Thesis

In Chapter II, we review the inverse scattering transform of the BO equation in detail by comparing to that of the KdV equation. To provide a better understanding of the inverse scattering transform, the calculation of an example is given to illustrate the method to calculate the scattering data of the BO equation. In Chapter III, the

zero-dispersion limit of the Cauchy problem of the BO equation is studied via an analogue of the Lax-Levermore method. Moreover, some generalizations of these results are given in Chapter IV. In Chapter V, three different numerical methods: the Fourier pseudospectral method, the Radial Basis Function (RBF) method and the Christov method are described to solve the Cauchy problem of the BO equation in infinite spatial domains. Furthermore, a comparison of these three methods is made and the numerical illustrations of the theoretical results are given. Finally, some discussion about the future work is provided in Chapter VI.

1.4 Notation

In this dissertation, we use capital and lowercase letters in bold font to represent matrixes and vectors respectively. If $n(\lambda)$ is a function defined on the complex λ -plane, we use $n_+(\lambda)$ ($n_-(\lambda)$) for $\lambda \in \mathbb{R}$ to represent the boundary value of $n(\lambda)$ taken from the upper (lower) half λ -plane.

CHAPTER II

The Inverse-Scattering Transform for Integrable Evolution Equations

In this chapter, we first introduce the inverse scattering transform of the KdV equation and then we discuss the inverse scattering transform of the BO equation in detail. For those who are familiar with the inverse scattering transform of the KdV equation, the inverse scattering transform of the BO equation will become easier to understand by comparing with that of the KdV equation.

2.1 The Inverse-Scattering Transform for the KdV Equation

The Lax pair of the KdV equation [42] is

$$(2.1) \quad \epsilon^2 \psi_{xx} + \frac{1}{3} u \psi = -k^2 \psi$$

$$(2.2) \quad \epsilon \psi_t = (\epsilon u_x + \rho) \psi - \epsilon \left(\frac{2}{3} u - 4k^2 \right) \psi_x$$

where ρ is a constant and k is a complex spectral parameter. By letting $\lambda = k^2$, the equation (2.1) can be viewed as an eigenvalue problem for the Schrödinger operator $-\epsilon^2 \frac{d^2}{dx^2} - u/3$, where λ is the spectral parameter. If u is a real function, the Schrödinger operator is a self-adjoint operator on $L^2(\mathbb{R})$ and its continuous spectrum is \mathbb{R}^+ .

2.1.1 The Direct Scattering Problem

The equation (2.1) is a second order ordinary differential equation (ODE). By assuming the potential u lies in $L^2(\mathbb{R})$, one can find that if k is a real number, any solution of the equation (2.1) tends to $C_1 e^{ikx/\epsilon} + C_2 e^{-ikx/\epsilon}$ as $x \rightarrow \pm\infty$, where C_1 and C_2 are constants. Let $\phi(x; k)$, $\psi(x; k)$, $\bar{\phi}(x; k)$ and $\bar{\psi}(x; k)$ to be the solutions of (2.1) with the boundary conditions:

$$(2.3) \quad \phi(x; k) = e^{-ikx/\epsilon}(1 + o(1)), \quad \bar{\phi}(x; k) = e^{ikx/\epsilon}(1 + o(1)), \quad \text{as } x \rightarrow -\infty,$$

$$(2.4) \quad \psi(x; k) = e^{ikx/\epsilon}(1 + o(1)), \quad \bar{\psi}(x; k) = e^{-ikx/\epsilon}(1 + o(1)), \quad \text{as } x \rightarrow \infty,$$

where $k \in \mathbb{R}$. Then the functions $\phi(x; k)$, $\psi(x; k)$, $\bar{\phi}(x; k)$ and $\bar{\psi}(x; k)$ satisfy the following Volterra type integral equations [1]:

$$(2.5) \quad \phi(x; k) = e^{-ikx/\epsilon} - \frac{1}{3\epsilon} \int_{-\infty}^x \frac{\sin(k(x-y)/\epsilon)}{k} u(y) \phi(y; k) dy,$$

$$(2.6) \quad \bar{\phi}(x; k) = e^{ikx/\epsilon} - \frac{1}{3\epsilon} \int_{-\infty}^x \frac{\sin(k(x-y)/\epsilon)}{k} u(y) \bar{\phi}(y; k) dy,$$

$$(2.7) \quad \psi(x; k) = e^{ikx/\epsilon} + \frac{1}{3\epsilon} \int_x^{\infty} \frac{\sin(k(x-y)/\epsilon)}{k} u(y) \psi(y; k) dy,$$

$$(2.8) \quad \bar{\psi}(x; k) = e^{-ikx/\epsilon} + \frac{1}{3\epsilon} \int_x^{\infty} \frac{\sin(k(x-y)/\epsilon)}{k} u(y) \bar{\psi}(y; k) dy.$$

Here, each of these Volterra type integral equations (2.5)-(2.8) has a unique solution.

The functions $\psi(x; k)$ and $\bar{\psi}(x; k)$ are linearly independent of each other if the real

number $k \neq 0$, because the Wronskian

$$(2.9) \quad W[\psi, \bar{\psi}] = \psi_x \bar{\psi} - \psi \bar{\psi}_x = 2ik \neq 0.$$

Since the equation (2.1) is a second order ODE, any solution of the equation (2.1) can be written as a linear combination of $\psi(x; k)$ and $\bar{\psi}(x; k)$. This fact implies that there exist $a(k)$, $b(k)$, $\bar{a}(k)$ and $\bar{b}(k)$ such that

$$(2.10) \quad \phi(x; k) = a(k)\bar{\psi}(x; k) + b(k)\psi(x; k); \quad \bar{\phi}(x; k) = \bar{a}(k)\psi(x; k) + \bar{b}(k)\bar{\psi}(x; k),$$

where $\bar{a}(k) = -a^*(k)$ and $\bar{b}(k) = b^*(k)$. The functions $\phi(x; k)$ and $\psi(x; k)$ have analytic extensions to the upper half complex k -plane and $\bar{\phi}(x; k)$ and $\bar{\psi}(x; k)$ have analytic extensions to the lower half complex k -plane. A complex number k_n is defined to be an eigenvalue, if k_n satisfies $a(k_n) = 0$. In fact, $\lambda_n = k_n^2$ is an eigenvalue of the eigenvalue problem (2.1) for the Schrödinger operator. A complex number c_n is defined to be the norming constant corresponding to the eigenvalue k_n , if c_n satisfies

$$(2.11) \quad v_n \sim c_n e^{ik_n x/\epsilon}, \quad \text{as } x \rightarrow \infty,$$

where v_n is the eigenfunction of the eigenvalue problem (2.1) for the Schrödinger operator corresponding to $\lambda_n = k_n^2$ and satisfies

$$(2.12) \quad \int_{-\infty}^{\infty} v_n^2 dx = 1.$$

Since the Schrödinger operator is a self-adjoint on operator $L^2(\mathbb{R})$ and its continuous spectrum is \mathbb{R}^+ , the eigenvalue λ_n has to be a negative number, which implies k_n is a purely imaginary number and if k_n is an eigenvalue, the complex conjugate k_n^* is also an eigenvalue. In fact, the norming constant corresponding to k_n^* is the complex conjugate of c_n . So we will use k_n and k_n^* to represent the eigenvalues in the rest of this section, where imaginary part of k_n is positive and that of k_n^* is negative.

Here the functions $a(k, t)$ and $r(k, t) = b(k, t)/a(k, t)$ and the constants $\{k_n\}_{n=1}^N$, $\{k_n^*\}_{n=1}^N$, $\{c_n\}_{n=1}^N$ and $\{c_n^*\}_{n=1}^N$ are called the “scattering data”.

2.1.2 Time Dependence of the Scattering Data

The time evolution of the scattering data for the KdV equation is given by

$$(2.13) \quad k_n(t) = k_n(0), \quad c_n(t) = c_n(0)e^{4k_n^3 t/\epsilon^3},$$

$$(2.14) \quad a(k, t) = a(k, 0), \quad r(k, t) = r(k, 0)e^{8ik^3 t/\epsilon^3}.$$

2.1.3 The Inverse Scattering Problem

If the scattering data are given, one can construct a Gel’fand-Levitan-Marchenko equation [1]:

$$(2.15) \quad K(x, y) + F(x + y) + \int_x^\infty K(x, s)F(s + y)da = 0, \quad y \geq x,$$

where

$$(2.16) \quad F(x) = \frac{1}{2\pi} \int_{-\infty}^\infty r(k, t)e^{ikx/\epsilon} dk + \sum_{n=1}^N (c_n^2(t)e^{-ik_n x/\epsilon} + (c_n^*)^2(t)e^{-ik_n^* x/\epsilon}).$$

The potential $u(x, t)$ can be calculated by solving the equation (2.15) and using the relation between the potential $u(x, t)$ and the function $K(x, y)$:

$$(2.17) \quad u(x, t) = -2\epsilon \frac{\partial}{\partial x} K(x, x).$$

This calculation can also be done by solving a Riemann-Hilbert Problem.

2.1.4 The Riemann-Hilbert Problem

According to the properties of $\phi(x; k)$, $\psi(x; k)$, $\bar{\phi}(x; k)$ and $\bar{\psi}(x; k)$ discussed in §2.1.1, one can find that the row vector function $\mathbf{m}(k; x, t) = (m_1(k; x, t), m_2(k; x, t))$, where

$$(2.18) \quad m_1(k; x, t) = \frac{\phi e^{ikx/\epsilon}}{a(k)} \quad \text{and} \quad m_2(k; x, t) = \psi e^{-ikx/\epsilon} \quad \text{for} \quad \Im(k) > 0,$$

$$(2.19) \quad m_1(k; x, t) = \frac{\bar{\phi}e^{-ikx/\epsilon}}{-\bar{a}(k)} \quad \text{and} \quad m_2(k; x, t) = \bar{\psi}e^{ikx/\epsilon} \quad \text{for} \quad \Im(k) < 0,$$

satisfies the following Riemann–Hilbert Problem.

Riemann-Hilbert problem II.1.

Analyticity: $\mathbf{m}(k)$ is analytic in $\mathbb{C} \setminus (\mathbb{R} \cup \{k_1, k_2, \dots, k_n\})$

Residue condition:

$$(2.20) \quad \text{Res}_{k=k_j} \mathbf{m}(k) = \lim_{k \rightarrow k_j} \mathbf{m}(k) \begin{bmatrix} 0 & 0 \\ -ic_n(t)e^{2ik_n x/\epsilon} & 0 \end{bmatrix},$$

$$(2.21) \quad \text{Res}_{k=k_j^*} \mathbf{m}(k) = \lim_{k \rightarrow k_j^*} \mathbf{m}(k) \begin{bmatrix} 0 & ic_n^*(t)e^{-2ik_n^* x/\epsilon} \\ 0 & 0 \end{bmatrix},$$

Jump conditions: The boundary values taken on \mathbb{R} satisfy: $\mathbf{m}_+(k) = \mathbf{m}_-(k)\mathbf{v}_{x,t}(k)$

for $k \in \mathbb{R}$, where

$$(2.22) \quad \mathbf{v}_{x,t} = \begin{bmatrix} 1 - |r(k, t)|^2 & -r^*(k, t)e^{-2ikx} \\ r(k, t)e^{2ikx} & 1 \end{bmatrix}$$

Normalization: $\mathbf{m}(k)$ is normalized at infinity:

$$(2.23) \quad \mathbf{m}(k) \rightarrow (1, 1) \quad \text{as} \quad k \rightarrow \infty.$$

The potential $u(x, t)$ can be evaluated by solving Riemann-Hilbert Problem II.1 and using the relation between $u(x, t)$ and $\mathbf{m}(k)$:

$$(2.24) \quad u(x, t) = -2i\epsilon \frac{\partial}{\partial x} m_{11}(x, t),$$

where

$$(2.25) \quad m_{11} = \lim_{k \rightarrow \infty} k(m_1 - 1).$$

2.2 The Inverse-Scattering Transform for the BO Equation

The Lax pair of the BO equation [6, 57] is

$$(2.26) \quad i\epsilon w_x^+ + \lambda(w^+ - w^-) = -uw^+$$

$$(2.27) \quad iw_t^\pm - 2i\lambda w_x^\pm + \epsilon w_{xx}^\pm - 2i\mathcal{C}_\pm(u_x)w^\pm = -\rho w^\pm$$

where ρ is a constant and \mathcal{C}_\pm are the Cauchy operators defined by

$$(2.28) \quad \mathcal{C}_\pm(u) = \pm \frac{1}{2}u - \frac{1}{2}i\mathcal{H}(u).$$

In fact, the Cauchy operators \mathcal{C}_\pm can be equivalently defined as

$$(2.29) \quad \mathcal{C}_\pm(u)(x) = \lim_{\delta \downarrow 0} \left(\frac{1}{2\pi i} \int_{-\infty}^{\infty} \frac{u(y)}{y - (x \pm \delta i)} dy \right).$$

The constant ρ will be determined later to match the boundary conditions. Here, the functions $w^\pm(x)$ represent the boundary values of a function which is analytic in the upper (+) and lower (-) half x -plane. In this section, we introduce the inverse scattering transform of the BO equation, most of which was discussed by Fokas and Ablowitz in [25]. We also introduce some results given by Kaup and Matsuno [39, 49, 50]. Moreover, we fill in some mathematical details and mathematical gaps in this section to consummate the theory and make it easy to understand. Before talking about that, we discuss the definitions of the Cauchy operators \mathcal{C}_\pm and the Hilbert transform \mathcal{H} and introduce the definition of the Hardy space and some basic properties of the Cauchy operators \mathcal{C}_\pm , which will be used later. The Hilbert transform \mathcal{H} and the Cauchy operators \mathcal{C}_\pm are operators on $L^2(\mathbb{R})$. The Hilbert transform is defined in terms of a principal value integral by (1.2) where the principal value integral is defined by

$$(2.30) \quad \int_{-\infty}^{\infty} \frac{f(y)}{y - x} dy = \lim_{\delta \downarrow 0} \left(\int_{-\infty}^{x-\delta} \frac{f(y)}{y - x} dy + \int_{x+\delta}^{\infty} \frac{f(y)}{y - x} dy \right).$$

To provide a better understanding of two equivalent definitions of the Cauchy operators, we calculate the function $\mathcal{C}_+(u)(x)$ via two different definitions, where $u(x) = 1/(x^2 + 1)$. First we use the equation (2.29) to calculate $\mathcal{C}_+(u)(x)$. By adding an integral on a contour on the upper half complex plane connecting ∞ and $-\infty$ to the right hand side of the equation (2.29), one can obtain an integral on a closed contour. After applying Cauchy residue theorem to the right hand side of the equation (2.29) and letting the contour on the upper half plane go to ∞ , one can find that the integral on the contour on the upper half plane vanishes and that

$$(2.31) \quad \begin{aligned} \mathcal{C}_+(u)(x) &= -\lim_{\delta \downarrow 0} \left(\text{Res}_{y=-i} \left[\frac{1}{(y - (x + \delta i))(y^2 + 1)} \right] \right) \\ &= \frac{i}{2(x + i)}. \end{aligned}$$

One the other hand, we first calculate $\mathcal{H}(u)(x)$. Since

$$(2.32) \quad \begin{aligned} \frac{1}{(y-x)(y^2+1)} &= \frac{1}{x^2+1} \left(\frac{1+xy}{(y-x)(y^2+1)} - \frac{x}{y^2+1} \right) \\ &= \frac{1}{x^2+1} \left(\frac{1}{y-x} - \frac{y}{y^2+1} - \frac{x}{y^2+1} \right), \end{aligned}$$

then the function $\mathcal{H}(u)(x)$ can be written as

$$(2.33) \quad \mathcal{H}(u)(x) = \frac{1}{\pi(x^2+1)} \int_{-\infty}^{\infty} \frac{1+xy}{(y-x)(y^2+1)} dy - \frac{x}{\pi(x^2+1)} \left(\int_{-\infty}^{\infty} \frac{1}{y^2+1} dy \right).$$

The first integral on the right hand side of the equation (2.33) vanishes based on the following calculation.

$$(2.34) \quad \begin{aligned} \int_{-\infty}^{\infty} \frac{(1+xy)dy}{(y-x)(y^2+1)} &= \lim_{L \rightarrow \infty} \left(\lim_{\delta \downarrow 0} \left(\int_{-L}^{x-\delta} \frac{(1+xy)dy}{(y-x)(y^2+1)} + \int_{x+\delta}^L \frac{(1+xy)dy}{(y-x)(y^2+1)} \right) \right) \\ &= \lim_{L \rightarrow \infty} \left(\lim_{\delta \downarrow 0} \left(\int_{-L}^{x-\delta} \left(\frac{1}{y-x} - \frac{y}{y^2+1} \right) dy \right) \right) \\ &\quad + \lim_{L \rightarrow \infty} \left(\lim_{\delta \downarrow 0} \left(\int_{x+\delta}^L \left(\frac{1}{y-x} - \frac{y}{y^2+1} \right) dy \right) \right). \end{aligned}$$

The fact that $y/(y^2 + 1)$ is an odd function tells us that

$$\begin{aligned}
 \int_{-\infty}^{\infty} \frac{(1 + xy)dy}{(y - x)(y^2 + 1)} &= \lim_{L \rightarrow \infty} \left(\lim_{\delta \downarrow 0} \left(\int_{-L}^{x-\delta} \frac{1}{y - x} dy + \int_{x+\delta}^L \frac{1}{y - x} dy \right) \right) \\
 (2.35) \qquad \qquad \qquad &= \lim_{L \rightarrow \infty} \left(\log \left(\frac{|L - x|}{|L + x|} \right) \right) \\
 &= 0.
 \end{aligned}$$

Therefore, one can obtain

$$\begin{aligned}
 \mathcal{H}(u)(x) &= -\frac{x}{\pi(x^2 + 1)} \left(\int_{-\infty}^{\infty} \frac{1}{y^2 + 1} dy \right) \\
 (2.36) \qquad \qquad \qquad &= -\frac{x}{x^2 + 1}.
 \end{aligned}$$

Then it is easy to see that

$$(2.37) \qquad \qquad \qquad \mathcal{C}_+(u)(x) = \frac{1}{2}u(x) - \frac{1}{2}i\mathcal{H}(u)(x) = \frac{i}{2(x + i)}.$$

The above calculation verifies the fact these two definitions of the Cauchy operator are equivalent. Next, we introduce the definition of the Hardy space and some basic properties of the Cauchy operators \mathcal{C}_{\pm} .

Definition II.2. The Hardy space \mathbb{H}^+ (\mathbb{H}^-) on the upper half-plane (lower half-plane) is defined to be the space of holomorphic functions f on the upper half-plane (lower half-plane) with bounded norm given by

$$(2.38) \qquad \qquad \qquad \|f\|_{\mathbb{H}^{\pm}} = \sup_{y \in \mathbb{R}^{\pm}} \left[\int_{\mathbb{R}} |f(x + iy)|^2 dx \right]^{1/2}.$$

The most well-known property of the Cauchy operators is the Plemelj formula (2.39) [19, 73, 26] in the following theorem. In fact, the Cauchy operator \mathcal{C}_{\pm} are orthogonal and complementary projections onto the Hardy spaces \mathbb{H}^{\pm} respectively [73, 26]. This fact implies the first two statements in Theorem II.3 and the identities (2.40) and (2.41).

Theorem II.3. [19, 73, 26] For any function $f \in L^2(\mathbb{R})$, the function $\mathcal{C}_+(f)$ ($\mathcal{C}_-(f)$) belongs to \mathbb{H}^+ (\mathbb{H}^-). On the other hand, if $g \in \mathbb{H}^+$ (\mathbb{H}^-), then there exists a function $f \in L^2(\mathbb{R})$ such that $g = \mathcal{C}_+(f)$ ($g = \mathcal{C}_-(f)$). Moreover, for any functions $f, q \in L^2$, the following identities hold true:

$$(2.39) \quad \mathcal{C}_+(f) - \mathcal{C}_-(f) = f,$$

$$(2.40) \quad \mathcal{C}_+(\mathcal{C}_-(f)) = \mathcal{C}_-(\mathcal{C}_+(f)) = 0,$$

$$(2.41) \quad \mathcal{C}_\pm(\mathcal{C}_\pm(f)) = \mathcal{C}_\pm(f),$$

$$(2.42) \quad \int_{-\infty}^{\infty} \mathcal{C}_\pm(f)(x)\mathcal{C}_\pm(q)(x)dx = 0,$$

$$(2.43) \quad \int_{-\infty}^{\infty} \mathcal{C}_+(f)(x)q(x)dx = - \int_{-\infty}^{\infty} f(x)\mathcal{C}_-(q)(x)dx.$$

Here, the identities (2.42) and (2.43) can be directly obtained from an alternative interpretation of the Cauchy operators (see the identity (2.2) in [26]).

2.2.1 The Direct Scattering Problem

In §2.1, the first equation in the Lax pair can be written as an eigenvalue problem. Here, this fact also holds true. If $w^\pm \in \mathbb{H}^\pm$, by applying the Cauchy operator \mathcal{C}_+ to each side of the equation (2.26) and using (2.40) and (2.41), the equation (2.26) becomes

$$(2.44) \quad i\epsilon w_x^+ + \lambda w^+ = -\mathcal{C}_+(uw^+).$$

Then after using the fact $w^+ = \mathcal{C}_+(w^+)$, one can write (2.44) in the form

$$(2.45) \quad \mathcal{L}w^+ = \lambda w^+,$$

where the operator \mathcal{L} is defined by:

$$(2.46) \quad \mathcal{L} := -i\epsilon \frac{d}{dx} - \mathcal{C}_+ u \mathcal{C}_+.$$

This is an eigenvalue problem of the operator \mathcal{L} . If u is a real function, the operator \mathcal{L} is an essentially self-adjoint operator on \mathbb{H}^+ and its continuous spectrum is \mathbb{R}^+ .

For $\lambda \in \mathbb{R}$, if w^\pm are bounded, then $uw^\pm \in L^2(\mathbb{R})$. The identity (2.39) implies that $uw^\pm = \mathcal{C}_+(uw^\pm) - \mathcal{C}_-(uw^\pm)$. Then the equation (2.26) can be written as:

$$(2.47) \quad i\epsilon w_x^\pm + \lambda w^\pm + \mathcal{C}_+(uw^\pm) = \lambda w^\mp + \mathcal{C}_-(uw^\pm).$$

Since each side of the equation (2.47) is bounded and analytic in the upper and lower half x -plane, according to Liouville's Theorem, each side of the equation (2.47) is equal to a constant denoted by λw_0 . Then one can obtain an equation for w^+ :

$$(2.48) \quad i\epsilon w_x^+ + \lambda(w^+ - w_0) = -\mathcal{C}_+(uw^+).$$

With the use of an integrating factor, one can write w^+ as:

$$(2.49) \quad w^+ = w_0 + C e^{ikx/\epsilon} + \frac{i}{\epsilon} \int_{-\infty}^x \mathcal{C}_+(uw^+)(y) e^{ik(x-y)/\epsilon} dy,$$

where C is a constant. It implies

$$(2.50) \quad w^+ \rightarrow w_0 + C e^{ikx/\epsilon} \quad \text{as } x \rightarrow -\infty$$

$$(2.51) \quad w^+ \rightarrow w_0 + \left(C + \frac{i}{\epsilon} \int_{-\infty}^{\infty} \mathcal{C}_+(uw^+)(y) e^{-iky/\epsilon} dy \right) e^{ikx/\epsilon} \quad \text{as } x \rightarrow \infty$$

For $\lambda > 0$, the functions $M(x; \lambda)$, $\overline{M}(x; \lambda)$, $N(x; \lambda)$ and $\overline{N}(x; \lambda)$ are assumed to be the solutions of the equation (2.26) with the following boundary conditions:

$$(2.52) \quad M(x; \lambda) = 1 + o(1), \quad \text{as } x \rightarrow -\infty,$$

$$(2.53) \quad \overline{M}(x; \lambda) = e^{i\lambda x/\epsilon}(1 + o(1)), \quad \text{as } x \rightarrow -\infty,$$

$$(2.54) \quad N(x; \lambda) = e^{i\lambda x/\epsilon}(1 + o(1)), \quad \text{as } x \rightarrow \infty,$$

$$(2.55) \quad \overline{N}(x; \lambda) = 1 + o(1), \quad \text{as } x \rightarrow \infty.$$

After applying the Fourier Transform, one can show that for $\lambda > 0$, the functions $M(x; \lambda)$, $\overline{M}(x; \lambda)$, $N(x; \lambda)$ and $\overline{N}(x; \lambda)$ satisfy the following Fredholm integral equations:

$$(2.56) \quad M(x; \lambda) = 1 + \frac{1}{\epsilon} \int_{-\infty}^{\infty} G_+(x, y; \lambda) u(y) M(y; \lambda) dy,$$

$$(2.57) \quad \overline{M}(x; \lambda) = e^{i\lambda x/\epsilon} + \frac{1}{\epsilon} \int_{-\infty}^{\infty} G_+(x, y; \lambda) u(y) \overline{M}(y; \lambda) dy,$$

$$(2.58) \quad N(x; \lambda) = e^{i\lambda x/\epsilon} + \frac{1}{\epsilon} \int_{-\infty}^{\infty} G_-(x, y; \lambda) u(y) N(y; \lambda) dy,$$

$$(2.59) \quad \overline{N}(x; \lambda) = 1 + \frac{1}{\epsilon} \int_{-\infty}^{\infty} G_-(x, y; \lambda) u(y) \overline{N}(y; \lambda) dy,$$

where

$$(2.60) \quad G_{\pm}(x, y; \lambda) = \lim_{\delta \downarrow 0} \frac{1}{2\pi} \int_0^{\infty} \frac{e^{i(x-y)p/\epsilon}}{p - (\lambda \pm i\delta)} dp.$$

In fact, $G_{\pm}(x, y; \lambda)$ are the boundary values of $G(x, y; \lambda)$ taken from the upper and lower half λ -plane respectively. Here the function $G(x, y; \lambda)$ is given by

$$(2.61) \quad G(x, y; \lambda) = \frac{1}{2\pi} \int_0^{\infty} \frac{e^{i(x-y)p/\epsilon}}{p - \lambda} dp \quad \text{for } \lambda \notin \mathbb{R}^+.$$

By using the definition of G_{\pm} and applying Cauchy's residue theorem, one can show that the difference between $G_+(x, y; \lambda)$ and $G_-(x, y; \lambda)$ is given by

$$(2.62) \quad G_+(x, y; \lambda) - G_-(x, y; \lambda) = ie^{i(x-y)\lambda/\epsilon} \quad \text{for } \lambda > 0.$$

If $\lambda \notin \mathbb{R}^+$, after integration by parts, one can find the asymptotic behavior of $G(x, y; \lambda)$ as $|x| \rightarrow \infty$ is given by

$$(2.63) \quad G(x, y; \lambda) = \frac{1}{2\pi i x \lambda} + O(x^{-2}) \quad \text{for } \lambda \notin \mathbb{R}^+.$$

By taking derivative with respect to λ and integration by parts, one can obtain

$$(2.64) \quad \frac{\partial}{\partial \lambda}(G(x, y; \lambda)) = -\frac{1}{2\pi \lambda} + \frac{i(x-y)}{\epsilon} G(x, y; \lambda),$$

which implies $G_{\pm}(x, y; \lambda)$, the boundary values of $G(x, y; \lambda)$ also satisfy

$$(2.65) \quad \frac{\partial}{\partial \lambda}(G_{\pm}(x, y; \lambda)) = -\frac{1}{2\pi \lambda} + \frac{i(x-y)}{\epsilon} G_{\pm}(x, y; \lambda).$$

The corresponding integral equations in §2.1 are Volterra type integral equations, which are easier to analyze. Here, a different method is used to investigate these Fredholm integral equations. To investigate the relation between $M(x; \lambda)$ and $\bar{N}(x; \lambda)$, we introduce a new function $\Delta_{M\bar{N}}(x; \lambda) = M(x; \lambda) - \bar{N}(x; \lambda)$. By subtracting (2.59) from (2.56) and using (2.62), one can find that the function $\Delta(x; \lambda)$ satisfies

$$(2.66) \quad \Delta_{M\bar{N}}(x; \lambda) = \beta(\lambda)e^{i\lambda x/\epsilon} + \frac{1}{\epsilon} \int_{-\infty}^{\infty} G_-(x, y; \lambda)u(y)\Delta_{M\bar{N}}(y; k)dy$$

where

$$(2.67) \quad \beta(\lambda) = \frac{i}{\epsilon} \int_{-\infty}^{\infty} u(y)M(y; \lambda)e^{-i\lambda y/\epsilon} dy.$$

The equation (2.66) implies $\Delta_{M\bar{N}}(x; \lambda)/\beta(\lambda)$ is a solution of the equation (2.58). Since $N(x; \lambda)$ is the unique solution of the equation (2.58), one can obtain

$$(2.68) \quad \Delta_{M\bar{N}}(x; \lambda) = \beta(\lambda)N(x; \lambda).$$

Therefore, the relation between $M(x; \lambda)$ and $\bar{N}(x; \lambda)$ is given by

$$(2.69) \quad M(x; \lambda) = \bar{N}(x; \lambda) + \beta(\lambda)N(x; \lambda) \quad \text{for } \lambda > 0.$$

The same strategy can be used to write $N(x; \lambda)$ in terms of $\bar{N}(x; \lambda)$. After multiplying each side of the equation (2.58) by $e^{-i\lambda x/\epsilon}$, differentiating them with respect to λ and applying the equation (2.65), it is easy to show

$$(2.70) \quad \Delta_N(x; \lambda) = e^{-i\lambda x/\epsilon} f(\lambda) + \frac{1}{\epsilon} \int_{-\infty}^{\infty} G_-(x, y; \lambda) e^{-i\lambda(x-y)/\epsilon} u(y) \Delta_N(y; \lambda) dy,$$

where

$$(2.71) \quad \Delta_N(x; \lambda) = \frac{\partial}{\partial \lambda} (N(x; \lambda) e^{-i\lambda x/\epsilon}) \quad \text{and} \quad f(\lambda) = -\frac{1}{2\pi\lambda\epsilon} \int_{-\infty}^{\infty} u(y) N(y; \lambda) dy.$$

Then it is obvious that $\Delta_N(x; \lambda) e^{i\lambda x/\epsilon} / f(\lambda)$ is a solution of the equation (2.59). The uniqueness of the equation (2.59) and the asymptotic behavior of $\bar{N}(x; \lambda)$ as $\lambda \rightarrow 0+$ given in [39] indicate

$$(2.72) \quad N(x; \lambda) = e^{i\lambda x/\epsilon} \int_0^\lambda f(k) e^{-ixk/\epsilon} \bar{N}(x, k) dk.$$

By simply substituting it into (2.69), one can obtain a nonlocal relation between $M(x; \lambda)$ and $\bar{N}(x; \lambda)$:

$$(2.73) \quad M(x; \lambda) = \bar{N}(x; \lambda) + \beta(\lambda) e^{i\lambda x/\epsilon} \int_0^\lambda f(k) e^{-ixk/\epsilon} \bar{N}(x, k) dk.$$

Fokas and Ablowitz introduced the functions $M(x; \lambda)$, $\bar{M}(x; \lambda)$, $N(x; \lambda)$ and $\bar{N}(x; \lambda)$ in their paper [25] and kept using these notations throughout the paper. To provide

a better understanding of the theory, we introduce a new function $W(x, \lambda)$. In fact, the functions $M(x; \lambda)$ and $\overline{N}(x; \lambda)$ are the boundary values of a function $W(x, \lambda)$ taken from the upper and lower half λ -plane respectively:

$$(2.74) \quad M(x; \lambda) = \lim_{\lambda' \rightarrow \lambda + i0} W(x, \lambda'); \quad \overline{N}(x; \lambda) = \lim_{\lambda' \rightarrow \lambda - i0} W(x, \lambda') \quad \text{for } \lambda \in \mathbb{R}^+.$$

The function $W(x, \lambda)$ is analytic in $\mathbb{C} \setminus (\mathbb{R}^+ \cup \{\lambda_1, \dots, \lambda_n\})$ and satisfies the equation (2.26) and the following Fredholm integral equation

$$(2.75) \quad W(x; \lambda) = 1 + \frac{1}{\epsilon} \int_{-\infty}^{\infty} G(x, y; \lambda) u(y) W(y; \lambda) dy$$

for $\lambda \notin \mathbb{R}^+ \cup \{\lambda_1, \dots, \lambda_n\}$. Here $\lambda_1, \dots, \lambda_n$ are simple eigenvalues of the eigenvalue problem (2.45) (In [25], Fokas and Ablowitz assumed all the eigenvalues corresponding to the problem they discussed are simple eigenvalues), which are negative real numbers. Assume $\Phi_j(x) \in \mathbb{H}^+$ is the eigenfunction of the eigenvalue problem (2.45) corresponding to λ_j and satisfies

$$(2.76) \quad \lambda_j = \frac{1}{2\pi i} \int_{-\infty}^{\infty} u(y) \Phi_j(y) dy,$$

then it also satisfies the equation (2.26). By applying the Fourier Transform to the equation (2.26), one can show that $\Phi_j(x)$ satisfies the following Fredholm integral equation:

$$(2.77) \quad \Phi_j(x) = \frac{1}{\epsilon} \int_{-\infty}^{\infty} G(x, y; \lambda_j) u(y) \Phi_j(y) dy.$$

After using (2.63) and (2.76), the (2.77) tells us that

$$(2.78) \quad \Phi_j(x) \sim \frac{1}{x} \quad \text{as } |x| \rightarrow \infty.$$

By applying the analytic Fredholm theorem [65] to the Fredholm integral equation (2.75), one expects a pole at $\lambda = \lambda_j$. Since the eigenvalues are assumed to be simple

eigenvalues above, one can write $W(x; \lambda)$ as

$$(2.79) \quad W(x; \lambda) = W^{(j)}(x; \lambda) + C_j \frac{\Phi_j(x)}{\lambda - \lambda_j}$$

where C_j is a constant and $W^{(j)}(x; \lambda)$ is analytic at $\lambda = \lambda_j$. Then by substituting it into the equation (2.75), using (2.77), letting λ tend to λ_j and using (2.64) and (2.77), one can obtain

$$(2.80) \quad W_{\Delta}^{(j)}(x; \lambda_j) - \frac{1}{\epsilon} \int_{-\infty}^{\infty} G(x, y; \lambda_j) u(y) W_{\Delta}^{(j)}(y; \lambda_j) dy = a_j,$$

where

$$(2.81) \quad W_{\Delta}^{(j)}(x; \lambda_j) = W^{(j)}(x; \lambda_j) - \frac{iC_j}{\epsilon} x \Phi_j(x); \quad a_j = 1 - \frac{C_j}{2\pi\epsilon\lambda_j} \int_{-\infty}^{\infty} \Phi_j(y) u(y) dy.$$

Here $W_{\Delta}^{(j)}(x; \lambda_j)$ is analytic at $\lambda = \lambda_j$. By the Fredholm theory, a_j is equal to 0. It implies that $W_{\Delta}^{(j)}(x; \lambda_j)$ is a solution of the equation (2.77). Then $W_{\Delta}^{(j)}(x; \lambda_j) = \gamma_j \Phi_j(x)$, where γ_j is a constant. The constant γ_j plays a similar role as the norming constant c_n in §2.1. Moreover, after using the fact $a_j = 0$ and the equation (2.76), one can find the constant $C_j = -i\epsilon$. Therefore,

$$(2.82) \quad \lim_{\lambda \rightarrow \lambda_j} \left\{ W(x; \lambda) + \epsilon \frac{i\Phi_j(x)}{\lambda - \lambda_j} \right\} = (x + \gamma_j(t)) \Phi_j(x).$$

The above calculation is valid for all complex potential $u(x, t)$. The function $u(x, t)$ we are interested in is a real function. With the assumption that the potential $u(x, t)$ is real, Kaup and Matsuno [39] showed

$$(2.83) \quad f(\lambda) = \frac{\beta^*(\lambda)}{2\pi i \lambda}, \quad \text{for } \lambda > 0,$$

and

$$(2.84) \quad \Im(\gamma_j(0)) = -\frac{1}{2\lambda_j}.$$

The eigenvalues λ_j $j = 1 \cdots n$, the constants γ_j $j = 1 \cdots n$, and the reflection coefficient $\beta(\lambda)$ where $\lambda > 0$ constitute the *scattering data*, which can be used to calculate the potential $u(x, t)$ as will be shown later.

2.2.2 Time Dependence of the Scattering Data

Since the potential $u(x, t)$ varies as time t varies, one expects the scattering data also vary as time t varies. The variation of the scattering data can be derived from the equation (2.27). By substituting $M(x; \lambda)$ into equation (2.27) and applying the boundary condition (2.52), one can find that the constant ρ in equation (2.27) is equal to zero. Therefore,

$$(2.85) \quad iM_t - 2i\lambda M_x + \epsilon M_{xx} - 2i\mathcal{C}_+(u_x)M = 0.$$

After applying the same strategy to $\bar{N}(x; \lambda)$, one can obtain

$$(2.86) \quad i\bar{N}_t - 2i\lambda\bar{N}_x + \epsilon\bar{N}_{xx} - 2i\mathcal{C}_+(u_x)\bar{N} = 0.$$

Then by substituting (2.69) into (2.85) and using (2.86), it is easy to show $N(x; \lambda)$ satisfies

$$(2.87) \quad i\beta_t(\lambda)N + i\beta(\lambda)N_t - 2i\lambda\beta(\lambda)N_x + \epsilon\beta(\lambda)N_{xx} - 2i\mathcal{C}_+(u_x)\beta(\lambda)N = 0.$$

After using the boundary condition (2.54) and considering the asymptotic behavior of each side of the equation (2.87), one can obtain $\beta_t(\lambda) = i\lambda^2\beta(\lambda)/\epsilon$, which implies

$$(2.88) \quad \beta(\lambda, t) = \beta(\lambda, 0)e^{i\lambda^2 t/\epsilon}.$$

It follows from (2.83) and (2.88) that the variation of $f(\lambda, t)$ is given by

$$(2.89) \quad f(\lambda, t) = f(\lambda, 0)e^{-i\lambda^2 t/\epsilon}.$$

In [25], Fokas and Ablowitz stated the number of eigenvalues and the eigenvalues themselves are constants without a rigorous proof or a detailed calculation. Here, we provide the proof of this statement. By differentiating each side of the equation

(2.76) with respect to t and using (1.1), (2.27) and (2.45), we obtain

$$\begin{aligned}
(\lambda_j)_t &= \frac{1}{2\pi i} \int_{-\infty}^{\infty} (u(\Phi_j)_t + u_t \Phi_j) dy \\
(2.90) \quad &= \frac{1}{2\pi i} \int_{-\infty}^{\infty} (u(2\lambda_j(\Phi_j)_y + i\epsilon(\Phi_j)_{yy} + 2\mathcal{C}_+(u_y)\Phi_j) + u_t \Phi_j) dy \\
&= \frac{1}{2\pi i} \int_{-\infty}^{\infty} (u(2\mathcal{C}_+(u_y)\Phi_j - i\epsilon(\Phi_j)_{yy} - 2\mathcal{C}_+((u\Phi_j)_y)) + u_t \Phi_j) dy
\end{aligned}$$

Since the function Φ_j belongs to \mathbb{H}^+ , Φ_j is a eigenfunction of the Hilbert transform and satisfies $H(\Phi_j) = i\Phi_j$. After using this fact, the skew-adjointness of the Hilbert transform and the asymptotic behavior of u and Φ_j , we obtain

$$(2.91) \quad \int_{-\infty}^{\infty} iu(\Phi_j)_{yy} dy = - \int_{-\infty}^{\infty} H(u_{yy})\Phi_j dy$$

and

$$\begin{aligned}
(2.92) \quad \int_{-\infty}^{\infty} u\mathcal{C}_+(u_y)\Phi_j dy - \int_{-\infty}^{\infty} u\mathcal{C}_+((u\Phi_j)_y) dy &= \int_{-\infty}^{\infty} (u\mathcal{C}_+(u_y)\Phi_j - \mathcal{C}_-(u_y)u\Phi_j) dy \\
&= \int_{-\infty}^{\infty} uu_y\Phi_j dy.
\end{aligned}$$

Then the equation (2.90) becomes

$$\begin{aligned}
(2.93) \quad (\lambda_j)_t &= \frac{1}{2\pi i} \int_{-\infty}^{\infty} ((2uu_y + \epsilon H(u_{yy}))\Phi_j + u_t \Phi_j) dy \\
&= \frac{1}{2\pi i} \int_{-\infty}^{\infty} (-u_t \Phi_j + u_t \Phi_j) dy \\
&= 0,
\end{aligned}$$

which implies the number of eigenvalues and the eigenvalues themselves do not vary as time varies. Since $W(x; \lambda)$ and $\Phi_j(x)$ satisfy the equation (2.27), the equation (2.82) indicates the function $(x + \gamma_j(t))\Phi_j(x, t)$ also satisfies the equation (2.27). By substituting this function into (2.27) and considering the asymptotic behavior as x tends to infinity, one can obtain $(\gamma_j)_t = 2\lambda_j$, which implies the explicit time dependence of the constants γ_j is given by

$$(2.94) \quad \gamma_j(t) = 2\lambda_j t + \gamma_j(0).$$

2.2.3 The Inverse Scattering Problem

If the scattering data are given, then one can use them to calculate the potential $u(x, t)$ by analyzing the function $W(x; \lambda)$. The equation (2.79) indicates one can write the function $W(x; \lambda)$ as

$$(2.95) \quad W(x; \lambda) = 1 - \epsilon \sum_j \frac{i\Phi_j(x)}{\lambda - \lambda_j} + n(x; \lambda),$$

where $n(x; \lambda)$ is analytic in $\mathbb{C} \setminus \mathbb{R}^+$. By substituting it into (2.69), one can obtain the jump condition for $n(x; \lambda)$ on \mathbb{R}^+ :

$$(2.96) \quad n^+(x, \lambda) = n^-(x, \lambda) + \beta(\lambda)N(x, \lambda),$$

where $n^\pm(x, \lambda)$ represent the boundary values of the function $n(x, \lambda)$. Since $n(x; \lambda)$ is analytic in $\mathbb{C} \setminus \mathbb{R}^+$ and $n(x, \lambda) \rightarrow 0$ as $\lambda \rightarrow \infty$, we learn from the jump condition (2.96) that

$$(2.97) \quad n(x, \lambda) = \frac{1}{2\pi i} \int_0^\infty \frac{\beta(k)N(x, k)}{k - \lambda} dk.$$

The equation (2.97) implies that

$$(2.98) \quad W(x; \lambda) = 1 + \frac{1}{2\pi i} \int_0^\infty \frac{\beta(k)N(x, k)}{k - \lambda} dk - i\epsilon \sum_j \frac{1}{\lambda - \lambda_j} \Phi_j(x).$$

By substituting (2.98) into (2.82), it is easy to show that

$$(2.99) \quad (x + \gamma_j)\Phi_j(x) + i\epsilon \sum_{j \neq q} \frac{1}{\lambda_j - \lambda_q} \Phi_q(x) - \frac{1}{2\pi i} \int_0^\infty \frac{\beta(k)N(x, k)}{k - \lambda_j} dk = 1.$$

This formula can be used to calculate soliton solutions of the BO equation, which will be discussed later. After letting λ go to the positive real axis from the lower half λ -plane, the left hand side of the equation (2.98) becomes $\bar{N}(x; \lambda)$:

$$(2.100) \quad \bar{N}(x; \lambda) = 1 + \lim_{\delta \downarrow 0} \left(\frac{1}{2\pi i} \int_0^\infty \frac{\beta(k)N(x, k)}{k - \lambda + i\delta} dk \right) - i\epsilon \sum_j \frac{1}{\lambda - \lambda_j} \Phi_j(x).$$

By substituting it into (2.72) and changing the order of integration, one can show

$$(2.101) \quad N(x; \lambda) = \bar{f}(x, \lambda) + \frac{1}{2\pi i} \int_0^\infty \hat{f}(x, k) \beta(k) N(x; k) dk - i\epsilon \sum_j \hat{f}_j(x, \lambda) \Phi_j(x),$$

where

$$(2.102) \quad \bar{f}(x, \lambda) = e^{i\lambda x/\epsilon} \int_0^\lambda f(k) e^{-ikx/\epsilon} dk; \quad \hat{f}_j(x, \lambda) = e^{i\lambda x/\epsilon} \int_0^\lambda \frac{f(k) e^{-ikx/\epsilon} dk}{k - \lambda_j}$$

and

$$(2.103) \quad \hat{f}(x, \lambda) = \lim_{\delta \downarrow 0} \left(e^{i\lambda x/\epsilon} \int_0^\lambda \frac{f(k) e^{-ikx/\epsilon} dk}{\lambda - k + i\delta} \right).$$

By using the equation (2.75) and the asymptotic behavior of $W(x; \lambda)$ and $G(x, y; \lambda)$, one can obtain

$$(2.104) \quad W(x; \lambda) \longrightarrow 1 - \frac{\mathcal{C}_+(u)}{\lambda}, \quad \text{as } \lambda \rightarrow \infty.$$

By substituting (2.98) into (2.104), it is easy to show that $\mathcal{C}_+(u)(x)$ can be written in the form

$$(2.105) \quad \mathcal{C}_+(u)(x) = \frac{1}{2\pi i} \int_0^\infty \beta(k) N(x, k) dk + i\epsilon \sum_j \Phi_j(x).$$

If one can obtain $N(x, \lambda)$ and $\Phi_j(x)$ by solving the equations (2.99) and (2.101), the potential $u(x, t)$ can be calculated via (2.105). It is very difficult to use the equations (2.99) and (2.101) to analyze the asymptotic properties of the BO equation. However, there is a more powerful tool, the Riemann–Hilbert Problem, available.

2.2.4 The Riemann–Hilbert Problem

Based on the properties of $W(x, \lambda, t)$ given above, $W(x, \lambda, t)$ is the solution of the following nonlocal Riemann-Hilbert Problem. Here $W(x, \lambda, t)$ is viewed as a function of λ and x and t are parameters.

Riemann-Hilbert problem II.4.

Analyticity: $W(\lambda)$ is analytic in $\mathbb{C} \setminus (\mathbb{R}^+ \cup \{\lambda_1, \lambda_2, \dots, \lambda_n\})$

Residue condition:

$$(2.106) \quad \operatorname{Res}_{\lambda=\lambda_j}(W(\lambda)) = \frac{-i\epsilon}{x + \gamma_j(t)} \frac{\partial}{\partial \lambda} (W(\lambda)(\lambda - \lambda_j)) \Big|_{\lambda=\lambda_j}$$

Jump conditions: The boundary values taken on \mathbb{R}^+ satisfy

$$(2.107) \quad W_+(\lambda) = W_-(\lambda) + \beta(\lambda) e^{i\lambda x/\epsilon} \int_0^\lambda f(k) W_-(k) e^{-ikx/\epsilon} dk, \quad \text{for } \lambda \in \mathbb{R}^+$$

Normalization: $W(\lambda)$ is normalized at infinity:

$$(2.108) \quad W(\lambda) \rightarrow 1 \quad \text{as } \lambda \rightarrow \infty.$$

Compared to Riemann-Hilbert problem II.1 in §2.1, Riemann-Hilbert problem II.4 is much more complicated. The residue condition and the jump condition in Riemann-Hilbert problem II.1 are local conditions and those in Riemann-Hilbert problem II.4 are nonlocal conditions.

The equation (2.104) can be rewritten as

$$(2.109) \quad \mathcal{C}_+(u) = \lim_{\lambda \rightarrow \infty} \lambda(1 - W(\lambda)).$$

If one can solve Riemann-Hilbert Problem II.4, then $u(x, t)$ can be obtained via (2.109).

2.2.5 The Soliton Solutions

Soliton solutions are very important special solutions for nonlinear integrable evolution equations. The soliton solutions of the BO equation are rational functions and the corresponding scattering data are reflectionless (the reflection coefficient

$\beta(\lambda) \equiv 0$). If the potential $u(x, t)$ is a soliton solution, then the equation (2.99) becomes

$$(2.110) \quad (x + \gamma_j)\Phi_j(x) + i\epsilon \sum_{j \neq q} \frac{1}{\lambda_j - \lambda_q} \Phi_q(x) = 1.$$

The soliton solutions can be calculated by solving this linear algebra problem and using (2.105). The soliton solutions also can be obtained by solving Riemann–Hilbert Problem II.4. Since $\beta(\lambda) \equiv 0$, $W(x; \lambda)$ is analytic in the whole complex λ -plane except some simple poles on the negative real axis. The normalization condition of $W(x; \lambda)$ suggests the function $W(x; \lambda)$ can be written as

$$(2.111) \quad W(x; \lambda) = \frac{\lambda^N + a_{N-1}\lambda^{N-1} + \cdots + a_0}{(\lambda - \lambda_1) \cdots (\lambda - \lambda_N)}$$

where a_0, a_1, \dots, a_{N-1} are constants to be determined to match the residue condition. One can turn it into a linear algebra problem by substituting (2.111) into the residue condition. In fact, the formulas of the soliton solutions obtained via these two methods are same as the N -soliton formula obtained by Matsuno [48] via a bilinear transformation method. Matsuno’s N -soliton formula is

$$(2.112) \quad u(x, t) = 2\epsilon \frac{\partial}{\partial x} \Im(\log(\tau_\epsilon(x, t))),$$

where the “tau-function” $\tau_\epsilon(x, t) := \det(\mathbb{I} + i\epsilon^{-1}\mathbf{A}_\epsilon)$. Here \mathbf{A}_ϵ is an $N \times N$ Hermitean matrix given by

$$(2.113) \quad (\mathbf{A}_\epsilon)_{nm} = -2\lambda_n(x + 2\lambda_n t + \gamma_n(0)), \quad \text{for } n = m,$$

and

$$(2.114) \quad (\mathbf{A}_\epsilon)_{nm} = \frac{2i\epsilon(\lambda_n\lambda_m)^{1/2}}{\lambda_n - \lambda_m}, \quad \text{for } n \neq m.$$

2.2.6 The Multi-phase Solutions

The periodic solutions of the BO equation obtained by Benjamin [5], Ono [59], Satsuma and Ishimori [66] are given by

$$(2.115) \quad u(x, t) = \frac{k \tanh \phi}{1 + \operatorname{sech} \phi \cos \xi}$$

with

$$(2.116) \quad \xi = k(x - at)/\epsilon + \xi_0 \quad \text{and} \quad a = k \coth \phi,$$

where k and ϕ are real constants and ξ_0 is the phase constant. Satsuma and Ishimori [66] also constructed multi-phase solutions of the BO equation (also called N -periodic wave solutions in [66]) via a bilinear transformation method. Later, Dobrokhotov and Krichever [22] obtained the same multi-phase solutions of the BO equation by using a different approach, which is given by

$$(2.117) \quad u(x, t) = C + \sum_{n=1}^N (a_n - b_n) - 2\Im \left(\frac{\partial}{\partial x} (\log(\det(\mathbf{Q}(x, t)))) \right)$$

where $C < a_1 < b_1 < a_2 < b_2 < \dots < a_N < b_N$ are real constants. The matrix $\mathbf{Q}(x, t)$ is given by

$$(2.118) \quad (\mathbf{Q})_{jm} = c_m e^{i(a_m - b_m)x/\epsilon - i(a_m^2 - b_m^2)t/\epsilon} \delta_{jm} - \frac{1}{b_j - a_m},$$

where δ_{jm} is Kronecker delta and the constant c_m is defined by

$$(2.119) \quad c_m = \sqrt{-\frac{(b_m - C) \prod_{j \neq i} (a_i - a_j)(b_i - b_j)}{(a_m - C) \prod_{j=1}^N (b_i - a_j)(a_i - b_j)}}.$$

In fact, the solutions given by (2.117) are the periodic solutions of the BO equation when N is equal to 1. The discussion in [22] suggests that the periodic solutions of the BO equation can be also written in the form

$$(2.120) \quad u(x, t) = C + a_1 - b_1 + 2\Re(r(x, t)),$$

where $r(x, t)$ satisfies that the function $R(\lambda; x, t)$ given by

$$(2.121) \quad R(\lambda; x, t) = 1 + \frac{r(x, t)}{\lambda - a_1}$$

is a solution of the following Riemann-Hilbert problem

Riemann-Hilbert problem II.5.

Analyticity: $R(\lambda; x, t)$ is analytic in $\mathbb{C} \setminus \{a_1\}$

Residue condition:

$$(2.122) \quad \operatorname{Res}_{\lambda=a_1}(R(\lambda; x, t)) = R(b_1; x, t)(c_1)^{-1} e^{i(b_1 - a_1)x/\epsilon - i(b_1^2 - a_1^2)t/\epsilon}$$

Normalization: $R(\lambda; x, t)$ is normalized at infinity:

$$(2.123) \quad R(\lambda; x, t) \rightarrow 1 \quad \text{as } \lambda \rightarrow \infty.$$

2.2.7 The Conservation Laws

Kaup and Matsuno discussed the conservation laws of the BO equation in [39], which is introduced below. By employing the strategy used in §2.2.2 to show the eigenvalues do not vary as time changes, one can show

$$(2.124) \quad \int_{-\infty}^{\infty} (u(y)\overline{N}(y; \lambda))_t dy = 0.$$

The equation (2.124) implies that I is a conserved quantity, where

$$(2.125) \quad I = \int_{-\infty}^{\infty} u(y)\overline{N}(y; \lambda) dy.$$

By multiplying each side of the equation (2.100), changing the order of integration, using (2.71), (2.76) and (2.83), one can write I in terms of u , $\beta(\lambda)$ and λ_j :

$$(2.126) \quad I = \int_{-\infty}^{\infty} u(y) dy + \frac{\epsilon}{2\pi} \lim_{\delta \downarrow 0} \left(\int_0^{\infty} \frac{|\beta(k)|^2}{k - \lambda + i\delta} dk \right) + 2\pi\epsilon \sum_j \frac{\lambda_j}{\lambda - \lambda_j}.$$

Kaup and Matsuno [39] expanded $\bar{N}(x; \lambda)$ as

$$(2.127) \quad \bar{N}(x; \lambda) = \sum_{k=0}^{\infty} \frac{(-1)^k \bar{N}_{k+1}(x)}{\lambda^k}.$$

By substituting it into (2.26), they obtained that $\bar{N}_1 = 1$ and

$$(2.128) \quad \bar{N}_{k+1}(x) = \mathcal{C}_+(u\bar{N}_k)(x) + i\epsilon \frac{\partial \bar{N}_k}{\partial x}(x).$$

The conserved quantity I then can be expanded as

$$(2.129) \quad I = \sum_{k=0}^{\infty} \frac{(-1)^k I_{k+1}}{\lambda^k},$$

where

$$(2.130) \quad I_k = \int_{-\infty}^{\infty} u(y) \bar{N}_k(y) dy.$$

By expanding the right hand side of the equation (2.126) in inverse powers of λ , Kaup and Matsuno [39] obtained

$$(2.131) \quad I_k = \frac{(-1)^m \epsilon}{2\pi} \int_0^{\infty} |\beta(\lambda)|^2 \lambda^{k-2} d\lambda + 2\pi\epsilon \sum_{j=1}^N (-\lambda_j)^{k-1} \quad \text{for } k = 2, 3, \dots,$$

where N is the number of eigenvalues. They showed that the equation (2.131) is also valid for $m = 1$ by multiplying (2.100) by $u(x)$, integrating over \mathbb{R} , letting λ tend to 0 and using the asymptotic behavior of $\bar{N}(x; \lambda)$ as $\lambda \rightarrow 0+$ given in [39]. In particular, for $m = 1, 2$, it is easy to see that

$$(2.132) \quad 2\pi N\epsilon = \frac{\epsilon}{2\pi} \int_0^{\infty} \frac{|\beta(\lambda)|^2}{\lambda} d\lambda + \int_{-\infty}^{\infty} u(x) dx$$

and

$$(2.133) \quad \int_{-\infty}^{\infty} \frac{1}{2} u^2(x) dx = 2\pi\epsilon \sum_{j=1}^n (-\lambda_j) + \frac{\epsilon}{2\pi} \int_0^{\infty} |\beta(\lambda)|^2 d\lambda.$$

2.2.8 Matsuno's Method

Matsuno provided a remarkable method to approximate the eigenvalues corresponding to an ϵ -independent smooth positive initial condition u_0 valid for small $\epsilon > 0$ by using the conservation laws (2.131) in his papers [49, 50]. Here, we introduce his method by following the reorganized calculation in [56].

By using the recurrence relation (2.128) with $\epsilon = 0$, one can calculate the limits of I_k as ϵ tend to 0:

$$(2.134) \quad \lim_{\epsilon \downarrow 0} I_k = \int_{\mathbb{R}} u(x) \mathcal{C}_+(u \mathcal{C}_+(u \mathcal{C}_+(\cdots u \mathcal{C}_+(u) \cdots)))(x) dx, \quad k \in \mathbb{Z}^+,$$

where the Cauchy operator \mathcal{C}_+ appears $k - 1$ times in the integrand. Since I_k are conserved quantities, their limits are also independent of time t , which suggests the limits of I_k also can be written in the form:

$$(2.135) \quad \lim_{\epsilon \downarrow 0} I_k = \int_{\mathbb{R}} u_0(x) \mathcal{C}_+(u_0 \mathcal{C}_+(u_0 \mathcal{C}_+(\cdots u_0 \mathcal{C}_+(u_0) \cdots)))(x) dx, \quad k \in \mathbb{Z}^+.$$

With the use of an identity

$$(2.136) \quad \int_{\mathbb{R}} u_0(x) \mathcal{C}_+(u_0 \mathcal{C}_+(u_0 \mathcal{C}_+(\cdots u_0 \mathcal{C}_+(u_0) \cdots)))(x) dx = \frac{1}{k} \int_{\mathbb{R}} u_0(x)^k dx, \quad k \in \mathbb{Z}^+$$

we proved for the first time (see Appendix B), one can simplify the equation (2.135) as follow:

$$(2.137) \quad \lim_{\epsilon \downarrow 0} I_k = \frac{1}{k} \int_{\mathbb{R}} u_0(x)^k dx, \quad k \in \mathbb{Z}^+.$$

In fact, the equation (2.137) can also be obtained by an older argument given in Nakamura's paper [58].

After substituting (2.131) into (2.137), one can obtain

$$(2.138) \quad \lim_{\epsilon \downarrow 0} \frac{(-1)^k \epsilon}{2\pi} \int_0^\infty |\beta(\lambda)|^2 \lambda^{k-2} d\lambda + 2\pi \lim_{\epsilon \downarrow 0} \epsilon \sum_{n=1}^N (-\lambda_n)^{k-1} = \frac{1}{k} \int_{\mathbb{R}} u_0(x)^k dx,$$

for $k \in \mathbb{Z}^+$. In [49, 50], Matsuno assumed the integral in the first term on the left hand side of the equation (2.138) is bounded for small $\epsilon > 0$ and $k \in \mathbb{Z}^+$, if the initial condition u_0 is positive and smooth. Here the upper and lower bounds are independent of ϵ . This assumption is based on a physical argument. By using this hypothesis, it is obvious the first term on the left hand side of the equation (2.138) is equal to 0. Then the equation (2.138) becomes

$$(2.139) \quad \lim_{\epsilon \downarrow 0} \epsilon \sum_{n=1}^N (-\lambda_n)^{k-1} = \frac{1}{2\pi k} \int_{\mathbb{R}} u_0(x)^k dx, \quad k \in \mathbb{Z}^+.$$

The finite sum in the equation (2.139) can be written in terms of an integral and then the equation (2.139) becomes

$$(2.140) \quad \lim_{\epsilon \downarrow 0} \int_{-\infty}^0 (-\lambda)^{k-1} \left(\sum_{n=1}^N \epsilon \delta(\lambda - \lambda_n) \right) d\lambda = \frac{1}{2\pi k} \int_{\mathbb{R}} u_0(x)^k dx, \quad k \in \mathbb{Z}^+,$$

where $\delta(\lambda)$ is the Dirac delta function. The finite sum in the equation (2.140) converges to an eigenvalue density function $F(\lambda)$ as $\epsilon \downarrow 0$ in some weak sense. Then the equation (2.140) becomes

$$(2.141) \quad \int_{-\infty}^0 (-\lambda)^{k-1} F(\lambda) d\lambda = \frac{1}{2\pi k} \int_{\mathbb{R}} u_0(x)^k dx, \quad k \in \mathbb{Z}^+.$$

Matsuno calculated the function $F(\lambda)$ explicitly by solving the classical moment problem (2.141). He noticed the integral on the left hand side of the equation (2.141) can be written as

$$(2.142) \quad \int_{-\infty}^0 (-\lambda)^{k-1} F(\lambda) d\lambda = (-i)^{k-1} \frac{d^{k-1} \hat{F}}{d\xi^{k-1}}(0)$$

where $\hat{F}(\xi)$ is the Fourier transform of F :

$$(2.143) \quad \hat{F}(\xi) := \int_{-\infty}^0 F(\lambda) e^{-i\xi\lambda} d\lambda.$$

Then the equation (2.141) becomes

$$(2.144) \quad \frac{d^{k-1} \hat{F}}{d\xi^{k-1}}(0) = \frac{i^{k-1}}{2\pi k} \int_{\mathbb{R}} u_0(x)^k dx, \quad k \in \mathbb{Z}^+.$$

If $u_0(x) \in L^1(\mathbb{R}) \cap L^\infty(\mathbb{R})$, then by expanding $\hat{F}(\xi)$ about $\xi = 0$ and using the equation (2.144) to estimate the coefficients, one can find $\hat{F}(\xi)$ is an entire function, which implies the Taylor series of $\hat{F}(\xi)$ at 0 converges to $\hat{F}(\xi)$ for $\xi \in \mathbb{R}$. Then the function $\hat{F}(\xi)$ can be written in the form:

$$\begin{aligned}
 \hat{F}(\xi) &= \sum_{k=1}^{\infty} \frac{1}{(k-1)!} \frac{d^{k-1} \hat{F}}{d\xi^{k-1}}(0) \xi^{k-1} \\
 (2.145) \quad &= \sum_{k=1}^{\infty} \frac{(i\xi)^{k-1}}{2\pi k!} \int_{\mathbb{R}} u_0(x)^k dx \\
 &= \frac{1}{2\pi i\xi} \sum_{k=1}^{\infty} \int_{\mathbb{R}} \frac{[i\xi u_0(x)]^k}{k!} dx.
 \end{aligned}$$

Based on the absolute convergence of the combined sum and integral in the equation (2.145), one can interchange the infinite sum and integral and write $\hat{F}(\xi)$ as

$$\begin{aligned}
 \hat{F}(\xi) &= \frac{1}{2\pi i\xi} \int_{\mathbb{R}} \sum_{k=1}^{\infty} \frac{[i\xi u_0(x)]^k}{k!} dx \\
 (2.146) \quad &= \frac{1}{2\pi i\xi} \int_{\mathbb{R}} (e^{i\xi u_0(x)} - 1) dx \\
 &= \frac{1}{\pi\xi} \int_{\mathbb{R}} e^{i\xi u_0(x)/2} \sin\left(\frac{1}{2}\xi u_0(x)\right) dx.
 \end{aligned}$$

After applying the inverse Fourier transform to each side of the equation (2.146), the equation (2.146) becomes

$$(2.147) \quad F(\lambda) = \frac{1}{2\pi} \lim_{R \uparrow \infty} \int_{-R}^{+R} e^{i\xi\lambda} \int_{\mathbb{R}} \frac{e^{i\xi u_0(x)/2}}{\pi\xi} \sin\left(\frac{1}{2}\xi u_0(x)\right) dx d\xi.$$

According to Fubini's Theorem, one can change the order of integration and pass the limit through the integral in (2.147). Then the equation (2.147) becomes

$$\begin{aligned}
 (2.148) \quad F(\lambda) &= \frac{1}{2\pi} \int_{\mathbb{R}} \left(\int_{\mathbb{R}} e^{i\xi(\lambda+u_0(x)/2)} \frac{\sin\left(\frac{1}{2}\xi u_0(x)\right)}{\pi\xi} d\xi \right) dx. \\
 &= \frac{1}{2\pi} \int_{\mathbb{R}} \chi_{[-u_0(x), 0]}(\lambda) dx.
 \end{aligned}$$

where $\chi_{[-u_0(x), 0]}(\lambda)$ is the indicator function of an interval $[-u_0(x), 0]$. If $\lambda \notin [-L, 0]$ where L is the maximum of the initial condition $u_0(x)$ for $x \in \mathbb{R}$, then the indicator

function in (2.148) is always equal to 0. This fact implies $F(\lambda) \equiv 0$ for $\lambda \notin [-L, 0]$. If $\lambda \in (-L, 0)$, the equation (2.148) can be simplified as:

$$(2.149) \quad F(\lambda) = \frac{1}{2\pi} \int_{\{x \in \mathbb{R}, u_0(x) > -\lambda\}} dx, \quad -L < \lambda < 0.$$

2.3 An Example for the Scattering theory of the BO Equation

Kodama, Ablowitz, and Satsuma [40] calculated eigenvalues and eigenfunctions in the inverse scattering transform of the BO equation with special initial conditions of the form

$$(2.150) \quad u(x, 0) = \frac{2v}{x^2 + 1},$$

where v is a constant. In this section, we illustrate their method to calculate the scattering data corresponding to these special initial conditions.

The eigenfunctions $\Phi_j(x; k_j)$ and the functions $M(x; k)$, $\overline{M}(x; k)$, $N(x; k)$ and $\overline{N}(x; k)$ all satisfy the following equation:

$$(2.151) \quad i\epsilon w_x^+ + \lambda(w^+ - w^-) = -uw^+.$$

The right side of the equation (2.151) can be broken down into two parts $-\mathcal{C}_+(uw^+)$ and $\mathcal{C}_-(uw^+)$ with the use of the identity (2.39). Then the equation (2.151) becomes

$$(2.152) \quad i\epsilon w_x^+ + \lambda w^+ + \mathcal{C}_+(uw^+) = \lambda w^- + \mathcal{C}_-(uw^+).$$

Since the solutions of the equation (2.151) discussed here are bounded, each side of the equation (2.152) has analytic and bounded extensions to both the upper and lower half planes. According to Liouville's Theorem, each side of the equation (2.152) is equal to a constant denoted by λw_0 , then the equation (2.152) becomes,

$$(2.153) \quad i\epsilon w_x^+ + \lambda(w^+ - w_0) = -\mathcal{C}_+(uw^+) \quad \text{and} \quad \lambda(w^- - w_0) = -\mathcal{C}_-(uw^+).$$

By using the definition of the Cauchy operator \mathcal{C}_- , w^- can be written as:

$$(2.154) \quad w^- = w_0 - \lim_{\delta \downarrow 0} \left(\frac{1}{2\pi i \lambda} \int_{-\infty}^{\infty} \frac{1}{y - (x - i\delta)} \left(\frac{2v}{y^2 + 1} \right) w^+(y) dy \right).$$

After applying Cauchy's residue theorem to the right side of (2.154), one can write w^- as:

$$(2.155) \quad w^- = w_0 - \lim_{\delta \downarrow 0} \left(\frac{1}{\lambda} \operatorname{Res}_{y=i} \left[\frac{1}{y - (x - i\delta)} \left(\frac{2v}{y^2 + 1} \right) w^+(y) \right] \right) = w_0 - \frac{ivw^+(i)}{\lambda(x - i)}.$$

Then one can obtain a first order ordinary differential equation for w^+ by substituting (2.155) into (2.151):

$$(2.156) \quad i\epsilon w_x^+ + \lambda(w^+ - w_0) + \frac{2v}{x^2 + 1} w^+ + \frac{ivw^+(i)}{x - i} = 0.$$

With the use of an integrating factor, one can obtain a general solution of (2.156) given by

$$(2.157) \quad w^+(x) = w_0 + e^{i\lambda x/\epsilon} \left(\frac{x - i}{x + i} \right)^{v/\epsilon} \left(C - \frac{1}{\epsilon} \int_{-\infty}^x \frac{vw^+(i)}{y - i} e^{-i\lambda y/\epsilon} \left(\frac{y + i}{y - i} \right)^{v/\epsilon} dy + \int_{-\infty}^x \frac{2w_0vi}{y^2 + 1} e^{-i\lambda y/\epsilon} \left(\frac{y + i}{y - i} \right)^{v/\epsilon} dy \right)$$

where C is a constant.

If λ_j is an eigenvalue and $\Phi_j(x) \in \mathbb{H}^+$ is the corresponding eigenfunction, then $\Phi_j(x)$ is a solution of the equation (2.151) for $\lambda = \lambda_j$. This fact tells us that $\Phi_j(x)$ can be written as the right hand side of the equation (2.157) with $w_0 = C = 0$:

$$(2.158) \quad \Phi_j(x) = -\frac{v}{\epsilon} \Phi_j(i) e^{i\lambda_j x/\epsilon} \left(\frac{x - i}{x + i} \right)^{v/\epsilon} \int_{-\infty}^x \frac{1}{y - i} e^{-i\lambda_j y/\epsilon} \left(\frac{y + i}{y - i} \right)^{v/\epsilon} dy.$$

Here, the constants w_0 and C are chosen to be equal to 0, because $\Phi_j(x) \rightarrow 0$ as $|x| \rightarrow \infty$. But, the equation (2.158) only guarantees $\Phi_j(x) \rightarrow 0$ as $x \rightarrow -\infty$. If it is also true that $\Phi_j(x) \rightarrow 0$ as $x \rightarrow +\infty$, the eigenvalue λ_j has to satisfy the following equation:

$$(2.159) \quad \int_{-\infty}^{\infty} \frac{1}{y - i} e^{-i\lambda_j y/\epsilon} \left(\frac{y + i}{y - i} \right)^{v/\epsilon} dy = 0.$$

In fact, that the equation (2.159) holds true is a necessary and sufficient condition of λ_j is an eigenvalue.

If v/ϵ is a positive integer, then the left hand side of the equation (2.159) can be calculated explicitly by a recurrence relation. Assume the function $D_n(\lambda)$ is defined by

$$(2.160) \quad D_n(\lambda) = \int_{-\infty}^{\infty} \frac{1}{y-i} e^{-i\lambda y/\epsilon} \left(\frac{y+i}{y-i} \right)^n dy,$$

then by integration by parts and applying Cauchy's residue theorem, one can obtain $D_1(\lambda) = 2\pi i(1 + 2\lambda/\epsilon)e^{\lambda/\epsilon}$. After applying integration by parts to $D_{n+1}(\lambda)$, one can obtain

$$(2.161) \quad D_{n+1}(\lambda) = \frac{2n+1+2\lambda/\epsilon}{n+1} D_n(\lambda) - \frac{n}{n+1} D_{n-1}(\lambda),$$

which is related to the famous three-term recurrence relation for the Laguerre polynomials [3]. Thus $D_n(\lambda)$ can be written in terms of the Laguerre polynomials:

$$(2.162) \quad D_n(\lambda) = 2\pi i e^{\lambda/\epsilon} L_n(-2\lambda/\epsilon),$$

where $L_n(\lambda)$ is the Laguerre polynomial of degree n . Therefore, if $v/\epsilon = n$, then the eigenvalues are equal to the roots of the Laguerre polynomial of degree n scaled by $-2/\epsilon$, which implies the number of eigenvalues is n .

If v/ϵ is a positive number but not an integer, then there exists an integer n such that $n-1 < v/\epsilon < n$. By solving the equation (2.159) numerically, one can find that the number of eigenvalues is n .

The method introduced above cannot be directly applied to general rational initial conditions because with general rational initial conditions, the right hand side of the equation (2.158) may become a sum of two terms with two unknown coefficients and the relation between these two coefficients is also unknown. In that case, besides the

eigenvalue λ_j , the equation (2.159) has another unknown parameter. So, one cannot calculate the eigenvalue λ_j only by using the equation (2.159).

If v/ϵ is equal to an integer n , then from (2.132), one can find that the reflection coefficient $\beta(\lambda) \equiv 0$ by the following calculation:

$$(2.163) \quad \frac{1}{2\pi} \int_0^\infty \frac{|\beta(\lambda)|^2}{\lambda} d\lambda = 2\pi n - \frac{1}{\epsilon} \int_{-\infty}^\infty u(x) dx = 2\pi n - 2\pi v/\epsilon = 0.$$

According to the discussion in §2.2.5, a solution of the BO equation is a soliton solution if the corresponding reflection coefficient is identically equal to zero. This argument shows that if v/ϵ is an integer, the solution of the BO equation with the initial condition (2.150) is a soliton solution.

Kodama, Ablowitz, and Satsuma only calculated the eigenvalues corresponding to the special initial condition (2.150) in [40]. Since the functions $M(x; \lambda)$, $N(x; \lambda)$, $\bar{M}(x; \lambda)$ and $\bar{N}(x; \lambda)$ satisfy the equation (2.151), one can calculate them also by using the equation (2.157) and choosing appropriate values for w_0 and C based on their asymptotic behaviors as $|x| \rightarrow \infty$. We provide this calculation here. From the boundary condition (2.53), by choosing $w_0 = 0$ and $C = 1$ in the equation (2.157), the function $\bar{M}(x; \lambda)$ can be written in the form

$$(2.164) \quad \bar{M}(x; \lambda) = e^{i\lambda x/\epsilon} \left(\frac{x-i}{x+i} \right)^{v/\epsilon} - \frac{v}{\epsilon} \bar{M}(i; \lambda) e^{i\lambda x/\epsilon} \left(\frac{x-i}{x+i} \right)^{v/\epsilon} \int_{-\infty}^x \frac{1}{y-i} e^{-i\lambda y/\epsilon} \left(\frac{y+i}{y-i} \right)^{v/\epsilon} dy.$$

According to the boundary condition (2.54), by letting $w_0 = 0$ and

$$(2.165) \quad C = e^{-2\pi v i/\epsilon} + \frac{v}{\epsilon} \int_{-\infty}^\infty \frac{w^+(i)}{y-i} e^{-i\lambda y/\epsilon} \left(\frac{y+i}{y-i} \right)^{v/\epsilon} dy,$$

the function $N(x; \lambda)$ can be written as:

$$(2.166) \quad N(x; \lambda) = e^{i\lambda x/\epsilon} \left(\frac{x-i}{x+i} \right)^v e^{-2\pi v i/\epsilon} \\ + \frac{v}{\epsilon} N(i; \lambda) e^{i\lambda x/\epsilon} \left(\frac{x-i}{x+i} \right)^{v/\epsilon} \int_x^\infty \frac{1}{y-i} e^{-i\lambda y/\epsilon} \left(\frac{y+i}{y-i} \right)^{v/\epsilon} dy.$$

Similarly, from the boundary condition (2.52), by choosing $w_0 = 1$ and $C = 0$, the function $M(x; \lambda)$ can be written in the form

$$(2.167) \quad M(x; \lambda) = 1 + \frac{v}{\epsilon} e^{i\lambda x/\epsilon} \left(\frac{x-i}{x+i} \right)^{v/\epsilon} \left(- \int_{-\infty}^x \frac{M(i; \lambda)}{y-i} e^{-i\lambda y/\epsilon} \left(\frac{y+i}{y-i} \right)^{v/\epsilon} dy \right. \\ \left. + \int_{-\infty}^x \frac{2i}{y^2+1} e^{-i\lambda y/\epsilon} \left(\frac{y+i}{y-i} \right)^{v/\epsilon} dy \right).$$

According to the boundary condition (2.55), by letting $w_0 = 1$ and

$$(2.168) \quad C = \frac{v}{\epsilon} \left(\int_{-\infty}^\infty \frac{w^+(i)}{y-i} e^{-i\lambda y/\epsilon} \left(\frac{y+i}{y-i} \right)^{v/\epsilon} dy - \int_{-\infty}^\infty \frac{2i}{y^2+1} e^{-i\lambda y/\epsilon} \left(\frac{y+i}{y-i} \right)^{v/\epsilon} dy \right),$$

the function $\bar{N}(x; \lambda)$ can be written as:

$$(2.169) \quad \bar{N}(x; \lambda) = 1 + \frac{v}{\epsilon} e^{i\lambda x/\epsilon} \left(\frac{x-i}{x+i} \right)^{v/\epsilon} \left(\int_x^\infty \frac{\bar{N}(i; \lambda)}{y-i} e^{-i\lambda y/\epsilon} \left(\frac{y+i}{y-i} \right)^{v/\epsilon} dy \right. \\ \left. - \int_x^\infty \frac{2i}{y^2+1} e^{-i\lambda y/\epsilon} \left(\frac{y+i}{y-i} \right)^{v/\epsilon} dy \right).$$

After letting x in each side of the equation (2.167) tend to infinity and using the jump condition (2.69) and the boundary conditions (2.52), (2.54) and (2.55), one can write $\beta(\lambda)$ in the form

$$(2.170) \quad \beta(\lambda) = \frac{v}{\epsilon} e^{2v\pi i/\epsilon} \left(\int_{-\infty}^\infty \frac{2i}{y^2+1} e^{-i\lambda y/\epsilon} \left(\frac{y+i}{y-i} \right)^{v/\epsilon} dy \right. \\ \left. - \int_{-\infty}^\infty \frac{M(i; \lambda)}{y-i} e^{-i\lambda y/\epsilon} \left(\frac{y+i}{y-i} \right)^{v/\epsilon} dy \right).$$

In fact, the formulas (2.164), (2.166), (2.167), (2.169) and (2.170) do not determine $M(x; \lambda)$, $\overline{M}(x; \lambda)$, $N(x; \lambda)$, $\overline{N}(x; \lambda)$ and $\beta(\lambda)$, because $M(i; \lambda)$, $\overline{M}(i; \lambda)$, $N(i; \lambda)$ and $\overline{N}(i; \lambda)$ can not be determined from them.

As discussed above, the eigenvalues corresponding to the special initial condition (2.150) are the roots of the Laguerre polynomial of degree n scaled by $-2/\epsilon$, if $n = v/\epsilon$ is a positive integer. Here we use this fact and the asymptotic distribution of the roots of the Laguerre polynomial studied in [20, 47] to verify Matsuno's results given in §2.2.8, which has not previous been done. We first recall the definition of weak-* convergence.

Definition II.6. Let \mathbb{X} be a normed vector space. Then the dual space of \mathbb{X} consists of all bounded linear functionals on \mathbb{X} and is denoted by \mathbb{X}^* .

Definition II.7. Let \mathbb{X} be a normed vector space and \mathbb{X}^* be the dual space of \mathbb{X} . If $\phi_n, \phi \in \mathbb{X}^*$ and $\phi_n(x)$ converges pointwise to $\phi(x)$ for all $x \in \mathbb{X}$, then ϕ_n weak-* converges to $\phi(x)$.

The eigenvalues $\lambda_1, \lambda_2, \dots, \lambda_n$ are the roots of the polynomial $L_n(-2\lambda/\epsilon)$. Since the positive integer n is equal to v/ϵ , the polynomial $L_n(-2\lambda/\epsilon)$ can be written as $L_n(-2\lambda/\epsilon) = L_n(-2n\lambda/v)$. Then k_1, k_2, \dots, k_n are the roots of the polynomial $L_n(nk)$, where $k_j = -2\lambda_j/v$ for $j = 1, 2, \dots, n$. Let μ_n be the normalized counting measure of $\lambda_1, \lambda_2, \dots, \lambda_n$ defined by

$$(2.171) \quad \mu_n(\lambda) := \frac{1}{n} \sum_{j=1}^n \delta(\lambda - \lambda_j).$$

According to Theorem 3.1 in [20] and Theorem 1 in [47], $\lambda_1, \lambda_2, \dots, \lambda_n$ belong to the interval $[-2v, 0]$ and the measure μ_n converges in the weak-* sense to μ , where μ is a measure with density $f(\lambda)$ defined by

$$(2.172) \quad f(\lambda) = -\frac{\sqrt{-2v\lambda - \lambda^2}}{\pi\lambda v} d\lambda, \quad \lambda \in [-2v, 0]$$

and the support of the measure μ is $[-2v, 0]$. That is, for each continuous function $g : [-2v, 0] \rightarrow \mathbb{C}$,

$$(2.173) \quad \lim_{n \rightarrow \infty} \int_{-2v}^0 g(k) d\mu_n(k) = \int_{-2v}^0 g(k) d\mu(k).$$

Here, μ_n and μ belong to the dual space of $\mathbb{C}([-2v, 0])$, where $\mathbb{C}([-2v, 0])$ is the function space consisting of all continuous functions on $[-2v, 0]$.

Based on this result, the equation (2.141) with $k = 1$ and the definition of the eigenvalue density function $F(\lambda)$ given in §2.2.8, one can find $F(\lambda) \equiv 0$ for $\lambda \notin [-2v, 0]$ and

$$(2.174) \quad \begin{aligned} F(\lambda) &= -\frac{\sqrt{-2v\lambda - \lambda^2}}{\pi\lambda v} \times \frac{1}{2\pi} \int_{-\infty}^{\infty} u(x, 0) dx \\ &= -\frac{\sqrt{-2v\lambda - \lambda^2}}{\pi\lambda v} \times v \\ &= -\frac{\sqrt{-2v\lambda - \lambda^2}}{\pi\lambda}, \quad \lambda \in [-2v, 0]. \end{aligned}$$

On the other hand, one can use Matsuno's results introduced in §2.2.8 to calculate the eigenvalue density function $F(\lambda)$ directly. Since the maximum of the function $u_0(x)$ is $2v$, $F(\lambda) \equiv 0$ for $\lambda \notin [-2v, 0]$. Then by using the equation (2.149), one can calculate $F(\lambda)$ for $\lambda \in [-2v, 0]$:

$$(2.175) \quad \begin{aligned} F(\lambda) &= \frac{1}{2\pi} \int_{\{x \in \mathbb{R}, u_0(x) > -\lambda\}} dx \\ &= \frac{1}{2\pi} \int_{-\sqrt{-2v/\lambda-1}}^{\sqrt{-2v/\lambda-1}} dx \\ &= -\frac{\sqrt{-2v\lambda - \lambda^2}}{\pi\lambda}, \quad \lambda \in [-2v, 0]. \end{aligned}$$

The formulas for the eigenvalue density function $F(\lambda)$ obtained via two different methods are the same, which verifies Matsuno's result.

CHAPTER III

Zero dispersion limit of the BO equation for positive initial conditions

In this chapter, we study the zero-dispersion limit of the Cauchy problem of the BO equation with a suitable initial condition¹.

3.1 The Scattering Data in the Zero-Dispersion Limit

In this section, we give the definition of admissible initial conditions and an asymptotic approximation of the scattering data $\{\beta(\lambda), \{\lambda_n\}_{n=1}^N, \{\gamma_n\}_{n=1}^N\}$ corresponding to admissible initial conditions valid for small $\epsilon > 0$. Even though u_0 is independent of ϵ , the scattering data depend on ϵ since the parameter ϵ appears in the equation (2.26). The asymptotic approximation of $\beta(\lambda)$ and $\{\lambda_n\}_{n=1}^N$ is based on Matsuno's method introduced in §2.2.8.

3.1.1 Admissible Initial Conditions

The initial conditions for the BO equation (1.1) that we will consider in this chapter are the admissible initial conditions defined in Definition III.1. Many of the conditions in Definition III.1 are imposed for our convenience; we make no claim that they are necessary.

¹The content of this chapter is taken almost verbatim from [56] and some modifications and reorganization are done to make this dissertation more readable.

Definition III.1. A function $u_0 : \mathbb{R} \rightarrow \mathbb{R}$ is called an *admissible initial condition* if the following properties hold true:

Smoothness: $u_0 \in C^3(\mathbb{R})$.

Positivity: $u_0(x) > 0$ for all $x \in \mathbb{R}$.

Existence of a Unique Critical Point: There is a unique point $x_0 \in \mathbb{R}$ for which $u_0'(x_0) = 0$. Moreover,

$$(3.1) \quad u_0''(x_0) < 0,$$

making x_0 the global maximizer of u_0 .

Tail Behavior: $\lim_{x \rightarrow \pm\infty} u_0(x) = 0$, and

$$(3.2) \quad \lim_{x \rightarrow \pm\infty} |x|^{q+1} u_0'(x) = C_{\pm} \quad \text{for some } q > 1,$$

where $C_+ < 0$ and $C_- > 0$ are constants. These two conditions imply that an admissible initial condition u_0 also satisfies

$$(3.3) \quad \lim_{x \rightarrow \pm\infty} |x|^q u_0(x) = \mp \frac{C_{\pm}}{q}.$$

Inflection Points: In each bounded interval there exist at most finitely many points $x = \xi$ at which $u_0''(\xi) = 0$, and each is a simple inflection point: $u_0'''(\xi) \neq 0$.

An admissible initial condition $u_0(x)$ satisfies all the conditions used in §2.2.8 where we introduced Matsuno's method. The results in §2.2.8 are valid for the admissible initial condition $u_0(x)$. From the equation (2.141), one can see that the function $F(\lambda)$ introduced in §2.2.8 satisfies

$$(3.4) \quad \int_{-L}^0 F(\lambda) d\lambda = M,$$

where the positive constant L is defined by

$$(3.5) \quad L := \max_{x \in \mathbb{R}} u_0(x),$$

and the *mass* M is defined by

$$(3.6) \quad M := \frac{1}{2\pi} \int_{\mathbb{R}} u_0(x) dx.$$

Here, the tail behavior (3.3) and the boundness of u_0 ensure that the mass M is finite. In fact, since u_0 is an admissible initial condition, the function $F(\lambda)$ can be written in the form

$$(3.7) \quad F(\lambda) := \frac{1}{2\pi} (x_+(\lambda) - x_-(\lambda)), \quad -L \leq \lambda < 0,$$

where the *turning points* $x_{\pm} : [-L, 0) \rightarrow \mathbb{R}$ are two monotone branches of the inverse function of u_0 and satisfy

$$(3.8) \quad u_0(x_{\pm}(\lambda)) = -\lambda \quad \text{and} \quad x_-(\lambda) \leq x_0 \leq x_+(\lambda) \quad \text{for} \quad -L \leq \lambda < 0.$$

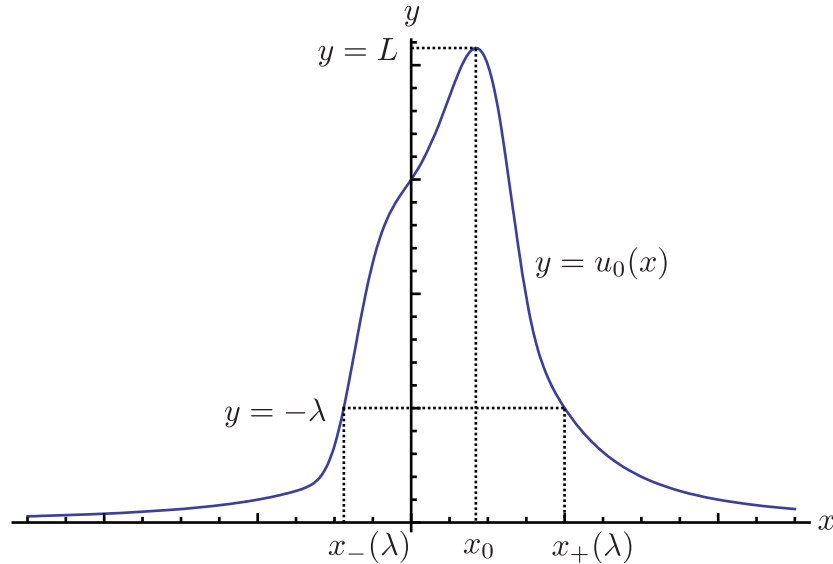


Figure 3.1: The graph of an admissible initial condition and the turning points $x_{\pm}(\lambda)$.

By choosing $k = 1$ in the equation (2.139), one can obtain

$$(3.9) \quad \lim_{\epsilon \downarrow 0} \epsilon N = M,$$

which suggests the number of eigenvalues is asymptotically proportional to $1/\epsilon$.

3.1.2 Formula for Phase Constants

The WKB methods recalled by Lax and Levermore [43] to analyze the Schrödinger equation in the forward problem for the zero-dispersion limit of the KdV equation were sufficiently powerful to provide asymptotic formulae for both the discrete spectrum (via Bohr-Sommerfeld quantization of the Weyl formula that is the analogue in the KdV theory of the function $F(\lambda)$ obtained by Matsuno) and also for the “norming constants” that in the KdV theory are the analogues of the phase constants $\{\gamma_n\}_{n=1}^N$ in the BO theory. However, we have not found a way to apply these methods to the nonlocal operator \mathcal{L} , and unfortunately Matsuno’s method does not provide approximations of the phase constants $\{\gamma_n\}_{n=1}^N$ since they do not enter into the equation (2.131).

Our contribution to the theory of the spectral analysis of the nonlocal operator \mathcal{L} in the zero-dispersion limit is to provide a new asymptotic formula for the phase constants. It is difficult to motivate the formula as it arises from the analysis of the inverse problem that we will describe in the next section, but it is nonetheless quite easy to present. If $\lambda < 0$ is an eigenvalue of \mathcal{L} with potential u given by an admissible initial condition u_0 , then our approximation to the corresponding phase constant is given in terms of the turning points $x_{\pm}(\lambda)$ as follows:

$$(3.10) \quad \gamma \approx \gamma(\lambda) := -\frac{1}{2}(x_+(\lambda) + x_-(\lambda)), \quad -L \leq k < 0.$$

Remark III.2. Our choice of $\gamma(\lambda)$ in terms of u_0 is specifically designed to ensure the convergence of $\tilde{u}_{\epsilon}(x, t)$ (to be defined precisely in Definition III.3 below) at $t = 0$ to the given ϵ -independent initial condition u_0 .

3.1.3 Modification of the Cauchy Data

Based on the above considerations, we may now make very precise definitions of formal (not rigorously justified) approximations of the scattering data corresponding to an admissible condition u_0 . The first approximation is to neglect the reflection coefficient by setting

$$(3.11) \quad \tilde{\beta}(\lambda) := 0, \quad \lambda > 0.$$

Next we define the exact number of approximate eigenvalues (hopefully also the approximate number of exact eigenvalues) by setting

$$(3.12) \quad N(\epsilon) := \left\lfloor \frac{M}{\epsilon} \right\rfloor,$$

which in particular implies that

$$(3.13) \quad \lim_{\epsilon \downarrow 0} \epsilon N(\epsilon) = M.$$

Then we define approximations to the eigenvalues themselves as an ordered set of numbers $\{\tilde{\lambda}_n\}_{n=1}^{N(\epsilon)} \subset (-L, 0)$ obtained by quantizing the Matsuno eigenvalue density given by (3.7):

$$(3.14) \quad \int_{-L}^{\tilde{\lambda}_n} F(\lambda) d\lambda = \epsilon \left(n - \frac{1}{2} \right), \quad n = 1, 2, \dots, N(\epsilon).$$

Finally, we define approximations to the corresponding phase constants as numbers $\{\tilde{\gamma}_n\}_{n=1}^{N(\epsilon)}$ given precisely by

$$(3.15) \quad \tilde{\gamma}_n := \gamma(\tilde{\lambda}_n), \quad n = 1, \dots, N(\epsilon).$$

where $\gamma(\cdot)$ is defined by (3.10).

Now in our analysis of the Cauchy problem for the BO equation with admissible initial data u_0 we take a sideways step that is not *a priori* justified: we simply

replace the true solution $u_\epsilon(x, t)$ of the Cauchy problem with a family $\tilde{u}_\epsilon(x, t)$ of exact solutions of the BO equation (1.1) with the property that for each $\epsilon > 0$ the scattering data for $\tilde{u}_\epsilon(x, t)$ at time $t = 0$ is *exactly* the approximate scattering data just defined. This step was also an important part of the method of Lax and Levermore [43]. We formalize this modification of the initial data in the following definition.

Definition III.3. Let u_0 be an admissible initial condition. Then, by $\tilde{u}_\epsilon(x, t)$ we mean the exact solution of the BO equation (1.1) given for each $\epsilon > 0$ by the reflectionless inverse-scattering formula

$$(3.16) \quad \tilde{u}_\epsilon(x, t) := 2\epsilon \frac{\partial}{\partial x} \Im \{ \log(\tilde{\tau}_\epsilon(x, t)) \},$$

where

$$(3.17) \quad \tilde{\tau}_\epsilon(x, t) := \det \left(\mathbb{I} + i\epsilon^{-1} \tilde{\mathbf{A}}_\epsilon \right)$$

and where $\tilde{\mathbf{A}}_\epsilon = \tilde{\mathbf{A}}_\epsilon(x, t)$ is an $N(\epsilon) \times N(\epsilon)$ Hermitean matrix with elements

$$(3.18) \quad (\tilde{\mathbf{A}}_\epsilon)_{nm} := \frac{2i\epsilon \sqrt{\tilde{\lambda}_n \tilde{\lambda}_m}}{\tilde{\lambda}_n - \tilde{\lambda}_m}, \quad n \neq m$$

and

$$(3.19) \quad (\tilde{\mathbf{A}}_\epsilon)_{nn} := -2\tilde{\lambda}_n(x + 2\tilde{\lambda}_n t + \tilde{\gamma}_n) = -2\tilde{\lambda}_n(x + 2\tilde{\lambda}_n + \gamma(\tilde{\lambda}_n)).$$

Here the number $N(\epsilon)$ is defined by (3.12) and the components of the scattering data $\{\tilde{\lambda}_n\}_{n=1}^{N(\epsilon)}$ and $\{\tilde{\gamma}_n\}_{n=1}^{N(\epsilon)}$ are given explicitly by (3.14) and (3.15) respectively.

While it is not the case that $\tilde{u}_\epsilon(x, 0) = u_0(x)$ in general, the relevance of this definition in connection with the Cauchy problem with initial condition u_0 is a consequence of Corollary III.6 in §3.2, which guarantees convergence in the mean square

sense of $\tilde{u}_\epsilon(\cdot, 0)$ to $u_0(\cdot)$ as $\epsilon \downarrow 0$. This modification of the initial data is an analogue of the replacement of the true scattering data by its reflectionless WKB approximation in the Lax-Levermore theory.

Before introducing our main result about $\tilde{u}_\epsilon(x, t)$ we note that Definition III.1 implies a number of properties of the functions F and γ that will be useful later, so we take the opportunity to record these here. Note that F and γ will frequently occur in the context of the following functions:

$$(3.20) \quad D(\lambda; x, t) := -2\lambda(x + 2\lambda t + \gamma(\lambda)), \quad -L < \lambda < 0,$$

and

$$(3.21) \quad \varphi(\lambda) := \sqrt{-\lambda F(\lambda)}, \quad -L < \lambda < 0.$$

Lemma III.4. *Let u_0 be an admissible initial condition with decay exponent $q > 1$, and let $F : [-L, 0) \rightarrow \mathbb{R}$ be defined by (3.7) and $\gamma : [-L, 0) \rightarrow \mathbb{R}$ be defined by (3.10). Then F and γ both belong to $C^{(1)}(-L, 0)$ and F and F' are strictly positive on this open interval. Also, there exists a sufficiently small constant $\delta > 0$ and positive constants C_{-L} and C_0 such that*

$$(3.22) \quad \frac{1}{2}C_{-L}\sqrt{L + \lambda} < F(\lambda) < C_{-L}\sqrt{L + \lambda},$$

and

$$(3.23) \quad \frac{1}{4} \frac{C_{-L}}{\sqrt{L + \lambda}} < F'(\lambda) < \frac{1}{2} \frac{C_{-L}}{\sqrt{L + \lambda}}$$

both hold for $-L < \lambda < -L + \delta$, while

$$(3.24) \quad \frac{1}{2}C_0(-\lambda)^{-1/q} < F(\lambda) < C_0(-\lambda)^{-1/q},$$

and

$$(3.25) \quad \frac{1}{2} \frac{C_0}{q} (-\lambda)^{-1/q-1} < F'(\lambda) < \frac{C_0}{q} (-\lambda)^{-1/q-1}$$

both hold for $-\delta < \lambda < 0$. Also,

$$(3.26) \quad |\gamma(\lambda) + x_0| \leq \pi F(\lambda) \quad \text{and} \quad |\gamma'(\lambda)| \leq \pi F'(\lambda), \quad -L \leq \lambda < 0,$$

inequalities that when combined with (3.22)–(3.25) imply obvious upper bounds for $|\gamma(\lambda) + x_0|$ and $|\gamma'(\lambda)|$.

In particular, these estimates show that $F(\lambda)$ is integrable, and $\varphi(\lambda)$ and $D(\lambda; x, t)$ (and hence also $\lambda x_{\pm}(\lambda)$) are bounded, and that with $\sigma = \min(\frac{1}{2}, 1 - \frac{1}{q}) \in (0, 1)$, $\varphi(\cdot)$ is Hölder continuous with exponent $\sigma/2$ while $D(\cdot; x, t)$ is Hölder continuous with exponent σ uniformly for (x, t) in compact sets, on $(-L, 0)$.

Proof. The turning points $x_{\pm}(\lambda)$ are clearly of class $C^{(1)}(-L, 0)$, by definition $x_+(\lambda) > x_0 > x_-(\lambda)$ on this open interval, and moreover $x_+(\lambda)$ is strictly increasing while $x_-(\lambda)$ is strictly decreasing on $(-L, 0)$. These facts immediately imply the desired basic smoothness properties of F and γ , and the positivity and monotonicity of F , as well as the inequalities (3.26).

Since $u_0(x_0) = L$ and $u'_0(x_0) = 0$, the $C^{(2)}(\mathbb{R})$ function u_0 satisfies

$$(3.27) \quad \lim_{x \rightarrow x_0} \frac{u_0(x) - L}{(x - x_0)^2} = \frac{u''_0(x_0)}{2} \quad \text{and} \quad \lim_{x \rightarrow x_0} \frac{u'_0(x)}{x - x_0} = u''_0(x_0).$$

Using these together with the inequality $u''_0(x_0) < 0$, the definition of $x_{\pm}(\lambda)$ as branches of the inverse function of u_0 shows that

$$(3.28) \quad \lim_{\lambda \downarrow -L} \frac{\pm(x_{\pm}(\lambda) - x_0)}{\sqrt{L + \lambda}} = \sqrt{\frac{2}{-u''_0(x_0)}} \quad \text{and} \quad \lim_{\lambda \downarrow -L} \pm x'_{\pm}(\lambda) \sqrt{L + \lambda} = \sqrt{\frac{1}{-2u''_0(x_0)}}.$$

Using these relations in (3.7) and (3.10) establishes the existence of the limits

$$(3.29) \quad \lim_{\lambda \downarrow -L} \frac{F(\lambda)}{\sqrt{L + \lambda}} = \frac{1}{\pi} \sqrt{\frac{2}{-u''_0(x_0)}} \quad \text{and} \quad \lim_{\lambda \downarrow -L} F'(\lambda) \sqrt{L + \lambda} = \frac{1}{2\pi} \sqrt{\frac{2}{-u''_0(x_0)}},$$

which prove the two-sided estimates (3.22) and (3.23).

Next, note that the decay conditions (3.2) and (3.3) for u_0 and its derivative together imply that

$$(3.30) \quad \lim_{\lambda \uparrow 0} x_{\pm}(\lambda)(-\lambda)^{\frac{1}{q}} = \pm \left(\mp \frac{C_{\pm}}{q} \right)^{\frac{1}{q}} \quad \text{and} \quad \lim_{\lambda \uparrow 0} x'_{\pm}(\lambda)(-\lambda)^{\frac{1}{q}+1} = \pm \frac{1}{q} \left(\mp \frac{C_{\pm}}{q} \right)^{\frac{1}{q}},$$

where $\mp C_{\pm}$ are the positive constants in (3.2) and (3.3). It follows from (3.7) that

$$(3.31) \quad \lim_{\lambda \uparrow 0} F(\lambda)(-\lambda)^{\frac{1}{q}} = \frac{1}{2\pi} \left[\left(-\frac{C_+}{q} \right)^{\frac{1}{q}} + \left(\frac{C_-}{q} \right)^{\frac{1}{q}} \right],$$

which proves (3.24) and

$$(3.32) \quad \lim_{\lambda \uparrow 0} F'(\lambda)(-\lambda)^{\frac{1}{q}+1} = \frac{1}{2\pi q} \left[\left(-\frac{C_+}{q} \right)^{\frac{1}{q}} + \left(\frac{C_-}{q} \right)^{\frac{1}{q}} \right],$$

which proves (3.25). □

3.2 The Inverse-Scattering Problem in the Zero-Dispersion Limit

In this section, we provide our main result and its proof.

3.2.1 Main Theorem

The main result of our analysis is easy to state, but first we need to recall some basic facts about the inviscid Burgers equation obtained from (1.1) simply by setting $\epsilon = 0$. For general sufficiently smooth initial data $u^B(x, 0) = u_0(x)$ the inviscid Burgers equation

$$(3.33) \quad \frac{\partial u^B}{\partial t} + 2u^B \frac{\partial u^B}{\partial x} = 0$$

does not have a global solution due to gradient catastrophe (shock formation) in finite time. It does have a global solution as a real multi-sheeted surface over the (x, t) -plane, which can be obtained by the method of characteristics. The sheets of this surface are obtained as the real solutions of the implicit equation

$$(3.34) \quad u^B = u_0(x - 2u^B t),$$

and by implicit differentiation it is easy to verify that away from singularities each sheet of the surface is a function $u^B = u^B(x, t)$ that satisfies (3.33). A simple consequence of the Implicit Function Theorem is that for sufficiently small $|t|$ there is a unique solution of (3.34) for all $x \in \mathbb{R}$. New sheets of the multivalued solution are born from *breaking points* in the (x, t) -plane that are in one-to-one correspondence with generic inflection points ξ of u_0 for which $u'_0(\xi) \neq 0$ but $u''_0(\xi) = 0$. If $\xi \in \mathbb{R}$ is such a point, then the corresponding breaking point is given by

$$(3.35) \quad (x_\xi, t_\xi) := \left(\xi - \frac{u_0(\xi)}{u'_0(\xi)}, -\frac{1}{2u'_0(\xi)} \right).$$

Each such breaking point is the location of a pitchfork bifurcation for u^B with respect to t holding $x - 2u_0(\xi)t = \xi$ fixed, with two new branches emerging as $|t|$ increases. Thus, assuming that u'_0 is a bounded function of total integral zero, the solution of the Cauchy problem for (3.33) is classical for

$$(3.36) \quad T_- := -\frac{1}{2 \max_{x \in \mathbb{R}} u'_0(x)} < t < -\frac{1}{2 \min_{x \in \mathbb{R}} u'_0(x)} =: T_+.$$

Note that under our assumptions on u'_0 we have $T_- < 0 < T_+$. Also, T_- is the supremum of all $t_\xi < 0$ while T_+ is the infimum of all $t_\xi > 0$. When we consider the Cauchy problem for $t > 0$, we will refer to $T := T_+$ as the *breaking time*.

For $t/t_\xi > 1$ there are *caustic curves* $x_\xi^-(t) < x_\xi^+(t)$ with limiting values as $t \rightarrow t_\xi$ given by $x_\xi^-(t_\xi) = x_\xi^+(t_\xi) = x_\xi$ that bound the triply-folded region emerging from (x_ξ, t_ξ) . The caustic curves correspond to double roots of (3.34), and crossing one of them at a generic point results in a change in the number of sheets by exactly two. Except along the union of the caustic curves and the breaking points from which they emerge, the number of solutions of (3.34) is always odd, and all are simple roots. See Figure 3.2.

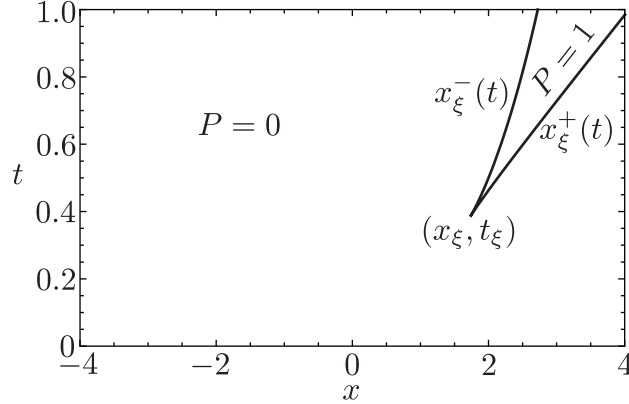


Figure 3.2: Except along the caustic curves $x = x_\xi^-(t)$ and $x = x_\xi^+(t)$ the number of solutions of (3.34) is of the form $2P + 1$, and these solutions are simple roots. For this figure, $u_0(x) := 2(1 + x^2)^{-1}$.

For the initial data $u_0(x) = 2(1 + x^2)^{-1}$ used in Figure 1.1, the breaking time before which there is a unique solution for all $x \in \mathbb{R}$ and after which there is an expanding interval in which there are three solutions, is exactly $T = 2\sqrt{3}/9 \approx 0.3849$. Snapshots of the evolution of the multivalued solution of (3.33) for this initial data are shown in Figure 3.3. Our result is then the following.

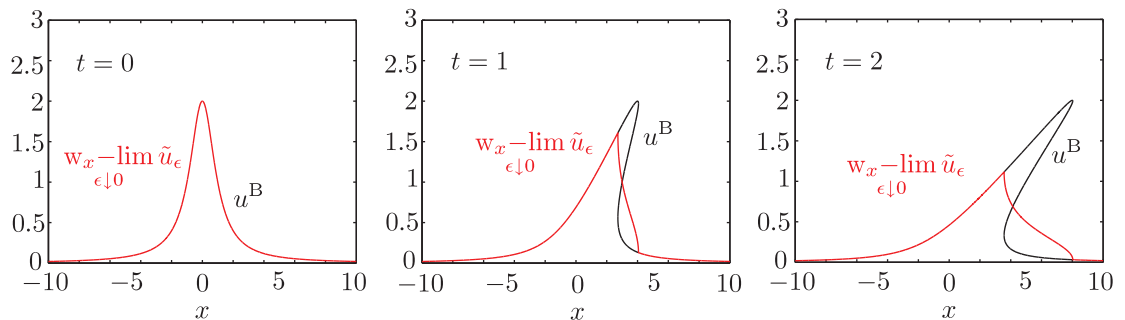


Figure 3.3: The multivalued solution (black) of (3.33) and the signed sum of branches (red) corresponding to $u_0(x) = 2(1 + x^2)^{-1}$. Left: $t = 0$. Middle: $t = 1$. Right: $t = 2$. Before the breaking time as well as afterwards but outside the oscillation interval there is only one solution branch and hence no difference between the red and black curves.

Theorem III.5. Let $u_0^B(x, t) < u_1^B(x, t) < \dots < u_{2P}^B(x, t)$ be the branches of

the multivalued (method of characteristics) solution of the inviscid Burgers' equation (3.33) subject to an admissible initial condition $u^{\text{B}}(x, 0) = u_0(x)$. Then, the weak $L^2(\mathbb{R})$ (in x) limit of $\tilde{u}_\epsilon(x, t)$ is given by

$$(3.37) \quad \text{w}_x\text{-}\lim_{\epsilon \downarrow 0} \tilde{u}_\epsilon(x, t) = \sum_{n=0}^{2P(x,t)} (-1)^n u_n^{\text{B}}(x, t),$$

uniformly for t in arbitrary bounded intervals. Note that the right-hand side extends by continuity to the caustic curves.

The signed sum of branches that is the weak limit is illustrated with red curves in Figure 3.3 for the same initial data as in Figure 1.1. Of course convergence in the weak $L^2(\mathbb{R})$ (in x) topology means that for every $v \in L^2(\mathbb{R})$, we have

$$(3.38) \quad \lim_{\epsilon \downarrow 0} \int_{\mathbb{R}} \tilde{u}_\epsilon(x, t) v(x) dx = \int_{\mathbb{R}} \left[\sum_{n=0}^{2P(x,t)} (-1)^n u_n^{\text{B}}(x, t) \right] v(x) dx$$

with the limit being uniform with respect to t in arbitrary bounded intervals. Thus, the weak limit essentially smooths out the rapid oscillations seen in Figure 1.1 and (if we think of v as the indicator function of a mesoscale interval) represents a kind of local average in x .

For t before the breaking time T for the inviscid Burgers' equation, the weak limit guaranteed by Theorem III.5 may be strengthened as follows.

Corollary III.6. *Suppose that $0 \leq t < T$, so that $P(x, t) = 0$ for all $x \in \mathbb{R}$ (that is, the solution $u^{\text{B}} = u_0^{\text{B}}(x, t)$ of the inviscid Burgers' equation with initial data $u_0(x)$ is classical). Then*

$$(3.39) \quad \lim_{\epsilon \downarrow 0} \tilde{u}_\epsilon(x, t) = u_0^{\text{B}}(x, t)$$

with the limit being in the (strong) $L^2(\mathbb{R}_x)$ topology.

It should be pointed out that the weak limit formula (3.37) is much more explicit than the corresponding formula found by Lax and Levermore [43, 44, 45] for the weak zero-dispersion limit of the Cauchy problem for the KdV equation. Indeed, the latter requires the solution, for each x and t , of a constrained functional variational problem, which can be solved in closed form only for the simplest initial data.

3.2.2 Basic Strategy. Outline of the Proof of Main Theorem

According to Definition III.3, $\tilde{u}_\epsilon(x, t)$ is expressed in terms of the determinant $\tilde{\tau}_\epsilon$ as follows:

$$(3.40) \quad \tilde{u}_\epsilon(x, t) = \frac{\partial \tilde{U}_\epsilon}{\partial x}(x, t), \quad \tilde{U}_\epsilon(x, t) = 2\epsilon \Im\{\log(\tilde{\tau}_\epsilon(x, t))\}.$$

As the logarithm of a complex-valued quantity is involved, $\tilde{U}_\epsilon(x, t)$ is only defined modulo $4\pi\epsilon$ for each (x, t) , and naturally one should choose the appropriate branch for each (x, t) to achieve continuity. We do this concretely in equation (3.42) below.

At this very early point our analysis must take a very different path than that followed by Lax and Levermore [43] in their study of the zero-dispersion limit for the KdV equation. Indeed, the expansion of $\tilde{\tau}_\epsilon$ in principal minors that is at the heart of the Lax-Levermore method would be a poor choice in this situation. One reason for this is simply that the principal-minors expansion of $\tilde{\tau}_\epsilon(x, t)$ consists of complex-valued terms of indefinite phase, so the sum cannot be easily estimated by its largest term. But a more important reason is that the formula (3.40) for $\tilde{U}_\epsilon(x, t)$ involves not $\log(\tilde{\tau}_\epsilon)$ but rather $\Im\{\log(\tilde{\tau}_\epsilon)\}$, that is, we require an estimate of the *phase* of the determinant and we are not interested in its magnitude.

So instead of expanding the determinant as a sum, we write it as a product. Let $\{\alpha_n\}_{n=1}^{N(\epsilon)}$ be the real eigenvalues of $\tilde{\mathbf{A}}_\epsilon(x, t)$. Then the corresponding eigenvalues of $\mathbb{I} + i\epsilon^{-1}\tilde{\mathbf{A}}_\epsilon(x, t)$ are of course $\{1 + i\epsilon^{-1}\alpha_n\}_{n=1}^{N(\epsilon)}$, so we may expand $\tilde{\tau}_\epsilon$ as a product

over eigenvalues in the form:

$$(3.41) \quad \tilde{\tau}_\epsilon(x, t) = \prod_{n=1}^{N(\epsilon)} (1 + i\epsilon^{-1}\alpha_n).$$

This yields a suggestive formula for $\tilde{U}_\epsilon(x, t)$ in terms of the eigenvalues of $\tilde{\mathbf{A}}_\epsilon$:

$$(3.42) \quad \tilde{U}_\epsilon(x, t) := \epsilon \sum_{n=1}^{N(\epsilon)} 2 \arctan(\epsilon^{-1}\alpha_n).$$

Here $-\pi/2 < \arctan(\cdot) < \pi/2$, so in particular by this definition we have made an unambiguous choice of the branch of the logarithm. This formula seems at first not to be of much use because, unlike the principal minor determinants in the Lax-Levermore method which can be written explicitly in terms of the matrix elements, the eigenvalues of $\tilde{\mathbf{A}}_\epsilon$ are only implicitly known. However, numerical experiments suggest that some structure emerges in the limit $\epsilon \downarrow 0$. Indeed, the plots shown in Figure 3.4 provide good evidence that the normalized (to mass M) counting measures

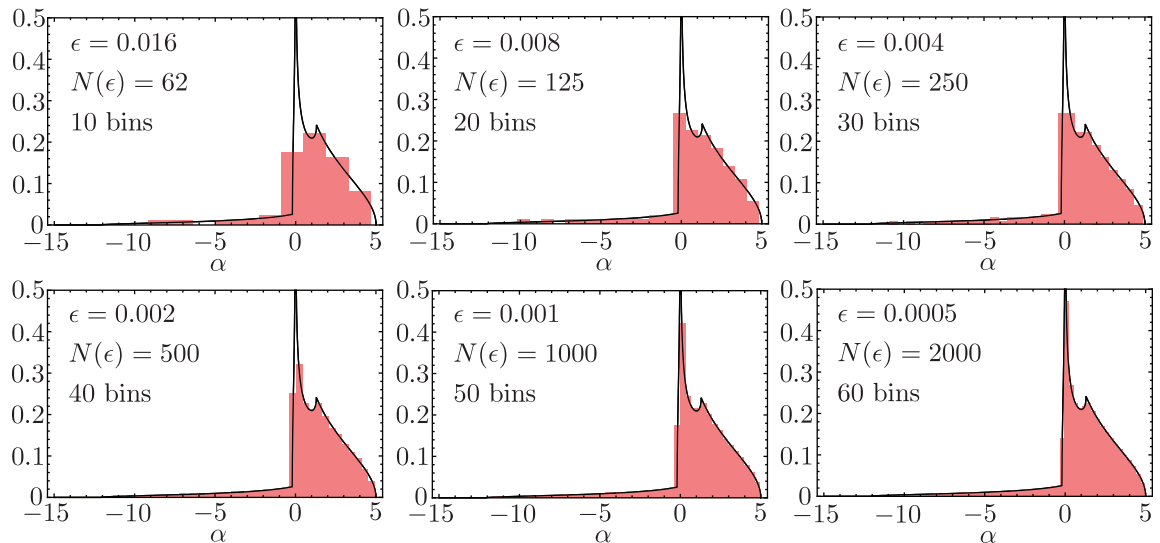


Figure 3.4: Histograms of eigenvalues of $\tilde{\mathbf{A}}_\epsilon$ corresponding to the initial condition $u_0(x) := 2(1+x^2)^{-1}$, $x = 5$, and $t = 2$, normalized to have total area $M = 1$, compared with the density $G(\alpha; x, t)$ of the limiting absolutely continuous measure μ .

μ_ϵ given for $\epsilon > 0$ by

$$(3.43) \quad \mu_\epsilon := \frac{M}{N(\epsilon)} \sum_{n=1}^{N(\epsilon)} \delta_{\alpha_n}, \quad \{\alpha_n\}_{n=1}^{N(\epsilon)} \text{ eigenvalues of } \tilde{\mathbf{A}}_\epsilon$$

might converge in some sense to a measure μ having a density $G(\alpha; x, t)$. This convergence suggests further that the formula (3.42) could be interpreted as a Riemann sum, for the integral of $\pi \operatorname{sgn}(\alpha)$ (the pointwise limit as $\epsilon \downarrow 0$ of the summand) against the limiting measure μ . We will prove that indeed $\tilde{U}_\epsilon(x, t)$ converges, uniformly with respect to x and t in compact sets, to a limit function $U(x, t)$ given by such an integral in the limit $\epsilon \downarrow 0$.

To obtain an effective formula for $U(x, t)$ we need to analyze the asymptotic behavior of the measures μ_ϵ . This part of our analysis is modeled after the work of Wigner [71, 72] on the statistical distribution of eigenvalues of random Hermitian matrices with independent and identically distributed matrix elements. Like Wigner, we use the method of moments because while the measures themselves are not easy to express in terms of the matrix elements, their moments are:

$$(3.44) \quad \int_{\mathbb{R}} \alpha^p d\mu_\epsilon(\alpha) = \frac{M}{N(\epsilon)} \sum_{n=1}^{N(\epsilon)} \alpha_n^p = \frac{M}{N(\epsilon)} \operatorname{tr}(\tilde{\mathbf{A}}_\epsilon^p), \quad p = 0, 1, 2, \dots$$

We prove the existence of the limit of the right-hand side in equation (3.44) as $\epsilon \downarrow 0$ for every p using the fact that for small ϵ the matrix $\tilde{\mathbf{A}}_\epsilon$ concentrates near the diagonal, where it can be approximated by the product of a diagonal matrix and the Toeplitz matrix corresponding to the symbol $f(\theta) := i(\pi - \theta)$, $0 < \theta < 2\pi$ (of singular Fisher-Hartwig type due to jump discontinuities). The result of this asymptotic analysis of moments is the following Proposition, the proof of which will be given below in §3.2.3.

Proposition III.7. *For each nonnegative integer p ,*

$$(3.45) \quad \lim_{\epsilon \downarrow 0} \int_{\mathbb{R}} \alpha^p d\mu_\epsilon(\alpha) = Q_p,$$

with the limit being uniform with respect to (x, t) in any compact set, where

$$(3.46) \quad Q_p := \frac{1}{2\pi(p+1)} \int_{-L}^0 [(x + 2\lambda t - x_-(\lambda))^{p+1} - (x + 2\lambda t - x_+(\lambda))^{p+1}] (-2\lambda)^p d\lambda.$$

Given these limiting moments, the next task is to establish the existence of a corresponding limiting measure μ with these moments, and to prove the existence of the limit $\tilde{U}_\epsilon(x, t) \rightarrow U(x, t)$. A remarkable feature of this analysis is that the solution of the moment problem for μ is carried out by virtually the same procedure as Matsuno used to obtain the function $F(\lambda)$ from u_0 (see §2.2.8). Our result is the following Proposition, that will be proved in all details in §3.2.4.

Proposition III.8. *Uniformly for (x, t) in compact sets,*

$$(3.47) \quad \lim_{\epsilon \downarrow 0} \tilde{U}_\epsilon(x, t) = U(x, t),$$

where

$$(3.48) \quad U(x, t) := \int_{\mathbb{R}} \pi \operatorname{sgn}(\alpha) d\mu(\alpha)$$

and where μ is an absolutely continuous measure of mass M with density $G(\alpha; x, t)$, and

$$(3.49) \quad G(\alpha; x, t) := -\frac{1}{4\pi} \int_{-L}^0 \chi_{[-2\lambda(x+2\lambda t-x_+(\lambda)), -2\lambda(x+2\lambda t-x_-(\lambda))]}(\alpha) \frac{d\lambda}{\lambda}.$$

Here, $\chi_{[a,b]}(z)$ denotes the indicator function of the interval $[a, b]$.

The limiting measure μ is the closest analogue in the zero-dispersion theory of the BO equation of the equilibrium (or extremal) measure arising in the Lax-Levermore theory of the KdV equation. But a significant difference is that in this case the measure μ is specified *explicitly* rather than implicitly as the solution of a variational problem.

The region of integration in the double integral obtained by combining (3.49) with (3.48) is illustrated for three different values of (x, t) in Figure 3.5. The points

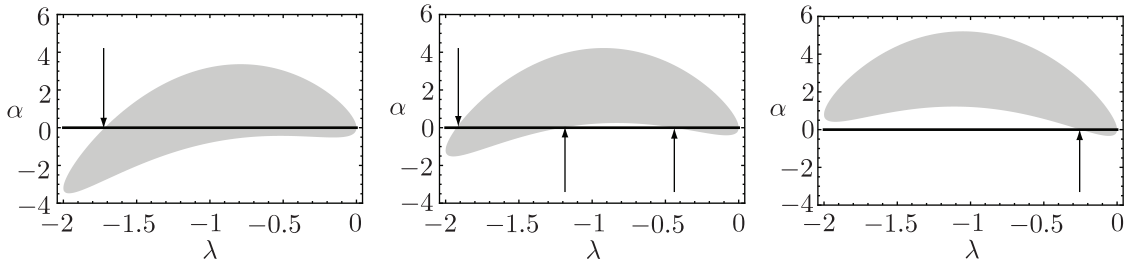


Figure 3.5: The region of integration $-2\lambda(x + 2\lambda t - x_+(\lambda)) < \alpha < -2\lambda(x + 2\lambda t - x_-(\lambda))$ for $u_0(x) = 2(1 + x^2)^{-1}$ with $t = 0.7$. Left: $x = 2$ (to the left of the oscillatory region for $u_\epsilon(x, t)$). Center: $x = 2.5$ (within the oscillatory region for $u_\epsilon(x, t)$). Right: $x = 3$ (to the right of the oscillatory region for $u_\epsilon(x, t)$). The line $\alpha = 0$ of discontinuity of the integrand is superimposed, and the intersections of the boundary with this line are indicated with arrows.

where the boundary curves of this region intersect the line $\alpha = 0$ (where the integrand is discontinuous) obviously will play an important role in the differentiation of $U(x, t)$ with respect to x . Moreover, these intersection points correspond (simply by changing the sign) to the branches of the multivalued solution of Burgers' equation with initial data u_0 . This explains their appearance in the formula for the weak limit of $u_\epsilon(x, t)$. All details of this calculation will be given in §3.2.5, which will complete the proof of Theorem III.5.

3.2.3 Asymptotics of Traces of Powers of \tilde{A}_ϵ . Proof of Proposition III.7

The definition (3.14) implies that where $F(\lambda)$ is bounded and bounded away from zero, the numbers $\{\tilde{\lambda}_n\}_{n=1}^{N(\epsilon)}$ are locally nearly equally spaced, but they are more dilute near the “soft edge” of the spectrum $\lambda = -L$ and more dense near the “hard edge” of the spectrum $\lambda = 0$. Taking into account the soft edge behavior we may obtain a uniform estimate:

Lemma III.9. *There is a constant $C_\lambda > 0$ independent of ϵ such that*

$$(3.50) \quad |\tilde{\lambda}_n - \tilde{\lambda}_m| \leq C_\lambda \epsilon^{2/3} |n - m|^{2/3}$$

holds for all n and m between 1 and $N(\epsilon)$.

Proof. Since F is a monotone increasing function with $F(-L) = 0$, it is bounded away from zero except in a right-neighborhood of $\lambda = -L$. Using the lower bound given in (3.22) from Lemma III.4 we obtain a lower bound $F(\lambda) \geq C\sqrt{L + \lambda}$ valid uniformly for $-L < \lambda < 0$ with $0 < C \leq C_{-L}/2$. Then, using the definition (3.14) we have (assuming $n \geq m$ without loss of generality)

$$(3.51) \quad \epsilon |n - m| = \int_{\tilde{\lambda}_m}^{\tilde{\lambda}_n} F(\lambda) d\lambda \geq C \int_{\tilde{\lambda}_m}^{\tilde{\lambda}_n} \sqrt{L + \lambda} d\lambda \geq C \int_0^{|\tilde{\lambda}_n - \tilde{\lambda}_m|} \sqrt{\xi} d\xi = \frac{2C}{3} |\tilde{\lambda}_n - \tilde{\lambda}_m|^{3/2},$$

so the desired inequality follows with $C_\lambda := (2C/3)^{-2/3}$. \square

We decompose the matrix $\tilde{\mathbf{A}}_\epsilon$ into a sum $\tilde{\mathbf{A}}_\epsilon = \mathbf{D} + \mathbf{H}$ of its diagonal part

$$(3.52) \quad \mathbf{D} := \text{diag}(D_1, D_2, \dots, D_{N(\epsilon)}), \quad D_k := D(\tilde{\lambda}_k; x, t),$$

where $D(\lambda; x, t)$ is defined by (3.20), and its off-diagonal part \mathbf{H} whose matrix elements are given by

$$(3.53) \quad (\mathbf{H})_{nm} = \frac{2i\epsilon \sqrt{\tilde{\lambda}_n \tilde{\lambda}_m}}{\tilde{\lambda}_n - \tilde{\lambda}_m}, \quad \text{for } n \neq m, \text{ and } (\mathbf{H})_{nn} = 0.$$

We also will soon need the quantities $\{\varphi_n\}_{n=1}^{N(\epsilon)}$ defined by

$$(3.54) \quad \varphi_n := \varphi(\tilde{\lambda}_n), \quad n = 1, \dots, N(\epsilon),$$

where $\varphi(\lambda)$ is given by (3.21).

Lemma III.10. *There is a constant $C_\varphi > 0$ and for each $R > 0$ there is a constant $C_{D,R} > 0$ such that*

$$(3.55) \quad |\varphi_n| \leq C_\varphi$$

and

$$(3.56) \quad \sup_{x^2+t^2 \leq R^2} |D_n| \leq C_{D,R}$$

both hold for all $\epsilon > 0$ and all n between 1 and $N(\epsilon)$. Also,

$$(3.57) \quad |\varphi_n - \varphi_m| \leq C_\varphi \epsilon^{\sigma/3} |n - m|^{\sigma/3}$$

and

$$(3.58) \quad \sup_{x^2+t^2 \leq R^2} |D_n - D_m| \leq C_{D,R} \epsilon^{\sigma/3} |n - m|^{\sigma/3}$$

both hold for all $\epsilon > 0$ and for all n and m between 1 and $N(\epsilon)$. Here σ is the positive Hölder exponent of Lemma III.4.

Proof. This is an easy consequence of the Hölder continuity of $\varphi(\cdot)$ and $D(\cdot; x, t)$ guaranteed by Lemma III.4, and of the spacing estimate for $\{\tilde{\lambda}_k\}_{k=1}^{N(\epsilon)}$ given in Lemma III.9. In fact, since D is Hölder continuous with exponent σ while φ has exponent $\sigma/2$ the most natural bound for $|D_n - D_m|$ is proportional to $\epsilon^{2\sigma/3} |n - m|^{2\sigma/3}$, and to obtain (3.58) we use the fact that $\epsilon |n - m| \leq 2\epsilon N(\epsilon)$ is uniformly bounded to reduce the exponent to $\sigma/3$. \square

Lemma III.11. *There is a constant $C_H > 0$ such that*

$$(3.59) \quad |(n - m)(\mathbf{H})_{nm}| \leq C_H$$

and

$$(3.60) \quad |(n - m)(\mathbf{H})_{nm} - 2i\varphi_n\varphi_m| \leq C_H \epsilon^{\sigma/3} |n - m|^{\sigma/3}$$

both hold for all $\epsilon > 0$ and all $n \neq m$ between 1 and $N(\epsilon)$. Again, $\sigma > 0$ is the Hölder exponent of Lemma III.4.

Proof. Suppose without loss of generality that $n > m$, implying that $\tilde{\lambda}_m < \tilde{\lambda}_n < 0$.

Then

$$\begin{aligned}
 -i(n-m)(\mathbf{H})_{nm} &= 2\sqrt{-\tilde{\lambda}_n}\sqrt{-\tilde{\lambda}_m}\frac{\epsilon(n-m)}{\tilde{\lambda}_n-\tilde{\lambda}_m} \\
 (3.61) \qquad \qquad &\leq ([-\tilde{\lambda}_n] + [-\tilde{\lambda}_m])\frac{\epsilon(n-m)}{\tilde{\lambda}_n-\tilde{\lambda}_m} \\
 &= \epsilon(n-m) - 2\tilde{\lambda}_n\frac{\epsilon(n-m)}{\tilde{\lambda}_n-\tilde{\lambda}_m}.
 \end{aligned}$$

Now, recalling the definition (3.14) of the numbers $\{\tilde{\lambda}_k\}_{k=1}^{N(\epsilon)}$ and applying the Mean Value Theorem we may write the latter difference quotient as $F(\xi)$ for some ξ with $\tilde{\lambda}_m \leq \xi \leq \tilde{\lambda}_n$, and since F is increasing we have $F(\xi) \leq F(\tilde{\lambda}_n)$, so

$$(3.62) \qquad -i(n-m)(\mathbf{H})_{nm} \leq 2\epsilon(n-m) - 2\tilde{\lambda}_n F(\tilde{\lambda}_n) = 2\epsilon(n-m) + 2\varphi_n^2,$$

where we have also replaced $\epsilon(n-m)$ with $2\epsilon(n-m)$. On the other hand, we may write

$$(3.63) \qquad -i(n-m)(\mathbf{H})_{nm} = 2\epsilon(n-m)\frac{\sqrt{-\tilde{\lambda}_n}\sqrt{-\tilde{\lambda}_m} + \tilde{\lambda}_m}{\tilde{\lambda}_n - \tilde{\lambda}_m} - 2\tilde{\lambda}_m\frac{\epsilon(n-m)}{\tilde{\lambda}_n - \tilde{\lambda}_m}.$$

Again the difference quotient may be replaced by $F(\xi) \geq F(\tilde{\lambda}_m)$, and since

$$(3.64) \qquad \frac{\sqrt{-\tilde{\lambda}_n}\sqrt{-\tilde{\lambda}_m}}{\tilde{\lambda}_n - \tilde{\lambda}_m} = -\frac{\sqrt{-\tilde{\lambda}_m}}{\sqrt{\tilde{\lambda}_n} + \sqrt{\tilde{\lambda}_m}} \geq -1,$$

we obtain

$$(3.65) \qquad -i(n-m)(\mathbf{H})_{nm} \geq -2\epsilon(n-m) - 2\tilde{\lambda}_m F(\tilde{\lambda}_m) = -2\epsilon(n-m) + 2\varphi_m^2.$$

Combining (3.62) and (3.65) gives

$$(3.66) \qquad |(n-m)(\mathbf{H})_{nm} - 2i\varphi_n\varphi_m| \leq 2\epsilon|n-m| + 2\max\{\varphi_n, \varphi_m\}|\varphi_n - \varphi_m|,$$

and then applying Lemma III.10 we obtain

$$(3.67) \quad |(n-m)(\mathbf{H})_{nm} - 2i\varphi_n\varphi_m| \leq 2\epsilon|n-m| + 2C_\varphi^2\epsilon^{\sigma/3}|n-m|^{\sigma/3}.$$

Now, $0 \leq \epsilon|n-m| \leq 2\epsilon N(\epsilon)$, and this upper bound has a limit as $\epsilon \downarrow 0$, so $\epsilon|n-m|$ is nonnegative and bounded. Since $\sigma \leq 3$ we have therefore proved (3.60). Since $\varphi_n\varphi_m$ and $\epsilon|n-m|$ are bounded, (3.59) then follows from (3.60). \square

For any nonnegative integer power p , the p th moment of the measure μ_ϵ can be written in terms of \mathbf{D} and \mathbf{H} with the use of (3.44):

$$(3.68) \quad \int_{\mathbb{R}} \alpha^p d\mu_\epsilon(\alpha) = \sum_{j=0}^p Z_{pj},$$

where Z_{pj} contains the contribution to the trace coming from products of matrices involving exactly j factors of \mathbf{H} :

$$(3.69) \quad Z_{pj} := \frac{M}{N(\epsilon)} \sum_{\substack{d_1+d_2+\dots+d_s=p-j \\ h_1+h_2+\dots+h_s=j}} \text{tr}(\mathbf{D}^{d_1}\mathbf{H}^{h_1}\dots\mathbf{D}^{d_s}\mathbf{H}^{h_s}),$$

and where $d_1 \geq 0$ and $h_s \geq 0$, while $d_k > 0$ for $2 \leq k \leq s$ and $h_k > 0$ for $1 \leq k \leq s-1$. Since p is a fixed number, it will suffice to compute the limit of Z_{pj} as $\epsilon \downarrow 0$ for $j = 0, \dots, p$. Actually, it will be enough to consider even values of j as the following result shows.

Lemma III.12. *If j is an odd number, then $Z_{pj} = 0$.*

Proof. Since $\text{tr}(\mathbf{M}) = \text{tr}(\mathbf{M}^\top)$ for all square matrices \mathbf{A} ,

$$(3.70) \quad \begin{aligned} \frac{N(\epsilon)}{M} Z_{pj} &= \sum_{\substack{d_1+d_2+\dots+d_s=p-j \\ h_1+h_2+\dots+h_s=j}} \text{tr}\left(\left(\mathbf{D}^{d_1}\mathbf{H}^{h_1}\dots\mathbf{D}^{d_s}\mathbf{H}^{h_s}\right)^\top\right) \\ &= (-1)^j \sum_{\substack{d_1+d_2+\dots+d_s=p-j \\ h_1+h_2+\dots+h_s=j}} \text{tr}\left(\mathbf{H}^{h_s}\mathbf{D}^{d_s}\dots\mathbf{H}^{h_1}\mathbf{D}^{d_1}\right) \end{aligned}$$

where in the second line we have used the facts that $\mathbf{D}^\top = \mathbf{D}$ and $\mathbf{H}^\top = -\mathbf{H}$. By relabeling the terms in the sum we therefore obtain

$$(3.71) \quad \frac{N(\epsilon)}{M} Z_{pj} = (-1)^j \frac{N(\epsilon)}{M} Z_{pj}.$$

Since $N(\epsilon) > 0$ and $M < \infty$, the desired result follows. \square

An important role will be played below by the Toeplitz (discrete convolution) operator $\mathcal{T}_f : \ell^2(\mathbb{Z}) \rightarrow \ell^2(\mathbb{Z})$ defined by

$$(3.72) \quad (\mathcal{T}_f c)_n := \sum_{m \in \mathbb{Z}} f_{n-m} c_m, \quad \{c_m\}_{m \in \mathbb{Z}} \in \ell^2(\mathbb{Z}),$$

where $\{f_n\}_{n \in \mathbb{Z}} \in \ell^2(\mathbb{Z})$ is the sequence

$$(3.73) \quad f_n := \begin{cases} n^{-1}, & n \neq 0 \\ 0, & n = 0. \end{cases}$$

Lemma III.13. *For any even positive integer j , we have*

$$(3.74) \quad \sum_{n_2, \dots, n_j \in \mathbb{Z}} f_{-n_2} \left[\prod_{\ell=2}^{j-1} f_{n_\ell - n_{\ell+1}} \right] f_{n_j} = \frac{(i\pi)^j}{j+1},$$

where the $j-1$ -fold infinite sum converges absolutely.

Proof. Note that since $\{f_n\}_{n \in \mathbb{Z}} \in \ell^2(\mathbb{Z})$, $\{g_n\}_{n \in \mathbb{Z}} \in \ell^2(\mathbb{Z})$ as well, where $g_n := |f_n|$ for all $n \in \mathbb{Z}$. The corresponding Fourier series converge in the mean-square sense to functions $f(\cdot)$ and $g(\cdot)$ in $L^2[0, 2\pi]$:

$$(3.75) \quad f(\theta) := \sum_{n \in \mathbb{Z}} f_n e^{in\theta} = i(\pi - \theta), \quad 0 < \theta < 2\pi$$

and

$$(3.76) \quad g(\theta) := \sum_{n \in \mathbb{Z}} g_n e^{in\theta} = -\log(2(1 - \cos(\theta))), \quad 0 < \theta < 2\pi.$$

First we establish the absolute convergence of the series on the left-hand side of (3.74). Using (3.72), observe that

$$(3.77) \quad \sum_{n_2, \dots, n_j \in \mathbb{Z}} |f_{-n_2}| \left[\prod_{\ell=2}^{j-1} |f_{n_\ell - n_{\ell+1}}| \right] |f_{n_j}| = (\mathcal{T}_g^{j-1} g)_0$$

where \mathcal{T}_g is the Toeplitz operator associated with the sequence $\{g_n\}_{n \in \mathbb{Z}}$. Now, $g(\cdot)$ has a logarithmic singularity at $\theta = 0 \pmod{2\pi}$, but this is sufficiently mild that $g(\cdot)^m \in L^2[0, 2\pi] \subset L^1[0, 2\pi]$ for any positive integer power m . Now for any function $k(\cdot) \in L^2[0, 2\pi]$, the corresponding Fourier coefficients are

$$(3.78) \quad k_n := \frac{1}{2\pi} \int_0^{2\pi} k(\theta) e^{-in\theta} d\theta,$$

so in particular we see that $(\mathcal{T}_g^{j-1} g)_0$ is the average value of the function whose Fourier coefficients are $\{(\mathcal{T}_g^{j-1} g)_n\}_{n \in \mathbb{Z}}$. But by the convolution theorem:

$$(3.79) \quad w_n := \sum_{m \in \mathbb{Z}} u_{n-m} v_m \quad \iff \quad w(\theta) = u(\theta)v(\theta),$$

so it follows that

$$(3.80) \quad (\mathcal{T}_g^{j-1} g)_0 = \frac{1}{2\pi} \int_0^{2\pi} g(\theta)^j d\theta$$

which is finite because $g(\cdot)^j \in L^1[0, 2\pi]$.

Now we find the exact value of the $j - 1$ -fold infinite sum by the same reasoning:

$$(3.81) \quad \sum_{n_2, \dots, n_j \in \mathbb{Z}} f_{-n_2} \left[\prod_{\ell=2}^{j-1} f_{n_\ell - n_{\ell+1}} \right] f_{n_j} = (\mathcal{T}_f^{j-1} f)_0 = \frac{1}{2\pi} \int_0^{2\pi} f(\theta)^j d\theta,$$

and by direct calculation using (3.75),

$$(3.82) \quad \frac{1}{2\pi} \int_0^{2\pi} f(\theta)^j d\theta = \frac{1}{2\pi} \int_0^{2\pi} [i(\pi - \theta)]^j d\theta = \frac{(i\pi)^j}{j+1}$$

for j even (the integral vanishes by symmetry for j odd). □

Now we consider separately each of the terms in Z_{pj} for j even.

Lemma III.14. *If j is an even number and $h_1 + \dots + h_s = j$ while $d_1 + \dots + d_s = p - j$, then*

$$(3.83) \quad \lim_{\epsilon \downarrow 0} \frac{M}{N(\epsilon)} \operatorname{tr} (\mathbf{D}^{d_1} \mathbf{H}^{h_1} \dots \mathbf{D}^{d_s} \mathbf{H}^{h_s}) = \frac{(2\pi)^j}{j+1} \int_{-L}^0 D(\lambda; x, t)^{p-j} \varphi(\lambda)^{2j} F(\lambda) d\lambda,$$

with the limit being uniform with respect to (x, t) in any compact set.

Proof. Recalling the matrix elements D_n and $(\mathbf{H})_{nm}$ of \mathbf{D} and \mathbf{H} respectively, we have

$$(3.84) \quad \operatorname{tr} (\mathbf{D}^{d_1} \mathbf{H}^{h_1} \dots \mathbf{D}^{d_s} \mathbf{H}^{h_s}) = \sum_{a_1, a_2, \dots, a_j=1}^{N(\epsilon)} \left[\prod_{i=1}^j D_{a_i}^{m_i} \right] \left[\prod_{\ell=1}^{j-1} H_{a_\ell a_{\ell+1}} \right] H_{a_j a_1},$$

where the exponents m_1, \dots, m_j are given by

$$(3.85) \quad m_i := \begin{cases} d_1, & i = 1 \\ d_{b+1}, & i = 1 + h_1 + h_2 + \dots + h_b \quad \text{for some } 0 < b < s \\ 0, & \text{otherwise.} \end{cases}$$

Note that $m_1 + m_2 + \dots + m_j = d_1 + d_2 + \dots + d_s = p - j$.

Now, the matrix element $(\mathbf{H})_{nm}$ is relatively small unless $n \approx m$, and this suggests that the j -fold sum in (3.84) should concentrate near the diagonal, where $a_k = a_1$ for all k . Making this precise, given any $r > 0$ we will first show that

$$(3.86) \quad \lim_{\epsilon \downarrow 0} Z_{\text{OD}}(\epsilon) = 0,$$

where

$$(3.87) \quad Z_{\text{OD}}(\epsilon) := \frac{M}{N(\epsilon)} \sum_{\substack{a_1, a_2, \dots, a_j=1 \\ \exists k: |a_k - a_1| > \epsilon^{-r}}}^{N(\epsilon)} \left[\prod_{i=1}^j D_{a_i}^{m_i} \right] \left[\prod_{\ell=1}^{j-1} H_{a_\ell a_{\ell+1}} \right] H_{a_j a_1},$$

with the limit being uniform for (x, t) in compact sets. Indeed, if $x^2 + t^2 \leq R^2$, then

using (3.56) from Lemma III.10 and (3.59) from Lemma III.11 we obtain

$$\begin{aligned}
(3.88) \quad |Z_{\text{OD}}(\epsilon)| &\leq \frac{MC_{D,R}^{p-j} C_H^j}{N(\epsilon)} \sum_{\substack{a_1, a_2, \dots, a_j=1 \\ \exists k: |a_k - a_1| > \epsilon^{-r}}}^{N(\epsilon)} \left[\prod_{\ell=1}^{j-1} |f_{a_\ell - a_{\ell+1}}| \right] |f_{a_j - a_1}| \\
&= \frac{MC_{D,R}^{p-j} C_H^j}{N(\epsilon)} \sum_{a_1=1}^{N(\epsilon)} \sum_{\substack{a_2, a_3, \dots, a_j=1 \\ \exists k: |a_k - a_1| > \epsilon^{-r}}}^{N(\epsilon)} \left[\prod_{\ell=1}^{j-1} |f_{a_\ell - a_{\ell+1}}| \right] |f_{a_j - a_1}| \\
&\leq \frac{MC_{D,R}^{p-j} C_H^j}{N(\epsilon)} \sum_{a_1=1}^{N(\epsilon)} \sum_{\substack{a_2, a_3, \dots, a_j \in \mathbb{Z} \\ \exists k: |a_k - a_1| > \epsilon^{-r}}} \left[\prod_{\ell=1}^{j-1} |f_{a_\ell - a_{\ell+1}}| \right] |f_{a_j - a_1}|.
\end{aligned}$$

With the inner sum extended over \mathbb{Z}^{j-1} in this way, it becomes independent of the outer sum index a_1 as can be seen by the substitution $n_k = a_k - a_1$ for $k = 2, 3, \dots, j$.

Thus

$$(3.89) \quad |Z_{\text{OD}}(\epsilon)| \leq MC_{D,R}^{p-j} C_H^j \sum_{\substack{n_2, n_3, \dots, n_j \in \mathbb{Z} \\ \exists k: |n_k| > \epsilon^{-r}}} |f_{-n_2}| \left[\prod_{\ell=2}^{j-1} |f_{n_\ell - n_{\ell+1}}| \right] |f_{n_j}|,$$

and the latter upper bound is of course independent of (x, t) with $x^2 + t^2 \leq R^2$ and tends to zero for $r > 0$ by Lemma III.13.

It follows from (3.86) that

$$(3.90) \quad \lim_{\epsilon \downarrow 0} \frac{M}{N(\epsilon)} \text{tr} (\mathbf{D}^{d_1} \mathbf{H}^{h_1} \dots \mathbf{D}^{d_s} \mathbf{H}^{h_s}) = \lim_{\epsilon \downarrow 0} Z_{\text{D}}(\epsilon)$$

where the diagonally-concentrated terms are

$$(3.91) \quad Z_{\text{D}}(\epsilon) := \frac{M}{N(\epsilon)} \sum_{\substack{a_1, a_2, \dots, a_j=1 \\ \forall k: |a_k - a_1| \leq \epsilon^{-r}}}^{N(\epsilon)} \left[\prod_{i=1}^j D_{a_i}^{m_i} \right] \left[\prod_{\ell=1}^{j-1} H_{a_\ell a_{\ell+1}} \right] H_{a_j a_1}.$$

We will analyze $Z_{\text{D}}(\epsilon)$ under the additional assumption that $r < 1$.

The first step is show that if $r < 1$ each occurrence of $(\mathbf{H})_{nm}$ in (3.91) may be replaced by $2i\varphi_n \varphi_m f_{n-m}$ without affecting the limiting value of $Z_{\text{D}}(\epsilon)$ as $\epsilon \downarrow 0$. Indeed, by making this substitution j times in succession each time keeping track

of the error using Lemma III.11 along with the estimates (3.55) and (3.56) from Lemma III.10, one sees that with $K_R > 0$ defined by

$$(3.92) \quad K_R := C_{D,R}^{p-j} \sum_{k=1}^j (2C_\varphi^2)^{k-1} C_H^{j-k+1},$$

for all j -tuples of integers a_1, \dots, a_j between 1 and $N(\epsilon)$ satisfying $|a_k - a_1| \leq \epsilon^{-r}$ for all k ,

$$(3.93) \quad \left| \left[\prod_{i=1}^j D_{a_i}^{m_i} \right] \left[\prod_{\ell=1}^{j-1} H_{a_\ell a_{\ell+1}} \right] H_{a_j a_1} - (2i)^j \left[\prod_{i=1}^j D_{a_i}^{m_i} \varphi_{a_i}^2 \right] \left[\prod_{\ell=1}^{j-1} f_{a_\ell - a_{\ell+1}} \right] f_{a_j - a_1} \right| \\ \leq K_R \epsilon^{(1-r)\sigma/3} \left[\prod_{\ell=1}^{j-1} |f_{a_\ell - a_{\ell+1}}| \right] |f_{a_j - a_1}|.$$

Therefore, if we define a modification of $Z_D(\epsilon)$ by

$$(3.94) \quad Z_D^1(\epsilon) := \frac{(2i)^j M}{N(\epsilon)} \sum_{\substack{a_1, a_2, \dots, a_j=1 \\ \forall k: |a_k - a_1| \leq \epsilon^{-r}}}^{N(\epsilon)} \left[\prod_{i=1}^j D_{a_i}^{m_i} \varphi_{a_i}^2 \right] \left[\prod_{\ell=1}^{j-1} f_{a_\ell - a_{\ell+1}} \right] f_{a_j - a_1},$$

we have

$$(3.95) \quad |Z_D(\epsilon) - Z_D^1(\epsilon)| \leq \frac{MK_R \epsilon^{(1-r)\sigma/3}}{N(\epsilon)} \sum_{\substack{a_1, a_2, \dots, a_j=1 \\ \forall k: |a_k - a_1| \leq \epsilon^{-r}}}^{N(\epsilon)} \left[\prod_{\ell=1}^{j-1} |f_{a_\ell - a_{\ell+1}}| \right] |f_{a_j - a_1}| \\ \leq \frac{MK_R \epsilon^{(1-r)\sigma/3}}{N(\epsilon)} \sum_{a_1=1}^{N(\epsilon)} \left(\sum_{a_2, a_3, \dots, a_j \in \mathbb{Z}} \left[\prod_{\ell=1}^{j-1} |f_{a_\ell - a_{\ell+1}}| \right] |f_{a_j - a_1}| \right).$$

By the substitution $n_\ell = a_\ell - a_1$ one sees that the inner sum is independent of a_1 , and it is finite by Lemma III.13. Since $\sigma > 0$ and $r < 1$, we therefore have

$$(3.96) \quad \lim_{\epsilon \downarrow 0} Z_D(\epsilon) = \lim_{\epsilon \downarrow 0} Z_D^1(\epsilon)$$

uniformly for $x^2 + t^2 \leq R^2$.

The second step is to show that if $r < 1$ we may replace $D_{a_i}^{m_i} \varphi_{a_i}^2$ with $D_{a_1}^{m_i} \varphi_{a_1}^2$ for each i in (3.94) without changing the limiting value of $Z_D^1(\epsilon)$. Indeed, applying Lemma III.10 we see that with $K_R^1 > 0$ defined by

$$(3.97) \quad K_R^1 := (p+j) C_{D,R}^{p-j} C_\varphi^{2j},$$

we see that for all j -tuples of integers a_1, \dots, a_j between 1 and $N(\epsilon)$ satisfying $|a_k - a_1| \leq \epsilon^{-r}$ for all k ,

$$(3.98) \quad \left| \prod_{i=1}^j D_{a_i}^{m_i} \varphi_{a_i}^2 - D_{a_1}^{p-j} \varphi_{a_1}^{2j} \right| \leq K_R^1 \epsilon^{(1-r)\sigma/3}.$$

Hence, defining a subsequent modification of $Z_D^I(\epsilon)$ by

$$(3.99) \quad Z_D^{II}(\epsilon) := \frac{(2i)^j M}{N(\epsilon)} \sum_{a_1=1}^{N(\epsilon)} D_{a_1}^{p-j} \varphi_{a_1}^{2j} \sum_{\substack{a_2, a_3, \dots, a_j=1 \\ \forall k: |a_k - a_1| \leq \epsilon^{-r}}}^{N(\epsilon)} \left[\prod_{\ell=1}^{j-1} f_{a_\ell - a_{\ell+1}} \right] f_{a_j - a_1},$$

we see that

$$(3.100) \quad \begin{aligned} |Z_D^I(\epsilon) - Z_D^{II}(\epsilon)| &\leq \frac{2^j M K_R^1 \epsilon^{(1-r)\sigma/3}}{N(\epsilon)} \sum_{a_1=1}^{N(\epsilon)} \sum_{\substack{a_2, a_3, \dots, a_j=1 \\ \forall k: |a_k - a_1| \leq \epsilon^{-r}}}^{N(\epsilon)} \left[\prod_{\ell=1}^{j-1} |f_{a_\ell - a_{\ell+1}}| \right] |f_{a_j - a_1}| \\ &\leq \frac{2^j M K_R^1 \epsilon^{(1-r)\sigma/3}}{N(\epsilon)} \sum_{a_1=1}^{N(\epsilon)} \left(\sum_{a_2, a_3, \dots, a_j \in \mathbb{Z}} \left[\prod_{\ell=1}^{j-1} |f_{a_\ell - a_{\ell+1}}| \right] |f_{a_j - a_1}| \right), \end{aligned}$$

and so exactly as before

$$(3.101) \quad \lim_{\epsilon \downarrow 0} Z_D^I(\epsilon) = \lim_{\epsilon \downarrow 0} Z_D^{II}(\epsilon)$$

uniformly for $x^2 + t^2 \leq R^2$.

The third step is to show that if $r < 1$ one may neglect a small fraction of the terms in the outer sum corresponding to $a_1 \leq 1 + \epsilon^{-r}$ and $a_1 \geq N(\epsilon) - \epsilon^{-r}$ without changing the limiting value of $Z_D^{II}(\epsilon)$. Indeed, defining the index set

$$(3.102) \quad S_\epsilon := \{n \in \mathbb{Z}, 1 + \epsilon^{-r} < n < N(\epsilon) - \epsilon^{-r}\},$$

and then setting

$$(3.103) \quad Z_D^{III}(\epsilon) := \frac{(2i)^j M}{N(\epsilon)} \sum_{a_1 \in S_\epsilon} D_{a_1}^{p-j} \varphi_{a_1}^{2j} \sum_{\substack{a_2, a_3, \dots, a_j=1 \\ \forall k: |a_k - a_1| \leq \epsilon^{-r}}}^{N(\epsilon)} \left[\prod_{\ell=1}^{j-1} f_{a_\ell - a_{\ell+1}} \right] f_{a_j - a_1},$$

we easily obtain from (3.55) and (3.56) in Lemma III.10 that

$$\begin{aligned}
(3.104) \quad |Z_D^{\text{II}}(\epsilon) - Z_D^{\text{III}}(\epsilon)| &\leq \frac{2^j M C_{D,R}^{p-j} C_\varphi^{2j}}{N(\epsilon)} \sum_{\substack{a_1=1 \\ a_1 \notin S_\epsilon}}^{N(\epsilon)} \sum_{\substack{a_2, a_3, \dots, a_j=1 \\ \forall k: |a_k - a_1| \leq \epsilon^{-r}}}^{N(\epsilon)} \left[\prod_{\ell=1}^{j-1} |f_{a_\ell - a_{\ell+1}}| \right] |f_{a_j - a_1}| \\
&\leq \frac{2^j M C_{D,R}^{p-j} C_\varphi^{2j}}{N(\epsilon)} \sum_{\substack{a_1=1 \\ a_1 \notin S_\epsilon}}^{N(\epsilon)} \sum_{a_2, a_3, \dots, a_j \in \mathbb{Z}} \left[\prod_{\ell=1}^{j-1} |f_{a_\ell - a_{\ell+1}}| \right] |f_{a_j - a_1}|.
\end{aligned}$$

But the inner sum is independent of a_1 and is convergent by Lemma III.13 and the outer sum has $O(\epsilon^{-r})$ terms while $N(\epsilon)$ is proportional to ϵ^{-1} , so with $r < 1$ we have

$$(3.105) \quad \lim_{\epsilon \downarrow 0} Z_D^{\text{II}}(\epsilon) = \lim_{\epsilon \downarrow 0} Z_D^{\text{III}}(\epsilon)$$

uniformly for $x^2 + t^2 \leq R^2$.

The next step in analyzing $Z_D(\epsilon)$ is to deal with the inner sum in the definition (3.103) of $Z_D^{\text{III}}(\epsilon)$. Taking into account the conditions on a_1 in the outer sum, it is obvious that the conditions $1 \leq a_k \leq N(\epsilon)$ are superfluous in the inner sum:

$$(3.106) \quad Z_D^{\text{III}}(\epsilon) = \frac{(2i)^j M}{N(\epsilon)} \sum_{a_1 \in S_\epsilon} D_{a_1}^{p-j} \varphi_{a_1}^{2j} \sum_{\substack{a_2, a_3, \dots, a_j \in \mathbb{Z} \\ \forall k: |a_k - a_1| \leq \epsilon^{-r}}} \left[\prod_{\ell=1}^{j-1} f_{a_\ell - a_{\ell+1}} \right] f_{a_j - a_1}.$$

By introducing the differences $n_k = a_k - a_1$ it now becomes clear that the inner sum is independent of a_1 :

$$(3.107) \quad Z_D^{\text{III}}(\epsilon) = \frac{(2i)^j M}{N(\epsilon)} \left(\sum_{a_1 \in S_\epsilon} D_{a_1}^{p-j} \varphi_{a_1}^{2j} \right) \left(\sum_{\substack{n_2, n_3, \dots, n_j \in \mathbb{Z} \\ \forall k: |n_k| \leq \epsilon^{-r}}} f_{-n_2} \left[\prod_{\ell=2}^{j-1} f_{a_\ell - a_{\ell+1}} \right] f_{n_j} \right).$$

Now, according to Lemma III.13, the latter sum has the limit $(i\pi)^j / (j+1)$ as $\epsilon \downarrow 0$ with $r > 0$, so

$$(3.108) \quad \lim_{\epsilon \downarrow 0} Z_D^{\text{III}}(\epsilon) = \lim_{\epsilon \downarrow 0} Z_D^{\text{IV}}(\epsilon),$$

uniformly for $x^2 + t^2 \leq R^2$, where

$$(3.109) \quad Z_D^{\text{IV}}(\epsilon) := \frac{(2\pi)^j}{j+1} \cdot \frac{M}{N(\epsilon)} \sum_{a_1 \in S_\epsilon} D_{a_1}^{p-j} \varphi_{a_1}^{2j}.$$

The final step in the analysis of $Z_D(\epsilon)$ is simply to evaluate the limit on the right-hand side of by recognizing the sum as a Riemann sum for an integral:

$$(3.110) \quad \lim_{\epsilon \downarrow 0} Z_D(\epsilon) = \lim_{\epsilon \downarrow 0} Z_D^{IV}(\epsilon) = \frac{(2\pi)^j}{j+1} \int_{-L}^0 D(\lambda; x, t)^{p-j} \varphi(\lambda)^{2j} F(\lambda) d\lambda.$$

Note that since the summand $D_{a_1}^{p-j} \varphi_{a_1}^{2j}$ is polynomial in x and t , the convergence of the Riemann sum is uniform for (x, t) in compact sets. Comparing with (3.90) we see that the proof is complete. \square

Now we may complete the proof of Proposition III.7. Lemma III.14 shows that each of the terms in the formula (3.69) for Z_{pj} has the same limit as $\epsilon \downarrow 0$. Therefore, for all even j ,

$$(3.111) \quad \begin{aligned} \lim_{\epsilon \downarrow 0} Z_{pj} &= \sum_{\substack{d_1+d_2+\dots+d_s=p-j \\ h_1+h_2+\dots+h_s=j}} \frac{(2\pi)^j}{j+1} \int_{-L}^0 D(\lambda; x, t)^{p-j} \varphi(\lambda)^{2j} F(\lambda) d\lambda \\ &= \binom{p}{j} \frac{(2\pi)^j}{j+1} \int_{-L}^0 D(\lambda; x, t)^{p-j} \varphi(\lambda)^{2j} F(\lambda) d\lambda. \end{aligned}$$

Combining this result with Lemma III.12 and the formula (3.68) for the p^{th} moment, we obtain

$$(3.112) \quad Q_p = \lim_{\epsilon \downarrow 0} \int_{\mathbb{R}} \alpha^p d\mu_\epsilon(\alpha) = \sum_{k=0}^{\lfloor p/2 \rfloor} \binom{p}{2k} \frac{(2\pi)^{2k}}{2k+1} \int_{-L}^0 D(\lambda; x, t)^{p-2k} \varphi(\lambda)^{4k} F(\lambda) d\lambda,$$

uniformly for (x, t) in compact sets. Now we apply the identity

$$(3.113) \quad \sum_{k=0}^{\lfloor p/2 \rfloor} \frac{1}{2k+1} \binom{p}{2k} a^{2k} b^{p-2k} = \frac{(b+a)^{p+1} - (b-a)^{p+1}}{2a(1+p)},$$

holding for any integer $p \geq 0$ and real numbers a and b . (This identity can be most easily obtained by expanding the binomials on the right-hand side.) Recalling the definitions (3.20) and (3.21) of $D(\lambda; x, t)$ and $\varphi(\lambda)$, and using the fact that $x_\pm(\lambda) = \pm\pi F(\lambda) - \gamma(\lambda)$ then completes the proof of Proposition III.7.

3.2.4 Convergence of Measures and Locally Uniform Convergence of \tilde{U}_ϵ . Proof of Proposition III.8

Recall the measures μ_ϵ defined by (3.43).

Lemma III.15. *For each nonnegative integer p ,*

$$(3.114) \quad \lim_{\epsilon \downarrow 0} \int_{\mathbb{R}} \alpha^p d\mu_\epsilon(\alpha) = \int_{\mathbb{R}} \alpha^p d\mu(\alpha)$$

where μ is the absolutely continuous (with respect to Lebesgue measure on \mathbb{R}) measure defined by $d\mu(\alpha) = G(\alpha; x, t) d\alpha$, and the compactly supported integrable density function $G(\alpha; x, t)$ is given by (3.49). The limit is uniform with respect to (x, t) in compact sets. Also, like each μ_ϵ , μ is a measure with mass M .

Proof. Recalling Proposition III.7, we first show that the given measure μ satisfies

$$(3.115) \quad \int_{\mathbb{R}} \alpha^p d\mu(\alpha) = Q_p,$$

where Q_p is given by (3.46), for all nonnegative $p \in \mathbb{Z}$. Equivalently, we may construct a measure with the desired moments as follows: the characteristic function of the measure μ is the Fourier transform

$$(3.116) \quad \hat{G}(\xi; x, t) := \int_{\mathbb{R}} G(\alpha; x, t) e^{-i\alpha\xi} d\alpha,$$

and this function necessarily has the desired moments $\{Q_p\}_{p=0}^\infty$ as its derivatives at $\xi = 0$:

$$(3.117) \quad \frac{d^p \hat{G}}{d\xi^p}(0; x, t) = (-i)^p Q_p.$$

So $\hat{G}(\xi; x, t)$ has the Taylor series

$$(3.118) \quad \hat{G}(\xi; x, t) = \sum_{p=0}^{\infty} \frac{(-i\xi)^p}{p!} Q_p.$$

Now from the obvious inequality $|x + 2\lambda t - x_{\pm}(\lambda)| \leq |x - x_0| + 2L|t| + 2\pi F(\lambda)$, we obtain

(3.119)

$$\begin{aligned} |Q_p| &\leq \frac{1}{\pi(p+1)} \int_{-L}^0 (|x - x_0| + 2L|t| + 2\pi F(\lambda))^{p+1} (-2\lambda)^p d\lambda \\ &\leq \frac{1}{\pi(p+1)} \int_{-L}^0 (2L|x - x_0| + 4L^2|t| - 4\pi\lambda F(\lambda))^p (|x - x_0| + 2L|t| + 2\pi F(\lambda)) d\lambda. \end{aligned}$$

Also, from Lemma III.4, there is a constant $K > 0$ such that $0 \leq -\lambda F(\lambda) \leq K$, so for $(x - x_0)^2 + t^2 \leq R^2$,

$$\begin{aligned} |Q_p| &\leq \frac{(2LR + 4L^2R + 4\pi K)^p}{\pi(p+1)} \int_{-L}^0 (|x - x_0| + 2L|t| + 2\pi F(\lambda)) d\lambda \\ (3.120) \quad &\leq \frac{(LR + 2L^2R + 2\pi M)}{\pi(p+1)} (2LR + 4L^2R + 4\pi K)^p \\ &\leq \frac{1}{\pi} (LR + 2L^2R + 2\pi M) (2LR + 4L^2R + 4\pi K)^p, \end{aligned}$$

where in the last step we used (3.4). This inequality implies that the Taylor series (3.118) converges for all $\xi \in \mathbb{C}$ to an entire function of exponential type.

Now we will sum the Taylor series (3.118) in closed form by substituting from the formula (3.46) and exchanging the order of summation and integration. Indeed, since

$$(3.121) \quad \sum_{p=0}^{\infty} \frac{(-i\xi)^p}{p!} \cdot \frac{(-2\lambda)^p (x + 2\lambda t - x_{\pm}(\lambda))^{p+1}}{p+1} = \frac{e^{2i\xi\lambda[x+2\lambda t-x_{\pm}(\lambda)]} - 1}{2i\xi\lambda},$$

we obtain the formula

$$(3.122) \quad \hat{G}(\xi; x, t) = \int_{-L}^0 \frac{e^{2i\xi\lambda[x+2\lambda t-x_-(\lambda)]} - e^{2i\xi\lambda[x+2\lambda t-x_+(\lambda)]}}{4\pi i\xi\lambda} d\lambda.$$

Computing the inverse Fourier transform

$$(3.123) \quad G(\alpha; x, t) = \frac{1}{2\pi} \int_{\mathbb{R}} \hat{G}(\xi; x, t) e^{i\alpha\xi} d\xi$$

by exchanging the order of integration leads directly to the claimed formula (3.49).

It is obvious that $G(\alpha; x, t)$ is a nonnegative function, and since by Lemma III.4

(3.124)

$$\inf_{-L < \lambda < 0} -2\lambda(x + 2\lambda t - x_+(\lambda)) > -\infty \quad \text{and} \quad \sup_{-L < \lambda < 0} -2\lambda(x + 2\lambda t - x_-(\lambda)) < +\infty$$

for every (x, t) , it is clear that $G(\alpha; x, t)$ has compact support. It is also straightforward to verify that μ has mass M :

$$\begin{aligned} \int_{\mathbb{R}} d\mu(\alpha) &= \int_{\mathbb{R}} G(\alpha; x, t) d\alpha \\ &= -\frac{1}{4\pi} \int_{\mathbb{R}} \int_{-L}^0 \chi_{[-2\lambda(x+2\lambda t-x_+(\lambda)), -2\lambda(x+2\lambda t-x_-(\lambda))]}(\alpha) \frac{d\lambda}{\lambda} d\alpha \\ &= -\frac{1}{4\pi} \int_{-L}^0 \frac{1}{\lambda} \int_{\mathbb{R}} \chi_{[-2\lambda(x+2\lambda t-x_+(\lambda)), -2\lambda(x+2\lambda t-x_-(\lambda))]}(\alpha) d\alpha d\lambda \\ (3.125) \quad &= -\frac{1}{4\pi} \int_{-L}^0 \frac{1}{\lambda} \int_{-2\lambda(x+2\lambda t-x_+(\lambda))}^{-2\lambda(x+2\lambda t-x_-(\lambda))} d\alpha d\lambda \\ &= \int_{-L}^0 F(\lambda) d\lambda \\ &= M, \end{aligned}$$

according to (3.4). Therefore μ is indeed an absolutely continuous compactly supported (nonnegative) measure of mass M . \square

Note that the reconstruction of the the measure μ from its moments is virtually the same calculation as took place on the direct scattering side in our discussion of Matsuno's method in §2.2.8.

Lemma III.16. *There is a compact interval $\Omega \subset \mathbb{R}$ containing the support of all of the measures $\{\mu_\epsilon\}_{\epsilon>0}$ as well as that of the measure μ , and Ω may be chosen independent of (x, t) in any given compact set.*

Proof. Since μ has compact support certainly contained within the interval

$$(3.126) \quad \inf_{-L < \lambda < 0} [2\lambda x_+(\lambda)] - 2L|x| - 4L^2|t| \leq \alpha \leq \sup_{-L < \lambda < 0} [2\lambda x_-(\lambda)] + 2L|x| + 4L^2|t|$$

that is clearly bounded uniformly for (x, t) in any compact set, it is enough to show that the support of μ_ϵ is uniformly bounded as $\epsilon \downarrow 0$. But by definition of μ_ϵ this is equivalent to showing that the eigenvalue of \mathbf{A}_ϵ with the largest magnitude remains uniformly bounded as $\epsilon \downarrow 0$.

Since the matrix $\tilde{\mathbf{A}}_\epsilon$ is Hermitian, we have

$$(3.127) \quad \|\tilde{\mathbf{A}}_\epsilon\|_2 = \max_{1 \leq j \leq N(\epsilon)} |\alpha_j|,$$

so to prove that the eigenvalue of $\tilde{\mathbf{A}}_\epsilon$ with the largest magnitude remains uniformly bounded, it is completely equivalent to prove that the ℓ^2 (induced) matrix norm of $\tilde{\mathbf{A}}_\epsilon$ is uniformly bounded as $\epsilon \downarrow 0$ independent of (x, t) in any given compact set.

Recalling the decomposition $\tilde{\mathbf{A}}_\epsilon = \mathbf{D} + \mathbf{H}$ from the proof of Proposition III.7 given in §3.2.3, the triangle inequality gives $\|\tilde{\mathbf{A}}_\epsilon\|_2 \leq \|\mathbf{D}\|_2 + \|\mathbf{H}\|_2$, and since \mathbf{D} is diagonal,

$$(3.128) \quad \begin{aligned} \|\mathbf{D}\|_2 &= \max_{1 \leq n \leq N(\epsilon)} |2\tilde{\lambda}_n(x + 2\tilde{\lambda}_n t + \gamma(\tilde{\lambda}_n))| \\ &\leq \sup_{-L < \lambda < 0} |2\lambda(x + 2\lambda t + \gamma(\lambda))| \\ &\leq \sup_{-L < \lambda < 0} |2\lambda\gamma(\lambda)| + 2L|x| + 4L^2|t|, \end{aligned}$$

so since $\lambda\gamma(\lambda)$ is bounded according to Lemma III.4, and \mathbf{H} is independent of x and t , it is sufficient to show that $\|\mathbf{H}\|_2$ remains bounded as $\epsilon \downarrow 0$.

To estimate $\|\mathbf{H}\|_2$, we write \mathbf{H} in the following form: $\mathbf{H} = \mathbf{B}\mathbf{T}\mathbf{B} + \mathbf{E}$ where

$$(3.129) \quad \mathbf{B} = \text{diag} \left(e^{i\pi/4} \sqrt{-2\tilde{\lambda}_1 F(\tilde{\lambda}_1)}, \dots, e^{i\pi/4} \sqrt{-2\tilde{\lambda}_{N(\epsilon)} F(\tilde{\lambda}_{N(\epsilon)})} \right),$$

and \mathbf{T} is the $N(\epsilon) \times N(\epsilon)$ Toeplitz matrix with elements $(\mathbf{T})_{nm} = f_{n-m}$, where the sequence $\{f_n\}_{n \in \mathbb{Z}}$ is defined by (3.73). Of course $\mathbf{E} := \mathbf{H} - \mathbf{B}\mathbf{T}\mathbf{B}$. Therefore $\|\mathbf{H}\|_2 \leq \|\mathbf{B}\|_2^2 \|\mathbf{T}\|_2 + \|\mathbf{E}\|_2$. Because \mathbf{B} is diagonal,

$$(3.130) \quad \|\mathbf{B}\|_2^2 \leq \max_{1 \leq n \leq N(\epsilon)} [-2\tilde{\lambda}_n F(\tilde{\lambda}_n)] \leq \sup_{-L < \lambda < 0} [-2\lambda F(\lambda)]$$

which is finite by Lemma III.4. The Toeplitz matrix \mathbf{T} can be written as $\mathbf{T} = \mathcal{P}\mathcal{T}_f\mathcal{P}$, where \mathcal{P} is the orthogonal projection from $\ell^2(\mathbb{Z})$ onto \mathbb{C}^N viewed as a subset of $\ell^2(\mathbb{Z})$ associated with components having indices $\{1, 2, \dots, N(\epsilon)\} \subset \mathbb{Z}$, and where $\mathcal{T}_f : \ell^2(\mathbb{Z}) \rightarrow \ell^2(\mathbb{Z})$ is the Toeplitz operator defined by (3.72) from §3.2.3. The $\ell^2(\mathbb{Z})$ operator norm of \mathcal{P} is clearly equal to one, and since

$$(3.131) \quad \sum_{l \in \mathbb{Z}} f_l e^{il\theta} = i(\pi - \theta), \quad 0 < \theta < 2\pi,$$

the Pythagorean Theorem in $L^2(0, 2\pi)$ gives

$$(3.132) \quad \begin{aligned} \sum_{n \in \mathbb{Z}} |(\mathcal{T}c)_n|^2 &= \frac{1}{2\pi} \int_0^{2\pi} \left| \sum_{n \in \mathbb{Z}} (\mathcal{T}c)_n e^{in\theta} \right|^2 d\theta \\ &= \frac{1}{2\pi} \int_0^{2\pi} \left| \sum_{n \in \mathbb{Z}} \sum_{m \in \mathbb{Z}} f_{n-m} c_m e^{in\theta} \right|^2 d\theta \\ &= \frac{1}{2\pi} \int_0^{2\pi} \left| \sum_{m \in \mathbb{Z}} c_m e^{im\theta} \sum_{n \in \mathbb{Z}} f_{n-m} e^{i[n-m]\theta} \right|^2 d\theta \\ &= \frac{1}{2\pi} \int_0^{2\pi} (\pi - \theta)^2 \left| \sum_{m \in \mathbb{Z}} c_m e^{im\theta} \right|^2 d\theta \\ &\leq \pi^2 \frac{1}{2\pi} \int_0^{2\pi} \left| \sum_{m \in \mathbb{Z}} c_m e^{im\theta} \right|^2 d\theta \\ &= \pi^2 \sum_{m \in \mathbb{Z}} |c_m|^2, \end{aligned}$$

the $\ell^2(\mathbb{Z})$ operator norm of \mathcal{T}_f is bounded by π . It follows that $\|\mathbf{H}\|_2 \leq \pi + \|\mathbf{E}\|_2$, so it suffices to show that $\|\mathbf{E}\|_2$ remains bounded as $\epsilon \downarrow 0$.

So far, we have exploited the special structure of the dominant parts of the matrix $\tilde{\mathbf{A}}_\epsilon$ and applied correspondingly specialized norm estimates to these terms. The error term \mathbf{E} has less structure, but is it smaller; to estimate its norm it will be sufficient to use the rather crude inequality $\|\mathbf{E}\|_2 \leq \|\mathbf{E}\|_{\text{HS}}$ and work with the Hilbert-Schmidt norm

$$(3.133) \quad \|\mathbf{E}\|_{\text{HS}}^2 := \sum_{n=1}^{N(\epsilon)} \sum_{m=1}^{N(\epsilon)} |(\mathbf{E})_{nm}|^2,$$

where the elements of \mathbf{E} are explicitly given by

$$(3.134) \quad (\mathbf{E})_{nm} := 2i \left[\frac{\epsilon \sqrt{\tilde{\lambda}_n \tilde{\lambda}_m}}{\tilde{\lambda}_n - \tilde{\lambda}_m} - \frac{\sqrt{\tilde{\lambda}_n F(\tilde{\lambda}_n) \tilde{\lambda}_m F(\tilde{\lambda}_m)}}{n - m} \right], \quad \text{for } n \neq m, \text{ and } (\mathbf{E})_{nn} = 0.$$

If we introduce continuous variables $a := (n - \frac{1}{2})\epsilon$ and $b := (m - \frac{1}{2})\epsilon$, then it is easy to see that the square of the Hilbert-Schmidt norm of \mathbf{E} is a Riemann sum approximation of a certain double integral:

$$(3.135) \quad \lim_{\epsilon \downarrow 0} \|\mathbf{E}\|_{\text{HS}}^2 = \iint_{[0, M]^2} e_0(a, b) da db,$$

provided the double integral exists, where

$$(3.136) \quad e_0(a, b) := 4 \left[\frac{\sqrt{m^{-1}(a)m^{-1}(b)}}{m^{-1}(a) - m^{-1}(b)} - \frac{\sqrt{m^{-1}(a)F(m^{-1}(a))m^{-1}(b)F(m^{-1}(b))}}{a - b} \right]^2,$$

and where $m^{-1}(\cdot)$ denotes the inverse function to the monotone function $m(\cdot)$ given by

$$(3.137) \quad m(\lambda) := \int_{-L}^{\lambda} F(\lambda') d\lambda'.$$

By changing variables to $\kappa = m^{-1}(a)$ and $\lambda = m^{-1}(b)$,

$$(3.138) \quad \iint_{[0, M]^2} e_0(a, b) da db = \iint_{[-L, 0]^2} e(\kappa, \lambda) d\kappa d\lambda,$$

where

$$(3.139) \quad e(\kappa, \lambda) := 4 \left[\frac{\sqrt{\kappa \lambda}}{\kappa - \lambda} - \frac{\sqrt{\kappa F(\kappa) \lambda F(\lambda)}}{m(\kappa) - m(\lambda)} \right]^2 F(\kappa) F(\lambda).$$

Note that since $F \geq 0$ by Lemma III.4, $e(\kappa, \lambda) \geq 0$ for $(\kappa, \lambda) \in [-L, 0]^2$. To complete the proof of the Lemma it is enough to show that the double integral on the right-hand side of (3.138) is finite.

In order to estimate the double integral, we divide the square $[-L, 0]^2$ into polygonal regions as follows (see Figure 3.6):

- The square $[-L, -L + \delta]^2$ contains those ordered pairs (κ, λ) for which both κ and λ are near the “soft edge” of the eigenvalue spectrum at $-L$. We divide this square into diagonal and off-diagonal parts according to whether $(\kappa + L)/2 \leq \lambda + L \leq 2(\kappa + L)$ (the diagonal part, S_D) or not (the off-diagonal parts, S_{OD}).
- The square $[-\delta, 0]^2$ contains those ordered pairs (κ, λ) for which both κ and λ are near the “hard edge” of the eigenvalue spectrum at 0. We divide this square into diagonal and off-diagonal parts according to whether $2\kappa < \lambda < \kappa/2$ (the diagonal part, H_D) or not (the off-diagonal parts H_{OD}).
- The remaining part of $[-L, 0]^2$ contains those ordered pairs (κ, λ) for which at least one of the coordinates lies in the “bulk” of the eigenvalue spectrum, bounded away from both edges. This is divided into a diagonal part B_D and two off-diagonal parts B_{OD} along two straight line segments parallel to the diagonal as indicated in Figure 3.6.

Here, the constant $\delta > 0$ is as specified in Lemma III.4. As $e(\kappa, \lambda) = e(\lambda, \kappa)$ it will be enough to show integrability of e over the part of $[-L, 0]^2$ with $\kappa < \lambda$, an inequality that we will assume tacitly below.

First we consider integrating $e(\kappa, \lambda)$ over the “off-diagonal” shaded regions S_{OD} , B_{OD} , and H_{OD} shown in Figure 3.6. An upper bound for $e(\kappa, \lambda)$ useful in these regions is easily obtained from the inequality $(a - b)^2 \leq 2a^2 + 2b^2$:

(3.140)

$$e(\kappa, \lambda) \leq 8\kappa F(\kappa)\lambda F(\lambda) \left[\frac{1}{(\kappa - \lambda)^2} + \frac{F(\kappa)F(\lambda)}{(m(\kappa) - m(\lambda))^2} \right], \quad (\kappa, \lambda) \in (-L, 0)^2.$$

Applying the Mean Value Theorem to this estimate yields

$$(3.141) \quad e(\kappa, \lambda) \leq \frac{8\kappa F(\kappa)\lambda F(\lambda)}{(\kappa - \lambda)^2} \left[1 + \frac{F(\kappa)F(\lambda)}{F(\xi)^2} \right],$$

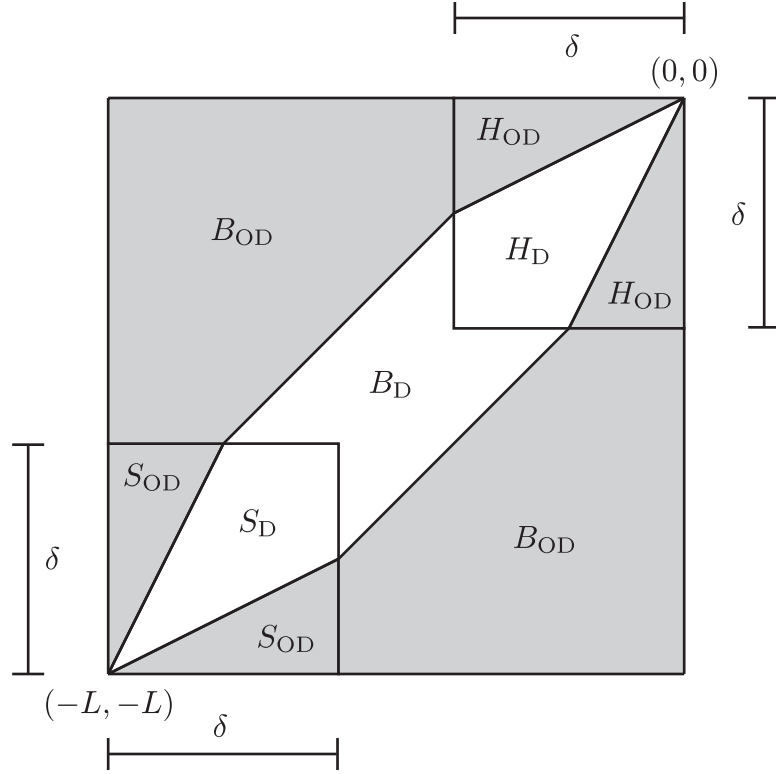


Figure 3.6: The square $[-L, 0]^2$ in the (κ, λ) -plane is covered by the six regions S_D , S_{OD} , B_D , B_{OD} , H_D , and H_{OD} .

where $\kappa \leq \xi \leq \lambda$. Finally, since F is monotone increasing according to Lemma III.4 we obtain

$$(3.142) \quad e(\kappa, \lambda) \leq \frac{8\kappa F(\kappa)\lambda F(\lambda)}{(\kappa - \lambda)^2} \left[1 + \frac{F(\lambda)}{F(\kappa)} \right] = \frac{8\kappa F(\kappa)\lambda F(\lambda)}{(\kappa - \lambda)^2} + \frac{8\kappa\lambda F(\lambda)}{(\kappa - \lambda)^2} F(\lambda).$$

Now, for $(\kappa, \lambda) \in B_{OD}$, we have that $\kappa - \lambda$ is bounded away from zero while by Lemma III.4 $\kappa F(\kappa)$ and $\lambda F(\lambda)$ are bounded (and of course $|\kappa| < L$) while $F(\lambda)$ is integrable. Hence we easily conclude that $e(\kappa, \lambda)$ is integrable on B_{OD} .

If $(\kappa, \lambda) \in H_{OD}$ with $\kappa < \lambda$, then we have the inequality

$$(3.143) \quad (\kappa - \lambda)^2 = \left(\left[\lambda - \frac{\kappa}{2} \right] + \left[-\frac{\kappa}{2} \right] \right)^2 \geq \frac{\kappa^2}{4},$$

and also since both $-\delta < \kappa < 0$ and $-\delta < \lambda < 0$ we may use the upper bound for F

given in (3.24) from Lemma III.4 to replace (3.142) with

$$(3.144) \quad e(\kappa, \lambda) \leq 32C_0^2(-\kappa)^{-1-1/q}(-\lambda)^{1-1/q} + 32C_0^2(-\kappa)^{-1}(-\lambda)^{1-2/q},$$

where $C_0 > 0$ and $q > 1$ are the constants in (3.24). This estimate is easily seen to be integrable on the component of H_{OD} with $\kappa < \lambda$ by direct calculation of the iterated integrals.

If $(\kappa, \lambda) \in S_{\text{OD}}$ with $\kappa < \lambda$, then we have the inequality

$$(3.145) \quad (\kappa - \lambda)^2 = \left(\left[\frac{\lambda + L}{2} \right] + \left[\frac{\lambda + L}{2} - (\kappa + L) \right] \right)^2 \geq \frac{(\lambda + L)^2}{4},$$

and also since both $-L < \kappa < -L + \delta$ and $-L < \lambda < -L + \delta$ we may use the upper bound for F given in (3.22) from Lemma III.4 along with the inequalities $|\kappa| < L$ and $|\lambda| < L$ to replace (3.142) with

$$(3.146) \quad e(\kappa, \lambda) \leq 32L^2C_{-L}^2(\kappa + L)^{1/2}(\lambda + L)^{-3/2} + 32L^2C_{-L}^2(\lambda + L)^{-1}.$$

This upper bound is obviously integrable on the component of S_{OD} with $\kappa < \lambda$.

Now we consider integrating $e(\kappa, \lambda)$ over the “diagonal” unshaded regions S_{D} , B_{D} , and H_{D} shown in Figure 3.6. By the Mean Value Theorem and the monotonicity of F guaranteed by Lemma III.4, we obtain an upper bound more useful when $\kappa \approx \lambda$:

$$(3.147) \quad e(\kappa, \lambda) \leq 4\kappa F(\kappa)\lambda F(\lambda) \left[\frac{F(\kappa) - F(\lambda)}{m(\kappa) - m(\lambda)} \right]^2, \quad (\kappa, \lambda) \in (-L, 0)^2.$$

Again using the Mean Value Theorem and monotonicity of F we may make the upper bound larger for $\kappa < \lambda$:

$$(3.148) \quad e(\kappa, \lambda) \leq \frac{4\kappa\lambda F(\lambda)F'(\xi)^2}{F(\kappa)},$$

where $\kappa \leq \xi \leq \lambda$.

For $(\kappa, \lambda) \in B_{\text{D}}$ with $\kappa < \lambda$, both κ and λ are bounded away from the soft and hard edges of the eigenvalue spectrum, so Lemma III.4 guarantees that F and F'

are bounded, and F is also bounded away from zero by strict monotonicity and the boundary condition $F(-L) = 0$. It follows from (3.148) that $e(\kappa, \lambda)$ is bounded and hence integrable on B_D .

If $(\kappa, \lambda) \in H_D$ then we may use the estimates (3.24) and (3.25) from Lemma III.4 to replace (3.148) with

$$(3.149) \quad e(\kappa, \lambda) \leq \frac{8C_0^2}{q^2} (-\kappa)^{1+1/q} (-\lambda)^{1-1/q} (-\xi)^{-2/q-2} \leq \frac{8C_0^2}{q^2} (-\kappa)^{1+1/q} (-\lambda)^{-1-3/q}.$$

The double integral of this upper bound over the region H_D with $\kappa < \lambda$ is easily computed by iterated integration and is clearly finite as a consequence of the fact that $q > 1$.

Finally, if $(\kappa, \lambda) \in S_D$ with $\kappa < \lambda$, then we may use the estimates (3.22) and (3.23) from Lemma III.4 together with the inequalities $|\kappa| < L$ and $|\lambda| < L$ to replace (3.148) with

$$(3.150) \quad e(\kappa, \lambda) \leq 2L^2 C_{-L}^2 (\kappa + L)^{-1/2} (\lambda + L)^{1/2} (\xi + L)^{-1} \leq 2L^2 C_{-L}^2 (\kappa + L)^{-3/2} (\lambda + L)^{1/2},$$

an upper bound that is clearly integrable over the part of S_D with $\kappa < \lambda$. \square

Lemma III.17. *The measure μ_ϵ converges in the weak-* sense to μ , uniformly for (x, t) in compact sets. That is, for each continuous function $f : \mathbb{R} \rightarrow \mathbb{C}$,*

$$(3.151) \quad \lim_{\epsilon \downarrow 0} \int_{\mathbb{R}} f(\alpha) d\mu_\epsilon(\alpha) = \int_{\mathbb{R}} f(\alpha) d\mu(\alpha),$$

with the limit being uniform with respect to (x, t) in compact sets.

Proof. According to Lemma III.15, for each polynomial $p(\alpha)$ we have the following limit, uniform for (x, t) in compact sets:

$$(3.152) \quad \lim_{\epsilon \downarrow 0} \int_{\mathbb{R}} p(\alpha) d\mu_\epsilon(\alpha) = \int_{\mathbb{R}} p(\alpha) d\mu(\alpha).$$

But by Lemma III.16 we can equivalently integrate over the compact interval Ω (independent of (x, t) in any given compact set) with the same result. Now by the Weierstraß Approximation Theorem, given any continuous function $f : \mathbb{R} \rightarrow \mathbb{C}$ and any $\rho > 0$ there is a polynomial $p_\rho^f(\alpha)$ for which

$$(3.153) \quad \sup_{\lambda \in \Omega} |f(\alpha) - p_\rho^f(\alpha)| < \frac{\rho}{M},$$

so for any measure ν of mass M with support in Ω (like μ_ϵ and μ),

$$(3.154) \quad \left| \int_{\mathbb{R}} [f(\alpha) - p_\rho^f(\alpha)] d\nu(\alpha) \right| \leq \int_{\Omega} |f(\alpha) - p_\rho^f(\alpha)| d\nu(\alpha) < \rho.$$

Let $\omega > 0$ be an arbitrarily small positive number. Then if we write

$$(3.155) \quad \nu[g] := \int_{\Omega} g(\alpha) d\nu(\alpha),$$

we have

$$(3.156) \quad \begin{aligned} \left| \int_{\mathbb{R}} f(\alpha) d\mu_\epsilon(\alpha) - \int_{\mathbb{R}} f(\alpha) d\mu(\alpha) \right| &= |\mu_\epsilon[f] - \mu[f]| \\ &= \left| \left[\mu_\epsilon[p_{\omega/3}^f] - \mu[p_{\omega/3}^f] \right] + \mu_\epsilon[f - p_{\omega/3}^f] - \mu[f - p_{\omega/3}^f] \right| \\ &\leq \left| \mu_\epsilon[p_{\omega/3}^f] - \mu[p_{\omega/3}^f] \right| + \left| \mu_\epsilon[f - p_{\omega/3}^f] \right| + \left| \mu[f - p_{\omega/3}^f] \right| \\ &< \left| \mu_\epsilon[p_{\omega/3}^f] - \mu[p_{\omega/3}^f] \right| + \frac{2}{3}\omega, \end{aligned}$$

with the last inequality following from (3.154). But with $\omega > 0$ fixed, (3.152) implies that $\epsilon > 0$ may be chosen sufficiently small, independently of (x, t) in any given compact set, that

$$(3.157) \quad \left| \mu_\epsilon[p_{\omega/3}^f] - \mu[p_{\omega/3}^f] \right| < \frac{1}{3}\omega,$$

which implies

$$(3.158) \quad \left| \int_{\mathbb{R}} f(\alpha) d\mu_\epsilon(\alpha) - \int_{\mathbb{R}} f(\alpha) d\mu(\alpha) \right| < \omega$$

thereby completing the proof. \square

Now we are in a position to complete the proof of Proposition III.8. We begin by writing $\tilde{U}_\epsilon(x, t)$ as defined by (3.42) in terms of the normalized (to mass M) counting measure μ_ϵ :

$$(3.159) \quad \tilde{U}_\epsilon(x, t) = \left[\frac{\epsilon N(\epsilon)}{M} \right] \int_{\mathbb{R}} 2 \arctan(\epsilon^{-1} \alpha) d\mu_\epsilon(\alpha).$$

Define the continuous functions

$$(3.160) \quad a_+(\alpha) := \pi + 4H(-\alpha) \arctan(\alpha), \quad a_-(\alpha) := -a_+(-\alpha), \quad \alpha \in \mathbb{R},$$

where $H(\cdot)$ denotes the Heaviside step function. It is then easy to check (see Figure 3.7) that for any $E > 0$,

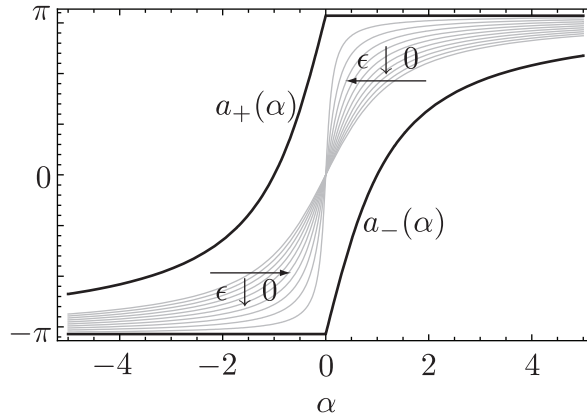


Figure 3.7: The graphs of $a_-(\alpha) < a_+(\alpha)$ (black) and several graphs of $2 \arctan(\epsilon^{-1}\alpha)$ for $\epsilon \leq 1$ (gray).

$$(3.161) \quad 0 < \epsilon \leq E \quad \implies \quad a_-(E^{-1}\alpha) \leq 2 \arctan(\epsilon^{-1}\alpha) \leq a_+(E^{-1}\alpha), \quad \alpha \in \mathbb{R}.$$

Therefore, for any $E > 0$ and all $0 < \epsilon < E$,

$$(3.162) \quad \int_{\mathbb{R}} a_-(E^{-1}\alpha) d\mu_\epsilon(\alpha) \leq \int_{\mathbb{R}} 2 \arctan(\epsilon^{-1}\alpha) d\mu_\epsilon(\alpha) \leq \int_{\mathbb{R}} a_+(E^{-1}\alpha) d\mu_\epsilon(\alpha).$$

Using Lemma III.17 we may pass to the limit $\epsilon \downarrow 0$ in the lower and upper bounds to obtain

$$(3.163) \quad \liminf_{\epsilon \downarrow 0} \int_{\mathbb{R}} 2 \arctan(\epsilon^{-1}\alpha) d\mu_\epsilon(\alpha) \geq \int_{\mathbb{R}} a_-(E^{-1}\alpha) d\mu(\alpha)$$

and also

$$(3.164) \quad \limsup_{\epsilon \downarrow 0} \int_{\mathbb{R}} 2 \arctan(\epsilon^{-1} \alpha) d\mu_{\epsilon}(\alpha) \leq \int_{\mathbb{R}} a_{+}(E^{-1} \alpha) d\mu(\alpha).$$

In these statements, $E > 0$ is an arbitrary parameter, and the limits are uniform for (x, t) in compact sets. But $a_{\pm}(E^{-1} \alpha)$ are uniformly bounded functions that both tend pointwise for $\alpha \neq 0$ to the same limit function $\pi \operatorname{sgn}(\lambda)$ as $E \downarrow 0$, while μ is a fixed measure that is absolutely continuous with respect to Lebesgue measure on \mathbb{R} , so by the Lebesgue Dominated Convergence Theorem,

$$(3.165) \quad \lim_{E \downarrow 0} \int_{\mathbb{R}} a_{\pm}(E^{-1} \alpha) d\mu(\alpha) = \int_{\mathbb{R}} \pi \operatorname{sgn}(\alpha) d\mu(\alpha).$$

By letting $E \downarrow 0$, it then follows from (3.163) and (3.164) that

$$(3.166) \quad \lim_{\epsilon \downarrow 0} \int_{\mathbb{R}} 2 \arctan(\epsilon^{-1} \alpha) d\mu_{\epsilon}(\alpha) = \int_{\mathbb{R}} \pi \operatorname{sgn}(\alpha) d\mu(\alpha)$$

with the limit being uniform for (x, t) in any given compact set. Finally, according to (3.13), we have (independent of x and t)

$$(3.167) \quad \lim_{\epsilon \downarrow 0} \frac{\epsilon N(\epsilon)}{M} = 1,$$

so combining this result with (3.166) and noting that $d\mu(\alpha) = G(\alpha; x, t) d\alpha$ completes the proof of Proposition III.8.

3.2.5 Differentiation of \tilde{U}_{ϵ} . Burgers' Equation and Weak Convergence of \tilde{u}_{ϵ}

Let $\phi \in \mathcal{D}(\mathbb{R})$ be a test function. Then by integration by parts and the uniform convergence of $\tilde{U}_{\epsilon}(x, t)$ to $U(x, t)$ on compact sets in the (x, t) -plane guaranteed by Proposition III.8,

$$(3.168) \quad \begin{aligned} \lim_{\epsilon \downarrow 0} \int_{\mathbb{R}} \tilde{u}_{\epsilon}(x, t) \phi(x) dx &= \lim_{\epsilon \downarrow 0} \int_{\mathbb{R}} \frac{\partial \tilde{U}_{\epsilon}}{\partial x}(x, t) \phi(x) dx \\ &= - \lim_{\epsilon \downarrow 0} \int_{\mathbb{R}} \tilde{U}_{\epsilon}(x, t) \phi'(x) dx \\ &= - \int_{\mathbb{R}} U(x, t) \phi'(x) dx. \end{aligned}$$

Lemma III.18. *The limit function $U(x, t)$ is continuously differentiable with respect to x , and if (x, t) is a point for which there are $2P(x, t) + 1$ solutions $u_0^B(x, t) < \dots < u_{2P(x,t)}^B(x, t)$ of the implicit equation (3.173),*

$$(3.169) \quad \frac{\partial U}{\partial x}(x, t) = \sum_{n=0}^{2P(x,t)} (-1)^n u_n^B(x, t),$$

and the above formula is extended to nongeneric (x, t) by continuity.

Proof. Exchanging the order of integration in the double-integral formula for $U(x, t)$ obtained by substituting $d\mu(\alpha) = G(\alpha; x, t) d\alpha$ with G given by (3.49) into (3.48), we obtain

$$(3.170) \quad U(x, t) = \int_{-L}^0 J(\lambda; x, t) d\lambda,$$

where

$$(3.171) \quad J(\lambda; x, t) := -\frac{1}{4\lambda} \int_{-2\lambda(x+2\lambda t-x_+(\lambda))}^{-2\lambda(x+2\lambda t-x_-(\lambda))} \operatorname{sgn}(\alpha) d\alpha.$$

Note that for $\lambda \in [-L, 0]$ the upper limit of integration is greater than or equal to the lower limit. Moreover the integral in $J(\lambda; x, t)$ is easily evaluated; for $-L < \lambda < 0$,

$$(3.172) \quad J(\lambda; x, t) = \begin{cases} -\pi F(\lambda), & x + 2\lambda t - x_-(\lambda) < 0, \\ x + 2\lambda t + \gamma(\lambda), & x + 2\lambda t - x_+(\lambda) \leq 0 \leq x + 2\lambda t - x_-(\lambda) \\ \pi F(\lambda), & x + 2\lambda t - x_+(\lambda) > 0. \end{cases}$$

It follows from the relations $x_{\pm}(\lambda) = \pm\pi F(\lambda) - \gamma(\lambda)$ that for an admissible initial condition u_0 , J is a continuous function of x for each fixed t , uniformly with respect to $\lambda \in [-L, 0]$, and hence also from (3.170) that $U(\cdot, t)$ is continuous on \mathbb{R} for each t . To prove that $U(\cdot, t)$ is continuously differentiable it will therefore suffice to establish continuous differentiability on the complement of a finite set of points and that the resulting piecewise formula for $\partial U/\partial x$ extends continuously to the whole real line.

To use the formula (3.172) in the representation (3.170) we therefore need to know those points $\lambda \in (-L, 0)$ at which one of the two quantities $x + 2\lambda t - x_+(\lambda) < x + 2\lambda t - x_-(\lambda)$ changes sign. Under the variable substitution $\lambda = -u^B$, the definition of the turning points $x_{\pm}(\lambda)$ as branches of the inverse function of u_0 implies that the union of solutions of the two equations $x + 2\lambda t - x_{\pm}(\lambda) = 0$ is exactly the totality of solutions of the implicit equation

$$(3.173) \quad u^B = u_0(x - 2u^B t).$$

In other words, the transitional points λ for the formula (3.172) correspond under the sign change $u^B = -\lambda$ to the branches of the multivalued solution of Burgers' equation

$$(3.174) \quad \frac{\partial u^B}{\partial t} + 2u^B \frac{\partial u^B}{\partial x} = 0$$

subject to the admissible initial condition $u^B(x, 0) = u_0(x)$.

Note that admissibility of u_0 implies (see Definition III.1) that given any $t \in \mathbb{R}$ there exist only a finite number of breaking points (x_{ξ}, t_{ξ}) with t_{ξ} in the closed interval between 0 and t . Indeed, the breaking points correspond to values of $\xi \in \mathbb{R}$ for which $u_0''(\xi) = 0$ but $u_0'''(\xi) \neq 0$, and the breaking times are $t_{\xi} = (-2u_0'(\xi))^{-1}$; since $u_0'(\xi)$ decays to zero for large ξ , bounded breaking times t_{ξ} correspond to bounded ξ , and there are only finitely many of these by hypothesis. Moreover, each breaking point (x_{ξ}, t_{ξ}) generates a new fold in the solution surface lying between two caustic curves emerging in the direction of increasing $|t|$ from (x_{ξ}, t_{ξ}) , and because $u_0'''(\xi) \neq 0$ there are exactly two more sheets of the multivalued solution of Burgers' equation born within the fold as a result of a simple pitchfork bifurcation. Therefore, the union of caustic curves and breaking points meets any line of constant t in the (x, t) -plane in a finite set of points $\{x_j^{\text{crit}}(t)\}$, and on every connected component of the set

$S_t := \{(x, t) | x \in \mathbb{R} \setminus \{x_j^{\text{crit}}(t)\}\}$, there is a finite, odd, and constant (with respect to x) number $2P(x, t) + 1$ of roots of the equation (3.173), and all roots are simple (and hence differentiable with respect to x).

If $t \geq 0$, then by admissibility of u_0 the quantity $b_-(\lambda; x, t) := x + 2\lambda t - x_-(\lambda)$ is strictly increasing as a function of λ on the interval $(-L, 0)$, and therefore in this interval there can exist at most one root of $b_-(\lambda; x, t)$, regardless of the value of $x \in \mathbb{R}$. Moreover, $b_-(\lambda; x, t) \rightarrow +\infty$ as $\lambda \uparrow 0$, so there will be exactly one root in $(-L, 0)$ if $b_-(-L; x, t) = x - x_0 - 2Lt < 0$ and no root in $(-L, 0)$ if $x - x_0 - 2Lt > 0$. Since $b_+(\lambda; x, t) := x + 2\lambda t - x_+(\lambda) < b_-(\lambda; x, t)$ for $-L < \lambda < 0$, if $x - x_0 - 2Lt < 0$, all roots of $b_+(\lambda; x, t)$ in $(-L, 0)$ must lie to the right of the root of $b_-(\lambda; x, t)$. Thus, for $x \in S_t \setminus \{x_0 + 2Lt\}$, we either have

$$(3.175) \quad \begin{aligned} U(x, t) &= \int_{-u_0^B}^0 (x + 2\lambda t + \gamma(\lambda)) d\lambda \\ &+ \sum_{p=1}^{P(x,t)} \left[\pi \int_{-u_{2p-1}^B}^{-u_{2p-2}^B} F(\lambda) d\lambda + \int_{-u_{2p}^B}^{-u_{2p-1}^B} (x + 2\lambda t + \gamma(\lambda)) d\lambda \right] \\ &+ \pi \int_{-L}^{-u_{2P(x,t)}^B} F(\lambda) d\lambda, \quad x \in S_t, \quad x > x_0 + 2Lt, \end{aligned}$$

in which case $u_0^B(x, t) < \dots < u_{2P(x,t)}^B(x, t)$ are all roots of $b_+(-u^B; x, t)$, or

$$(3.176) \quad \begin{aligned} U(x, t) &= \int_{-u_0^B}^0 (x + 2\lambda t + \gamma(\lambda)) d\lambda \\ &+ \sum_{p=1}^{P(x,t)} \left[\pi \int_{-u_{2p-1}^B}^{-u_{2p-2}^B} F(\lambda) d\lambda + \int_{-u_{2p}^B}^{-u_{2p-1}^B} (x + 2\lambda t + \gamma(\lambda)) d\lambda \right] \\ &- \pi \int_{-L}^{-u_{2P(x,t)}^B} F(\lambda) d\lambda, \quad x \in S_t, \quad x < x_0 + 2Lt, \end{aligned}$$

in which case $u_0^B(x, t) < \dots < u_{2P(x,t)-1}^B(x, t)$ are roots of $b_+(-u^B; x, t)$ while $u_{2P(x,t)}^B(x, t)$ with $u_{2P(x,t)}^B(x, t) > u_{2P(x,t)-1}^B(x, t)$ is a root of $b_-(-u^B; x, t)$. In both cases, the condition $x \in S_t$ guarantees that all roots are differentiable with respect to x , so we may

calculate $\partial U/\partial x$ by Leibniz' rule:

(3.177)

$$\begin{aligned} \frac{\partial U}{\partial x}(x, t) &= b_+(-u_{2P}^B(x, t); x, t) \frac{\partial u_{2P}^B}{\partial x}(x, t) + \sum_{n=0}^{2P-1} (-1)^n b_+(-u_n^B(x, t); x, t) \frac{\partial u_n^B}{\partial x}(x, t) \\ &\quad + \sum_{n=0}^{2P} (-1)^n u_n^B(x, t), \quad x \in S_t, \quad x > x_0 + 2Lt, \end{aligned}$$

or

(3.178)

$$\begin{aligned} \frac{\partial U}{\partial x}(x, t) &= b_-(-u_{2P}^B(x, t); x, t) \frac{\partial u_{2P}^B}{\partial x}(x, t) + \sum_{n=0}^{2P-1} (-1)^n b_+(-u_n^B(x, t); x, t) \frac{\partial u_n^B}{\partial x}(x, t) \\ &\quad + \sum_{n=0}^{2P} (-1)^n u_n^B(x, t), \quad x \in S_t, \quad x < x_0 + 2Lt, \end{aligned}$$

where in both cases $P = P(x, t)$ is a constant nonnegative integer on each connected component of S_t . The terms on the first line in each of these formulae arise from differentiating the limits of integration and using $x_{\pm}(\lambda) = \pm\pi F(\lambda) - \gamma(\lambda)$, while the terms on the second line arise from the explicit partial differentiation of the integrand $x + 2\lambda t + \gamma(\lambda)$ with respect to x . It follows from our division of the solutions of (3.173) among the roots of b_+ and b_- that in both cases the terms on the first line vanish identically, with the result that

$$(3.179) \quad \frac{\partial U}{\partial x}(x, t) = \sum_{n=0}^{2P(x,t)} (-1)^n u_n^B(x, t), \quad x \in S_t \setminus \{x_0 + 2Lt\}.$$

This expression is clearly continuous in x on each connected component of $S_t \setminus \{x_0 + 2Lt\}$. Moreover, it extends continuously to the finite complement in \mathbb{R}_x (at fixed $t \geq 0$) because at caustics pairs of solution branches entering into (3.179) with opposite signs simply coalesce. Therefore $U(\cdot, t)$ is indeed continuously differentiable for $t \geq 0$ and its derivative is given by the desired simple formula (3.169). Virtually the same argument applies to $t \leq 0$ with the roles of $b_{\pm}(\lambda; x, t)$ reversed, and the resulting formula for $\partial U/\partial x$ is the same. \square

It follows from this result that we may integrate by parts in (3.168) and obtain

$$(3.180) \quad \lim_{\epsilon \downarrow 0} \int_{\mathbb{R}} \tilde{u}_\epsilon(x, t) \phi(x) dx = \int_{\mathbb{R}} \frac{\partial U}{\partial x}(x, t) \phi(x) dx$$

for every test function $\phi \in \mathcal{D}(\mathbb{R})$. Now let $v \in L^2(\mathbb{R})$. Since $\mathcal{D}(\mathbb{R})$ is dense in $L^2(\mathbb{R})$, for each $\sigma > 0$ there exists a test function $\phi_\sigma \in \mathcal{D}(\mathbb{R})$ such that

$$(3.181) \quad \|\phi_\sigma - v\|_2^2 := \int_{\mathbb{R}} |\phi_\sigma(x) - v(x)|^2 dx < \sigma^2.$$

Then,

$$(3.182) \quad \begin{aligned} \int_{\mathbb{R}} \left[\tilde{u}_\epsilon(x, t) - \frac{\partial U}{\partial x}(x, t) \right] v(x) dx &= \int_{\mathbb{R}} \left[\tilde{u}_\epsilon(x, t) - \frac{\partial U}{\partial x}(x, t) \right] \phi_\sigma(x) dx \\ &+ \int_{\mathbb{R}} \frac{\partial U}{\partial x}(x, t) [\phi_\sigma(x) - v(x)] dx \\ &- \int_{\mathbb{R}} \tilde{u}_\epsilon(x, t) [\phi_\sigma(x) - v(x)] dx. \end{aligned}$$

Observe that, according to the definition (see Definition III.3) of $\tilde{u}_\epsilon(x, t)$ in terms of the modified scattering data, it follows from (2.133) that

$$(3.183) \quad \int_{\mathbb{R}} \tilde{u}_\epsilon(x, t)^2 dx = -4\pi\epsilon \sum_{n=1}^{N(\epsilon)} \tilde{\lambda}_n.$$

This Riemann sum converges as $\epsilon \downarrow 0$:

$$(3.184) \quad \lim_{\epsilon \downarrow 0} \int_{\mathbb{R}} \tilde{u}_\epsilon(x, t)^2 dx = -4\pi \int_{-L}^0 \lambda F(\lambda) d\lambda = \int_{\mathbb{R}} u_0(x)^2 dx,$$

where the second equality follows from the identities (2.141), which essentially define $F(\lambda)$ in terms of the admissible initial condition u_0 . Therefore, $\|\tilde{u}_\epsilon(\cdot, t)\|_2$ is bounded for sufficiently small ϵ , independently of t .

Also, $\partial U/\partial x$ is independent of ϵ and from the formula (3.169) it is easy to check that it is positive and bounded above by the constant L for all (x, t) . Therefore

$$(3.185) \quad \left\| \frac{\partial U}{\partial x}(\cdot, t) \right\|_2^2 \leq L \int_{\mathbb{R}} \frac{\partial U}{\partial x}(x, t) dx.$$

By the formula (3.169), the latter integral is equal to the area between the graph of the multivalued solution curve for Burgers' equation and the x -axis. Since points on the graph at the same height move with the same speed, this area is independent of time t , and hence we have

$$(3.186) \quad \left\| \frac{\partial U}{\partial x}(\cdot, t) \right\|_2^2 \leq 2\pi LM,$$

where the mass M is defined in terms of the initial condition u_0 by (3.6). In fact, for $0 \leq t < T$, where T is the breaking time, it follows from the fact that $\partial U/\partial x$ as given by (3.169) reduces to the classical solution $u_0^B(x, t)$ of Burgers' equation with initial data u_0 , which conserves exactly the $L^2(\mathbb{R}_x)$ norm, that

$$(3.187) \quad \left\| \frac{\partial U}{\partial x}(\cdot, t) \right\|_2^2 = \|u_0^B(\cdot, t)\|_2^2 = \int_{\mathbb{R}} u_0(x)^2 dx, \quad 0 \leq t < T.$$

We will use this fact below in §3.3 when we prove Corollary III.6. In any case, these considerations show that for all $\epsilon > 0$ sufficiently small there exists a constant $K > 0$ independent of t such that

$$(3.188) \quad \left\| \frac{\partial U}{\partial x}(\cdot, t) \right\|_2 + \|\tilde{u}_\epsilon(\cdot, t)\|_2 \leq K$$

holds for all $t \geq 0$.

Now, by Cauchy-Schwarz it follows that

$$(3.189) \quad \left| \int_{\mathbb{R}} \frac{\partial U}{\partial x}(x, t) [\phi_\sigma(x) - v(x)] dx - \int_{\mathbb{R}} \tilde{u}_\epsilon(x, t) [\phi_\sigma(x) - v(x)] dx \right| \leq K \|\phi_\sigma - v\|_2.$$

Given $\omega > 0$ arbitrarily small, we then choose $\sigma = \omega/(2M)$ and then (3.182) implies that

$$(3.190) \quad \left| \int_{\mathbb{R}} \left[\tilde{u}_\epsilon(x, t) - \frac{\partial U}{\partial x}(x, t) \right] v(x) dx \right| \leq \left| \int_{\mathbb{R}} \left[\tilde{u}_\epsilon(x, t) - \frac{\partial U}{\partial x}(x, t) \right] \phi_{\omega/(2M)}(x) dx \right| + \frac{\omega}{2}.$$

Finally, since $\phi_{\omega/(2M)}$ is a test function independent of ϵ , we may use (3.180) to choose $\epsilon > 0$ so small that the first term on the right-hand side is less than $\omega/2$.

This proves that

$$(3.191) \quad \text{w}_x\text{-}\lim_{\epsilon \downarrow 0} \tilde{u}_\epsilon(x, t) = \frac{\partial U}{\partial x}(x, t)$$

(weak L^2 convergence) uniformly for t in bounded intervals. Combining (3.169) with (3.191) completes the proof of Theorem III.5.

3.3 Strong Convergence Before Breaking

In this brief section we give a proof of Corollary III.6, following closely Lax and Levermore (see Theorem 4.5 in part II of [43]). Starting from the identity

$$(3.192) \quad \|\tilde{u}_\epsilon(\cdot, t) - u_0^{\text{B}}(\cdot, t)\|_2^2 = \int_{\mathbb{R}} \tilde{u}_\epsilon(x, t)^2 dx + \int_{\mathbb{R}} u_0^{\text{B}}(x, t)^2 dx - 2 \int_{\mathbb{R}} \tilde{u}_\epsilon(x, t) u_0^{\text{B}}(x, t) dx,$$

we note that for $0 \leq t < T$, where T is the breaking time, (3.184) and (3.187) imply that

$$(3.193) \quad \lim_{\epsilon \downarrow 0} \|\tilde{u}_\epsilon(\cdot, t) - u_0^{\text{B}}(\cdot, t)\|_2^2 = 2 \int_{\mathbb{R}} u_0(x)^2 dx - 2 \lim_{\epsilon \downarrow 0} \int_{\mathbb{R}} \tilde{u}_\epsilon(x, t) u_0^{\text{B}}(x, t) dx.$$

But $u_0^{\text{B}}(\cdot, t) \in L^2(\mathbb{R})$ is independent of ϵ , so by Theorem III.5,

$$(3.194) \quad \lim_{\epsilon \downarrow 0} \int_{\mathbb{R}} \tilde{u}_\epsilon(x, t) u_0^{\text{B}}(x, t) dx = \int_{\mathbb{R}} u_0^{\text{B}}(x, t)^2 dx = \int_{\mathbb{R}} u_0(x)^2 dx,$$

with the second equality following from (3.187) for $0 \leq t < T$. Therefore

$$(3.195) \quad \lim_{\epsilon \downarrow 0} \|\tilde{u}_\epsilon(\cdot, t) - u_0^{\text{B}}(\cdot, t)\|_2 = 0$$

as desired, and the proof is complete.

3.4 Numerical Verification

To illustrate the weak convergence of $\tilde{u}_\epsilon(x, t)$ as guaranteed by Theorem III.5, and to attempt to empirically quantify the rate of convergence, we have directly used the exact formula (3.42) for $\tilde{U}_\epsilon(x, t)$ having first chosen the modified scattering data corresponding to the admissible initial condition $u_0(x) = 2(1+x^2)^{-1}$ as specified in Definition III.3, and compared the result for several different values of ϵ with the limiting formula (3.48) for $U(x, t)$. Our results are shown in Figure 3.8. These plots clearly display the locally uniform convergence specified in Proposition III.8. An interesting feature is the apparent regular “staircase” form of the graph of $\tilde{U}_\epsilon(x, t)$ as a function of x ; that the steps have nearly equal height is a consequence of the fact that near the leading edge of the oscillation zone for u_ϵ (which lies approximately in the range $4 < x < 16$ in these plots) the undular bore wavetrain that is generated from the smooth initial data resolves into a train of solitons of the BO equation, each of which has a fixed mass proportional to ϵ (independent of amplitude and velocity).

To the eye, the size of the error between $\tilde{U}_\epsilon(x, t)$ and $U(x, t)$ appears to scale with ϵ . To confirm this more quantitatively, we collected numerical data from several experiments, each performed with a different value of ϵ at the fixed time $t = 4$. The supremum norm, calculated over the interval $-10 < x < 20$, of the error resulting from each of these experiments is plotted in Figure 3.9. On this plot with logarithmic axes, the data points appear to lie along a straight line, and we calculated the least squares linear fit to the data to be given by

$$(3.196) \quad \log_{10}(\|\tilde{U}_\epsilon(\cdot, 4) - U(\cdot, 4)\|_\infty) = 0.988 \log_{10}(\epsilon) + 0.523$$

where the slope and intercept are given to three significant digits. This strongly suggests a linear rate of convergence, in which the error is asymptotically proportional

to ϵ as $\epsilon \downarrow 0$.

The initial data $u_0(x) = 2(1+x^2)^{-1}$ was chosen for these experiments because it is the only initial condition (up to a constant multiple) for which the *exact* scattering data is known for a sequence of values of ϵ tending to zero. This is the result of a calculation of Kodama, Ablowitz, and Satsuma [40], which is introduced in §2.3. They showed that if $u_0(x) = 2(1+x^2)^{-1}$, then the reflection coefficient $\beta(\lambda)$ vanishes identically if $\epsilon = 1/N$ for any positive integer N . Moreover, there are in this case exactly N eigenvalues $\lambda_1 < \lambda_2 < \dots < \lambda_N$ of the operator \mathcal{L} defined by (2.46), and they are the roots of the following equation

$$(3.197) \quad L_N \left(-\frac{2\lambda}{\epsilon} \right) = L_N(-2N\lambda) = 0,$$

where L_N is the Laguerre polynomial of degree N . The corresponding phase constants γ_n all vanish exactly. The approximate eigenvalues determined from the initial condition u_0 via the formula (3.14) do not agree exactly with the scaled roots of the Laguerre polynomial of degree N (although the approximate phase constants agree exactly with the true phase constants), so it is a worthwhile exercise to compare the function $\tilde{u}_\epsilon(x, t)$ as specified by Definition III.3 with the true solution $u_\epsilon(x, t)$ of the Cauchy problem for the BO equation with initial data $u_0(x) = 2(1+x^2)^{-1}$. Of course Corollary III.6 guarantees strong convergence in L^2 at $t = 0$ (that is, $\tilde{u}_\epsilon(\cdot, 0)$ is L^2 -close to $u_0(\cdot)$) but this alone does not guarantee that $\tilde{u}_\epsilon(x, t)$ approximates $u_\epsilon(x, t)$ in any sense for $t > 0$. We made the comparison for several values of $\epsilon > 0$ corresponding to a reflectionless exact solution of the Cauchy problem constructed² from the

²In fact this is the numerical method we used to create the plots in Figure 1.1. This has a tremendous advantage over taking a more traditional numerical approach to the Cauchy problem for the BO equation (that is, one involving time stepping) since the calculations necessary to find the solution for any two given values of t are completely independent, so errors do not propagate (and to find the solution for any given time t it is not necessary to perform any calculations at all for intervening times from the initial instant). The only source of error in the use of the determinantal

determinantal formula (2.112) at the time $t = 4$, which is well beyond the breaking time. Our results are shown in Figure 3.10. These plots show that the modification of the scattering data used to construct $\tilde{u}_\epsilon(x, t)$ results in a phase shift relative to $u_\epsilon(x, t)$ that is proportional to ϵ , the approximate wavelength of the oscillations. In particular, $\tilde{u}_\epsilon(x, t)$ does not remain close to $u_\epsilon(x, t)$ after the breaking time in any strong sense, although it appears highly likely that convergence is restored in the weak topology.

formula (2.112), at least if the differentiation is carried out explicitly resulting in a sum of N determinants, is due to round-off.

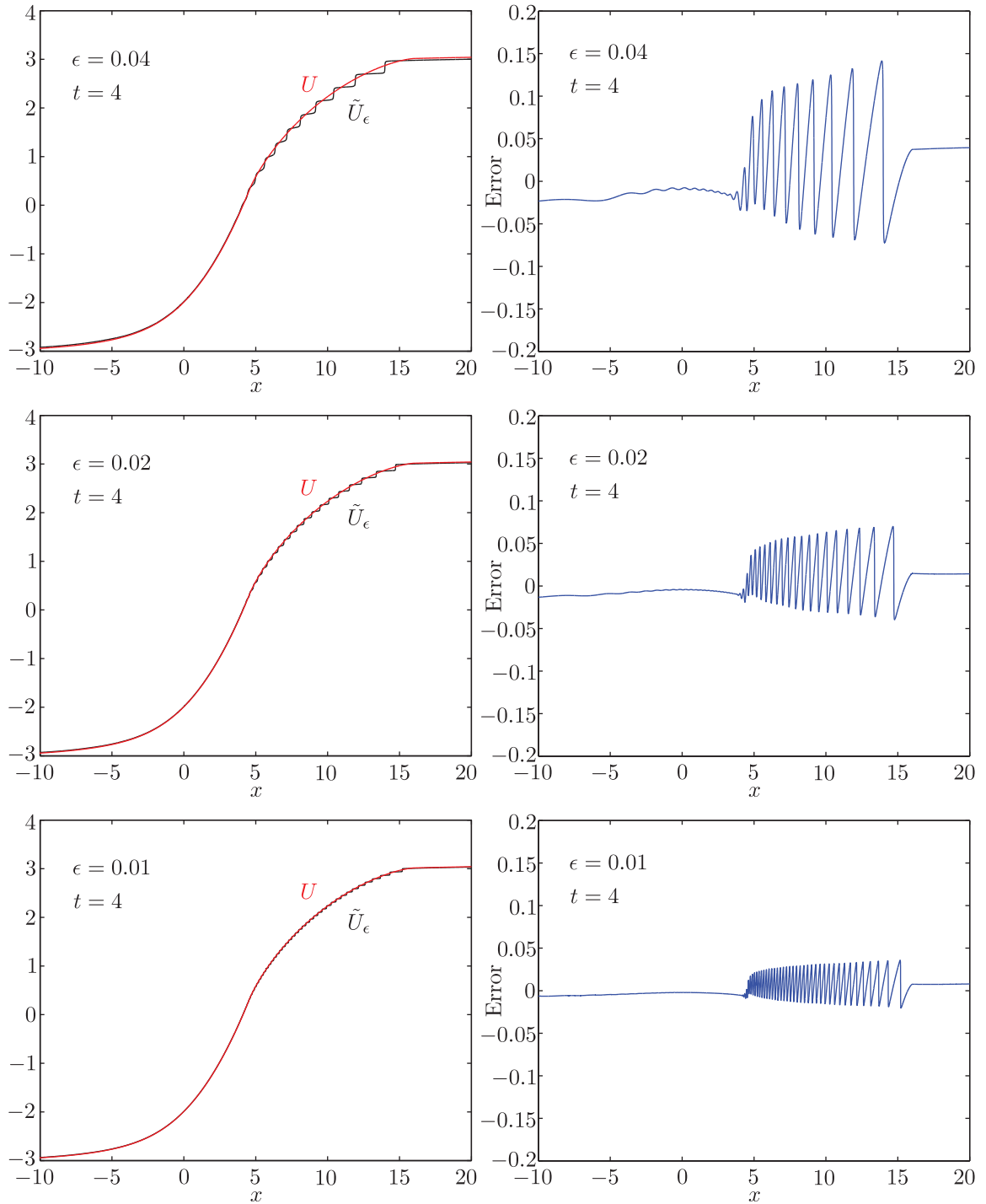


Figure 3.8: Left: plots of $\tilde{U}_\epsilon(x, t)$ (black) and its locally uniform limit $U(x, t)$ (red) at $t = 4$ for various values of ϵ . For these plots, $u_0(x) := 2(1 + x^2)^{-1}$. Right: corresponding plots of the error $U(x, t) - \tilde{U}_\epsilon(x, t)$.

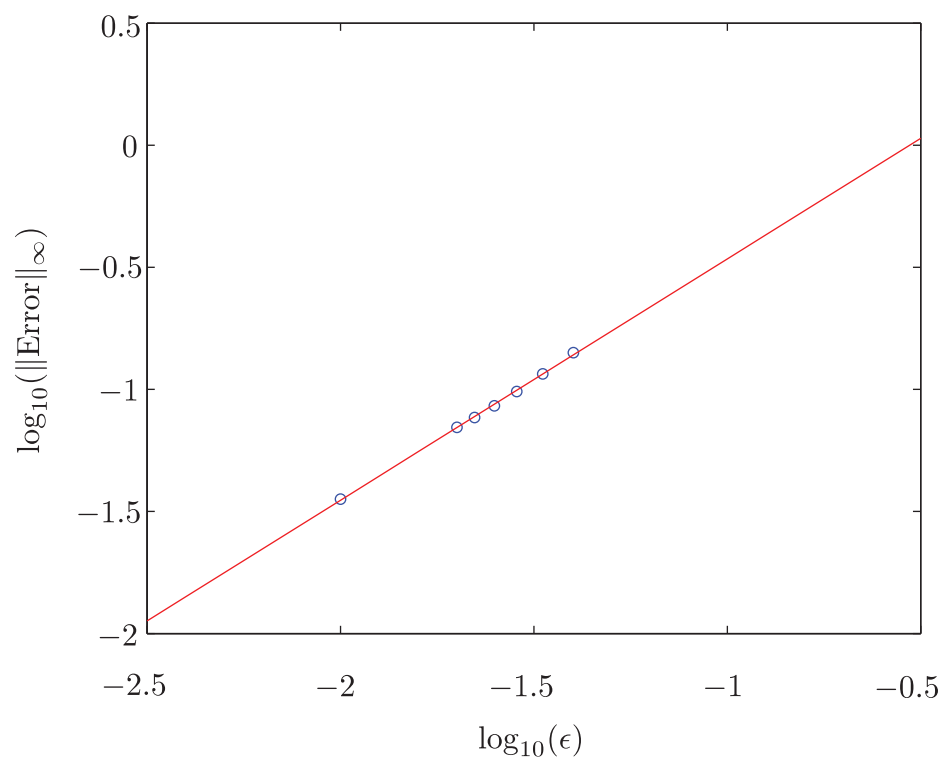


Figure 3.9: Circles: $\log_{10}(\|\tilde{U}_\epsilon(\cdot, 4) - U(\cdot, 4)\|_\infty)$ for $\epsilon = 1/25, 1/30, 1/35, 1/40, 1/45, 1/50,$ and $1/100$, as a function of $\log_{10}(\epsilon)$. In red: The least-squares linear fit.

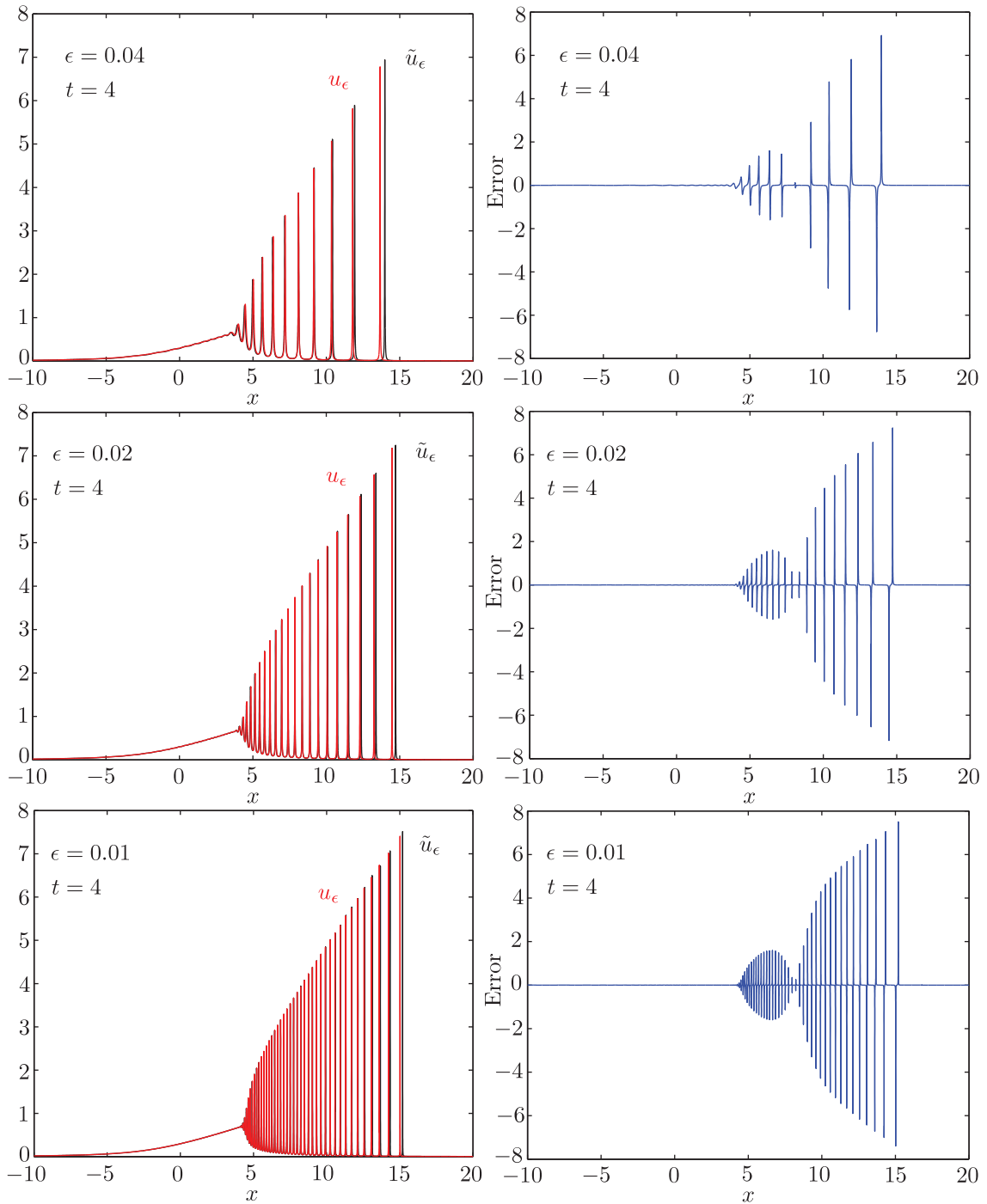


Figure 3.10: Left: plots of $\tilde{u}_\epsilon(x, t)$ (black) shown together with $u_\epsilon(x, t)$ (red) for the initial data $u_0(x) = 2(1 + x^2)^{-1}$ shown for several values of ϵ at $t = 4$. Right: The error $u_\epsilon(x, t) - \tilde{u}_\epsilon(x, t)$.

CHAPTER IV

Generalizations of the Zero-Dispersion Limit of the BO Equation

In this chapter, we provide generalizations of Theorem III.5 and their proof by introducing the higher-order BO equations.

4.1 Higher-Order BO Equations and Their Soliton Solutions

The higher-order BO equations introduced by Matsuno [51] are

$$(4.1) \quad u_t = -\frac{\partial K_n(u)}{\partial x}, \quad n = 3, 4, 5, \dots,$$

where the variational derivatives $K_n(u)$ are defined by

$$(4.2) \quad K_n(u) := \frac{\delta I_n}{\delta u}, \quad n = 3, 4, 5, \dots$$

Here I_n are defined by the equation (2.130) and the recurrence relation (2.128).

The variational derivatives $K_n(u)$ can be calculated by using the recurrence relation (2.128), the equation (2.130) and the definition of $K_n(u)$. It is easy to obtain that

$$(4.3) \quad K_3(u) = u^2 + \epsilon \mathcal{H}(u_x),$$

which implies the higher-order BO equation (4.1) is the BO equation (1.1) for $n = 3$.

The formula of the N -soliton solutions of the higher order BO equations for $n = 4, 5, 6$ obtained by Matsuno [51] via the bilinear transformation method is

$$(4.4) \quad u(x, t) = 2\epsilon \frac{\partial}{\partial x} \Im (\log(\tau_n(x, t; \epsilon))),$$

where the ‘‘tau-function’’ $\tau_n(x, t; \epsilon) := \det(\mathbb{I} + i\epsilon^{-1}\mathbf{A}_n(\epsilon))$. Here $\mathbf{A}_n(\epsilon)$ is an $N \times N$ Hermitean matrix given by

$$(4.5) \quad (\mathbf{A}_n(\epsilon))_{lm} = -2\lambda_m(x + (-1)^{n-1}(n-1)\lambda_m^{n-2}t + \gamma_m), \quad \text{for } l = m,$$

and

$$(4.6) \quad (\mathbf{A}_n(\epsilon))_{lm} = \frac{2i\epsilon(\lambda_l\lambda_m)^{1/2}}{\lambda_l - \lambda_m}, \quad \text{for } l \neq m.$$

In fact, the formula (4.4) is valid for $n = 3, 4, 5, \dots$, which is proved by Matsuno in [54].

4.2 Generalizations

By comparing the formula of the N -soliton solutions of the higher order BO equations and the formula of the N -soliton solutions of the BO equation, one can find the only difference between the formula (4.4) and the formula (2.112) is the diagonal entries of the matrix \mathbf{A}_ϵ are $-2\lambda_m(x + 2\lambda_m t + \gamma_m)$ and the diagonal entries of the matrix $\mathbf{A}_n(\epsilon)$ are $-2\lambda_m(x + (-1)^{n-1}(n-1)\lambda_m^{n-2}t + \gamma_m)$. Then we introduce a new function $\bar{u}_n(x, t; \epsilon)$:

$$(4.7) \quad \bar{u}_n(x, t; \epsilon) = 2\epsilon \frac{\partial}{\partial x} \Im (\log(\bar{\tau}_n(x, t; \epsilon))),$$

where the ‘‘tau-function’’ $\bar{\tau}_n(x, t; \epsilon) := \det(\mathbb{I} + i\epsilon^{-1}\bar{\mathbf{A}}_n(\epsilon))$. Here $\bar{\mathbf{A}}_n(\epsilon)$ is an $N(\epsilon) \times N(\epsilon)$ Hermitean matrix given by

$$(4.8) \quad (\bar{\mathbf{A}}_n(\epsilon))_{lm} = -2\tilde{\lambda}_m(x + (-1)^{n+1}(n+1)\tilde{\lambda}_m^n t + \gamma_m), \quad \text{for } l = m,$$

and

$$(4.9) \quad (\bar{\mathbf{A}}_n(\epsilon))_{lm} = \frac{2i\epsilon(\tilde{\lambda}_l\tilde{\lambda}_m)^{1/2}}{\tilde{\lambda}_l - \tilde{\lambda}_m}, \quad \text{for } l \neq m.$$

Here, the number $N(\epsilon)$ is defined by (3.12) and $\{\tilde{\lambda}_n\}_{n=1}^{N(\epsilon)}$ and $\{\tilde{\gamma}_n\}_{n=1}^{N(\epsilon)}$ are defined by (3.14) and (3.15) respectively. In fact, the function $\bar{u}_n(x, t; \epsilon)$ is a N -soliton solution of the $(n + 2)$ th order BO equation. The function $\bar{u}_n(x, t; \epsilon)$ is same as the function $\tilde{u}_\epsilon(x, t)$ defined by (3.16) when the integer $n = 1$. By following the approach used in Chapter III, one can obtain a generalization of Theorem III.5. The proof is provided in §4.3.

Theorem IV.1. *Let $u_n^0(x, t) < u_n^1(x, t) < \dots < u_n^{2P(x,t)}(x, t)$ be the branches of the multivalued (method of characteristics) solution of the following equation*

$$(4.10) \quad \frac{\partial u_n}{\partial t} + (n + 1)(u_n)^n \frac{\partial u_n}{\partial x} = 0$$

subject to an admissible initial condition

$$(4.11) \quad u_n(x, 0) = u_0(x).$$

Then, the weak $L^2(\mathbb{R})$ (in x) limit of $\bar{u}_n(x, t; \epsilon)$ is given by

$$(4.12) \quad \text{w}_x\text{-}\lim_{\epsilon \downarrow 0} \bar{u}_n(x, t; \epsilon) = \sum_{m=0}^{2P(x,t)} (-1)^m u_n^m(x, t),$$

uniformly for t in arbitrary bounded intervals.

Similarly as the inviscid Burgers equation, the multivalued solution of the equation (4.10) can be constructed by the method of characteristics. In fact, the multivalued solution of the equation (4.10) can be obtained by solving the following implicit equation

$$(4.13) \quad u_n = u_0(x - (n + 1)(u_n)^n t).$$

Furthermore, after substituting (4.4) into (4.1), one can find the N -soliton solutions of the higher order BO equations $u(x, t)$ given by (4.4) satisfy

$$(4.14) \quad \frac{\partial}{\partial t} \left(2\epsilon \frac{\partial}{\partial x} \mathfrak{S}(\log(\tau_\epsilon(x, t))) \right) = -\frac{\partial K_n(u)}{\partial x}, \quad n = 3, 4, 5, \dots$$

This equation suggests

$$(4.15) \quad K_n(u) = -2\epsilon \frac{\partial}{\partial t} \mathfrak{S}(\log(\tau_\epsilon(x, t))) + C(t) \quad \text{for } n = 3, 4, 5, \dots$$

where $C(t)$ is a function of t . According to the definitions of $K_n(u)$ and $\tau_\epsilon(x, t)$, the first term of the equation (4.15) and $K_n(u)$ tend to zero, as x tends to infinity. This fact implies $C(t) \equiv 0$. Then one can obtain the formula of $K_n(u)$ corresponding to the N -soliton solutions of the higher order BO equations:

$$(4.16) \quad K_n(u) = -2\epsilon \frac{\partial}{\partial t} \mathfrak{S}(\log(\tau_\epsilon(x, t))) \quad \text{for } n = 3, 4, 5, \dots$$

Since the function $u(x, 0)$ defined by the equation (4.4) with $\lambda_m = \tilde{\lambda}_m$ and $\gamma_m = 2\tilde{\lambda}_m \bar{t} + \gamma(\tilde{\lambda}_m)$ for $m = 1, 2, \dots, N$ is equal to $\tilde{u}_\epsilon(x, \bar{t})$ defined by (3.16), $K_n(u(x, 0))$ corresponding to $u(x, 0)$ is equal to $K_n(\tilde{u}_\epsilon(x, \bar{t}))$ corresponding to $\tilde{u}_\epsilon(x, \bar{t})$. Then the equation (4.16) suggests

$$(4.17) \quad K_{n+2}(\tilde{u}_\epsilon(x, \bar{t})) = -\frac{\partial \tilde{U}_\epsilon}{\partial t_n}(x, t_1, t_2, \dots, t_n) \Bigg|_{t_1=\bar{t}, t_2=\dots=t_n=0}$$

where $\tilde{U}_\epsilon(x, t_1, t_2, \dots, t_n)$ is given by (3.40) with $-2\tilde{\lambda}_k(x + 2\tilde{\lambda}_k t)$ replaced by $-2\tilde{\lambda}_k(x + 2\tilde{\lambda}_k t_1 - 3\tilde{\lambda}_k^2 t_2 + 4\tilde{\lambda}_k^3 t_3 - 5\tilde{\lambda}_k^4 t_4 + \dots + (-1)^{n+1}(n+1)\tilde{\lambda}_k^n t_n)$. Assume the limit of $\tilde{U}_\epsilon(x, t_1, t_2, \dots, t_n)$ as $\epsilon \rightarrow 0+$ exists:

$$(4.18) \quad U(x, t_1, t_2, \dots, t_n) = \lim_{\epsilon \downarrow 0} \tilde{U}_\epsilon(x, t_1, t_2, \dots, t_n),$$

then by following the approach used in Chapter III, one can obtain a formula for derivatives of $U(x, t_1, t_2, \dots, t_n)$, which are given in the following proposition. The proof is provided in §4.4.

Proposition IV.2. *Let $u_0^B(x, t) < u_1^B(x, t) < \dots < u_{2P(x,t)}^B(x, t)$ be the branches of the multivalued (method of characteristics) solution of the inviscid Burgers equation (3.33) subject to an admissible initial condition $u^B(x, 0) = u_0(x)$. Then the function $U(x, t_1, t_2, \dots, t_n)$ satisfies*

$$(4.19) \quad - \frac{\partial U}{\partial t_n}(x, t_1, t_2, \dots, t_n) \Big|_{t_1=t, t_2=\dots=t_n=0} = \sum_{m=0}^{2P(x,t)} (-1)^m u_m^B(x, t)^n.$$

If (x, t) satisfies $P(x, t) = 0$, then the following conjecture holds true because of Corollary III.6. If (x, t) satisfies $P(x, t) \neq 0$, then the solutions of the BO equation become approximately periodic traveling waves in finite time. An alternative interpretation of the weak limit in x (t_n) is that the weak limit can be viewed as the local average with respect to x (t_n). The formula of the periodic traveling solutions of the BO equation suggests that the weak limit in x is same as the weak limit in t_n , which suggests Conjecture IV.3 holds true. The proof will be finished in the future as a part of ongoing work.

Conjecture IV.3. *Let $u_0^B(x, t) < u_1^B(x, t) < \dots < u_{2P(x,t)}^B(x, t)$ be the branches of the multivalued (method of characteristics) solution of the inviscid Burgers equation (3.33) subject to an admissible initial condition $u^B(x, 0) = u_0(x)$. Then, the weak $L^2(\mathbb{R})$ (in x) limit of $K_{n+2}(\tilde{u}_\epsilon(x, t))$ where n is a positive integer, is given by*

$$(4.20) \quad \text{w}_x\text{-}\lim_{\epsilon \downarrow 0} K_{n+2}(\tilde{u}_\epsilon(x, t)) = \sum_{m=0}^{2P(x,t)} (-1)^m u_m^B(x, t)^n,$$

uniformly for t in arbitrary bounded intervals.

4.3 Proof of Theorem IV.1

According to the definition of the function $\bar{u}_n(x, t; \epsilon)$, one can write $\bar{u}_n(x, t; \epsilon)$ as:

$$(4.21) \quad \bar{u}_n(x, t; \epsilon) = \frac{\partial \bar{U}_n}{\partial x}(x, t; \epsilon), \quad \bar{U}_n(x, t; \epsilon) = 2\epsilon \Im(\log(\bar{\tau}_n(x, t; \epsilon))).$$

By the exactly same analysis as was done in Chapter III, one can obtain

$$(4.22) \quad \bar{U}_n(x, t) = \lim_{\epsilon \downarrow 0} \bar{u}_n(x, t; \epsilon) = \int_{-L}^0 \bar{J}_n(\lambda; x, t) d\lambda,$$

where

$$(4.23) \quad \bar{J}_n(\lambda; x, t) := -\frac{1}{4\lambda} \int_{-2\lambda(x+(-1)^{n+1}(n+1)\lambda^n t - x_+(\lambda))}^{-2\lambda(x+(-1)^{n+1}(n+1)\lambda^n t - x_-(\lambda))} \operatorname{sgn}(\alpha) d\alpha.$$

Since the union of solutions of the two equations $x + (-1)^{n+1}(n+1)\lambda^n t - x_{\pm}(\lambda) = 0$ is exactly $\{-u_n^0(x, t), -u_n^1(x, t), \dots, -u_n^{2P(x,t)}(x, t)\}$, by following the calculation done in §3.2.5, it is easy to show that

$$(4.24) \quad \lim_{\epsilon \downarrow 0} \bar{u}_n(x, t; \epsilon) = \frac{\partial \bar{U}_n(x, t)}{\partial x} = \sum_{m=0}^{2P(x,t)} (-1)^m u_n^m(x, t).$$

4.4 Proof of Proposition IV.2

By applying the exactly same method used in Chapter III, one can find that

$$(4.25) \quad U(x, t_1, t_2, \dots, t_n) = \int_{-L}^0 J(\lambda; x, t_1, t_2, \dots, t_n) d\lambda,$$

where the function $J(\lambda; x, t_1, t_2, \dots, t_n)$ is defined by

$$(4.26) \quad J(\lambda; x, t_1, t_2, \dots, t_n) := -\frac{1}{4\lambda} \int_{-2\lambda(x+2\lambda t_1+\dots+(-1)^{n+1}(n+1)\lambda^n t_n - x_+(\lambda))}^{-2\lambda(x+2\lambda t_1+\dots+(-1)^{n+1}(n+1)\lambda^n t_n - x_-(\lambda))} \operatorname{sgn}(\alpha) d\alpha.$$

By differentiating each side of the equation (4.25) and letting $t_1 = t$ and $t_2 = \dots = t_n = 0$, the equation (4.25) becomes

$$(4.27) \quad \frac{\partial U}{\partial t_n}(x, t, 0, \dots, 0) = \int_{-L}^0 \frac{\partial J}{\partial t_n}(\lambda; x, t, 0, \dots, 0) d\lambda.$$

Here, the integrand of the integral on the right hand side of the equation (4.27) can be written as

$$(4.28) \quad \begin{aligned} & \frac{\partial J}{\partial t_n}(\lambda; x, t, 0, \dots, 0) \\ &= \frac{(-1)^{n+1}(n+1)\lambda^n}{2} (\operatorname{sgn}(-2\lambda b_-(\lambda; x, t)) - \operatorname{sgn}(-2\lambda b_+(\lambda; x, t))) \\ &= \frac{(-1)^{n+1}(n+1)\lambda^n}{2} (\operatorname{sgn}(b_-(\lambda; x, t)) - \operatorname{sgn}(b_+(\lambda; x, t))) \quad \text{for } \lambda \in [-L, 0), \end{aligned}$$

where

$$(4.29) \quad b_{\pm}(\lambda; x, t) = x + 2\lambda t - x_{\pm}(\lambda).$$

According to the discussion in §3.2.5, the union of solutions of the two equations $b_{\pm}(\lambda; x, t) = 0$ is exactly $\{-u_0^B(x, t), -u_1^B(x, t), \dots, -u_{2P(x,t)}^B(x, t)\}$ and one of the two quantities $b_{\pm}(\lambda; x, t)$ changes sign at $\lambda = -u_m^B(x, t)$ for $m = 0, 1, \dots, 2P(x, t)$. Since $b_+(\lambda; x, t) \leq b_-(\lambda; x, t)$ for $\lambda \in [-L, 0)$, $\text{sgn}(b_-(\lambda; x, t)) - \text{sgn}(b_+(\lambda; x, t))$ is equal to 0 or 2. These facts imply $\text{sgn}(b_-(\lambda; x, t)) - \text{sgn}(b_+(\lambda; x, t))$ changes from 0 to 2 or changes from 2 to 0 at $\lambda = -u_m^B(x, t)$ for $m = 0, 1, \dots, 2P(x, t)$. Therefore, the fact $b_-(-L; x, t) = b_+(-L; x, t)$ and the equation (4.28) tell us that

$$(4.30) \quad \frac{\partial J}{\partial t_n}(\lambda; x, t, 0, \dots, 0) = (-1)^{n+1}(n+1)\lambda^n \quad \text{for } \lambda \in \Lambda$$

$$(4.31) \quad \frac{\partial J}{\partial t_n}(\lambda; x, t, 0, \dots, 0) = 0 \quad \text{for } \lambda \in [-L, 0) \setminus \Lambda$$

where Λ is defined by

$$(4.32) \quad \Lambda = [-u_0^B(x, t), 0] \cup [-u_2^B(x, t), -u_1^B(x, t)] \cdots [-u_{2P(x,t)}^B(x, t), -u_{2P(x,t)-1}^B(x, t)].$$

After substituting (4.30) and (4.31) into (4.27), the equation (4.27) becomes

$$(4.33) \quad \begin{aligned} & \frac{\partial U}{\partial t_n}(x, t, 0, \dots, 0) \\ &= \int_{-u_0^B(x,t)}^0 (-1)^{n+1}(n+1)\lambda^n d\lambda + \sum_{m=1}^{P(x,t)} \left(\int_{-u_{2m}^B(x,t)}^{-u_{2m-1}^B(x,t)} (-1)^{n+1}(n+1)\lambda^n d\lambda \right) \\ &= - \sum_{m=0}^{2P(x,t)} (-1)^m u_m^B(x, t)^{n+1}, \end{aligned}$$

which proves Proposition IV.2.

CHAPTER V

Numerical Methods

In this chapter, we choose the parameter ϵ in the BO equation (1.1) to be 1. Then the BO equation becomes

$$(5.1) \quad u_t + 2uu_x + \mathcal{H}(u_{xx}) = 0.$$

To numerically solve the BO equation, we first discretize the spatial domain. Assume the grid points are x_1, x_2, \dots, x_N . Then the evolutions of $u(x, t)$ at these grid points are given by:

$$(5.2) \quad u_t^m(t) = -2u^m(t)u_x(x_m, t) - \mathcal{H}(u_{xx})(x_m, t) \quad \text{for } m = 1, 2, \dots, N,$$

where the function $u^m(t)$ is the value of $u(x, t)$ at the grid point x_m

$$(5.3) \quad u^m(t) = u(x_m, t).$$

Since the function $u(x, t)$ is an unknown function, $u_x(x_m, t)$ and $\mathcal{H}(u_{xx})(x_m, t)$ cannot be written in terms of $u^1(t), u^2(t), \dots, u^N(t)$. However, $u_x(x_m, t)$ and $\mathcal{H}(u_{xx})(x_m, t)$ can be approximated in terms of $u^1(t), u^2(t), \dots, u^N(t)$. Assume the function $u(x, t)$ can be approximated by

$$(5.4) \quad u(x, t) \approx \sum_{k=1}^N a_k(t) \varrho_k(x),$$

where the functions $a_k(t)$ and $\varrho_k(x)$ satisfy

$$(5.5) \quad u(x_m, t) = \sum_{k=1}^N a_k(t) \varrho_k(x_m) \quad \text{for } m = 1, 2, \dots, N.$$

Here, $\varrho_1(x), \varrho_2(x), \dots, \varrho_N(x)$ are called basis functions. Different basis functions will be used in the different methods introduced below. The equation (5.5) can also be written as

$$(5.6) \quad \mathbf{u}(t) = \mathbf{A}\mathbf{a}(t)$$

where

$$(5.7) \quad \mathbf{u}(t) = (u(x_1, t), u(x_1, t), \dots, u(x_N, t))^T; \quad \mathbf{a}(t) = (a_1(t), a_2(t), \dots, a_N(t))^T$$

and the interpolation matrix \mathbf{A} is defined by

$$(5.8) \quad (\mathbf{A})_{mn} = \varrho_n(x_m).$$

Then $a_1(t), a_2(t), \dots, a_N(t)$ can be written in terms of $u^1(t), u^2(t), \dots, u^N(t)$:

$$(5.9) \quad \mathbf{a}(t) = \mathbf{A}^{-1}\mathbf{u}(t).$$

So $u_x(x_m, t)$ and $\mathcal{H}(u_{xx})(x_m, t)$ can be approximated by

$$(5.10) \quad u_x(x_m, t) \approx \sum_{k=1}^N (\mathbf{A}^{-1}\mathbf{u}(t))_k (\varrho_k)_x(x_m) \quad \text{for } m = 1, 2, \dots, N$$

$$(5.11) \quad \mathcal{H}(u_{xx})(x_m, t) \approx \sum_{k=1}^N (\mathbf{A}^{-1}\mathbf{u}(t))_k \mathcal{H}(\varrho_k)(x_m) \quad \text{for } m = 1, 2, \dots, N.$$

Then by using (5.10) and (5.11), the equation (5.2) can be approximated by a coupled system of nonlinear ordinary differential equations (ODEs) in time:

$$(5.12) \quad u_t^m(t) = \vartheta_m(u^1(t), \dots, u^N(t)) \quad \text{for } m = 1, 2, \dots, N,$$

where the function $\vartheta_m(u^1(t), \dots, u^N(t))$ is given by

$$(5.13) \quad \vartheta_m(u^1(t), \dots, u^N(t)) = - \sum_{k=1}^N (\mathbf{A}^{-1} \mathbf{u}(t))_k (2u^k(\varrho_k)_x(x_m) + \mathcal{H}(\varrho_k)(x_m)).$$

If $u^1(t), \dots, u^N(t)$ are known, the algorithm to calculate $a_1(t), \dots, a_N(t)$ by directly using the equation (5.9) is very expensive. However, this can be done via the Fast Fourier Transform (FFT) when some special basis functions $\varrho_1(x), \dots, \varrho_N(x)$ are used, which will be discussed later. In this chapter we use the ODEs (5.12). Moreover, the ODEs (5.12) is equivalent to the following ODEs.

$$(5.14) \quad \mathbf{a}_t = \mathbf{A}^{-1} \boldsymbol{\vartheta}((\mathbf{A}\mathbf{a})_1(t), (\mathbf{A}\mathbf{a})_2(t), \dots, (\mathbf{A}\mathbf{a})_N(t))$$

where

$$(5.15) \quad \boldsymbol{\vartheta} = (\vartheta_1, \vartheta_2, \dots, \vartheta_N)^T.$$

The method described above is called the “method of lines”, which will be applied to all of the algorithms used to solve the BO equation in this chapter. The time-marching scheme used to solve the ODEs (5.12) in this chapter is the fourth order Runge-Kutta method. In this chapter, three different numerical methods are described and a comparison of them is made. Here these three numerical methods are the Fourier pseudospectral method, the Christov method and the Gaussian radial basis function method. Furthermore, we numerically illustrate the theoretical results obtained in Chapter III and study the traveling wave solution of the cubic BO equation numerically. The new contributions of this chapter are the following: (1) the comparison of these three different numerical methods is made; (2) the Christov method and the Gaussian radial basis function method are applied to the BO equation for the first time; (3) the homotopy perturbation method has not previously used to study the traveling wave solutions of the cubic BO equation.

5.1 Fourier Pseudospectral Method

To use the Fourier pseudospectral method, one has to truncate the spatial domain to $[-\pi L, \pi L]$ and assume the function $u(x, t)$ satisfies the periodic boundary condition $u(-\pi L, t) = u(\pi L, t)$ for all $t \geq 0$, where L is a parameter used to determine the size of the spatial domain. The Fourier approximation of the function $u(x, t)$ is

$$(5.16) \quad u(x, t) \approx \sum_{k=-N/2+1}^{N/2} a_k(t) e^{ikx/L},$$

where N is the number of the grid points and $e^{ikx/L}$ are the basis functions. According to the definition of the discrete Fourier transform (DFT), the FFT can be used to calculate $a_k(t)$. The FFT algorithm is most efficient if the number of the grid points N is a power of two. To optimize the algorithm, typically, one chooses

$$(5.17) \quad N = 2^n,$$

where n is a positive integer.

The Hilbert transform of a function corresponds in the Fourier domain to multiplication of its Fourier transform by $i \operatorname{sgn}(k)$ in the Fourier domain. Since the Fourier pseudospectral method requires domain truncation, the interpretation of the Hilbert transform given (1.2) is not valid. So we use the interpretation introduced above. Under this interpretation, evaluating the dispersion term in the BO equation is trivial for the Fourier pseudospectral method because the Fourier basis functions are *eigenfunctions* of the Hilbert transform operator \mathcal{H} :

$$(5.18) \quad \mathcal{H}(e^{ikx}) = i \operatorname{sgn}(k) e^{ikx} \quad \text{for } k \neq 0.$$

The dispersion term in the BO equation is the Hilbert transform of the function u_{xx} . The derivative operator inside the Hilbert transform causes no difficulty because the derivative operator commutes with the Hilbert transform operator:

Proposition V.1. [61] For any function $f(x)$,

$$(5.19) \quad \frac{d}{dx} (\mathcal{H}(f)) = \mathcal{H} \left(\frac{df}{dx} \right).$$

In other words, the differential operator d/dx commutes with the Hilbert transform operator \mathcal{H} .

Therefore, to calculate the dispersion term in the BO equation, one can evaluate the Hilbert transform of the basis functions (for any of the three basis sets used here) and then take the second derivative of the result.

The fourth order Runge-Kutta time marching scheme for the Fourier method is stable if the time step δt satisfies the inequality

$$(5.20) \quad \delta t \leq 11.2 \frac{L^2}{N^2} = 0.28h^2,$$

which is derived in §5.4.

The Fourier pseudospectral method is easy to implement and its algorithm is made efficient by using the FFT. The Fourier pseudospectral method provides better approximations for periodic solutions of the BO equation, since the periodic boundary conditions built into the numerical scheme are consistent with the physical problem being studied. For nonperiodic solutions of the BO equation, for example, soliton solutions, a large domain has to be used to capture the features of these solutions in the region far from the origin, which is expensive. Moreover, there are other boundary difficulties which will be addressed later.

5.2 Rational Basis Function Method

One way to solve evolution equations with vanishing boundary conditions on an unbounded domain is to replace the Fourier harmonics with localized basis functions.

In particular, rational basis functions are a popular choice. In this section, we describe three different orthogonal rational basis function sets: the Higgins functions, the Christov functions, and the rational Chebyshev functions. These three basis function sets are defined as follows:

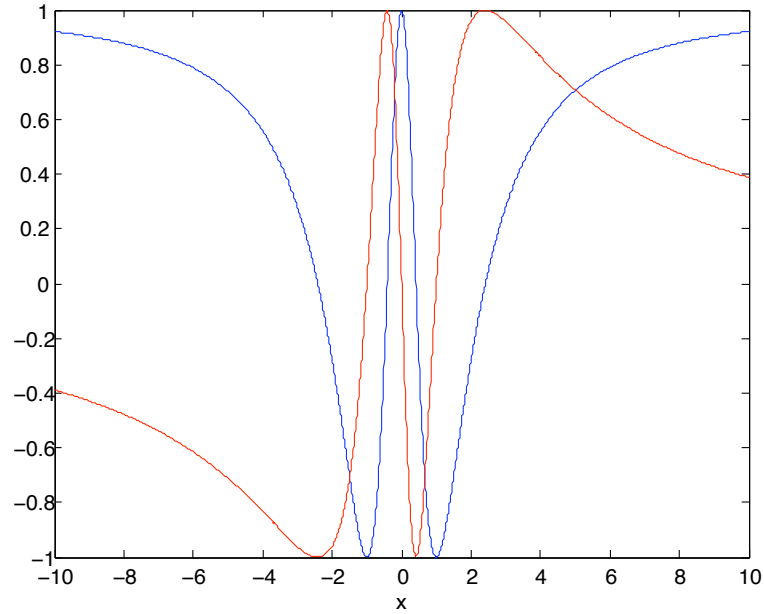


Figure 5.1: The graphs of the Higgins functions $CH_4(x)$ (blue) and $SH_3(x)$ (red) with $L = 1$

Definition V.2. [7] The functions $CH_{2n}(x)$ and $SH_{2n+1}(x)$ given by

$$(5.21) \quad CH_{2n}(x) = \frac{1}{2} (\mu_n(x) + \mu_{-n}(x)) \quad \text{for } n \in \mathbb{Z}^+ \cup \{0\}$$

and

$$(5.22) \quad SH_{2n+1}(x) = \frac{1}{2i} (\mu_{n+1}(x) - \mu_{-n-1}(x)) \quad \text{for } n \in \mathbb{Z}^+ \cup \{0\}$$

are called the Higgins functions, where

$$(5.23) \quad \mu_n(x) = \frac{(ix - L)^n}{(ix + L)^n} \quad \text{for } n \in \mathbb{Z}$$

and L is a positive real constant. The functions $\mu_n(x)$ are called the complex Higgins functions.

The Higgins functions were introduced by Higgins [35] in his book.

Definition V.3. [7] The functions $CC_{2n}(x)$ and $SC_{2n+1}(x)$ given by

$$(5.24) \quad CC_{2n}(x) = \frac{1}{2}(\phi_n(x) - \phi_{-n-1}(x)) \quad \text{for } n \in \mathbb{Z}^+ \cup \{0\}$$

and

$$(5.25) \quad SC_{2n+1}(x) = -\frac{1}{2i}(\phi_n(x) + \phi_{-n-1}(x)) \quad \text{for } n \in \mathbb{Z}^+ \cup \{0\}$$

are called the Christov functions, where

$$(5.26) \quad \phi_n = \frac{(ix - L)^n}{(ix + L)^{n+1}} \quad \text{for } n \in \mathbb{Z}$$

and L is a positive real constant. The functions $\phi_n(x)$ are called the complex Christov functions.

The Christov functions were introduced by Christov [14] in his paper.

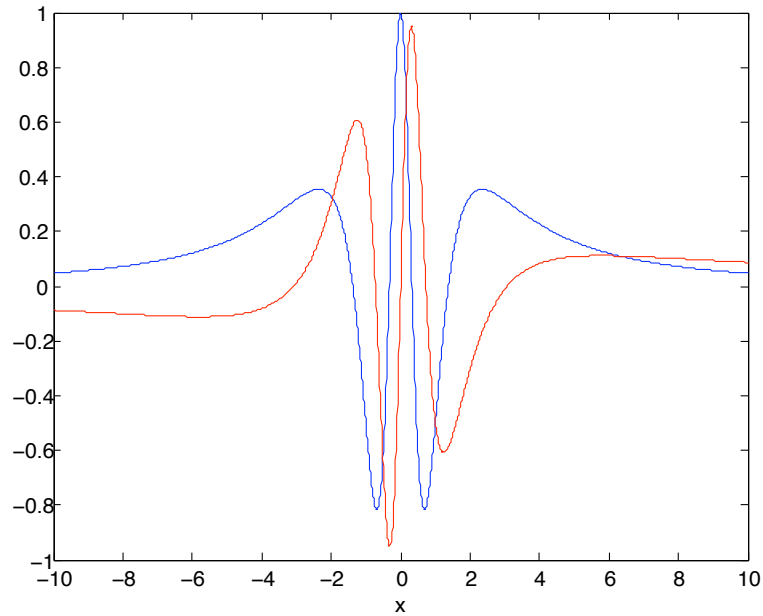


Figure 5.2: The graphs of the Christov functions $CC_4(x)$ (blue) and $SC_5(x)$ (red) with $L = 1$

Definition V.4. [7] The functions $TB_n(x)$ given by

$$(5.27) \quad TB_n(x) = T_n \left(\frac{y}{(L + y^2)^{\frac{1}{2}}} \right)$$

are called the rational Chebyshev functions of the first kind, where the functions $T_n(x)$ are the Chebyshev polynomials of the first kind and L is a positive real constant. The functions $UB_n(x)$ given by

$$(5.28) \quad UB_n(x) = U_n \left(\frac{y}{(L + y^2)^{\frac{1}{2}}} \right)$$

are called the rational Chebyshev functions of the second kind, where the functions $U_n(x)$ are the Chebyshev polynomials of the second kind and L is a positive real constant.

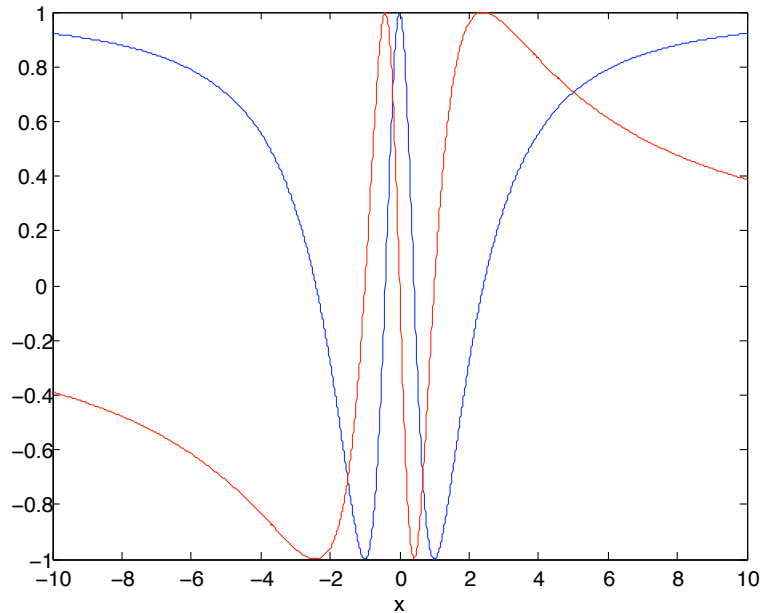


Figure 5.3: The graphs of the rational Chebyshev functions $TB_2(x)$ (blue) and $UB_2(x)$ (red) with $L = 1$

The rational Chebyshev functions were introduced by Boyd [7] in his paper. The relations among these three different basis function sets were also discussed by Boyd [7] and to describe them, we recall the following two propositions from his paper.

Proposition V.5. [7] *The Christov functions and the Higgins functions are related to the Chebyshev rational functions as*

$$(5.29) \quad CC_{2n}(x) = \frac{L}{L^2 + x^2} UB_{2n}(x); \quad SC_{2n+1}(x) = \frac{1}{(L^2 + x^2)^{\frac{1}{2}}} TB_{2n+1}(x),$$

$$(5.30) \quad CH_{2n}(x) = TB_{2n}(x); \quad SH_{2n+1}(x) = \frac{L}{(L^2 + x^2)^{\frac{1}{2}}} UB_{2n+1}(x).$$

Proposition V.6. [7] *With the mapping $x = L \cot(s/2)$, we have*

$$(5.31) \quad TB_n(x) = \cos\left(\frac{n}{2}s\right); \quad UB_n(x) = \frac{\sin\left(\frac{n+1}{2}s\right)}{\sin\left(\frac{s}{2}\right)},$$

$$(5.32) \quad CC_{2n}(x) = \frac{\cos(ns) - \cos((n+1)s)}{2L}; \quad SC_{2n+1}(x) = \frac{\sin((n+1)s) - \sin(ns)}{2L},$$

$$(5.33) \quad CH_{2n}(x) = \cos(ns); \quad SH_{2n+1}(x) = \sin((n+1)s).$$

Proposition V.6 also suggests that the FFT can be applied to all these rational basis function methods by a change of coordinate, which makes the algorithm to calculate $a_k(t)$ more efficient. However, there is no simple formula for the Hilbert transform of the Chebyshev functions $TB_n(x)$ and $UB_n(x)$ for odd integer n . The Higgins functions are not integrable in \mathbb{R} , which implies that the Hilbert transform of a Higgins function is not well-defined. The Hilbert transform of a Christov function is easy to calculate because of the following proposition.

Proposition V.7. *If $n \geq 0$, then*

$$(5.34) \quad \mathcal{H}(CC_{2n}(x)) = -SC_{2n+1}(x); \quad \mathcal{H}(SC_{2n+1}(x)) = CC_{2n}(x).$$

Proof. If $m \geq 0$, then the function $\phi_m(x)$ belongs to the Hardy space \mathbb{H}^- . According to the identity (2.40), one can have $\mathcal{C}_+(\phi_m) = 0$, which implies $\mathcal{H}(\phi_m) = -i\phi_m$. If $m < 0$, then the function $\phi_m(x)$ belongs to the Hardy space \mathbb{H}^+ . According to the identity (2.40), one can obtain $\mathcal{C}_-(\phi_m) = 0$, which implies $\mathcal{H}(\phi_m) = i\phi_m$. So, for any integer m , the function $\phi_m(x)$ is an eigenfunction of the Hilbert transform operator \mathcal{H} and satisfies

$$(5.35) \quad \mathcal{H}(\phi_0) = -i\phi_0; \quad \mathcal{H}(\phi_m) = -i\text{sgn}(m)\phi_m \quad \text{if } m \neq 0.$$

After applying the Hilbert transform \mathcal{H} to each side of the equations (5.24) and (5.25) and using (5.35), one can obtain

$$(5.36) \quad \begin{aligned} \mathcal{H}(\text{CC}_{2n}(x)) &= \frac{1}{2}(\mathcal{H}(\phi_n(x)) - \mathcal{H}(\phi_{-n-1}(x))) \\ &= \frac{1}{2}(-i\phi_n(x) - i\phi_{-n-1}(x)) \\ &= -\text{SC}_{2n+1}(x) \end{aligned}$$

and

$$(5.37) \quad \begin{aligned} \mathcal{H}(\text{SC}_{2n+1}(x)) &= -\frac{1}{2i}(\mathcal{H}(\phi_{-n-1}(x)) + \mathcal{H}(\phi_n(x))) \\ &= -\frac{1}{2i}(-i\phi_n(x) + i\phi_{-n-1}(x)) \\ &= \text{CC}_{2n}(x). \end{aligned}$$

□

James and Weideman [37] used the complex-valued rational functions

$$(5.38) \quad \varphi_n(x) = (-1)^{n+1}\phi_{-n-1}(x)$$

as basis functions to solve the BO equation, where $\phi_{-n-1}(x)$ are the complex Christov functions. The basis functions $\varphi_n(x)$ are closely related to the Christov functions. The algorithm is efficient and easy to implement because the functions $\varphi_n(x)$ are also

the eigenfunctions of the Hilbert transform operator \mathcal{H} and the FFT can be applied to it. Since we are interested in real-valued solutions of the BO equation, in this section, we use the real version of the basis functions used by James and Weideman, the Christov functions, as basis functions to solve the BO equation.

A Christov approximation is

$$(5.39) \quad u(x, t) \approx \sum_{n=0}^N a_n(t) \text{CC}_{2n}(x) + b_n(t) \text{SC}_{2n+1}(x).$$

Since the Christov functions are rational functions in \mathbb{R} and decay to zero algebraically, domain truncation is not necessary. To implement the Christov method by using the FFT requires the use of evenly spaced grid points after change of coordinate from x to s . Furthermore, because the soliton solutions of the BO equation are rational functions, the Christov method can provide good approximations for such solutions.

The constant L in definition V.3 is a parameter in the Christov method. To investigate the role of L in the Christov method, we calculate the errors of the numerical solutions obtained by applying the Christov method with different choices of the parameter L and the number of the grid points N . Here the errors are defined to be the maximum of the absolute value of the difference between the exact solutions and the numerical solutions. The results are provided in Figure 5.2. Figure 5.2 suggests that an appropriate choice of the parameter L provides a better accuracy.

5.3 Radial Basis Function Spectral Algorithm

Another choice of localized basis functions could be one with exponential decay, like Gaussian radial basis functions. Here a set of basis functions $\varrho_k(x)$ that can be written in the form $\varrho_k(x) = f(x - x_k)$ where f is a function and x_k are constants is called the radial basis functions.

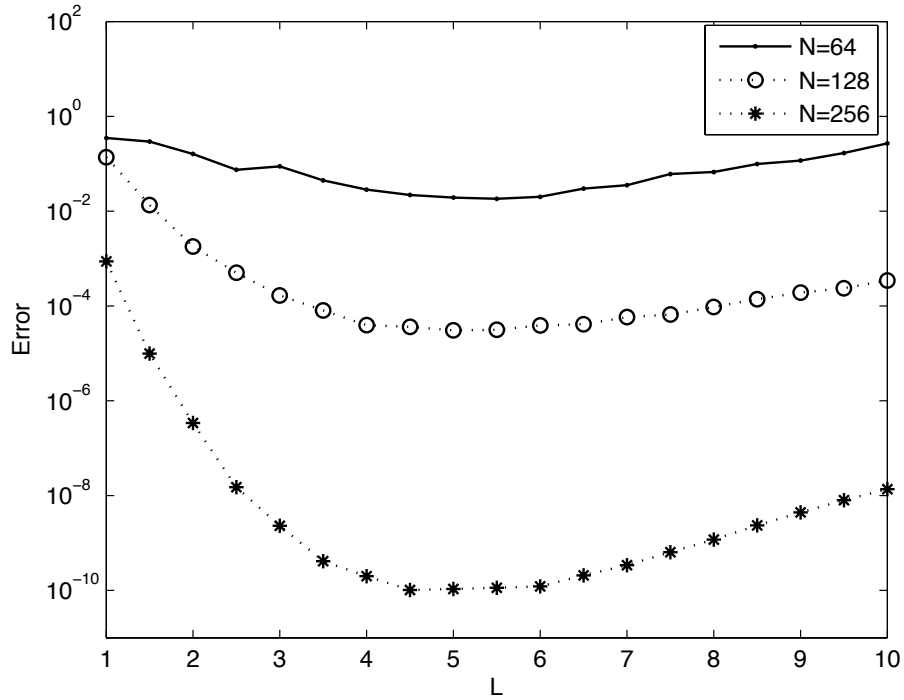


Figure 5.4: Comparison of the errors in $t \in [0, 5]$ using the Christov method to solve the BO equation with different choices of the parameter L and the number of the grid points N . Here the initial condition is $u(x, 0) = 2/(x^2 + 1)$ and the exact solution is $u(x, t) = 2/((x - t)^2 + 1)$.

5.3.1 Gaussian RBF Method

A Gaussian RBF approximation of $u(x, t)$ is

$$(5.40) \quad u(x, t) \approx \sum_{k=1}^N a_k(t) \exp\left(-\frac{\alpha^2}{h_k^2} (x - x_j)^2\right)$$

where x_k are “centers” and $\exp\left(-\frac{\alpha^2}{h_k^2} (x - x_j)^2\right)$ are the basis functions. In fact, usually the centers are chosen to be the grid points. The constant α in the equation (5.40) is the “relative inverse width”, which is typically chosen to satisfy

$$(5.41) \quad \frac{1}{4} \leq \alpha \leq \frac{1}{2}.$$

As discussed in [24, 70, 11], the interpolation matrix is very ill-conditioned for small α and very inaccurate for $\alpha \geq 1$. The parameters h_j in the equation (5.40) is chosen

to be equal to h for all j , if the grid spacing h is constant. If a nonuniform grid is used, the constants h_j is chosen to be approximately equal to the local grid spacing $x_{j+1} - x_j$. If nonuniform grid points are used, then one has to directly use the equation (5.9) to calculate the coefficients a_k , which is very expensive. On the other hand, if uniform grid points are used, then the FFT algorithm can be applied to calculate $a_k(t)$, which is discussed in §5.3.2.

The dispersion term in the BO equation is the Hilbert transform of the function u_{xx} . Using the Gaussian RBF method to solve the BO equation requires knowledge of evaluating the Hilbert transform of the Gaussian basis functions, which is provided in the following theorem.

Theorem V.8. [69] *The Hilbert transform of Gaussian functions can be written in the form*

$$(5.42) \quad \mathcal{H}(\exp(-a^2(y-s)^2))(x) = -\frac{2}{\sqrt{\pi}} \text{daw}(a[x-s]),$$

where $\text{daw}(x)$ is Dawson's Integral given by:

$$(5.43) \quad \text{daw}(y) \equiv e^{-y^2} \int_0^y e^{z^2} dz = -e^{-y^2} \frac{i}{2} \sqrt{\pi} \text{erf}(iy).$$

There are very efficient algorithms available to numerically evaluate Dawson's integral given in [15, 68, 69, 10].

5.3.2 Uniform Grid: Toeplitz Matrices

Proposition V.9. *The RBF interpolation matrix is a Toeplitz matrix if and only if the grid spacing is constant and the width of all RBFs is the same.*

Proof. A matrix \mathbf{A} with elements A_{jk} is a Toeplitz matrix if and only if A_{jk} can be written in the form

$$(5.44) \quad A_{jk} \equiv g(|j-k|) \quad \text{for a single variable function } g$$

For a uniform grid with $h_j = h$, the elements of the RBF interpolation matrix are

$$(5.45) \quad A_{jk} = \exp\left(-\frac{\alpha^2}{h^2}(x_j - x_k)^2\right) = \exp(-\alpha^2(j - k)^2).$$

It is obvious that the function A_{jk} in the equation (5.45) satisfies the Toeplitz condition (5.44). On the other hand, if the grid is not uniform, then

$$(5.46) \quad A_{j1} = \exp\left(-\frac{\alpha^2}{h_1^2}(x_j - x_1)^2\right)$$

cannot be written as $g(|j - 1|)$. If the grid is uniform but the constants h_j in the equation (5.40) are not same, then

$$(5.47) \quad A_{1k} = \exp\left(-\frac{\alpha^2}{h_k^2}(x_1 - x_k)^2\right)$$

cannot be written as $g(|1 - k|)$. □

According to Proposition V.9, if the uniform grid points are used, then the elements of the RBF interpolation matrix \mathbf{A} can be written as $A_{jk} = g(|j - k|)$. By using the convolution theorem, one can obtain

$$(5.48) \quad \mathbf{g} * \mathbf{a} = \mathcal{F}^{-1}(\mathcal{F}(\mathbf{g}) \cdot \mathcal{F}(\mathbf{a})),$$

where $\mathbf{g} = (g(0), g(1), \dots, g(N - 1))^T$ and \mathbf{a} is defined by (5.7). Here, \mathcal{F} represents the DFT and \mathcal{F}^{-1} represents the inverse DFT. Then according to the equation (5.6), one can have

$$(5.49) \quad \mathbf{u} = \mathcal{F}^{-1}(\mathcal{F}(\mathbf{g}) \cdot \mathcal{F}(\mathbf{a})).$$

The above line of reasoning leads us to conclude that \mathbf{a} can be calculated via the FFT algorithm.

5.3.3 Strengths of the RBF Method

Grid-Flexibility: There is no constraint on choosing the grid points in the RBF approximation given in §5.3.1. To capture the behavior of a solution that has very rapid oscillation in a small region and is very smooth in the remaining region, the use of a nonuniform grid that has many grid points in the oscillation region and few points elsewhere is very efficient. Such nonuniform grids can be easily handled with the RBF method. Moreover, the optimal grid can be adaptively chosen on the fly to follow moving structures. Driscoll and Heryudono [23] provide an adaptive algorithm for the RBF method in their paper.

Simple Implementation of the Hilbert Transform: The Gaussian basis functions are not eigenfunctions of the Hilbert transform. However, the Hilbert transform of a Gaussian basis function is a Dawson's function, which is easy to calculate numerically.

5.3.4 Drawbacks of the RBF Method

Relatively Expensive Algorithm: The Christov method and the Fourier pseudospectral method can be implemented by using the FFT, which makes the algorithms efficient. The FFT algorithms used in these two methods have an $O(n \log_2 n)$ complexity per time step. However, the FFT algorithm is not applicable to the RBF method with a nonuniform grid. To evaluate the nonlinear term and the dispersion term in the BO equation, multiplication of the interpolation matrix and the vector of coefficients is used, which has an $O(n^2)$ complexity. Compared to the Christov method and the Fourier pseudospectral method, the algorithm of the RBF method is more expensive.

5.4 Courant-Friedrichs-Lewy (CFL) Time Step Limit

If an explicit time-marching scheme is used to solve a nonlinear time evolution equation, to make the scheme stable, the time step has to be less than the ‘‘CFL limit’’ named after Courant, Friedrichs and Lewy [16, 17] who first discussed it in their paper for finite difference schemes. The CFL limit is determined by the time-marching algorithm, the time evolution equation and the spatial resolution. The wave dispersion mainly determines the CFL limit, if the wave dispersion is not too weak and the nonlinearity is not too strong. Therefore, one can obtain a good estimate of the CFL limit of a nonlinear time evolution equation by calculating the CFL limit of its linearization.

We will use a theoretical method to derive the formula of the CFL limit of the linear BO equation

$$(5.50) \quad u_t + \mathcal{H}(u_{xx}) = 0$$

for the Fourier pseudospectral method below and estimate the CFL limit for the BO equation by this formula. In fact, this theoretical method can be generalized to apply to other linear time evolution equations.

If one truncates the spatial domain to $[-\pi L, \pi L]$ and uses N grid points, then the grid spacing is $h = 2\pi L/N$ and the approximation of the function $u(x, t)$ is

$$(5.51) \quad u(x, t) = \sum_{k=-N/2+1}^{N/2} a_k(t) e^{ikx/L}.$$

By substituting it into the linear BO equation and using the identity (5.18), the linear BO equation becomes an uncoupled set of ordinary differential equations (ODE):

$$(5.52) \quad \frac{da_k}{dt} = i\omega \left(\frac{k}{L} \right) a_k \quad \text{for } k = -\frac{N}{2} + 1, -\frac{N}{2} + 2, \dots, \frac{N}{2},$$

where $\omega(\lambda) = -\text{sgn}(\lambda)\lambda^2$. If one applies the fourth order Runge-Kutta method to an ODE in the form:

$$(5.53) \quad \frac{du}{dt} = i\omega u,$$

where ω is real, the scheme is stable if and only if the time step δt satisfies the inequality [8]

$$(5.54) \quad \delta t \leq \frac{2.8}{|\omega|}.$$

In the equation (5.52), the wave number k satisfies $-N/2 + 1 \leq k \leq N/2$, which implies

$$(5.55) \quad \left| \omega \left(\frac{k}{L} \right) \right| \leq \frac{N^2}{4L^2}.$$

So the time marching scheme for the linear BO equation is stable if and only if the time step δt satisfies

$$(5.56) \quad \delta t \leq 11.2 \frac{L^2}{N^2} = 0.28h^2.$$

Therefore, $0.28h^2$ is our estimate for the CFL limit of the Fourier pseudospectral scheme for the BO equation. The CFL instability for the linear BO equation is also discussed in Fig. 11.5, pg. 209 of [8].

There is no simple theoretical analysis of the CFL limits of the linear BO equation for the Christov method and the RBF method. However, since the time marching scheme will quickly become unstable if the time step is larger than the CFL limit, one can estimate the CFL limits for these methods by implementing them with different choices of the time step. The CFL limits for different methods obtained by numerical experiments are given in Figure 5.5. Figure 5.5 suggests that the CFL limits for three different methods are inversely proportional to the square of the number of the grid

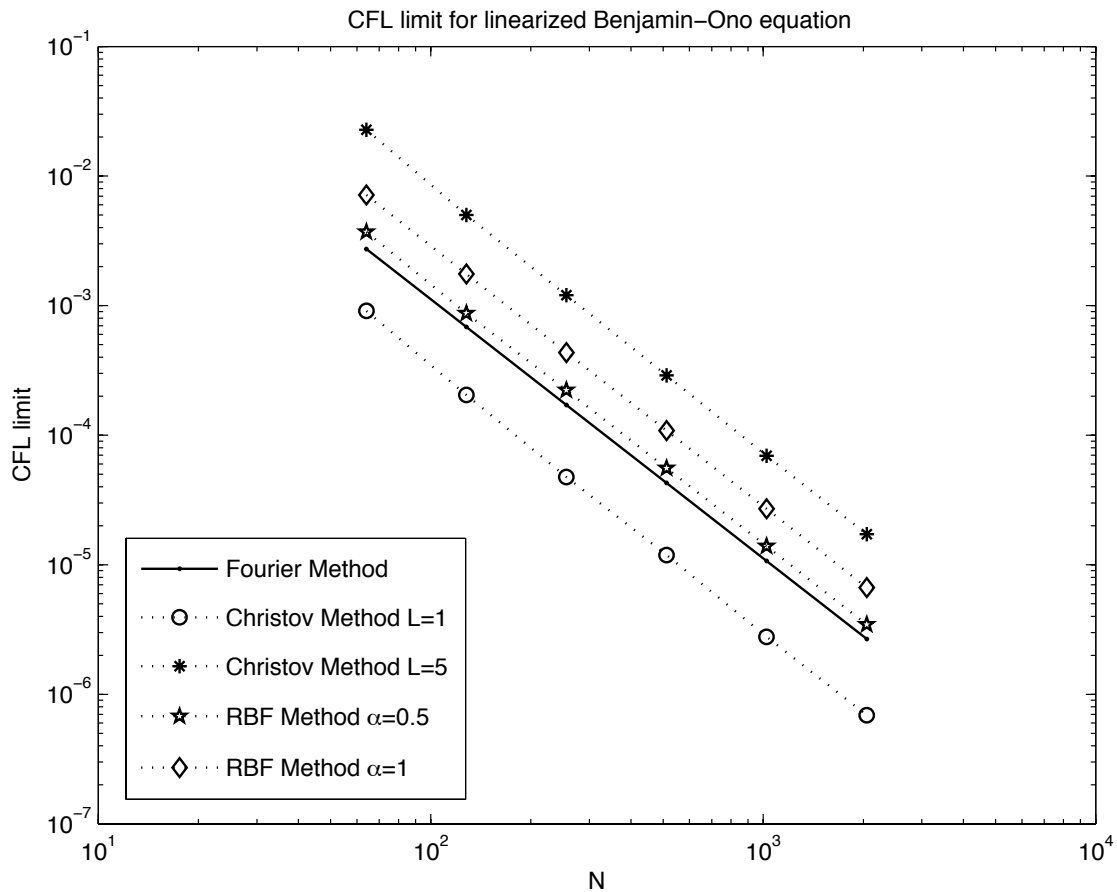


Figure 5.5: The CFL limit of the linear BO equation for the Fourier method, the RBF method and the Christov method.

points. Based on the numerical experiments and Figure 5.5, formulas of the CFL limits for three different methods are derived to provide a simple way to evaluate the CFL limit of the BO equation. These formulas are given in Table 5.1.

5.5 Aliasing Instability and Dealiasing

Aliasing instability, a strictly *nonlinear* phenomenon was discovered by Phillips [62]. He did a numerical experiment of his two-layer model, the first “general circulation model” (GCM) of the atmosphere. Several days later, the winds predicted by his simulation were supersonic and he was forced to stop. Phillips [63] later explained

Method and Parameter	Formula for the CFL limit δt
Fourier Method	$\delta t = 0.28(\Delta x)^2 = 0.28W^2/N^2$.
Christov Method	$\delta t = 2.9L^2/N^2$.
RBF Method with $\alpha = 0.5$	$\delta t = 0.36(\Delta x)^2 = 0.36W^2/N^2$.
RBF Method with $\alpha = 1$	$\delta t = 0.72(\Delta x)^2 = 0.72W^2/N^2$.

Table 5.1: Formulas for the CFL limit of the linear BO equation. The number W in the formulas is the width of the domain and L is a parameter in the Christov method.

this catastrophic failure as “aliasing instability”, which we now explain.

5.5.1 Aliasing Instability

If the spatial domain is $[-\pi L, \pi L]$ and the function $u(x, t)$ is approximated by a Fourier series:

$$(5.57) \quad u(x, t) = \sum_{k=-N/2+1}^{N/2} a_k(t) e^{ikx/L},$$

where N is the number of the grid points, then the grid spacing is $h = 2\pi L/N$. The shortest wavelength in this Fourier series is

$$(5.58) \quad \lambda = \frac{2\pi}{N/2L} = \frac{4\pi L}{N} = 2h.$$

On a discrete grid, short waves whose wavenumbers k are larger than the aliasing limit $k = \pi/h$, will be “aliased” to the long waves with lower wavenumbers as illustrated in Chapter 9 of [8], because the short and long waves are indistinguishable when sampled on the numerical grid. However, according to the following trigonometric identities:

$$(5.59) \quad \cos a \cos b = \frac{\cos(a-b) + \cos(a+b)}{2}; \quad \sin a \sin b = \frac{\cos(a-b) - \cos(a+b)}{2}$$

$$(5.60) \quad \sin a \cos b = \frac{\sin(a+b) + \sin(a-b)}{2}; \quad \cos a \sin b = \frac{\sin(a+b) - \sin(a-b)}{2},$$

a quadratically nonlinear term like uu_x in the BO equation is approximated by a Fourier series including waves whose wavenumbers are larger than the aliasing limit. Energy that should cascade to short waves is spuriously aliased to long waves, which often leads to explosive instability. To illustrate the phenomenology, we used the benchmark in Fig 5.6.

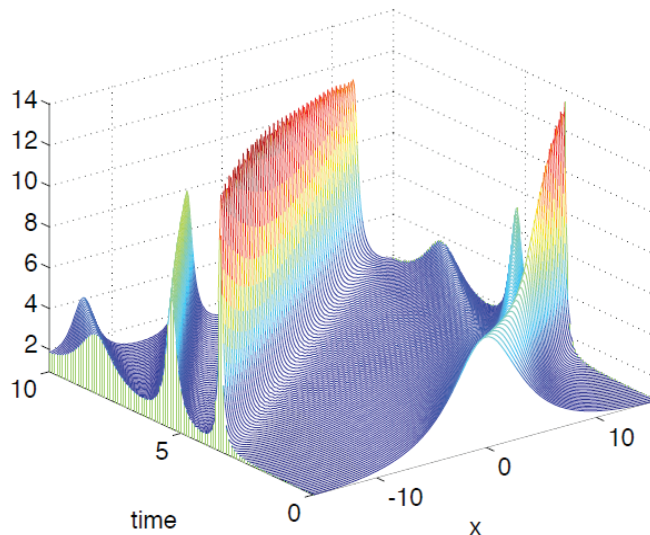


Figure 5.6: The benchmark case used to demonstrate aliasing instability in the BO equation. With 256 grids points, a timestep of $\delta t = 0.004$ is stable. The initial condition evolves into three solitons on the periodic domain $x \in [-5\pi, 5\pi]$.

One complication manifesting even in Phillips' computations is that a nonlinear computation may be accurate and stable for a considerable time and then suddenly crash with overflow errors. The reason is that it is common in fluid flows for a smooth initial condition to spontaneously evolve regions of higher spatial gradient and a plot of the Fourier coefficients becomes flatter as shown in Fig 5.7.

When the evolution equation is integrable, the flattening of the Fourier spectrum and the growth of narrow features do not proceed indefinitely. If the computation has not blown up by the time of flattest spectrum, then it can be integrated stably for

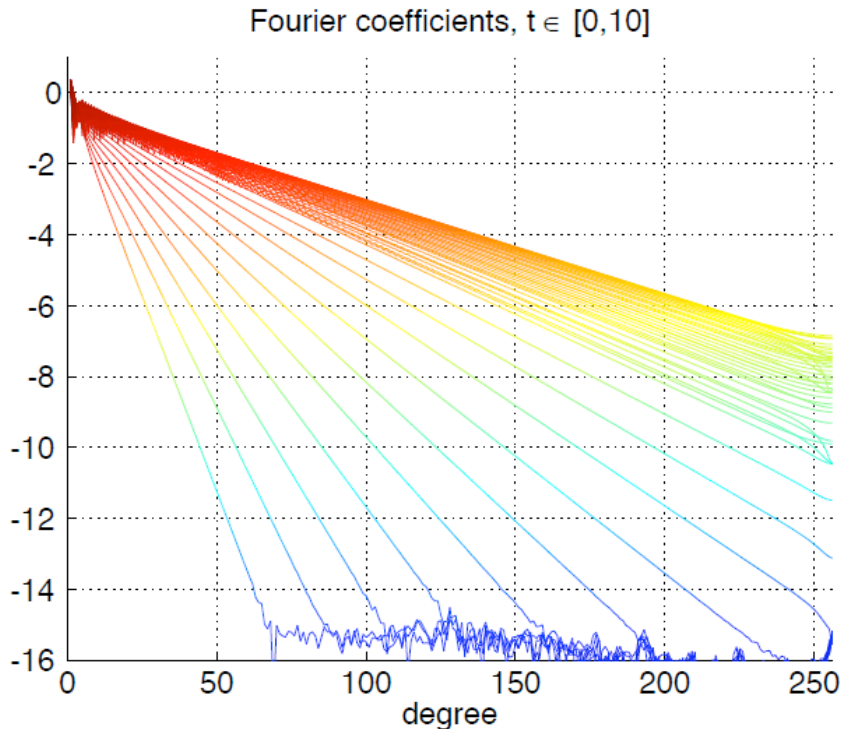


Figure 5.7: Canonical run but with $n = 512$ grid points and a timestep of $1/1000$. The Fourier coefficients are plotted every one-fifth in t with the lowest curve showing the initial curve; the slope monotonically decreases with time.

a very long time.

Shortening the time step cannot eliminate the aliasing instability. It is a fundamental difficulty caused by underresolution in the spatial domain. Figs. 5.6 and 5.7 show that the benchmark cases are stable with $N = 256$ and $N = 512$. When the spatial resolution is reduced to $N = 128$, instability begins.

The empirical precursor of aliasing instability is the appearance of waves whose wavelength is $2h$. From Fig 5.8 and 5.9, one can see that when the Fourier spectrum becomes sufficiently flat, the high wavenumbers near the aliasing limit go bad and deviate from the linear slope of the accurate solution shown in the previous figure. The noise can be seen in Fig. 5.9.

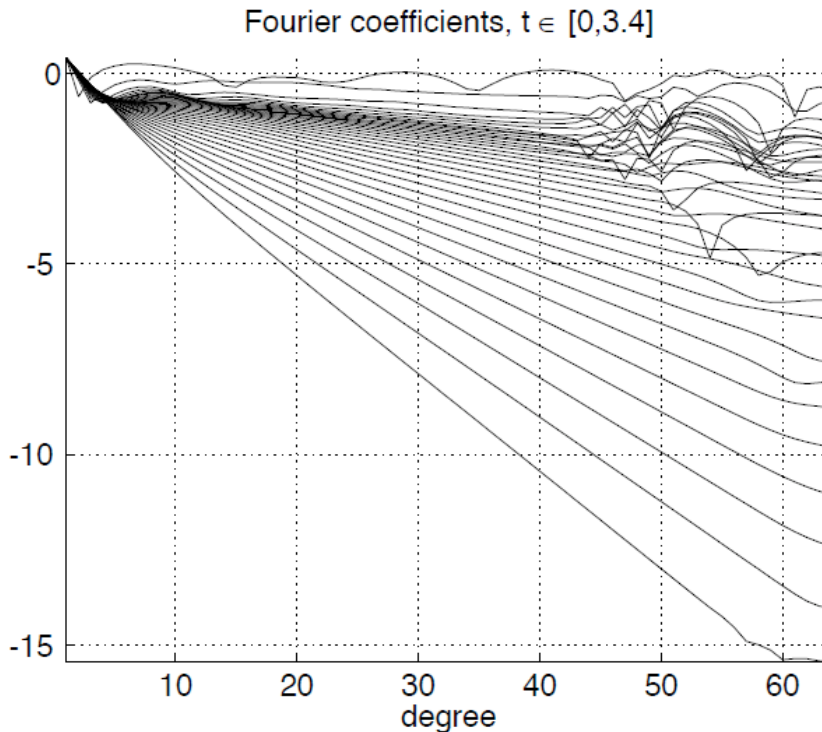


Figure 5.8: Canonical run but with $n = 128$ grid points and a timestep of $1/250$. The Fourier coefficients are plotted every one-tenth in t with the lowest curve showing the initial curve; the slope monotonically decreases with time. At the final time, the error in physical space is 5000% (not illustrated on this graph).

5.5.2 Dealiasing

Phillips [63] showed aliasing could be eliminated by taking the Fourier transform of $u(x, t)$ and filtering the upper one-half of the wavenumber spectrum. Later, Orszag pointed out, in a note, that it is actually sufficient to filter just the upper *one-third* of the wavenumber spectrum [60], which is called the “Orzag Two-Thirds Rule” [8].

Dealiasing is easy to implement in the Fourier method. The drawback of dealiasing is that additional FFTs are needed, so there is a significant jump in cost. Furthermore, the effective resolution is lowered to $(2/3)N$.

For the BO benchmark, dealiasing makes a tremendous difference. Without dealiasing or other forms of dissipation, the coarsest resolution which is stable for

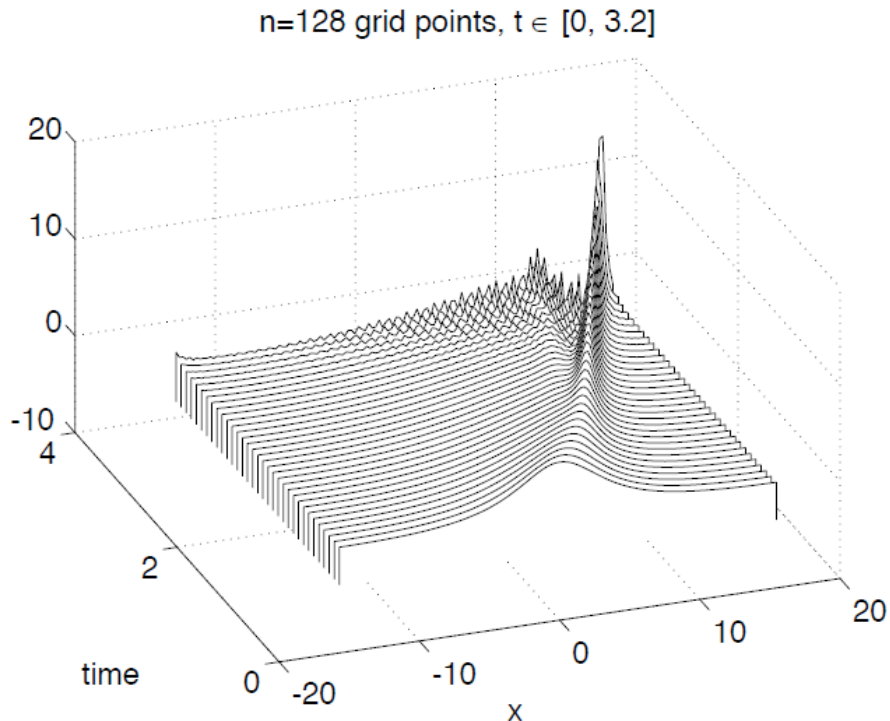


Figure 5.9: Canonical run but with $n = 128$ grid points and a timestep of $1/250$. $u(x, t)$ are plotted every one-tenth in t ; the slope monotonically decreases with time. The flow blows up catastrophically with overflow between $t = 3.4$ and $t = 3.5$.

the benchmark is $N = 256$.

With dealiasing, even a very coarse resolution of $N = 32$ is stable. A resolution of $N = 128$ is necessary to make the exact and computational solutions graphically indistinguishable. However, even the $N = 32$ solution is *qualitatively* correct: the initial hump splits into three solitons.

5.6 Boundary Difficulties

5.6.1 Moving Coordinate System

A common difficulty in numerically solving the Cauchy problem of the BO equation is that a soliton of the BO equation will move rightwards and eventually exit the region spanned by the spatial grid points. If the goal of the numerical calculation is

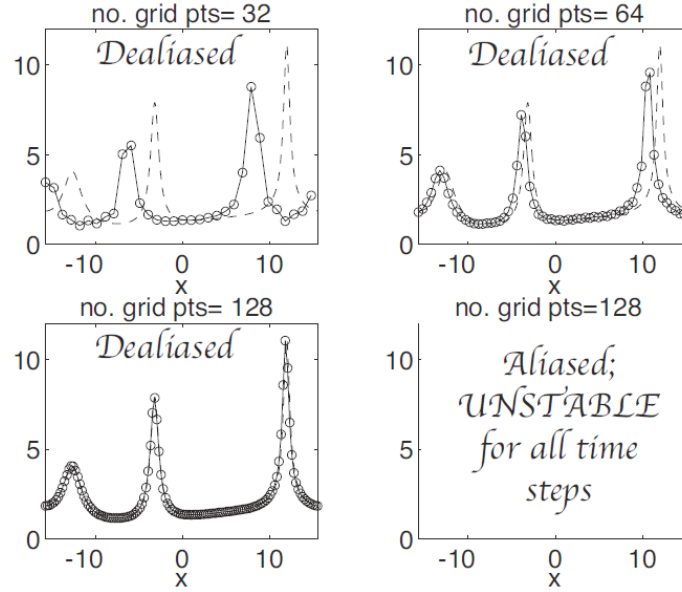


Figure 5.10: Comparison of the exact benchmark solution at $t = 10$ with the solution as computed using Orszag-Phillips dealiasing with resolutions of $N = 32$, $N = 64$ and $N = 128$ grid points. In each frame, the true solution is shown as the dashed curve; the solid curve with the circles is the lower resolution dealiased approximation. The lower right shows the $N = 128$ grid point solution without dealiasing: there is no graph because the aliased computation is unstable and overflows to Not-a-Number (NaN) at every grid point. This difficulty cannot be fixed by shortening the timestep.

to track a single feature, such as the largest soliton, or to make a movie in which the frame is centered on the largest soliton, it is helpful to shift into a moving coordinate system by writing

$$(5.61) \quad s = x - c_{trans}t$$

where c_{trans} is the speed of the moving coordinate. Then the BO equation becomes

$$(5.62) \quad u_t + (2u - c_{trans})u_s + \mathcal{H}(u_{ss}) = 0$$

which may be numerically solved in exactly the same way as the original unmodified BO equation.

5.6.2 Fourier Pseudospectral Method

The Fourier pseudospectral method requires domain truncation and periodic boundary conditions. So after a solution with non-negligible amplitude hits the right boundary of the domain, it will wrap around to reappear on the left, and similarly the left edge of the dispersing transient will wrap around to the right boundary. This phenomenon is illustrated in Fig 5.11. It is correct if the solution is a periodic solution. But if the solution is a non-periodic solution in \mathbb{R} , a collision between leftward-propagating (but wrapped-around) dispersive transients and the rightward-propagating solitons is completely unphysical.

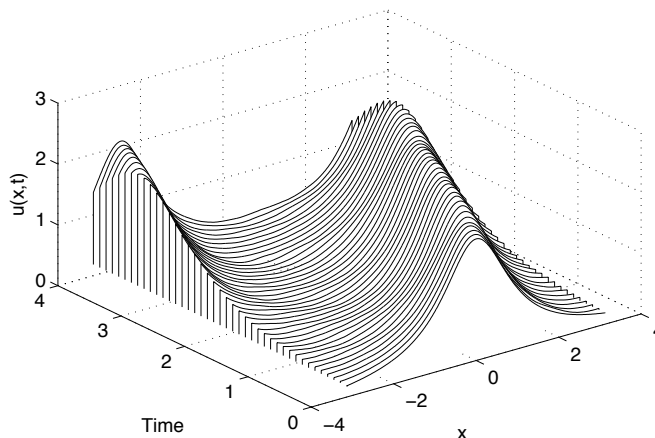


Figure 5.11: Waterfall plot using the Fourier pseudospectral method to solve the BO equation with $N = 512$ grid points and a timestep of $1/50000$. $u(x, t)$ plotted every one-tenth in t . The initial condition of $u(x, t)$ is $u(x, 0) = 2/(x^2 + 1)$ for $x \in [-\pi, \pi]$ and $u(x, 0) = u(x + 2\pi, 0)$ for all $x \in \mathbb{R}$.

5.6.3 Christov Method

We use evenly spaced grid points in the Christov method after change of coordinate from x to s . However, the grid used in x is nonuniform. Most of the grid points are in the region close to the origin and the grid spacing becomes very large in the

region far away from the origin. So when a solution moves away from the origin, it becomes more and more inaccurate because of underresolution. This phenomenon is illustrated in Fig 5.12.

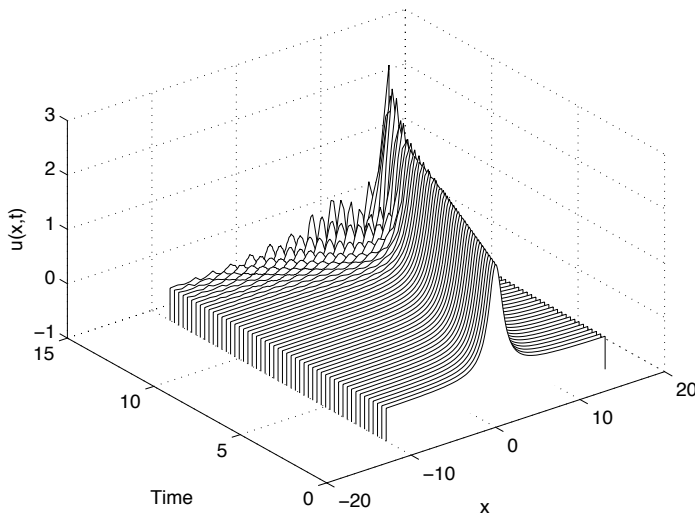


Figure 5.12: Waterfall plot using the Christov method to solve the BO equation with $N = 128$ grid points and a timestep of $1/1000$. $u(x, t)$ plotted every one-fourth in t . The initial condition of $u(x, t)$ is $u(x, 0) = 2/(x^2 + 1)$

5.6.4 RBF Method

The interpolation in §5.3 provides a good approximation in the domain of the grid points. However, the values of the interpolation function are very small outside the domain of the grid points because the Gaussian functions decay exponentially. This fact does not cause any problem if the function u_{xx} is very small outside the domain of the grid points. However, when a solution with non-negligible amplitude approaches the boundary of the domain of the grid points, it is not true any more and the solution becomes inaccurate. This phenomenon is illustrated in Fig 5.13.

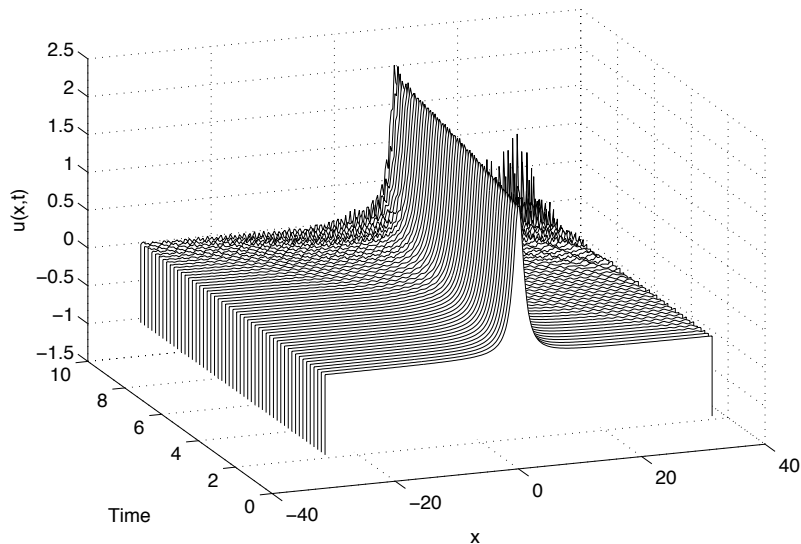


Figure 5.13: Waterfall plot using the RBF method to solve the BO equation with $N = 256$ grid points and a timestep of $1/5000$. $u(x, t)$ plotted every two-tenth in t . The initial condition of $u(x, t)$ is $u(x, 0) = 2/(x^2 + 1)$

5.7 Summary: Comparisons of Three Spectral Methods

In this section, we compare the three different spectral methods discussed in this chapter and list the results in Table 5.2 at the end.

5.7.1 Cost

The FFT can be applied to the Fourier pseudospectral method and the Christov method, which makes the algorithms fast. The implementations of the Fourier pseudospectral method and the Christov method have an $O(n \log_2 n)$ complexity per time step, if the FFT is used. On the other hand, the FFT cannot be applied to the RBF method, unless a uniform grid is used. To implement the RBF method with a nonuniform grid, one has to calculate the inverse of the interpolation matrix, which has an $O(n^3)$ complexity, but this must be done only once at the beginning of the implementation, unless an adaptive grid is used. Then, to evaluate the nonlinear

term and the dispersion term in the BO equation, multiplication of matrixes and vectors is used, which has an $O(n^2)$ complexity. Therefore, the RBF method is more expensive than the Fourier pseudospectral method and the Christov method.

5.7.2 Domain Truncation

The domain of the basis functions in the RBF method and the Christov method is \mathbb{R} . It is therefore not necessary to truncate the domain in order to solve a problem with a vanishing boundary condition on \mathbb{R} . To use the Fourier pseudospectral method, domain truncation is required since the basis functions in the Fourier pseudospectral method are periodic functions. However, there are boundary difficulties for the RBF method and the Christov method.

5.7.3 Boundary Difficulty

In the Fourier pseudospectral method, periodic boundary conditions are implicitly used by the scheme. As we discussed in §5.6, after a non-periodic solution hits the right (left) boundary of the domain, it will wrap around to reappear on the left (right) side of the domain, which is completely unphysical.

The grid used in the Christov method is nonuniform. Most of the grid points are concentrated in the region close to the origin. The numerical solution becomes inaccurate when it exits the vicinity of the origin because of underresolution.

In the RBF method, the method to evaluate the Hilbert transform of u_{xx} provides accurate results only when the function u_{xx} is very small outside the domain of the grid points. When a solution approaches the boundary of the domain, this condition is not satisfied and then the solution becomes inaccurate.

5.7.4 Grid-Flexibility

To use the FFT in the Christov method and the Fourier pseudospectral method, we have to choose evenly spaced grid points in the Fourier pseudospectral method and evenly spaced grid points in the Christov method after change of coordinate from x to s . There is no freedom to choose the grid points. Once the truncated domain and the number of the grid points in the Fourier pseudospectral method and the number of the grid points in the Christov method are chosen, the grid points are already determined. In contrast, nearly any grid at all can be used with the RBF method.

Table 5.2: Comparison of Numerical Methods

Term	Fourier	Christov	RBF
FFT-applicable	Yes	Yes	No
flops/timestep	$O(N \log_2(N))$	$O(N \log_2(N))$	$O(N^2)$
Domain Truncation	Yes	No	No
Grid-Flexible	No	No	Yes
Boundary Difficulty	Wrap around	Underresolution	Inaccuracy caused by the nonlocal operator \mathcal{H}

5.8 Numerical Experiments on the Zero-Dispersion Limit of the BO Equation

In Chapter III, the zero dispersion limit of the BO equation was studied analytically. In this section, we investigate this limit numerically to illustrate and verify our theoretical result. Here, we use the Fourier pseudospectral method. The number of the grid points N we use in the numerical experiments depends on the value of the small parameter ϵ in the BO equation. The number of the grid points N has to be large enough so that the numerical scheme is not subject to aliasing instability and that the numerical solutions are accurate. On the other hand, one has to choose N not too large, otherwise the numerical algorithm is too expensive. So we calculate

the errors of the numerical solutions with different choices of the small parameter ϵ and the number of the grid points N to help us make the best choice. Since we do not know the solutions of the BO equation for small ϵ , the error could be computed approximately as the difference between $u_{N_{max}}(x, t)$ and $u_N(x, t)$:

$$(5.63) \quad E(N) = \max_{x \in \mathbb{R}, t \in [0, 3]} |u_{N_{max}}(x, t) - u_N(x, t)|,$$

where N_{max} is the largest N chosen and $u_N(x, t)$ is the numerical solution obtained by using N grid points. The results are listed in Table 5.8.

	$\epsilon=0.1$ $N_{max} = 1024$	$\epsilon=0.05$ $N_{max} = 2048$	$\epsilon=0.025$ $N_{max} = 4096$	$\epsilon=0.0125$ $N_{max} = 8192$
N=64	NaN	NaN	NaN	NaN
N=128	NaN	NaN	NaN	NaN
N=256	1.7099E-04	NaN	NaN	NaN
N=512	1.7789E-09	1.5311E-03	NaN	NaN
N=1024		3.9309E-08	2.5320E-02	NaN
N=2048			2.4590E-07	4.0966E-01
N=4096				7.2139E-07

Table 5.3: Error of small dispersion limit calculation. The initial condition of $u(x, t)$ is $u(x, 0) = (\cos x + 1)/2$.

With this information in hand, we may now start to do the numerical experiments on the zero dispersion limit of the BO equation. According to Theorem III.5 in Chapter III, for any function $f \in L^2(\mathbb{R})$ and positive time t , the following equation holds true:

$$(5.64) \quad \lim_{\epsilon \downarrow 0} \int_{\mathbb{R}} f(y) u_{\epsilon}(y, t) dy = \int_{\mathbb{R}} f(y) \left(\sum_{n=0}^{2P(y,t)} (-1)^n u_n^B(y, t) \right) dy.$$

Here, we illustrate and verify the above theoretical result for the function f given by

$$(5.65) \quad f(y) = 1 \quad \text{for } y \in [-4\pi, x]; \quad f(y) = 0 \quad \text{for } y \notin [-4\pi, x].$$

Then by substituting (5.65) into (5.64), the equation (5.64) becomes

$$(5.66) \quad \lim_{\epsilon \downarrow 0} \int_{-4\pi}^x u_\epsilon(y, t) dy = \int_{-4\pi}^x \left(\sum_{n=0}^{2P(y,t)} (-1)^n u_n^B(y, t) \right) dy.$$

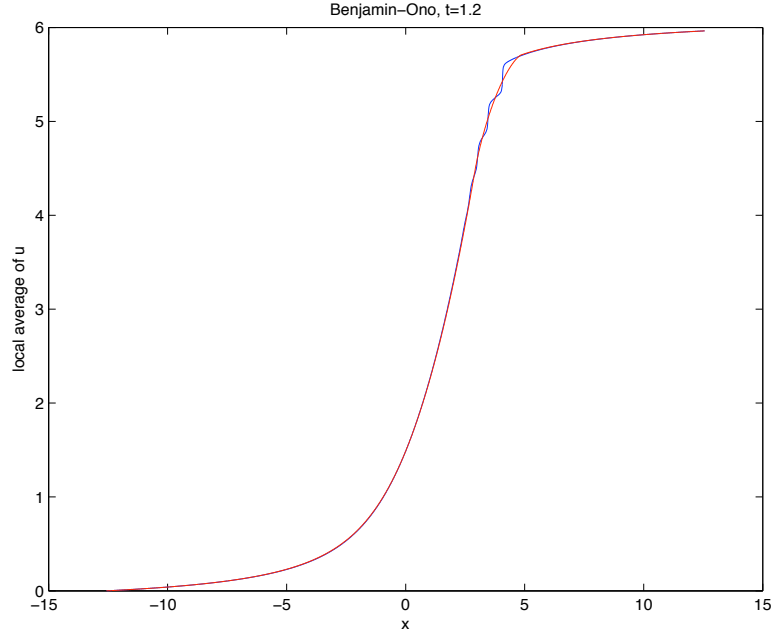


Figure 5.14: The red curve is the right hand side of the equation (5.66) and the blue curve is the left hand side of the equation (5.66) with $\epsilon = 0.05$. The initial condition used in the calculation is $u(x, 0) = 2/(x^2 + 1)$

Here, we numerically calculate the integral on the left hand side of the equation (5.66) with $\epsilon = 0.05$ and the integral on the right hand side of the equation (5.66), which theoretically are very close in value. We illustrate and verify this fact by plotting the numerical results in Figures 5.14–5.16.

5.9 Traveling Wave Solutions of the Cubic BO Equation

The numerical methods we discussed above can also be applied to the cubic BO equation:

$$(5.67) \quad u_t + 3u^2 u_x + \mathcal{H}(u_{xx}) = 0.$$

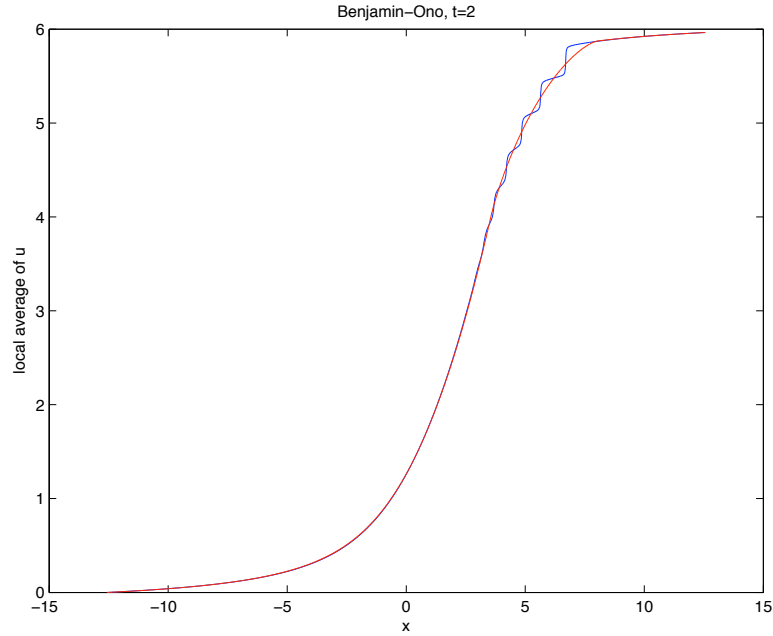


Figure 5.15: The red curve is the right hand side of the equation (5.66) and the blue curve is the left hand side of the equation (5.66) with $\epsilon = 0.05$. The initial condition used in the calculation is $u(x, 0) = 2/(x^2 + 1)$

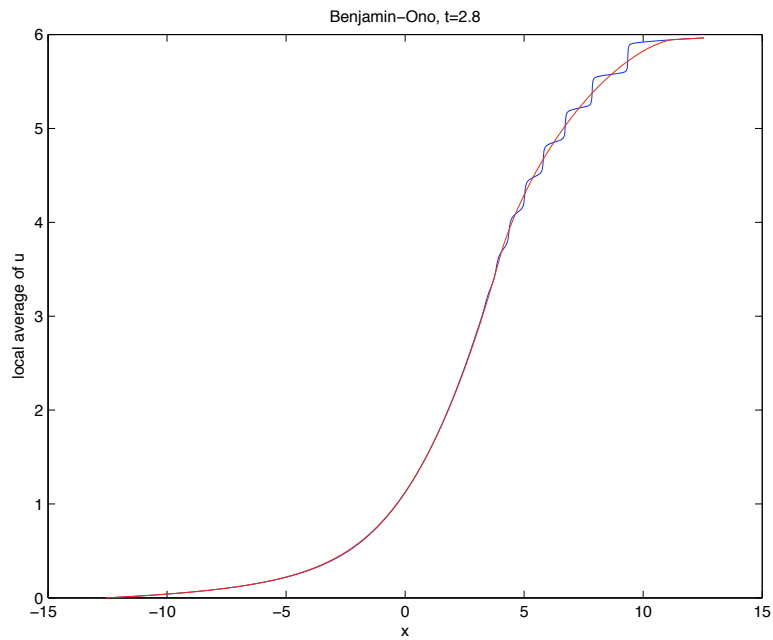


Figure 5.16: The red curve is the right hand side of the equation (5.66) and the blue curve is the left hand side of the equation (5.66) with $\epsilon = 0.05$. The initial condition used in the calculation is $u(x, 0) = 2/(x^2 + 1)$

This is really one of the best options for studying (5.67), since the equation (5.67) is not known to be integrable. Here, we apply the numerical methods to study the traveling wave solutions of the cubic BO equation.

5.9.1 Derivation of the Cubic BO Traveling Wave Equation and Its Scaling

If $u(x, t)$ is a traveling wave solution of the cubic BO equation with a vanishing boundary condition, then $u(x, t)$ can be written as $u(x, t) = f(x - ct)$ where the constant c is the speed of the traveling wave solution. Here the function f satisfies the following equation

$$(5.68) \quad (3f^2 - c)f_x + \mathcal{H}(f_{xx}) = 0$$

with the boundary condition

$$(5.69) \quad \lim_{x \rightarrow \pm\infty} f(x) = 0.$$

After integrating each side of the equation (5.68) from $-\infty$ to x and applying the boundary condition (5.69), one can obtain the cubic BO traveling wave equation:

$$(5.70) \quad f^3 - cf + H(f_x) = 0.$$

To study the traveling wave solutions of the cubic BO equation, without loss of generality, one can assume the constant c in (5.68) and (5.70) is equal to 1, based on the following proposition.

Proposition V.10. *If $v(x, t) = g(x - t)$ is a traveling wave solution of the cubic BO equation with speed 1, then $u(x, t) = f(x - ct)$ where $f(x) = \sqrt{c}g(cx)$ is a traveling wave solution of the cubic BO equation with positive speed c .*

5.9.2 A Numerical Method to Find A Traveling Wave Solution of the Cubic BO Equation

The formula for the traveling wave solution (the single soliton solution) of the BO equation is very simple. However, there is no explicit formula for the traveling wave solution of the cubic BO equation available in the literature. So we introduce a numerical method to find a traveling wave solution of the cubic BO equation with speed 1. Here, we use the cubic BO traveling wave equation (5.70) with $c = 1$ and the boundary condition (5.69). Assume the real function $f(x)$ can be written as:

$$(5.71) \quad f(x) = \sum_{n=-\infty}^{\infty} a_n \phi_n(x)$$

where a_n are complex numbers and $\phi_n(x)$ is the complex Christov function defined above by the equation (5.26) with $L = 1$:

$$(5.72) \quad \phi_n(x) = \frac{(ix - 1)^n}{(ix + 1)^{n+1}}.$$

Since the function $f(x)$ is a real function, the constants a_n satisfy $a_{-1-n} = -a_n^*$, where a_n^* is the complex conjugate of a_n . If $f(x)$ is a solution of the equation (5.70), then $f(x + d)$ is also a solution of the equation (5.70) for any constant d . Therefore, we also require the solution we are looking for to be an even function. Then a_n must satisfy that $a_{-1-n} = -a_n$ and a_n are real numbers. So the function $f(x)$ can be written as:

$$(5.73) \quad f(x) = \sum_{n=0}^{\infty} a_n \psi_n(x)$$

where the function $\psi_n(x)$ is defined by

$$(5.74) \quad \psi_n(x) = \phi_n(x) - \phi_{-1-n}(x) \quad \text{for } n \geq 0.$$

Combining the equation (5.35) and that the function $\phi_n(x)$ satisfies

$$(5.75) \quad (\phi_n(x))_x = i \left(\frac{n}{2} \phi_{n-1}(x) - \frac{2n+1}{2} \phi_n(x) + \frac{n+1}{2} \phi_{n+1}(x) \right),$$

one can show that $\mathcal{H}((\psi_n)_x)$ can be written in the form:

$$(5.76) \quad \begin{aligned} \mathcal{H}((\psi_n)_x) &= \mathcal{H}((\phi_n)_x) - \mathcal{H}((\phi_{-n-1})_x) \\ &= \frac{1}{2} (n\psi_{n-1} - (2n+1)\psi_n + (n+1)\psi_{n+1}). \end{aligned}$$

It is easy to see that the function $\mathcal{H}(f_x)$ can be written as

$$(5.77) \quad \mathcal{H}(f_x) = \frac{1}{2} \sum_{n=0}^{\infty} b_n \psi_n(x),$$

where the constants b_n are defined by

$$(5.78) \quad b_0 = a_1 - a_0; \quad b_n = na_{n-1} - (2n+1)a_n + (n+1)a_{n+1} \quad \text{for } n > 0.$$

By substituting (5.73) and (5.77) into (5.70), one can obtain

$$(5.79) \quad \sum_{n=0}^{\infty} \left(\frac{1}{2} b_n + a_n \right) \psi_n(x) = \left(\sum_{n=0}^{\infty} a_n \psi_n(x) \right)^3.$$

In practice, to use a numerical method, we approximate the function f by

$$(5.80) \quad f_N(x) \approx \sum_{n=0}^N a_n \psi_n(x),$$

then the equation (5.79) becomes

$$(5.81) \quad \sum_{n=0}^N \left(\frac{1}{2} b_n + a_n \right) \psi_n(x) = \left(\sum_{n=0}^N a_n \psi_n(x) \right)^3.$$

It is easy to show for any $n, m \in \mathbb{Z}$, the functions $\phi_n(x)\phi_m(x)$ can be written as:

$$(5.82) \quad \phi_n(x)\phi_m(x) = \frac{1}{2} (\phi_{n+m}(x) - \phi_{n+m+1}(x)),$$

which implies the function $\psi_n\psi_m$ can be written in the form:

$$(5.83) \quad \psi_n\psi_m = \frac{1}{2} (\psi_{m+n} - \psi_{m+n+1} + \psi_{n-m} - \psi_{n-m-1}) \quad \text{for } n > m$$

and

$$(5.84) \quad \psi_n\psi_m = \frac{1}{2} (\psi_{2n} - \psi_{2n+1} + 2\psi_0) \quad \text{for } n = m.$$

Therefore, the right hand side of the equation (5.81) can be written as a linear combination of ψ_n $n = 0, 1, 2, \dots, 3N + 2$. By matching the coefficients of ψ_n , $n = 0, 1, 2, \dots, N$, the equations (5.81) can be reduced to $N+1$ nonlinear equations for the $N+1$ coefficients a_0, a_1, \dots, a_N . Then one can calculate the values of a_0, a_1, \dots, a_N via Newton's method. However, to use Newton's method, we need have a pretty good first guess such that the iterations will converge. The first guess can be obtained by the homotopy perturbation method that we now describe.

5.9.3 Homotopy Perturbation Method

Lian [46] first developed the homotopy analysis method to study a simple pendulum. Later, the homotopy perturbation method, an analogue of the homotopy analysis method, was introduced by He [33, 34]. Here, we use He's homotopy perturbation method to find the traveling wave solution of the cubic BO equation. To use this method, we introduce the following equation

$$(5.85) \quad H(u_x) - u + u^2 = \delta(u^2 - u^3),$$

where δ is a parameter. In fact, the equation (5.85) is the equation (5.70) when $\delta = 1$.

We assume the solution of the equation (5.85) can be written as

$$(5.86) \quad u(x; \delta) = u_0(x) + \delta u_1(x) + \delta^2 u_2(x) + \dots$$

where

$$(5.87) \quad u_0(x) = \frac{2}{1+x^2} = \psi_0(x)$$

is a solution of the equation (5.85) with $\delta = 0$. Here the function $u_0(x)$ characterizes the known traveling wave solutions of the BO equation. By substituting (5.86) into

(5.85) and matching the coefficients of δ^n , one can obtain that the function $u_n(x)$ ($n > 0$) satisfies the following equation.

$$(5.88) \quad H((u_n)_x) - u_n + 2u_n u_0 = \sum_{m=0}^{n-1} u_m u_{n-1-m} - \sum_{m=0}^{n-1} \left(\sum_{j=0}^{n-1-m} u_m u_j u_{n-1-m-j} \right) - \sum_{m=1}^{n-1} u_m u_{n-m}$$

If $u_0(x), \dots, u_{n-1}(x)$ are known, then the equation (5.88) is an integro-differential equation for $u_n(x)$. Assume the functions $u_n(x)$ can be written as

$$(5.89) \quad u_n(x) = \sum_{j=0}^N a_j^{(n)} \psi_n(x) \quad \text{for } n > 0,$$

where $a_j^{(n)}$ are constants. By using the equations (5.83) and (5.84), the equation (5.88) can be reduced to $N + 1$ linear equations for $a_0^{(n)}, a_1^{(n)}, \dots, a_N^{(n)}$, which is easy to solve by Gaussian elimination. For small δ , the equation (5.86) provides a pretty good approximation of a solution for the equation (5.85). However, for relatively large δ , for example $\delta = 1$, the equation (5.86) is not able to give a good approximation. Instead of using the equation (5.86) directly, we calculate the Padé approximation [4] of the equation (5.86) with respect to δ , for relatively large δ . To show that the Padé approximation will provide a better approximation, we calculate the maximum value of δ such that $0 < \delta \leq 1$ and by using the solution we obtained as the first guess, Newton's method for the equation (5.85) will converge. From Table 5.4, we

Method	δ_{\max}	Method	δ_{\max}	Method	δ_{\max}
1st order	0.952	2nd order	0.537	Padé[1,1]	1
3rd order	0.688	4th order	0.541	Padé[2,2]	1
5th order	0.591	6th order	0.524	Padé[3,3]	1

Table 5.4: Maximum of δ such that $0 < \delta \leq 1$ and by using the solution we obtained as the first guess, Newton's method for the equation (5.85) will converge

find that the Padé does provide a better approximation. To evaluate the errors in Figure 5.17, we use different methods to calculate the solution of the equation (5.85)

$u(x)$ for different δ and compute the errors given by $\max |u(x) - u_{\text{exact}}(x)|$, where the function $u_{\text{exact}}(x)$ is obtained by using the Padé[1,1] solution as the first guess and applying Newton's method.

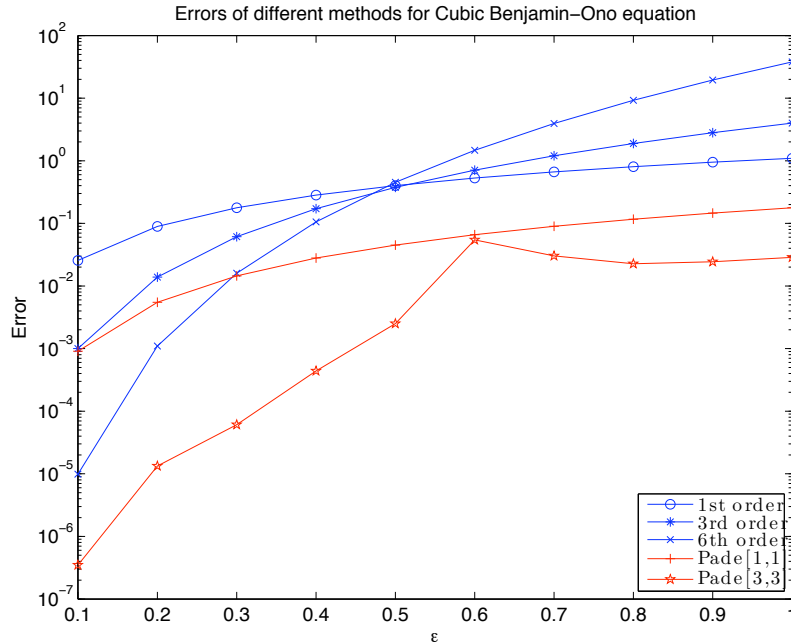


Figure 5.17: Comparison of the errors of different methods for the cubic BO equation

From Figure 5.17, one can find that the Padé approximation does provide a better approximation. One also can find that the sequence in the equation (5.86) converges for $0 \leq \delta < 0.5$ and diverges for $0.5 \leq \delta$, which explains the reason in Table 5.4 that the first order method provide a better first guess for Newton's method when $\delta > 0.5$.

CHAPTER VI

Future Work

6.1 The Zero-Dispersion Limit of the BO Equation with Negative Initial Conditions

6.1.1 Introduction

For negative initial conditions $u_0(x)$, the main contribution is from the reflection coefficient. Neglecting the discrete spectrum, Riemann-Hilbert Problem II.4 becomes

Riemann-Hilbert problem VI.1.

Analyticity: $W(\lambda)$ is analytic in for $\lambda \in \mathbb{C} \setminus \mathbb{R}^+$.

Jump conditions: The boundary values taken on \mathbb{R}^+ satisfy

$$(6.1) \quad W_+(\lambda) = W_-(\lambda) + \beta(\lambda) e^{i\lambda x/\epsilon} \int_0^\lambda \frac{\beta^*(k)}{2\pi i k} W_-(k) e^{-ikx/\epsilon} dk, \quad \text{for } \lambda \in \mathbb{R}^+.$$

Normalization: $W(\lambda)$ is normalized at infinity:

$$(6.2) \quad W(\lambda) \rightarrow 1 \quad \text{as } \lambda \rightarrow \infty.$$

And the conservation laws (2.131) for the BO equation become

$$(6.3) \quad \lim_{\epsilon \downarrow 0} I_k = \frac{(-1)^k \epsilon}{2\pi} \int_0^\infty |\beta(\lambda)|^2 \lambda^{k-2} d\lambda.$$

The equation (2.137) implies that the limit of the conserved quantity I_k can be written as

$$(6.4) \quad \lim_{\epsilon \downarrow 0} I_k = \frac{1}{k} \int_{\mathbb{R}} u_0(x)^k dx = \frac{(-1)^k}{2\pi} \lim_{\epsilon \downarrow 0} \left(\epsilon \int_0^\infty |\beta(\lambda)|^2 \lambda^{k-2} d\lambda \right).$$

This equation suggests that

$$(6.5) \quad \frac{1}{k} \int_{-\infty}^\infty (-u_0(x))^k dx = \frac{1}{2\pi} \int_0^\infty p(\lambda) \lambda^{k-1} d\lambda,$$

where the function $p(\lambda)$ is defined by

$$(6.6) \quad p(\lambda) = \lim_{\epsilon \downarrow 0} \epsilon \frac{|\beta(\lambda)|^2}{\lambda}.$$

Assume $g(\xi)$ is the Fourier transform of $p(\lambda)$. Then the n th derivative of $g(\xi)$ can be written in the form

$$(6.7) \quad g^{(n)}(\xi) = \int_0^\infty (-i\lambda)^n e^{-i\xi\lambda} p(\lambda) d\lambda \quad \text{for } n = 0, 1, 2, \dots.$$

After choosing $\xi = 0$ in (6.7) and substituting (6.5) into (6.7), we have

$$(6.8) \quad \begin{aligned} g^{(n)}(0) &= \int_0^\infty (-i\lambda)^n p(\lambda) d\lambda \\ &= \frac{2\pi i}{n+1} \int_{-\infty}^\infty (iu_0(x))^{n+1} dx \quad \text{for } n = 0, 1, 2, \dots \end{aligned}$$

If the initial condition $u_0(x) \in L^1(\mathbb{R}) \cap L^\infty(\mathbb{R})$, by expanding $g(\xi)$ about $\xi = 0$ and using the equation (6.8) to calculate the upper and lower bounds of the coefficients, one can obtain that $g(\xi)$ is an entire function, which implies $g(\xi)$ can be written as:

$$(6.9) \quad \begin{aligned} g(\xi) &= \sum_{n=0}^{\infty} g^{(n)}(0) \frac{\xi^n}{n!} \\ &= 2\pi i \int_{-\infty}^\infty \sum_{n=0}^{\infty} \left(\frac{(i\xi u_0(x))^{n+1}}{\xi(n+1)!} \right) dx \\ &= \frac{2\pi i}{\xi} \int_{-\infty}^\infty (e^{i\xi u_0(x)} - 1) dx \\ &= -4\pi \int_{-\infty}^\infty e^{i\xi u_0(x)/2} \frac{\sin(\xi u_0(x)/2)}{\xi} dx \end{aligned}$$

Since $g(\xi)$ is the Fourier transform of $p(\lambda)$, by simply applying the inverse Fourier transform to each side of the equation (6.9), we have

$$\begin{aligned}
(6.10) \quad p(\lambda) &= \frac{1}{2\pi} \int_{-\infty}^{\infty} e^{i\lambda\xi} g(\xi) d\xi \\
&= 2 \int_{-\infty}^{\infty} \int_{-\infty}^{\infty} e^{i\xi(u_0(x)/2+\lambda)} \frac{\sin(-\xi u_0(x)/2)}{\xi} dx d\xi \\
&= 2\pi \int_{-\infty}^{\infty} \chi_{[0, -u_0(x)]}(\lambda) dx \\
&= 2\pi \int_{-u_0(x) \geq \lambda} dx
\end{aligned}$$

where $L = \max_{x \in \mathbb{R}}(-u_0(x))$. Since $p(\lambda) \equiv 0$ for $\lambda > L$, the function $\beta(\lambda)$ satisfies $|\beta(\lambda)| = O(1)$ for $\lambda > L$ and

$$(6.11) \quad |\beta(\lambda)| = \left(\frac{2\pi\lambda}{\epsilon} \int_{-u_0(x) \geq \lambda} dx \right)^{1/2} + O(1) \quad \text{for } 0 < \lambda \leq L,$$

as $\epsilon \rightarrow 0+$.

Based on the above discussion, one can approximate the scattering data corresponding to the negative initial condition $u_0(x)$ as follows: there are no eigenvalues and the approximation of the reflection coefficient $\beta(\lambda, t)$ is given by

$$(6.12) \quad \bar{\beta}(\lambda, t) := r(\lambda) e^{i(\lambda^2 t + s_+(\lambda))/\epsilon},$$

where the function $s_+(\lambda)$ is given by the equation (6.16) below and the function $r(\lambda)$ is given by

$$(6.13) \quad r(\lambda) = \left(\frac{2\pi\lambda}{\epsilon} \int_{-u_0(x) \geq \lambda} dx \right)^{1/2}.$$

According to the equation (6.13), $r(\lambda) \equiv 0$ for $\lambda > L$. In the rest of this section, we will use $\bar{\beta}(\lambda, t)$ instead of $\beta(\lambda, t)$. Now, we introduce a new notation, which will be used below to simplify several equations.

Definition VI.2. The function $B_{\pm}(W)(\lambda)$ is defined for $\lambda \in \mathbb{R}^+$ by

$$(6.14) \quad B_{\pm}(W)(\lambda) = W(\lambda) \mp r(\lambda) e^{i\theta_{\pm}(\lambda)/\epsilon} \int_0^{\lambda} \frac{r(k)}{2\pi i k} W(k) e^{-i\theta_{\pm}(k)/\epsilon} dk,$$

where the function $\theta_{\pm}(\lambda)$ is defined by

$$(6.15) \quad \theta_{\pm}(\lambda) = x\lambda + t\lambda^2 + s_{\pm}(\lambda)$$

and the function $s_{\pm}(\lambda)$ is given by

$$(6.16) \quad s_{\pm}(\lambda) = - \int_0^{\lambda} x_{\mp}(k) dk \quad \text{for } \lambda \in [0, L].$$

By using $\bar{\beta}(\lambda, t)$ instead of $\beta(\lambda, t)$ in the jump condition in Riemann-Hilbert problem VI.1, Riemann-Hilbert problem VI.1 becomes the following Riemann-Hilbert problem.

Riemann-Hilbert problem VI.3.

Analyticity: $W(\lambda)$ is analytic in for $\lambda \in \mathbb{C} \setminus [0, L]$

Jump conditions: The boundary values taken on $[0, L]$ satisfy

$$(6.17) \quad W_+(\lambda) = B_-(W_-(\lambda)) \quad \text{for } \lambda \in [0, L]$$

which is equivalent to

$$(6.18) \quad W_-(\lambda) = B_+(W_+(\lambda)) \quad \text{for } \lambda \in [0, L]$$

Normalization: $W(\lambda)$ is normalized at infinity:

$$(6.19) \quad W(\lambda) \rightarrow 1 \quad \text{as } \lambda \rightarrow \infty.$$

By solving Riemann-Hilbert Problem VI.3 and using (2.109), one can obtain an approximation of $u(x, t)$, which we denote by $\hat{u}_{\epsilon}(x, t)$. If the initial condition $u_0(x)$ is a negative, “single hump”, smooth function, then one can obtain the asymptotic property of $\hat{u}_{\epsilon}(x, t)$ as $\epsilon \rightarrow 0+$, which is given in the following two conjectures.

Moreover, for such a initial condition, if $\lambda \in (0, L]$, the function $r(\lambda)$ can be written in terms of the turning points $x_{\pm}(\lambda)$

$$(6.20) \quad r(\lambda) = \left(\frac{2\pi\lambda}{\epsilon} (x_+(\lambda) - x_-(\lambda)) \right)^{1/2},$$

where the turning points $x_{\pm}(\lambda) : (0, L] \rightarrow \mathbb{R}$ are two monotone branches of the inverse function of $u_0(x)$ and satisfy

$$(6.21) \quad u_0(x_{\pm}(\lambda)) = -\lambda \quad \text{and} \quad x_-(\lambda) \leq x_0 \leq x_+(\lambda) \quad \text{for} \quad 0 < \lambda \leq L$$

and x_0 is the global minimum point of $u_0(x)$.

Conjecture VI.4. *If x and $t \geq 0$ satisfy that there is only one branch of the multivalued (method of characteristics) solution of the inviscid Burgers equation (3.33), which is denoted by $u^B(x, t)$, then*

$$(6.22) \quad \lim_{\epsilon \downarrow 0} \hat{u}_{\epsilon}(x, t) = u_0^B(x, t).$$

Conjecture VI.5. *If x and $t \geq 0$ satisfy that there are three branches of the multivalued (method of characteristics) solution of the inviscid Burgers equation (3.33), which are denoted by $u_0^B(x, t) < u_1^B(x, t) < u_2^B(x, t)$, then*

$$(6.23) \quad \hat{u}_{\epsilon}(x, t) = \sum_{n=0}^2 (-1)^n u_n^B + 2 \frac{(u_1^B - u_2^B)(u_1^B - u_0^B + \sqrt{(u_2^B - u_0^B)(u_1^B - u_0^B)} \cos \varphi)}{u_2^B + u_1^B - 2u_0^B + 2\sqrt{(u_2^B - u_0^B)(u_1^B - u_0^B)} \cos \varphi} + o(1)$$

as $\epsilon \rightarrow 0+$, where the functions $\varphi(x, t)$ and $A_3(\lambda)$ are defined by

$$(6.24) \quad \varphi = \frac{1}{\epsilon} (\theta_+(-u_2^B(x, t)) - \theta_+(-u_1^B(x, t))) + A_3(-u_1^B(x, t)) - A_3(-u_2^B(x, t))$$

and

$$(6.25) \quad A_3(\lambda) = -\frac{1}{2\pi} \int_{\bar{\Gamma}^m} \log \left(\left| \frac{\theta'_+(k)}{\theta'_-(k)} \right| \right) \frac{dk}{k - \lambda}.$$

Here the curve $\bar{\Gamma}^m$ is defined in §6.1.3.

The phase function $s_+(\lambda)$ in (6.12) is constructed such that $\hat{u}_\epsilon(x, 0)$ satisfies

$$(6.26) \quad \lim_{\epsilon \downarrow 0} \hat{u}_\epsilon(x, 0) = u_0(x).$$

The rigorous proof of Conjecture VI.4 and VI.5 have not been finished yet. However, the methodology and some preliminary results are provided in §6.1.2 and §6.1.3.

6.1.2 Methodology and Preliminary Results Related to Conjecture VI.4

The nonlocal jump condition in the Riemann-Hilbert problem is the main difficulty to prove Conjecture VI.4. Our strategy is to approximate the solution of the nonlocal Riemann-Hilbert problem by a solution of a Riemann-Hilbert problem with a local jump condition. For x and t satisfying $x + 2Lt < x_0$ ($x + 2Lt > x_0$), we construct a curve Γ^s in the lower half complex plane (the upper half complex plane) connecting the points 0 and L and satisfying

1. Γ^s is a smooth curve.
2. $\theta_-(\lambda)$ ($\theta_+(\lambda)$) and $r(\lambda)$ have analytic extensions from the real interval $[0, L]$ to Γ^s
3. There exists a point λ_0 on the curve Γ^s such that the imaginary part of $\theta_-(\lambda)$ ($\theta_+(\lambda)$) is increasing when λ moves from 0 or L to λ_0 along the curve Γ^s .

The area between the real axis and the curve Γ^s is denoted by Ω^s . Since the integrand of the integral in B_- (B_+) is analytic in Ω^s , we can move the jump from real axis to the curve Γ^s by making the following substitution:

$$(6.27) \quad \widehat{W}^s(\lambda) = W(\lambda) \quad \text{for } \lambda \notin \Omega^s; \quad \widehat{W}^s(\lambda) = B_{\mp}(W)(\lambda) \quad \text{for } \lambda \in \Omega^s.$$

Then the function $\widehat{W}^s(\lambda)$ satisfies the following Riemann-Hilbert problem.

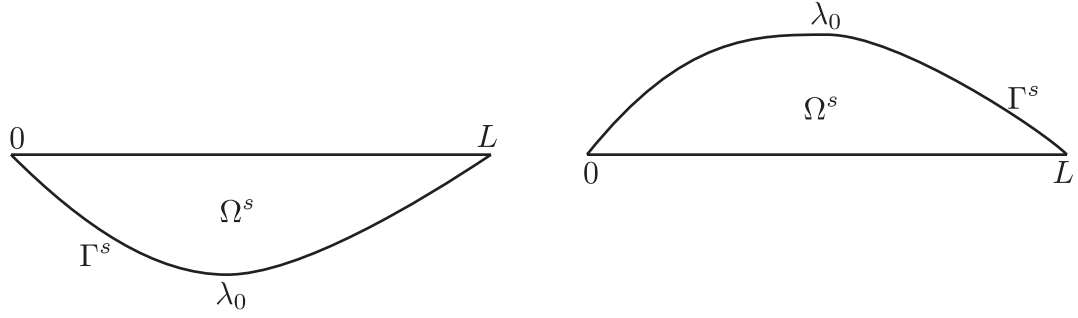


Figure 6.1: Left: the curve Γ^s corresponding to x and t satisfying $x + 2Lt < x_0$
 Right: the curve Γ^s corresponding to x and t satisfying $x + 2Lt > x_0$

Riemann-Hilbert problem VI.6.

Analyticity: $\widehat{W}^s(\lambda)$ is analytic in for $\lambda \in \mathbb{C} \setminus \Gamma^s$

Jump conditions: The boundary values taken on Γ^s satisfy

$$(6.28) \quad \widehat{W}_+^s(\lambda) = B_-(\widehat{W}_-^s)(\lambda) \quad \left(\widehat{W}_-^s(\lambda) = B_+(\widehat{W}_+^s)(\lambda) \right) \quad \text{for } \lambda \in \Gamma^s$$

Normalization: $\widehat{W}^s(\lambda)$ is normalized at infinity:

$$(6.29) \quad \widehat{W}^s(\lambda) \rightarrow 1 \quad \text{as } \lambda \rightarrow \infty.$$

Based on a formal calculation, a reasonable guess one can make is that the main contribution of the integral in B_- (B_+) in the jump condition is from the end points where Laplace's method [55] can be applied, which suggests that

$$(6.30) \quad \theta'_-(\lambda) \widehat{W}_+^s(\lambda) \approx \theta'_+(\lambda) \widehat{W}_-^s(\lambda) \quad \text{for } \lambda \in \Gamma^s.$$

Therefore, we use the solution of the following Riemann-Hilbert problem with local jump condition to approximate the solution of Riemann-Hilbert problem VI.6.

Riemann-Hilbert problem VI.7 (local).

Analyticity: $\overline{W}^s(\lambda)$ is analytic in for $\lambda \in \mathbb{C} \setminus \Gamma^s$

Jump conditions: The boundary values taken on Γ^s satisfy

$$(6.31) \quad \theta'_-(\lambda)\overline{W}_+^s(\lambda) = \theta'_+(\lambda)\overline{W}_-^s(\lambda)$$

Normalization: $\overline{W}^s(\lambda)$ is normalized at infinity:

$$(6.32) \quad \overline{W}^s(\lambda) \rightarrow 1 \quad \text{as } \lambda \rightarrow \infty.$$

Riemann-Hilbert problem VI.7 is easily solved, and the solution is characterized in the following Proposition.

Proposition VI.8. *Riemann-Hilbert Problem VI.7 has a unique solution $\overline{W}^s(\lambda)$ and $\widehat{W}^s(\lambda)$ satisfies*

$$(6.33) \quad \lim_{\lambda \rightarrow \infty} 2\Re((1 - \overline{W}^s(\lambda))\lambda) = u_0^B(x, t).$$

The next task is to show the solution of Riemann-Hilbert problem VI.6 is approximately equal to the solution of Riemann-Hilbert problem VI.7 for small $\epsilon > 0$. Let $\widehat{W}^s(\lambda) = \overline{W}^s(\lambda)E^s(\lambda)$. Then the *error* $E^s(\lambda)$ satisfies the following Riemann-Hilbert Problem.

Riemann-Hilbert problem VI.9 (error).

Analyticity: $E^s(\lambda)$ is analytic in for $\lambda \in \mathbb{C} \setminus \Gamma^s$

Jump conditions: The boundary values taken on Γ^s satisfy

$$(6.34) \quad \overline{W}_+^s(\lambda)E_+^s(\lambda) = B_-(\overline{W}_-^s E_-^s)(\lambda) \quad \text{for } \lambda \in \Gamma^s$$

which is equivalent to

$$(6.35) \quad \overline{W}_-^s(\lambda)E_-^s(\lambda) = B_+(\overline{W}_+^s E_+^s)(\lambda) \quad \text{for } \lambda \in \Gamma^s$$

Normalization: $E^s(\lambda)$ is normalized at infinity:

$$(6.36) \quad E^s(\lambda) \rightarrow 1 \quad \text{as} \quad \lambda \rightarrow \infty.$$

Before we discuss the properties of the function $E^s(\lambda)$, we give the definition of the Hölder spaces and Hölder norm.

Definition VI.10. The Hölder space $C^{0,\eta}(\Gamma)$ where $0 < \eta \leq 1$ consists of the functions f on Γ a bounded subset of \mathbb{C} for which

$$(6.37) \quad \|f\|_{C^{0,\eta}} = \sup_{x \in \Gamma} |f(x)| + \sup_{x,y \in \Gamma} \frac{|f(x) - f(y)|}{|x - y|^\eta}$$

is finite. The norm $\|\cdot\|_{C^{0,\eta}}$ is called the Hölder norm.

Since $E^s(\lambda)$ is analytic in \mathbb{C} except on the curve Γ^s , we assume that $E^s(\lambda)$ can be written as

$$(6.38) \quad E^s(\lambda) = 1 + \frac{1}{2\pi i} \int_{\Gamma^s} \frac{\rho(k)}{k - \lambda} dk,$$

where $\rho(\lambda)$ is in the Hölder space $C^{0,\eta}(\Gamma^s)$. The last step is to establish the following proposition using the theory of singular integral equations.

Proposition VI.11. *There exist a real number η satisfying $0 < \eta \leq 1$ and a unique function $\rho(\lambda)$ corresponding to η in the Hölder space $C^{0,\eta}(\Gamma^s)$ such that the function $E^s(\lambda)$ given by the equation (6.38) is a solution of Riemann-Hilbert Problem VI.9 and*

$$(6.39) \quad \|\rho(\lambda)\|_{C^{0,\eta}} = o(1) \quad \text{as} \quad \epsilon \rightarrow 0.$$

By using Proposition VI.8 and Proposition VI.11, one can prove Conjecture VI.4. However, the rigorous proof of Proposition VI.11 has not been completed yet. This remains work for the future.

6.1.3 Methodology and Preliminary Results Related to Conjecture VI.5

The strategy we use here is same as the strategy used in §6.1.2, which is to approximate the solution of the nonlocal Riemann-Hilbert problem by a solution of a Riemann-Hilbert problem with a local jump condition. We construct a curve Γ^m in the complex plane connecting the points 0 and L and satisfying

1. Γ^m is a smooth curve.
2. $\Gamma^m = \Gamma_+^m \cup \Gamma_-^m$, where Γ_+^m is in the upper half complex plane connecting the points λ_0 and L , Γ_-^m is in the lower half complex plane connecting the points 0 and λ_0 , and λ_0 is a point on real axis and satisfying $-u_1^B < \lambda_0 < -u_0^B$.
3. $\theta_-(\lambda)$ and $r(\lambda)$ have analytic extensions from the real interval $[0, \lambda_0]$ to Γ_-^m and $\theta_+(\lambda)$ and $r(\lambda)$ have analytic extensions from the real interval $[\lambda_0, L]$ to Γ_+^m .
4. There exist a point λ_1 on the curve Γ_-^m and a point λ_2 on the curve Γ_+^m such that the imaginary part of $\theta_-(\lambda)$ is increasing when λ moves from 0 or λ_0 to λ_1 along the curve Γ_-^m and the imaginary part of $\theta_+(\lambda)$ is increasing when λ moves from λ_0 or L to λ_2 along the curve Γ_+^m .

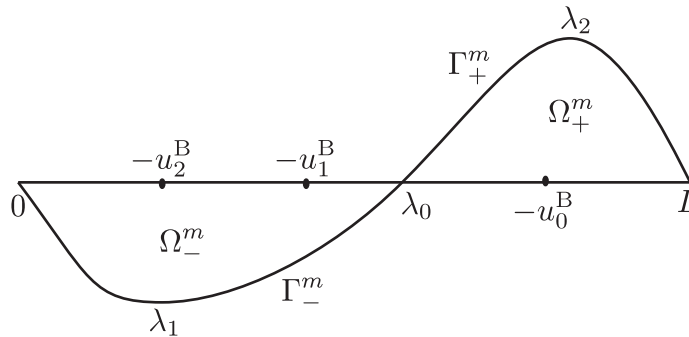


Figure 6.2: The graph of the curve Γ^M

The area between the real axis and the curve Γ_{\pm}^m is denoted by Ω_{\pm}^m . Since the integrand of the integral in B_{\pm} is analytic in Ω_{\pm}^m , we can move the jump from real axis to the curve Γ^m by making the following substitution:

$$(6.40) \quad \widehat{W}^m(\lambda) = W(\lambda) \quad \text{for } \lambda \notin \Omega_{+}^m \cup \Omega_{-}^m; \quad \widehat{W}^m(\lambda) = B_{\pm}(W)(\lambda) \quad \text{for } \lambda \in \Omega_{\pm}^m.$$

The function $\widehat{W}^m(\lambda)$ satisfies the following Riemann-Hilbert problem.

Riemann-Hilbert problem VI.12.

Analyticity: $\widehat{W}^m(\lambda)$ is analytic in for $\lambda \in \mathbb{C} \setminus \Gamma^m$

Jump conditions: The boundary values taken on Γ satisfy

$$(6.41) \quad \widehat{W}_{\pm}^m(\lambda) = B_{\mp}(\widehat{W}_{\mp}^m)(\lambda) \quad \text{for } \lambda \in \Gamma_{\mp}^m$$

Normalization: $\widehat{W}^m(\lambda)$ is normalized at infinity:

$$(6.42) \quad \widehat{W}^m(\lambda) \rightarrow 1 \quad \text{as } \lambda \rightarrow \infty.$$

Again formally applying Laplace's method to the integrals, a reasonable guess one can make is that the main contribution of the integral is from the end points, which suggests that

$$(6.43) \quad \theta'_{-}(\lambda) \widehat{W}_{+}^m(\lambda) \approx \theta'_{+}(\lambda) \widehat{W}_{-}^m(\lambda) \quad \text{for } \lambda \in \Gamma^m.$$

However, it may not be true for $\lambda \in \Gamma^m$ close to λ_0 because there are two points $-u_1^B$ and $-u_2^B$ on the path of integration in B_{-} , which are stationary points in asymptotic analysis. The contribution from these two stationary points is

$$(6.44) \quad e^{-i\pi/4} \frac{\varpi(-u_1^B)}{\sqrt{\theta'_{+}(-u_1^B)}} + e^{i\pi/4} \frac{\varpi(-u_2^B)}{\sqrt{-\theta'_{+}(-u_2^B)}}$$

where

$$(6.45) \quad \varpi(\lambda) = -\sqrt{\epsilon} e^{-i\theta_+(\lambda)/\epsilon} \frac{r(\lambda)}{-\sqrt{2\pi i \lambda}} \widehat{W}^m(\lambda).$$

By using the definition of $r(\lambda)$, the function $\varpi(\lambda)$ can be written as:

$$(6.46) \quad \varpi(\lambda) = -i e^{-i\theta_+(\lambda)/\epsilon} \sqrt{\frac{-\theta'_-(\lambda)}{\lambda}} \widehat{W}^m(\lambda).$$

The contribution from these two stationary points is not small compared to the contribution from the end points for $\lambda \in \Gamma^m$ close to λ_0 , if it is not equal to 0. Therefore, we will use a solution of the following Riemann-Hilbert problem with local jump condition and the condition that the above quantity is equal to 0 to approximate the solution of Riemann-Hilbert problem VI.12.

Riemann-Hilbert problem VI.13.

Analyticity: $\widetilde{W}^m(\lambda)$ is analytic in for $\lambda \in \mathbb{C} \setminus \Gamma^m$

Jump conditions: The boundary values taken on Γ^m satisfy

$$(6.47) \quad \theta'_-(\lambda) \widetilde{W}_+^m(\lambda) = \theta'_+(\lambda) \widetilde{W}_-^m(\lambda)$$

Cancellation condition: The values of $\widetilde{W}^m(\lambda)$ at $-u_1^B$ and $-u_2^B$ satisfy

$$(6.48) \quad e^{-i\pi/4} \frac{\varpi(-u_1^B)}{\sqrt{\theta''_+(-u_1^B)}} + e^{i\pi/4} \frac{\varpi(-u_2^B)}{\sqrt{-\theta''_+(-u_2^B)}} = 0$$

Normalization: $\widetilde{W}^m(\lambda)$ is normalized at infinity:

$$(6.49) \quad \widetilde{W}^m(\lambda) \rightarrow 1 \quad \text{as } \lambda \rightarrow \infty.$$

Next, we construct a solution of Riemann-Hilbert problem VI.13. As mentioned in Chapter I, the solutions of the BO equation become approximately periodic traveling waves in finite time for small ϵ . According to the discussion in [52, 53, 38],

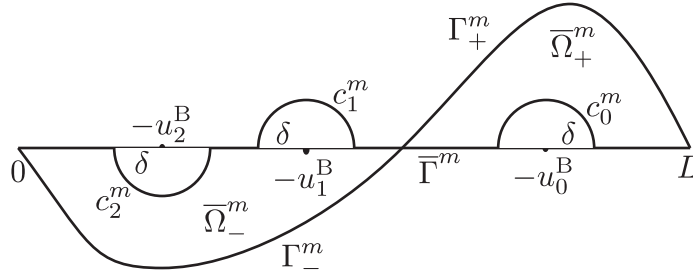


Figure 6.3: The graph of the curves Γ^m and $\bar{\Gamma}^m$

these approximately periodic traveling waves are well-modeled by periodic traveling solutions of the BO equation. This fact and the formula for the exact periodic traveling solutions of the BO equation (2.120) suggest a method to construct a solution of Riemann-Hilbert problem VI.13. Let

$$(6.50) \quad A_1(\lambda) = 1 + \frac{C}{\lambda + u_1^B}$$

where C is a constant that will be determined later to satisfy the cancellation condition and

$$(6.51) \quad A_2(\lambda) = \exp\left(\frac{1}{2\pi i} \int_{\bar{\Gamma}^m} \log\left(\frac{\theta'_+(k)}{\theta'_-(k)}\right) \frac{dk}{k - \lambda}\right).$$

Then $\widetilde{W}^m(\lambda)$ is given by

$$(6.52) \quad \widetilde{W}^m(\lambda) = A_1(\lambda)A_2(\lambda) \text{ for } \lambda \notin \bar{\Omega}^m; \quad \widetilde{W}^m(\lambda) = \left(\frac{\theta'_-(\lambda)}{\theta'_+(\lambda)}\right)^{\pm 1} A_1(\lambda)A_2(\lambda) \text{ for } \lambda \in \bar{\Omega}^m_{\pm},$$

where $\bar{\Omega}^m = \bar{\Omega}^m_+ \cup \bar{\Omega}^m_-$. In the following Proposition, we give the value of constant C such that $\widetilde{W}^m(\lambda)$ given by (6.52) is a solution of Riemann-Hilbert problem VI.13.

Proposition VI.14. *If*

$$(6.53) \quad C = \frac{(u_2^B - u_1^B)\sqrt{u_1^B - u_0^B}}{e^{i(\theta_+(-u_2^B) - \theta_+(-u_1^B))/\epsilon} e^{i(A_3(-u_1^B) - A_3(-u_2^B))} \sqrt{u_2^B - u_0^B} + \sqrt{u_1^B - u_0^B}}.$$

then $\widetilde{W}^m(\lambda)$ is a solution of Riemann-Hilbert problem VI.13 and satisfies

$$(6.54) \quad \lim_{\lambda \rightarrow \infty} 2\Re(-(\widetilde{W}^s(\lambda) - 1)\lambda) \\ = \sum_{j=0}^2 (-1)^j u_j^B + 2 \frac{(u_1^B - u_2^B)(u_1^B - u_0^B + \sqrt{(u_2^B - u_0^B)(u_1^B - u_0^B)} \cos \varphi)}{u_2^B + u_1^B - 2u_0^B + 2\sqrt{(u_2^B - u_0^B)(u_1^B - u_0^B)} \cos \varphi}.$$

To show the difference between $\widetilde{W}^m(\lambda)$ and $\widehat{W}^m(\lambda)$ is small, we introduce the following Riemann-Hilbert problem.

Riemann-Hilbert problem VI.15 (local).

Analyticity: $\overline{W}^m(\lambda)$ is analytic in for $\lambda \in \mathbb{C} \setminus \Gamma^m$

Jump conditions: The boundary values taken on Γ^m satisfy

$$(6.55) \quad \theta'_-(\lambda) \overline{W}_+^m(\lambda) = \theta'_+(\lambda) \overline{W}_-^m(\lambda)$$

Normalization: $\overline{W}^m(\lambda)$ is normalized at infinity:

$$(6.56) \quad \overline{W}^m(\lambda) \rightarrow 1 \quad \text{as } \lambda \rightarrow \infty.$$

The next task is to show the difference between the solution of Riemann-Hilbert problem VI.12 and the solution of Riemann-Hilbert problem VI.13 is small. Let $\widehat{W}^m(\lambda) = \widetilde{W}^m(\lambda) + \overline{W}^m(\lambda)E^m(\lambda)$. Then the error $E^m(\lambda)$ satisfies the following Riemann-Hilbert Problem.

Riemann-Hilbert problem VI.16 (error).

Analyticity: $E^m(\lambda)$ is analytic in for $\lambda \in \mathbb{C} \setminus \Gamma^m$

Jump conditions: The boundary values taken on Γ^m satisfy

$$(6.57) \quad \widetilde{W}_\pm^m(\lambda) + \overline{W}_\pm^m(\lambda)E_\pm^m(\lambda) = B_\mp(\widetilde{W}_\mp^m + \overline{W}_\mp^m E_\mp^m)(\lambda) \quad \text{for } \lambda \in \Gamma_\mp^m$$

Normalization: $E^m(\lambda)$ is normalized at infinity:

$$(6.58) \quad E^m(\lambda) \rightarrow 0 \quad \text{as } \lambda \rightarrow \infty.$$

We want now to establish the following Proposition.

Proposition VI.17. *There exist a real number η satisfying $0 < \eta \leq 1$ and a unique function $\rho(\lambda)$ corresponding to η in the Hölder space $C^{0,\eta}(\Gamma^s)$ such that the function $E^m(\lambda)$ given by*

$$(6.59) \quad E^m(\lambda) = \frac{1}{2\pi i} \int_{\Gamma^m} \frac{\rho(k)}{k - \lambda} dk,$$

is the unique solution of Riemann-Hilbert Problem VI.16 and

$$(6.60) \quad \|\rho(\lambda)\|_{C^{0,\eta}} = o(1) \quad \text{as } \epsilon \rightarrow 0.$$

By using Proposition VI.14 and Proposition VI.17, one can prove Conjecture VI.5. However, the rigorous proof of Proposition VI.17 has not been completed yet. We will try to prove them in the future.

6.2 Numerical Analysis for the Stability of the Traveling Wave Solution of the Cubic BO Equation and the Limited Area Model

The generalized BO equation

$$(6.61) \quad u_t + (p + 1)u^p u_x + \mathcal{H}(u_{xx}) = 0$$

where $p > 0$ is a constant is not known to be integrable if $p \neq 1$. So the inverse scattering transform cannot be applied to the generalized BO equation if $p \neq 1$. However, the numerical methods to solve the BO equation discussed in Chapter V can be used to study the generalized BO equation.

6.2.1 Instability of the Traveling Wave Solutions of the Cubic BO Equation

In §5.9.2, we use two different numerical methods to calculate the traveling wave solution of the cubic BO equation. The numerical simulations suggest that the traveling wave solutions of the cubic BO equation with small amplitude are stable and those with large amplitude are unstable. The instability of the traveling wave solutions of the cubic BO equation is an interesting phenomena, which will be studied by a numerical method, the limit area model, in the the future.

6.2.2 Limited Area Model

The limited area model is a mathematical model widely used in weather forecasting [21, 31, 27, 28, 9]. To provide accurate weather forecasting, a high resolution grid should be used. However, it is too expensive to use a high resolution grid in a global climate model. A compromise is to use a high resolution grid only in the area of interest, an approach called the limited area model. In that case, a coarse resolution global model is used to simulate the global climate, which provides the boundary condition for the limited area model.

A high resolution grid should be used to study the perturbed solution of the cubic BO equation. We will use the limited area model such that the high resolution grid is only used in the area we are interested in. This technique makes the algorithm cheaper.

APPENDICES

APPENDIX A

Derivation of the BO Equation

The calculation in this appendix is given in [13] and we fill in many mathematical details to make it easy to understand. Figure A.1 illustrates a two-layer inviscid and

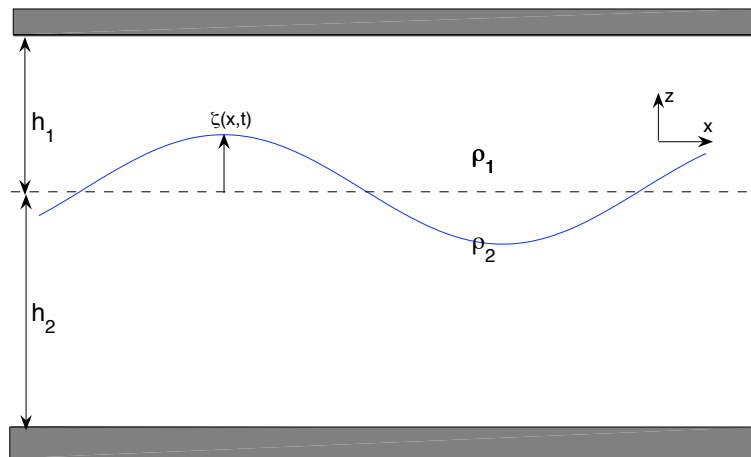


Figure A.1: Two-layer Fluid

incompressible fluid, where h_1 and h_2 are the undisturbed thicknesses of the upper and lower layers respectively. The BO equation describes internal gravity waves at the interface of these two layers with the assumption that the wavelength L is much larger than the thickness of the upper layer h_1 and the thickness of the lower layer h_2 is infinite. The wavelength L can be measured by the initial data. Moreover,

the upper layer is assumed to be initially irrotational and the lower layer is assumed to be irrotational for all time. Since the fluid is incompressible and inviscid, the density ρ_i , the velocity components in Cartesian coordinates (u_i, v_i) and the pressure p_i ($i = 1$ and $i = 2$ correspond to the top and bottom layers respectively) satisfy the continuity equation (corresponding to incompressibility)

$$(A.1) \quad \frac{\partial u_i}{\partial x} + \frac{\partial v_i}{\partial z} = 0$$

and the Euler equations (representing conservation of momentum)

$$(A.2) \quad \rho_i \left(\frac{\partial u_i}{\partial t} + u_i \frac{\partial u_i}{\partial x} + v_i \frac{\partial u_i}{\partial z} \right) = - \frac{\partial p_i}{\partial x}$$

$$(A.3) \quad \rho_i \left(\frac{\partial v_i}{\partial t} + u_i \frac{\partial v_i}{\partial x} + v_i \frac{\partial v_i}{\partial z} \right) = - \frac{\partial p_i}{\partial z} - \rho_i g,$$

where x is the horizontal coordinate, z is the vertical coordinate, and $g = 9.80665 \text{ m/s}^2$ is the gravitational constant. Here we assume $\rho_1 < \rho_2$ so that the fluid is stable and use $z = 0$ to represent the location of the unperturbed flat interface. The boundary conditions at the surface and the bottom of the fluid are assumed to be:

$$(A.4) \quad v_1(x, h_1, t) = 0; \quad v_2(x, -h_2, t) = 0.$$

At the interface, the kinematic boundary conditions are

$$(A.5) \quad \zeta_t + u_1 \zeta_x = v_1; \quad \zeta_t + u_2 \zeta_x = v_2; \quad p_1 = p_2 \quad \text{at} \quad z = \zeta(x, t),$$

where $\zeta(x, t)$ is the displacement of the interface.

In the upper layer, to non-dimensionalize all variables and functions in the equations (A.1)-(A.3) and the boundary conditions (A.4)-(A.5), we rescale all variables as

$$(A.6) \quad x = Lx^*; \quad z = h_1 z^*; \quad t = (L/U_0)t^*; \quad \zeta = h_1 \zeta^*,$$

and all functions as

$$(A.7) \quad p_1 = (\rho_1 U_0^2) p_1^*; \quad u_1 = U_0 u_1^*; \quad v_1 = U_0 v_1^*,$$

where $U_0 = \sqrt{gh_1}$ is an intrinsic velocity scale for the upper layer. Then the continuity equation (A.1) and the Euler equations (A.2) and (A.3) become

$$(A.8) \quad \frac{\partial u_1^*}{\partial x^*} + \gamma \frac{\partial v_1^*}{\partial z^*} = 0,$$

$$(A.9) \quad \frac{\partial u_1^*}{\partial t^*} + u_1^* \frac{\partial u_1^*}{\partial x^*} + \gamma v_1^* \frac{\partial u_1^*}{\partial z^*} = -\frac{\partial p_1^*}{\partial x^*},$$

$$(A.10) \quad \gamma \frac{\partial v_1^*}{\partial t^*} + \gamma u_1^* \frac{\partial v_1^*}{\partial x^*} + v_1^* \frac{\partial v_1^*}{\partial z^*} = -\frac{\partial p_1^*}{\partial z^*} - 1$$

and the boundary conditions (A.4) and (A.5) become

$$(A.11) \quad v_1^*(x^*, 1, t^*) = 0;$$

$$(A.12) \quad \zeta_{t^*}^* + u_1^* \zeta_{x^*}^* = \gamma v_1^* \quad \text{at} \quad z^* = \zeta^*(x^*, t^*),$$

where $\gamma = h_1/L$ is a dimensionless parameter. With the use of the assumption that the wavelength L is much larger than the thickness of the upper layer h_1 , we can assume that $\gamma \ll 1$. By rescaling v_1^* as $v_1^* = \gamma v_1^{**}$, the continuity equation (A.8) and the Euler equations (A.9) and (A.10) become

$$(A.13) \quad \frac{\partial u_1^*}{\partial x^*} + \frac{\partial v_1^{**}}{\partial z^*} = 0$$

$$(A.14) \quad \frac{\partial u_1^*}{\partial t^*} + u_1^* \frac{\partial u_1^*}{\partial x^*} + v_1^{**} \frac{\partial u_1^*}{\partial z^*} = -\frac{\partial p_1^*}{\partial x^*}$$

$$(A.15) \quad \frac{\partial p_1^*}{\partial z^*} = -1 - \gamma^2 \left(\frac{\partial v_1^{**}}{\partial t^*} + u_1^* \frac{\partial v_1^{**}}{\partial x^*} + v_1^{**} \frac{\partial v_1^{**}}{\partial z^*} \right)$$

and the boundary conditions (A.11) and (A.12) become

$$(A.16) \quad v_1^{**}(x^*, 1, t^*) = 0,$$

$$(A.17) \quad \zeta_{t^*}^* + u_1^* \zeta_{x^*}^* = v_1^{**} \quad \text{at} \quad z^* = \zeta^*(x^*, t^*).$$

After integrating each side of the continuity equation (A.13) with respect to z^* from ζ^* to 1 and using the boundary conditions (A.16) and (A.17), the continuity equation (A.13) becomes

$$(A.18) \quad (1 - \zeta^*) \overline{(u_1^*)_{x^*}} - \zeta_{t^*}^* - u_1^* \zeta_{x^*}^* = 0,$$

which can be written as

$$(A.19) \quad \eta^1_{t^*} + (\eta^1 \overline{u_1^*})_{x^*} = 0,$$

where $\eta^1 = 1 - \zeta^*$. Here \bar{g} is defined to be the vertical average given by

$$(A.20) \quad \bar{g}(x^*, t^*) = \frac{1}{\eta^1} \int_{\zeta^*}^1 g(x^*, z^*, t^*) dz^*$$

for any function g . Then by integrating each side of the equation (A.14) with respect to z^* from ζ^* to 1 and using the notation (A.20), the equation (A.14) becomes

$$(A.21) \quad \eta^1 \overline{(u_1^*)_{t^*}} + \frac{1}{2} \eta^1 \overline{(u_1^* u_1^*)_{x^*}} + \int_{\zeta^*}^1 v_1^{**} (u_1^*)_{z^*} dz^* = -\eta^1 \overline{(p_1^*)_{x^*}}.$$

After apply integration by parts to the third term on the left side of the equation (A.21) and using the equation (A.13) and the boundary conditions (A.16) and (A.17), the equation (A.21) can be written as

$$(A.22) \quad (\eta^1 \overline{u_1^*})_{t^*} + (\eta^1 \overline{u_1^* u_1^*})_{x^*} = -\eta^1 \overline{(p_1^*)_{x^*}}.$$

Then by integrating each side of the equation (A.15) with respect to z^* from ζ^* to z^* and using the boundary condition (A.17), one can obtain

$$(A.23) \quad p_1^* = -(z^* - \zeta^*) + P(x^*, t^*) + O(\gamma^2).$$

If one writes u_1^* as $u_1^* = u_1^{*(0)} + O(\gamma^2)$, then (A.14) and (A.23) suggest

$$(A.24) \quad u_1^{*(0)} = u_1^{*(0)}(x^*, t^*) \quad \text{if} \quad u_{1z^*}^{*(0)} = 0 \quad \text{at} \quad t = 0.$$

The assumption that the upper layer is initially irrotational indicates [12] that $u_{1z^*}^{*(0)} = 0$ at $t = 0$, which implies that $u_1^{*(0)}$ is independent of z^* . Therefore, $\eta^1 \overline{u_1^* u_1^*}$ can be written as

$$(A.25) \quad \eta^1 \overline{u_1^* u_1^*} = \eta^1 \overline{u_1^{*(0)} u_1^{*(0)}} + O(\gamma^2).$$

By substituting (A.23) and (A.25) into (A.22) and using (A.19), then the equation (A.22) becomes

$$(A.26) \quad (\overline{u_1^*})_{t^*} + \overline{u_1^* (u_1^*)_{x^*}} = -\zeta_{x^*}^* - P_{x^*} + O(\gamma^2).$$

In the lower layer, the assumption that the flow is irrotational implies that the velocity components u_2, v_2 can be written as $(u_2, v_2) = (\phi_x, \phi_z)$, where ϕ is the velocity potential. Then by substituting $(u_2, v_2) = (\phi_x, \phi_z)$ into (A.1)-(A.5), the continuity equation (A.1) and the Euler equations (A.2) and (A.3) become

$$(A.27) \quad \phi_{xx} + \phi_{zz} = 0.$$

$$(A.28) \quad \phi_{tx} + \frac{1}{2}(\phi_x^2 + \phi_z^2)_x = -\frac{1}{\rho_2}(p_2)_x$$

$$(A.29) \quad \phi_{tz} + \frac{1}{2}(\phi_x^2 + \phi_z^2)_z = -\frac{1}{\rho_2}(p_2)_z - g$$

and the boundary conditions (A.4) and (A.5) become

$$(A.30) \quad \phi_z(x, -h_2, t) = 0$$

$$(A.31) \quad \zeta_t + \phi_x \zeta_x = \phi_z, \quad \text{at} \quad z = \zeta(x, t).$$

Here, the Euler equations (A.28) and (A.29) imply that the pressure p_2 can be written as

$$(A.32) \quad p_2 = -\rho_2 \left(\phi_t + \frac{1}{2} (\phi_x^2 + \phi_z^2) + gz \right) + C(t)$$

where $C(t)$ is a function of t . After substituting $z = \zeta(x, t)$ into (A.32), differentiating it with respect to x and using the boundary condition (A.31), the equation (A.32) becomes

$$(A.33) \quad (p_2)_x = -\rho_2 \left(\frac{1}{2} (2\phi_t + \phi_x^2 + \phi_z^2)_x + \frac{\zeta_x}{2} (2\phi_t + \phi_x^2 + \phi_z^2)_z + g\zeta_x \right),$$

at $z = \zeta(x, t)$. In the lower layer, to non-dimensionalize all variables and functions in the equations (A.27)-(A.29) and the boundary conditions (A.30)-(A.31), we rescale all variables as

$$(A.34) \quad x = Lx^*, \quad z = Lz^{**}, \quad t = (L/U_0)t^*, \quad \zeta = h_1\zeta^*,$$

and all functions as

$$(A.35) \quad p_2 = (\rho_1 U_0^2) p_2^*, \quad \phi = \gamma U_0 L \phi^*.$$

Then the equations (A.27) and (A.33) become

$$(A.36) \quad \phi_{x^* x^*}^* + \phi_{z^{**} z^{**}}^* = 0,$$

$$(A.37) \quad (p_2^*)_{x^*} = -r (\gamma \phi_{t^* x^*}^* + \zeta_{x^*}^*) + O(\gamma) \quad \text{at} \quad z^{**} = \gamma \zeta^*(x^*, t^*),$$

where $r = \rho_2/\rho_1$ and the boundary conditions (A.30) and (A.31) become

$$(A.38) \quad \phi_{z^{**}}^*(x^*, -h_2/L, t^*) = 0,$$

$$(A.39) \quad \zeta_{t^*}^* + \gamma \phi_{x^*}^* \zeta_{x^*}^* = \phi_{z^{**}}^*, \quad \text{at} \quad z^{**} = \gamma \zeta^*(x^*, t^*).$$

With the use of the assumption that the thickness of the lower layer h_2 is infinite, one can write the boundary condition (A.38) as

$$(A.40) \quad \phi_{z^{**}}^*(x^*, -\infty, t^*) = 0.$$

After applying the Fourier transform with respect to x^* to each side of the equation (A.36), the equation (A.36) becomes

$$(A.41) \quad \widetilde{\phi}_{z^{**}z^{**}}^*(\xi, z^{**}, t^*) - \xi^2 \widetilde{\phi}^*(\xi, z^{**}, t^*) = 0,$$

where \widetilde{g} is defined to be the Fourier transform of g :

$$(A.42) \quad \widetilde{g}(\xi, z^{**}, t^*) = \int_{-\infty}^{\infty} g(x^*, z^{**}, t^*) e^{-i\xi x^*} dx^* \quad \text{for any function } g \in L^2(\mathbb{R}).$$

Then the general solution of the equation (A.41) is

$$(A.43) \quad \widetilde{\phi}^*(\xi, z^{**}, t^*) = C_1(\xi, t^*) e^{z^{**}\xi} + C_2(\xi, t^*) e^{-z^{**}\xi},$$

where $C_1(\xi, t^*)$ and $C_2(\xi, t^*)$ are functions of ξ and t^* . By imposing the boundary conditions (A.39) and (A.40), one can obtain the formula for $\widetilde{\phi}^*(\xi, z^{**}, t^*)$:

$$(A.44) \quad \widetilde{\phi}^*(\xi, z^{**}, t^*) = \text{sgn}(\xi) \frac{\widetilde{\zeta}_{t^*}^*}{\xi} e^{z^{**}\text{sgn}(\xi)} + O(\gamma).$$

After applying the inverse Fourier transform with respect to x^* to each side of the equation (A.44), differentiating it with respect to x^* and letting $z^{**} = \gamma\zeta^*(x^*, t^*)$, one can obtain

$$(A.45) \quad \begin{aligned} \phi_{x^*}^*(x^*, \gamma\zeta^*(x^*, t^*), t^*) &= \frac{1}{2\pi} \int_{-\infty}^{\infty} i \text{sgn}(\xi) \widetilde{\zeta}_{t^*}^* e^{i\xi x^*} d\xi + O(\gamma) \\ &= \frac{1}{2\pi} \int_{-\infty}^{\infty} \widetilde{\mathcal{H}(\zeta_{t^*}^*)} e^{i\xi x^*} d\xi + O(\gamma) \\ &= \mathcal{H}(\zeta_{t^*}^*) + O(\gamma). \end{aligned}$$

Then by substituting it into (A.37), the equation (A.37) becomes

$$(A.46) \quad (p_2^*)_{x^*} = -r (\gamma \mathcal{H}(\zeta_{t^*}^*) + \zeta_{x^*}^*) + O(\gamma^2) \quad \text{at } z^{**} = \gamma\zeta^*(x^*, t^*).$$

The boundary condition (A.5) implies that $p_1 = p_2$ at the interface. Moreover, the rescalings (A.6), (A.7), (A.34) and (A.35) indicate $(p_1^*)_{x^*} = (p_2^*)_{x^*}$ at the interface. Then by substituting $z^* = \zeta^*$ into (A.23) and differentiating each side of the equation (A.23) with respect to x^* , the equation (A.23) becomes

$$(A.47) \quad (p_1^*)_{x^*} = P_{x^*}(x^*, t^*) + O(\gamma^2) \quad \text{at} \quad z^* = \zeta^*(x^*, t^*).$$

After comparing (A.46) and (A.47), we have

$$(A.48) \quad P_{x^*} = -r(\gamma\mathcal{H}(\zeta_{t^*t^*}^*) + \zeta_{x^*}^*) + O(\gamma^2) \quad \text{at} \quad z^* = \zeta^*(x^*, t^*).$$

By writing $\mathcal{H}(\zeta_{t^*t^*}^*)$ as $\mathcal{H}(\zeta_{t^*t^*}^*) = -\mathcal{H}(\eta_{t^*t^*}^1)$ and using (A.19), the equation (A.48) becomes

$$(A.49) \quad P_{x^*} = -r(\gamma\mathcal{H}((\eta^1\overline{u}_1)_{x^*t^*}) + \zeta_{x^*}^*) + O(\gamma^2) \quad \text{at} \quad z^* = \zeta^*(x^*, t^*).$$

After letting $z^* = \zeta^*(x^*, t^*)$ in (A.26) and substituting (A.49) into (A.26), the equation (A.26) becomes

$$(A.50) \quad (\overline{u}_1^*)_{t^*} + \overline{u}_1^*(\overline{u}_1^*)_{x^*} + (1-r)\zeta_{x^*}^* = r\gamma\mathcal{H}((\eta^1\overline{u}_1)_{x^*t^*}) + O(\gamma^2) \quad \text{at} \quad z^* = \zeta^*(x^*, t^*).$$

Because of the weakly nonlinear assumption, we rescale \overline{u}_1^* as $\overline{u}_1^* = \gamma\overline{u}^{**}_1$ and rescale ζ^* as $\zeta^* = \gamma\zeta^{**}$, and then (A.19) and (A.50) become

$$(A.51) \quad \zeta_{t^*}^{**} - (\overline{u}^{**}_1)_{x^*} + \gamma(\zeta^{**}\overline{u}^{**}_1)_{x^*} = 0 \quad \text{at} \quad z^* = \zeta^*(x^*, t^*),$$

$$(A.52) \quad (\overline{u}^{**}_1)_{t^*} + \gamma\overline{u}_1^{**}(\overline{u}_1^{**})_{x^*} + (1-r)\zeta_{x^*}^{**} = r\gamma\mathcal{H}((\overline{u}^{**}_1)_{x^*t^*}) + O(\gamma^2)$$

at $z^* = \zeta^*(x^*, t^*)$. The leading order terms in (A.51) and (A.52) can be reduced to a linear wave equation with wave velocity $c_0 = \sqrt{r-1}$. We are interested in nonlinear and dispersive properties of the system. In order to best capture these, we introduce

the new coordinates corresponding to moving at the linear wave speed and speeding up the slow dynamics:

$$(A.53) \quad X = x^* - c_0 t^*, \quad T = \gamma t.$$

Then under the new coordinates, the equation (A.51) and (A.52) become

$$(A.54) \quad (\overline{u_1^{**}})_X = \gamma \zeta_T^{**} - c_0 \zeta_X^{**} + \gamma (\zeta^{**} \overline{u_1^{**}})_X,$$

$$(A.55) \quad \gamma (\overline{u_1^{**}})_T + (\gamma \overline{u_1^{**}} - c_0) (\overline{u_1^{**}})_X + (1 - r) \zeta_X^{**} = -c_0 r \gamma \mathcal{H}((\overline{u_1^{**}})_{XX}) + O(\gamma^2)$$

at the interface. Therefore, after substituting (A.54) into (A.55), one can obtain the BO equation:

$$(A.56) \quad \zeta_T^{**} + c_1 \zeta_X^{**} + c_2 \mathcal{H}(\zeta_{XX}^{**}) = 0,$$

where $c_1 = -3c_0/2$ and $c_2 = c_0 r/2$.

APPENDIX B

Proof of an Integral Identity

In this appendix, we provide the proof of an identity used in §2.2.8. The identity

$$(B.1) \quad \int_{\mathbb{R}} u_0(x) \mathcal{C}_+(u_0 \mathcal{C}_+(u_0 \mathcal{C}_+(\cdots u_0 \mathcal{C}_+(u_0) \cdots)))(x) dx = \frac{1}{k} \int_{\mathbb{R}} u_0(x)^k dx, \quad k \in \mathbb{Z}^+,$$

where the Cauchy projector \mathcal{C}_+ occurs $k - 1$ times in the integrand, holds true for any function $u_0(x) \in L^1(\mathbb{R}) \cap L^\infty(\mathbb{R})$. Here, we use \bar{I}_k to represent the left hand side of the identity (B.1) and rewrite \bar{I}_k as:

$$(B.2) \quad \bar{I}_k = \int_{\mathbb{R}} u_0(x) J_k^+(x) dx, \quad k = 1, 2, 3, \dots,$$

where the function $J_k^+(x)$ is given by the following recurrence relation:

$$(B.3) \quad J_1^+(x) = 1; \quad J_{k+1}^+(x) = \mathcal{C}_+(u_0 J_k^+)(x), \quad k = 1, 2, 3, \dots$$

To simplify the proof, we introduce new functions $J_k^-(x)$, which are given by the following recurrence relation:

$$(B.4) \quad J_1^-(x) = 1; \quad J_{k+1}^-(x) = \mathcal{C}_-(u_0 J_k^-)(x), \quad k = 1, 2, 3, \dots$$

Then we can write \bar{I}_k in the form

$$(B.5) \quad \bar{I}_k = \int_{\mathbb{R}} J_1^-(x) u_0(x) J_k^+(x) dx, \quad k = 1, 2, 3, \dots$$

By using the identity (2.43), we have, for $1 \leq s \leq k-1$

$$(B.6) \quad \int_{\mathbb{R}} J_s^-(x) u_0(x) J_{k+1-s}^+(x) dx = - \int_{\mathbb{R}} J_{s+1}^-(x) u_0(x) J_{k-s}^+(x) dx.$$

This equation implies that \bar{I}_k can also be written as:

$$(B.7) \quad \bar{I}_k = (-1)^{s-1} \int_{\mathbb{R}} J_s^-(x) u_0(x) J_{k+1-s}^+(x) dx, \quad \text{for } 1 \leq s \leq k.$$

Then after summing each side of the equation (B.7) from $s = 1$ to $s = k$, one can obtain

$$(B.8) \quad k\bar{I}_k = \int_{\mathbb{R}} u_0(x) \left(\sum_{j=1}^k (-1)^{k-j} J_j^+(x) J_{k+1-j}^-(x) \right) dx.$$

In fact, the sum in the equation (B.8) is equal to u_0^{k-1} , which will be proved below by the mathematical induction. We use O_k to represent the sum in the equation (B.8):

$$(B.9) \quad O_k = \sum_{j=1}^k (-1)^{k-j} J_j^+ J_{k+1-j}^-.$$

It is obvious that

$$(B.10) \quad O_1 = 1; \quad O_2 = u_0.$$

Assume $O_k = u_0^{k-1}$ for $k \leq m$, then we write O_{m+1} as:

$$(B.11) \quad O_{m+1} = \sum_{j=1}^m (-1)^{m+1-j} J_j^+ J_{m+2-j}^- + J_{m+1}^+.$$

To show $O_{m+1} = u_0^m$, we introduce new functions $J_{m+1,s}(x)$, which can be written in terms of $J_s^-(x)$ and $J_{m+1-s}^+(x)$:

$$(B.12) \quad J_{m+1,s} = \mathcal{C}_+(u_0 J_s^- J_{m+1-s}^+) \quad \text{for } s = 1, 2, \dots, m.$$

Then by using the identities (2.39), (2.40) and (2.41), we have, for $1 \leq s \leq m-1$,

$$\begin{aligned}
J_{m+1,s} &= \mathcal{C}_+(u_0 J_s^- J_{m+1-s}^+) \\
&= -\mathcal{C}_+(\mathcal{C}_-(u_0 J_s^-) J_{m+1-s}^+) + \mathcal{C}_+(u_0 J_s^-) J_{m+1-s}^+ \\
\text{(B.13)} \quad &= -\mathcal{C}_+(J_{s+1}^- J_{m+1-s}^+) + \mathcal{C}_+(u_0 J_s^-) J_{m+1-s}^+ \\
&= -\mathcal{C}_+(u_0 J_{s+1}^- J_{m-s}^+) + \mathcal{C}_+(u_0 J_s^-) J_{m+1-s}^+ \\
&= -J_{m+1,s+1} + \mathcal{C}_+(u_0 J_s^-) J_{m+1-s}^+.
\end{aligned}$$

From the definition of $J_{m+1,s}(x)$, it is obvious that

$$\text{(B.14)} \quad J_{m+1,m} = \mathcal{C}_+(u_0 J_m^-) J_1^+ \quad \text{and} \quad J_{m+1,1} = J_{m+1}^+.$$

The equations (B.13) and (B.14) imply that the last term on the right side of the equation (B.11) J_{m+1}^+ can be written as:

$$\text{(B.15)} \quad J_{m+1}^+ = J_{m+1,1} = \sum_{j=1}^m (-1)^{j-1} \mathcal{C}_+(u_0 J_j^-) J_{m+1-j}^+ = \sum_{j=1}^m (-1)^{m-j} J_j^+ \mathcal{C}_+(u_0 J_{m+1-j}^-).$$

Then after substituting it into (B.11) and using the identity (2.39) and the assumption $O_k = u_0^{k-1}$ for $k \leq m$, we have

$$\begin{aligned}
O_{m+1} &= \sum_{j=1}^m (-1)^{m-j} J_j^+ (\mathcal{C}_+(u_0 J_{m+1-j}^-) - J_{m+2-j}^-) \\
\text{(B.16)} \quad &= \sum_{j=1}^m (-1)^{m-j} J_j^+ u_0 J_{m+1-j}^- \\
&= u_0 O_m \\
&= u_0^m.
\end{aligned}$$

Thus, we conclude that $O_k = u_0^{k-1}$ for $k \in \mathbb{Z}^+$. By substituting this into (B.8), we complete the proof of the identity (B.1) as follows:

$$\text{(B.17)} \quad \bar{I}_k = \frac{1}{k} \int_{\mathbb{R}} u_0(x) O_k dx = \frac{1}{k} \int_{\mathbb{R}} u_0^k(x) dx \quad \text{for } k \in \mathbb{Z}^+.$$

BIBLIOGRAPHY

BIBLIOGRAPHY

- [1] M. J. Ablowitz and P. A. Clarkson. *Solitons, nonlinear evolution equations and inverse scattering*. Cambridge University Press, Cambridge, 1991.
- [2] M. J. Ablowitz, A. S. Fokas, and R. L. Anderson. The Direct Linearizing Transform and the Benjamin-Ono Equation. *Phys. Lett. A*, 93:375–378, 1983.
- [3] M. Abramowitz and I. A. Stegun. *Orthogonal Polynomials, Ch. 22 in Handbook of Mathematical Functions with Formulas, Graphs, and Mathematical Tables*. Dover, New York, 9th printing edition, 1972.
- [4] G. A. Baker and P. R. Graves-Morris. *Padé approximants*. Cambridge University Press, New York, 1996.
- [5] T. B. Benjamin. Internal waves of permanent form in fluids of great depth. *J. Fluid Mech.*, 29:559–592, 1967.
- [6] T. L. Bock and M.D. Kruskal. A two-parameter Miura transformation of the Benjamin-Ono equation. *Phys. Lett.*, 74A:173–176, 1979.
- [7] J. P. Boyd. The orthogonal rational functions of Higgins and Christov and Chebyshev polynomials. *J. Approx. Theor.*, 61:98–103, 1990.
- [8] J. P. Boyd. *Chebyshev and Fourier spectral methods*. Dover, New York, 2000.
- [9] J. P. Boyd. Limited-area Fourier spectral models and data analysis schemes: Windows, Fourier extension, Davies relaxation, and all that. *Mon. Weather Rev.*, 133:2030–2042, 2005.
- [10] J. P. Boyd. Evaluating of Dawson’s integral by solving its differential equation using orthogonal rational Chebyshev functions. *Appl. Math. Comput.*, 204:914–919, 2008.
- [11] J. P. Boyd and L. Wang. Truncated Gaussian RBF differences are always inferior to finite differences of the same stencil width. *Commun. Comput. Phys.*, 5:42–60, 2009.
- [12] W. Choi and R. Camassa. Weakly nonlinear internal waves in a two-fluid system. *J. Fluid. Mech.*, 313:83–103, 1996.

- [13] W. Choi and R. Camassa. Fully nonlinear internal waves in a two-fluid system. *J. Fluid Mech.*, 396:1–36, 1999.
- [14] C. I. Christov. A complete orthonormal system in $L^2(-\infty, \infty)$ space. *SIAM Journal of Applied Mathematics*, 42:1337–1344, 1982.
- [15] W. J. Cody, K. A. Paciorek, and H. C. Thacher. Chebyshev approximations for Dawson’s integral. *Math. Comput.*, 23:171–178, 1970.
- [16] R. Courant, K. Friedrichs, and H. Lewy. Über die partiellen Differenzgleichungen der mathematischen Physik. *Mathematische Annalen*, 100:32–74, 1928.
- [17] R. Courant, K. Friedrichs, and H. Lewy. On the partial difference equations of mathematical physics. *IBM Journal*, 11:215–234, 1967.
- [18] R. E. Davis and A. Acrivos. Solitary internal waves in deep water. *J. Fluid Mech.*, 29:593–607, 1967.
- [19] P. Deift, T. Kriecherbauer, K. T.-R. McLaughlin, S. Venakides, and X. Zhou. Strong asymptotics of orthogonal polynomials with respect to exponential weights. *Comm. Pure Appl. Math.*, 52:1491–1552, 1999.
- [20] H. Dette and W. J. Studden. Some new asymptotic properties for the zeros of Jacobi, Laguerre, and Hermite polynomials. *Constr. Approx.*, 11:227–238, 1995.
- [21] R. E. Dickinson, R. M. Errico, F. Giorgi, and G. T. Bates. A regional climate model for the western U.S. *Climatic Change*, 15:383–422, 1989.
- [22] S. Yu. Dobrokhotov and I. M. Krichever. Multi-phase solutions of the Benjamin-Ono equation and their averaging. *Mat. Zametki.*, 49:42–58, 1991.
- [23] T. A. Driscoll and A. R. H. Heryudono. Adaptive residual subsampling methods for radial basis function interpolation and collocation problems. *Comput. Math. Appl.*, 53:927–939, 2007.
- [24] G. F. Fasshauer. *Meshfree Approximation Methods with MATLAB*. Interdisciplinary Mathematical Sciences, World Scientific Publishing Company, Singapore, 2007.
- [25] A. S. Fokas and M. J. Ablowitz. The inverse scattering transform for the Benjamin-Ono equation: A pivot to multidimensional problems. *Stud. Appl. Math.*, 68:1–10, 1983.
- [26] C. Frayer, R. O. Hryniv, Ya V. Mykytyuk, and P. A. Perry. Inverse scattering for Schrödinger operators with Miura potentials: I. Unique Riccati representatives and ZS-AKNS systems. *Inverse Problems*, 25:115007–115031, 2009.
- [27] S. R. Fulton and W. H. Shubert. Chebyshev spectral methods for limited area models. Part I: model problem analysis. *Mon. Weather Rev.*, 115:1940–1953, 1987.

- [28] S. R. Fulton and W. H. Shubert. Chebyshev spectral methods for limited-area models. Part II: Shallow water model. *Mon. Weather Rev.*, 115:1954–1965, 1987.
- [29] C. S. Gardner, C. S. Greene, M. D. Kruskal, and R. M. Miura. Method for Solving the Korteweg-de Vries Equation. *Phys. Rev. Lett.*, 19:1095–1097, 1967.
- [30] C. S. Gardner, C. S. Greene, M. D. Kruskal, and R. M. Miura. Korteweg-de Vries and generalizations. VI. Methods for exact solution. *Comm. Pure Appl. Math.*, 27:97–133, 1974.
- [31] F. Giorgi. Simulation of regional climate using a limited area model nested in a general circulation model. *Journal of Climate*, 3:941–963, 1990.
- [32] A. V. Gurevich and L. P. Pitaevskii. Nonstationary structure of a collisionless shock wave. *Soviet Phys. JETP.*, 38:291–297, 1974.
- [33] J. H. He. An approximate solution technique depending upon an artificial parameter. *Commun. Nonlinear Sci. Numer. Simulat.*, 32:92–97, 1998.
- [34] J. H. He. Newton-like iteration method for solving algebraic equations. *Commun. Nonlinear Sci. Numer. Simulat.*, 32:106–109, 1998.
- [35] J. R. Higgins. *Completeness and basis properties of sets of special functions*. Cambridge Univ. Press, New York, 1977.
- [36] R. Hirota. Exact solution of the Korteweg-de Vries equation for multiple collisions of solitons. *Phys. Rev. Lett.*, 27:1192–1194, 1971.
- [37] R. L. James and J. A. C. Weideman. Pseudospectral Methods for the Benjamin-Ono Equation. *Advances in Computer Methods for Partial Differential Equations*, VII:371–377, 1992.
- [38] M. C. Jorge, A. A. Minzoni, and N. F. Smyth. Modulation solutions for the Benjamin-Ono equation. *Physica D*, 132:1–18, 1999.
- [39] D. J. Kaup and Y. Matsuno. the inverse scattering transform for the Benjamin-Ono equation. *Stud. Appl. Math.*, 101:73–98, 1998.
- [40] Y. Kodama, M. J. Ablowitz, and J. Satsuma. Direct and inverse scattering problems of the nonlinear intermediate long wave equation. *J. Math. Phys.*, 23:564–576, 1982.
- [41] D. J. Korteweg and F. de Vries. On the Change of Form of Long Waves Advancing in a Rectangular Canal, and on a New Type of Long Stationary Waves. *Philosophical Magazine*, 39:422–443, 1895.
- [42] P. Lax. Integrals of nonlinear equations of evolution and solitary waves. *Comm. Pure Applied Math.*, 21:467–490, 1968.

- [43] P. D. Lax and C. D. Levermore. The small dispersion limit of the Korteweg-de Vries equation. I. *Comm. Pure Appl. Math.*, 36:253–290, 1983.
- [44] P. D. Lax and C. D. Levermore. The small dispersion limit of the Korteweg-de Vries equation. II. *Comm. Pure Appl. Math.*, 36:571–593, 1983.
- [45] P. D. Lax and C. D. Levermore. The small dispersion limit of the Korteweg-de Vries equation. III. *Comm. Pure Appl. Math.*, 36:809–829, 1983.
- [46] S. J. Liao. A second-order approximate analytical solution of a simple pendulum by the process analysis method. *ASME J. Appl. Mech.*, 59:970–975, 1992.
- [47] A. Martinez-Finkelshtein, P. Martinez-Gonzalez, and R. Orive. On asymptotic zero distribution of Laguerre and generalized Bessel polynomials with varying parameters. *J. Comput. Appl. Math.*, 133:477–487, 2001.
- [48] Y. Matsuno. Exact multi-soliton solution of the Benjamin-Ono equation. *Journal of Physics A : Mathematics and General*, 12:619–621, 1979.
- [49] Y. Matsuno. Number density function of Benjamin-Ono solitons. *Physics Letters A*, 87:15–17, 1981.
- [50] Y. Matsuno. Asymptotic properties of the Benjamin-Ono equation. *J. Phys. Soc. Jpn.*, 51:667–674, 1982.
- [51] Y. Matsuno. *Bilinear transformation method*. Academic Press, Orlando, 1984.
- [52] Y. Matsuno. Nonlinear modulation of periodic waves in the small dispersion limit of the Benjamin-Ono equation. *Physical Review E*, 58:7934–7940, 1998.
- [53] Y. Matsuno. The small dispersion limit of the Benjamin-Ono equation and the evolution of a step initial condition. *J. Phys. Soc. Jpn.*, 67:1814–1817, 1998.
- [54] Y. Matsuno. The Lyapunov stability of the N -soliton solutions in the Lax hierarchy of the Benjamin-Ono equation. *J. Math. Phys.*, 47:3505–1–3505–13, 2006.
- [55] P. D. Miller. *Applied Asymptotic Analysis*. Graduate Studies in Mathematics **75**, American Mathematical Society, Providence, 2006.
- [56] P. D. Miller and Z. Xu. On the zero-dispersion limit of the Benjamin-Ono Cauchy problem for positive initial data. *Comm. Pure Appl. Math.*, 2010.
- [57] A. Nakamura. A direct method of calculating periodic wave solutions to nonlinear evolution equations I. Exact two-periodic wave solution. *J. Phys. Soc. Jpn.*, 47:1701–1705, 1979.
- [58] A. Nakamura. Bäcklund transform and conservation laws of the Benjamin-Ono equation. *J. Phys. Soc. Jpn.*, 47:1335–1340, 1979.

- [59] H. Ono. Algebraic solitary waves in stratified fluids. *J. Phys. Soc. Jpn.*, 39:1082–1091, 1975.
- [60] S. A. Orszag. On the elimination of aliasing in finite difference schemes by filtering high-wavenumber components. *J. Atmos. Sci.*, 28:p. 1074, 1971.
- [61] J. N. Pandey. *The Hilbert transform of Schwartz distributions and applications*. Wiley-Interscience, New York, 1996.
- [62] N. J. Phillips. The general circulation of the atmosphere: A numerical experiment. *Quart. J. Roy. Met. Soc.*, 82:123–164, 1956.
- [63] N. J. Phillips. *The atmosphere and the sea in motion*. Rockefeller Institute Press, New York, 1959.
- [64] A. Porter and N. F. Smyth. Modelling the morning glory of the Gulf of Carpentaria. *J. Fluid Mech.*, 454:1–20, 2002.
- [65] M. Reed and B. Simon. *Methods of Modern Mathematical Physics, Vol I: Functional Analysis*. Academic Press, New York, 1980.
- [66] J. Satsuma and Y. Ishimori. Periodic wave and rational soliton solutions of the Benjamin-Ono equation. *J. Phys. Soc. Jpn.*, 46(2):681–687, 1979.
- [67] V. Thomee and A. S. Vasudeva Murthy. A numerical method for the Benjamin-Ono equation. *BIT Numerical Mathematics*, 38:597–611, 1998.
- [68] J. A. C. Weideman. Computation of the complex error function. *SIAM J. Numer. Anal.*, 31:1497–1518, 1994.
- [69] J. A. C. Weideman. Computing the Hilbert transform on the real line. *Math. Comput.*, 64:745–762, 1995.
- [70] H. Wendland. *Scattered Data Approximation*. Cambridge Univ. Press, New York, 2005.
- [71] E. Wigner. Characteristic vectors of bordered matrices with infinite dimensions. *Ann. of Math.*, 62:548–564, 1955.
- [72] E. Wigner. On the distribution of the roots of certain symmetric matrices. *Ann. of Math.*, 67:325–328, 1958.
- [73] X. Zhou. Direct and inverse scattering transform with arbitrary spectral singularities. *Comm. Pure Appl. Math.*, 42:895–938, 1989.